INHERITED RETINAL DYSTROPHIES

Studies on the clinical and genetic characteristics

Ramon A.C. van Huet

©2015 , R.A.C. van Huet, Nijmegen, The Netherlands.

Lay-out: N. Nijhuis (binnenwerk), J. Hijkoop (cover), Gildeprint, Enschede.

Printed by Gildeprint, Enschede.

ISBN 978-94-6233-155-6

Inherited Retinal Dystrophies

Studies on the clinical and genetic characteristics

Proefschrift

door

Ramon Alexander Christian van Huet
geboren op 1 maart 1986 te Arnhem

Promotor

Prof. dr. Carel B. Hoyng

Co-promotoren

Dr. B. Jeroen Klevering
Dr. Rob W.J. Collin

Manuscriptcommissie:

Prof. dr. Baziel G.M. van Engelen (voorzitter)
Prof. dr. ir. Joris A. Veltman
Prof. dr. Bart P. Leroy (Universiteit van Gent, België)

Voor mijn ouders,
Voor Niels,

Table of Contents

Preface

In this thesis, the characteristics of a variety of inherited retinal dystrophies are described, which could cause significant visual disability. Each time a patient visited our outpatient clinic, sometimes after hours of travelling, the impact of being visually impaired became obvious to me. This does not only include the inability of doing your hobbies, but also includes the daily matters in life that are often done without thought by seeing individuals. I was pleasantly surprised to hear that one patient told me he ran under the guidance of a 'buddy' and that blind individuals even can ski like this. This is in contrast to inability to perform their profession that patients may face.

Inherited retinal dystrophies are not apparently visible from the outside. This sometimes leads to reactions of incomprehension among the patient's peers, for example when they are not recognized or noticed. On the other hand, the blind often have to put their – both literally and figuratively – blind trust in their peers or guide dog to maneuver in public. Despite the bad visual prognosis, many patients have shown an adaptability and positive mood that earns respect for both patients and their parents/family. I sincerely hope that the research described in this thesis will add to a future with improved counseling and prognosis with regard to these severe eye disorders.

Voorwoord

In dit proefschrift worden de kenmerken beschreven van enkele erfelijke netvliesaandoeningen die tot een ernstige visuele handicap kunnen leiden. Iedere keer wanneer er een patiënt, soms na uren reizen, bij ons op de polikliniek kwam voor onderzoeken, werd mij weer duidelijk welke impact slecht zien op je leven heeft. Hierbij speelt het niet het niet meer kunnen uitvoeren van hobby's, maar juist ook om de dagelijkse zaken in het leven, de dingen waar je als ziende vaak niet eens bij nadenkt. Ik was dan ook enigszins verbaasd toen een blinde patiënt mij uitlegde dat hij hard liep onder begeleiding van een zogenoemde 'buddy' en dat zelfs skiën tot de mogelijkheden behoorde. Daarentegen zijn het uitvoeren van beroepsmatige werkzaamheden dikwijls onmogelijk.

Erfelijke netvliesaandoeningen zijn niet zichtbaar aan de buitenkant en vraagt daarmee veel begrip van zowel patiënt als omgeving. Reacties van onbegrip vanuit de omgeving van de slechtziende komen geregeld voor, bijvoorbeeld wanneer iemand niet herkent of opgemerkt wordt. Hier staat lijnrecht tegenover dat de patiënt meestal – zowel letterlijk als figuurlijk – blind vertrouwen moet hebben in zijn medemens of een geleidehond om zich thuis of in het openbaar te manoeuvreren. Ondanks de vaak slechte visuele prognose tonen de meeste patiënten toch een aanpassingsvermogen en positiviteit die bewondering afdwingt voor zowel patiënten als ouders/familie. Ik hoop oprecht dat het onderzoek beschreven in dit proefschrift bij mag dragen aan een toekomst met een betere counseling en prognose ten aanzien van deze ernstige oogaandoeningen.

List of abbreviations

A2E   N-retinylidene-N-retinylethanolamine
ABCR   ATP-binding cassette transporter
AMD   Age-related macular degeneration
AON   Antisense oligonucleotidess
APEX   Arrayed-primer extension
arRP   autosomal recessive retinitis pigmentosa
ATP   Adenosine triphosphate
BBS   Bardet-Biedl syndrome
BCAMD   Benign concentric annular macular dystrophy
BCVA   Best corrected visual acuity
BDNF   Brain-derived neurotrophic factor
BEM   Bull's eye maculopathy
CAI   Carbonic anhydrase inhibitor
CD   Cone Dystrophy
cDNA   Complementary deoxynucleic acid
CFC   Cystoid fluid collection
CFT   Central foveal thickness
cGMP   Cyclic guanosine monophosphate
CI   Confidence interval
CL   Contact lens (electrodes)
CME   Cystoid macular edema
CNTF   Ciliary neurotrophic factor
CRALBP   Cellular retinaldehyde binding protein
CRBP   Cellular retinoid-binding protein
CRD   Cone-rod dystrophy
cSLO   Confocal scanning laser ophthalmoscopy
CSNB   Congenital stationary night blindness
DCMD   Dominant cystoid macular dystrophy
DNA   Deoxyribonucleic acid
DTL   Dawson-Trick-Litzkow (electrodes)
ELM   External limiting membrane
EOG   Electrooculography
ERG   Electroretinography
ERM   Epiretinal membrane
EVS   Exome variant server
FA   Fluorescein angiography
FAF   Fundus autofluorescence
ffERG   Full-field electroretinography

FP	Fundus photography
GAT	Gene augmentation therapy
GCL	Ganglion cell layer
GDNF	Glial-cell derived neurotrophic factor
GTP	Guanosine-5'-triphosphate
HGVS	Human genome variation society
HRM	High resolution melting
IFT	Intraflagellar transport
ILM	Internal limiting membrane
IMPG2	Interphotoreceptor matrix proteoglycan-2
INL	Inner nuclear layer
IPL	Inner plexiform layer
IPM	Interphotoreceptor matrix
iPSC	Induced pluripotent stem cells
IRBP	Interphotoreceptor retinoid-binding protein
IRD	Inherited retinal dystrophies
ISCEV	International Society for Clinical Electrophysiology of Vision
LCA	Leber congenital amaurosis
LogMAR	Logarithm of the minmal angle of resolution
LRAT	Lecithin:retinol acetyltransferase
MD	Macular dystrophy
mfERG	Multifocal electroretinography
MLPA	Multiplex ligation-dependent probe amplification
mRNA	Messenger ribonucleic acid
NGS	Next-generation sequencing
NMD	Nonsense-mediated decay
OCT	Optical coherence tomography
ONL	Outer nuclear layer
OPL	Outer plexiform layer
PCR	Polymerase chain reaction
PHARC	(Acronym) polyneuropathy, hearing loss, ataxia, retinitis pigmentosa and cataract
PR+RPE	Photoreceptor-Retinal pigment epithelium complex
PSC	Posterior subcapsular cataract
PTA	Pure tone average
RD	Retinal dystrophies
RdCVF	Rod-derived cone viability factor
RDH	All-*trans*-retinal dehydrogenase
RDH5	11-cis-retinol dehydrogenase
RNA	Ribonucleic acid
RP	Retinitis pigmentosa
RPE	Retinal pigment epithelium
RPE65	RPE specific protein 65 kDa
RT	Retinal thickness

SD-OCT   Spectral domain optical coherence tomography
STGD1   Stargardt disease
TD-OCT   Time domain optical coherence tomography
tRNA   Transport ribonucleic acid
UPSIT   University of Pennsylvania Smell Identification Test
VA   Visual acuity
VEGF   Vascular endothelial growth factor
VMD   Vitelliform macular dystrophy
VPA   Valproic acid
WES   Whole exome sequencing
XIAP   X-linked inhibitor of apoptosis

Gene names are not generally included in this list. The Retinal Network (RetNet), available at www. https://sph.uth.edu/retnet/, can used for reference of gene names.

General introduction

1

Historical background

The field of inherited retinal disease rapidly expanded after the invention of the ophthalmo-scope by Hermann Helmholtz in 1851. This device enabled examination of the retina and optic disc and caused a true revolution in ophthalmology.[1] Few years later in 1853, Van Trigt published a colored atlas depicting the normal retina as well as a variety of pathological disorders, including retinitis pigmentosa.[2] The first description of retinitis pigmentosa as a distinct clinical entity is generally ascribed to the Dutch ophthalmologist Franciscus C. Donders in 1855.[3] More than a century earlier, however, Rüdiger F. Ovelgün described a form of familial night blindness that closely resembled the disorder that would later become known as retinitis pigmentosa.[4] Even though the term 'retinitis' was an obvious misnomer, the name endured till present time.

In 1909, the German ophthalmologist Karl Stargardt described seven patients from two families who experienced vision loss starting in the first two decades of life.[5] Although the patients initially revealed a normal fundus, in time Stargardt observed the development of macular atrophy and yellowish retinal flecks. This disorder was soon referred to as Stargardt's macular dystrophy. Years later, in 1965, Franceschetti described a similar disease, which he named 'fundus flavimaculatus', characterized by retinal flecks that reached into the peripheral retina and a supposedly milder clinical course with a later age at onset.[6] In fact, fundus flavimaculatus was similar to the phenotypic characteristics of a second patient from Stargardt's original families published by Rosehr in 1954.[7,8] These days, especially after the identification of the molecular genetic cause, Stargardt disease (STGD1) and fundus flavimaculatus are considered subtypes of the same clinical entity.

Retinal disorders are prominently featured in the milestones in human genetics. One of the earliest and most extensive documented pedigree showing an autosomal dominant mode of inheritance involves the family of Jean Nougaret (1637-1719), who suffered from congenital stationary night blindness (CSNB).[9,10] In 1911, Wilson localized the locus of color blindness to the human X-chromosome, which was the first disease gene ever mapped.[11] The era of molecular genetics in retinal disease commenced with the discovery of a locus on the X chromosome in patients with X-linked retinitis pigmentosa by Bhattacharya and colleagues in 1984.[12] In 1990, Dryja and co-workers identified *Rhodopsin* as the first gene to be associated with autosomal dominant retinitis pigmentosa, and the same year Cremers *et al* found mutations in the *REP-1* gene responsible for choroideremia.[13,14] In 1991, the *peripherin-2* (*PRPH2,* formerly known as *RDS/peripherin*) gene was identified as a cause of autosomal dominant retinitis pigmentosa.[15,16] Its involvement in various macular dystrophies was discovered in the following years.[17,18] Up to date, over 200 genes have been identifiedthat have been associated with a wide variety of inherited retinal dystrophies (RetNet, available at https://sph.uth.edu/retnet/).
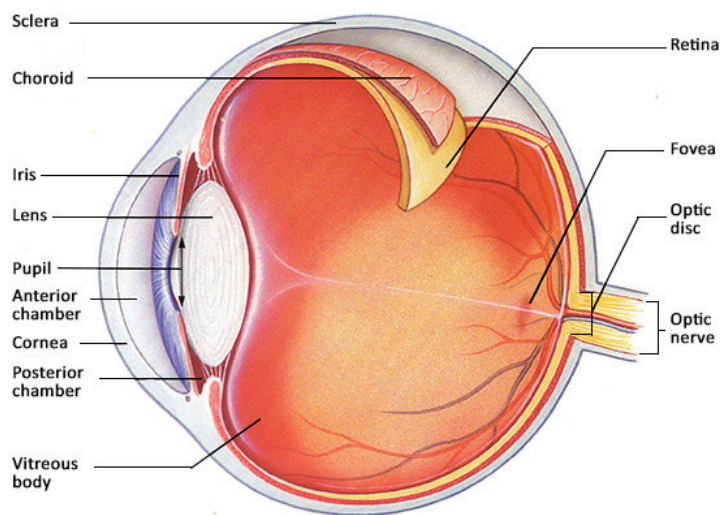
Figure 1.1. Anatomy of the human eye.

Anatomy and physiology of the eye

The eye is a highly specialized organ that enables us to perceive light and thereby our surroundings. The light that is emitted or reflected by the objects around us enters the eye through the cornea. The lens focuses the light beams on the retina, which lines the inner surface of the posterior segment of the orbital globe (Figure 1.1). The anatomy of the posterior part of the globe consists of three major tissue layers: the sclera, the choroid and the retina. The sclera is the outer shell of the orbital globe and is build of collagen fibrils and a few elastic fibers embedded in a matrix of proteoglycans. The choroid is a vascular layer that nourishes the retina; these layers are separated by Bruch membrane. The choroid and retina will be reviewed in detail in the following paragraphs.

The retina

The retina is part of the central nervous system. It originates from an evagination from the future diencephalon of the prosencephalon (forebrain) called the optic vesicle, as early as day 24 of embryologic development. The optic vesicle folds into the optic cup, which includes the tissue that will develop into the pigmented retina, which will develop into the retinal pigment epithelium (RPE), and the neural retina.[19,20] These two layers form a functional unit.

The neuroretina

The neuroretina is the transparent multilayered tissue adjacent to the RPE layer. Its layered architecture includes three nuclear layers containing the neurons, and two plexiform layers of synapses (Figure 1.2). The outer nuclear layer (ONL) contains the cell bodies of the photoreceptors. The inner nuclear layer (INL) contains the cell bodies of the bipolar, amacrine, horizontal and Müller cells, and the ganglion cell layer (GCL) contains the cell bodies of the ganglion cells. These cell layers interconnect via synapses that are present in the outer and

inner plexiform layer (OPL and IPL, respectively). Histologists as well as ophthalmologists recognize an additional intraretinal 'membrane': the external limiting membrane (ELM), which actually reflexes a linear confluence of junctional complexes between Müller cells and photoreceptors. The innermost layer of the retina that borders on the vitreous cavity is named the internal limiting membrane (ILM).

The neuroretina is responsible for the transition of photonic stimuli to electrical neuronal signals, structuring of these signals and the first step of the transport to the central visual pathway. The fundamental synaptic chain that facilitates vision is photoreceptor → bipolar cell → ganglion cell.[21] Horizontal cells in the OPL provide lateral interactions in this chain.[22] Amacrine cells help in signal processing by responding to specific alterations in retinal stimuli, for example sudden changes in light intensity. Müller glial cells span all layers of the neuroretina, and thereby provide a soft embedding for the neurons.[23] Additionally, Müller cells are responsible for the homeostatic and metabolic support of the neuroretina, including regulation of vasoconstriction and vasodilatation of retinal vessels.[24]
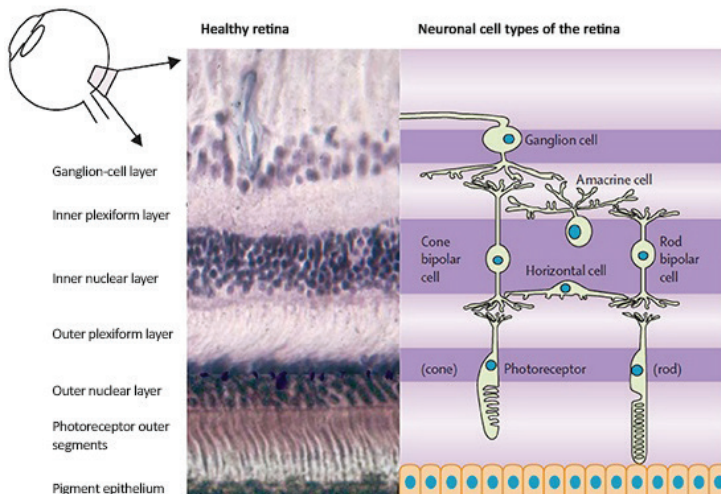
Figure 1.2. Histologic and schematic appearance of the healthy human retina. (Adapted from: Hartong DT et al, 2006.[25])

The central retina, called macula (or *macula lutea*, yellow spot), is located at the posterior pole of the ocular orbit between the optic disc and the vascular arcades and measures 5.5 mm in diameter (Figure 1.3A). This area contains accumulated oxygenated carotenoids, especially lutein and zeaxanthin, which contribute to its yellow color. The macula contains two or more ganglion cell layers, totaling half of all the ganglion cells in the retina.

The fovea (or *fovea centralis*) covers the central 1.5 mm of the macula and contains high numbers of cone photoreceptor cells that provide high spatial acuity. Its 0.35-mm-diameter center, called *foveola*, is densely packed with slender, elongated cone photoreceptors, and has a laterally displaced inner nuclear layer and ganglion cell layer. This configuration leads to a central depression: the foveal pit (Figure 1.3B).
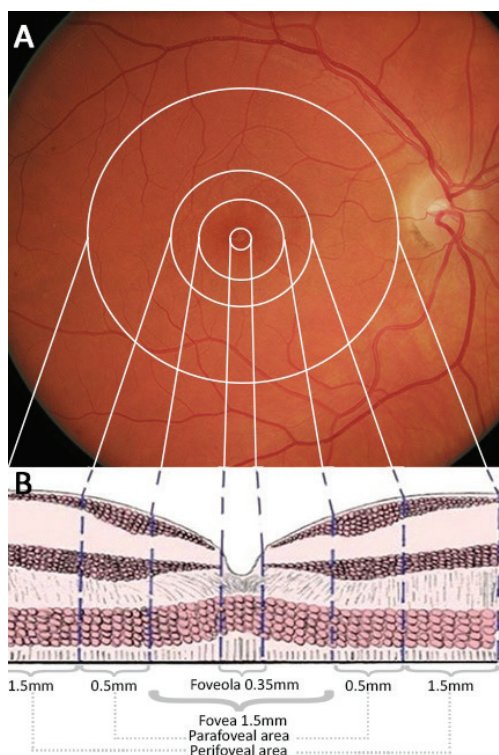
Figure 1.3. The topography of the posterior retina. A, Color fundus photograph with overlaying ETDRS grid chart to define the subfields of the macula. B, Cross-sectional presentation of the macular retina that highlights the anatomical differences between the macular subfields.

Photoreceptors. After light has travelled through the entire neuroretina it meets the photoreceptors where the photonic energy is converted into an electrical neuronal current. Photoreceptors are highly specialized neurons that can be segmented in a synaptic end facing the bipolar cells in the OPL, the cell body containing the nucleus, and inner and outer segments that are linked by the connecting cilium (Figure 1.4).

The connecting cilium is a primary immotile cilium that contains a 9+0 axoneme, consisting of 9 doublets of microtubules without a central microtubule, which is connected to the basal body in the distal tip of the inner segment.[26] Along this axoneme, bidirectional intraflagellar transport takes place, carried out by two distinct multiprotein complexes, IFT-A and IFT-B, and microtubule based motor assemblies kinesin-2 (anterograde transport) and cytoplasmic dynein (retrograde transport).[27] This mechnanism allows for efficient transportation of vital components used in the visual (retinoid) cycle, the phototransduction cascade and disc formation from the cell body to the outer segment.

The axoneme extends into the photoreceptor's outer segment, where cytoplasmic membranous discs are stacked. Within these discs, the phototransduction takes place that starts with the the capture of photons by visual pigments, which initiate the electrical neuronal signal (see below).[28,29] New discs evaginate from the plasma membrane around the connecting cilium, old discs are shed at the tip of the outer segment and phagocytized and further processed by the RPE.[30,31]

The inner segment can be divided into the myoid and ellipsoid sections. The ellipsoid is adjacent to the connecting cilium and contains the metabolic machinery including large numbers of mitochondria. The myoid is closer to the photoreceptor nucleus and has ribosomes, some endoplasmic reticulum, Golgi bodies and small numbers of mitochondria.[32]

Based on morphology and visual pigment, two types of photoreceptors are recognized: rods and cones. Cone photoreceptor cells function best in bright light, due to a relatively low sensitivity to light in combination with a high level of visual pigment regeneration, and facilitate high spatial resolution.
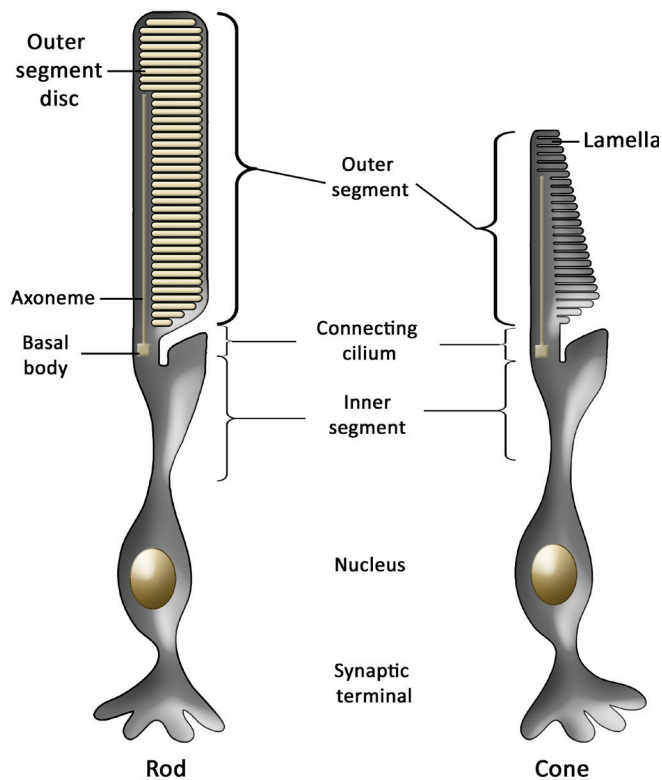
Figure 1.4. Schematic representation of a rod (left) and cone (right) photoreceptor. The outer segments of rods contain discs, whereas cones contain lamellae that are continuous with the plasma membrane.

There are three subtypes of cones: the S ('blue') cones, the M ('green') cones and the L ('red') cones that allow for color vision. The S cones contain iodopsin that is most sensitive to short wavelength light, whereas the iodopsin in M and L cones are sensitive to medium and long wavelength light, respectively.[33,34] Rod photoreceptors cells contain rhodopsin and are far more sensitive to light compared to cones. Therefore, rods provide vision in dim light conditions and sense brightness, contrast and motion.

The distribution of rods and cones varies with the topographical location in the retina. On average, the retina contains 4.6 million cones, and approximately 92 million rods that are mainly distributed in the (mid)peripheral retina.[35] The foveola contains the highest density of M- and L-cones, on average at 199,000 cones/mm^2 and is highly variable between individuals (100,000-324,000 cones/mm^2), but cone density falls steeply with increasing eccentricity (Figure 1.5); S-cones however are virtually absent in the foveola.[35,36] Over the (mid)peripheral retina, the cone subtypes are equally distributed.[37] Rod photoreceptors are also absent in the foveola, but rapidly grow in number with increasing eccentricity with a maximal density of ~160,000/mm^2 at ~20° eccentricity, which decreases towards the periphery (Figure 1.5).[35,38]

Although the peak rod density is high, visual acuity is limited in this region. This is the result of summation of multiple rod responses to a single ganglion cell in each receptive field, which increases sensitivity at the cost of image resolution. This is in contrast with the one to one ratio between cones and ganglion cells at the fovea.
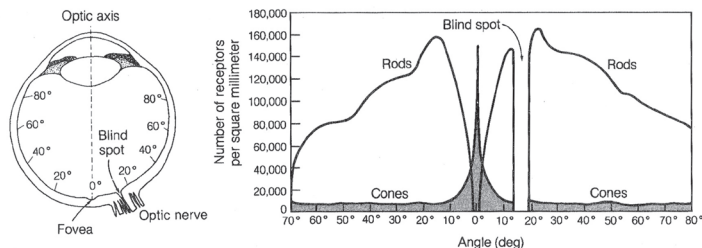
Figure 1.5. The distribution of rod and cone photoreceptors throughout the retina. (Source: Lindsay P et al, 1977[39])

The retinal pigment epithelium

The RPE consists of a monolayer of hexagonal cuboidal cells that are located between the Bruch membrane and the neuroretina (Figure 1.6). The apical side of RPE cells has villous processes that extend in the extracellular matrix between the photoreceptors and envelope the photoreceptor outer segments.[40,41] Every 24 hours, RPE cells phagocytize the outer 10% of the rod and cone outer segments, which contains the 'oldest' discs with the highest load of (toxic) by-products of the visual cycle (see below). Each RPE cell generally contacts multiple photoreceptor outer segments and therefore is the most phagocytic cell in the human body.[42] The phagosome with the shed outer segment subsequently fuses with organelles filled with lytic enzymes called lysosomes, and the phagosome's content is digested. During lifetime, a single RPE cell phagocytoses ~3 billion photoreceptor outer segments.[43]

The lateral surfaces of RPE cells contain tight junctions (zonulae occludentes) that closely connect the adjacent RPE cells. These bonds prevent the free movement of water-soluble molecules through the RPE layer, forming the outer blood-retina barrier. RPE cells closely regulate transport by a wide variety of active channels and pumps to actively transport ions and metabolites from the neuroretina to the choriocapillaris and vice versa.[44] Additionally, the RPE keeps the neuroretina attached by draining the subretinal space from water, a process for which the RPE has a large reserve capacity (up to 2 mL per 24 hours).[45-47]

The pigmentation of RPE cells is caused by melanin-containing spheroidal cytoplasmic organelles called melanosomes, which provide the ability to absorb light. By this, the RPE absorbs scattered light and minimizes phototoxic effects. Furthermore, melanin has anti-oxidative abilities.[48] However, during life, an increasing portion of the available melanin becomes oxidized and accordingly the number of melanosomes decreases with age.[49,50]

In addition to these functions, the RPE plays an important role in the maintenance of the interphotoreceptor matrix, Bruch membrane and the choriocapillaris by the secretion of a variety of factors, including hyaluronan, VEGF and tissue inhibitor of metalloproteinases-3 (TIMP-3),[51-55] Its role in the visual (retinoid) cycle is discussed separately below.
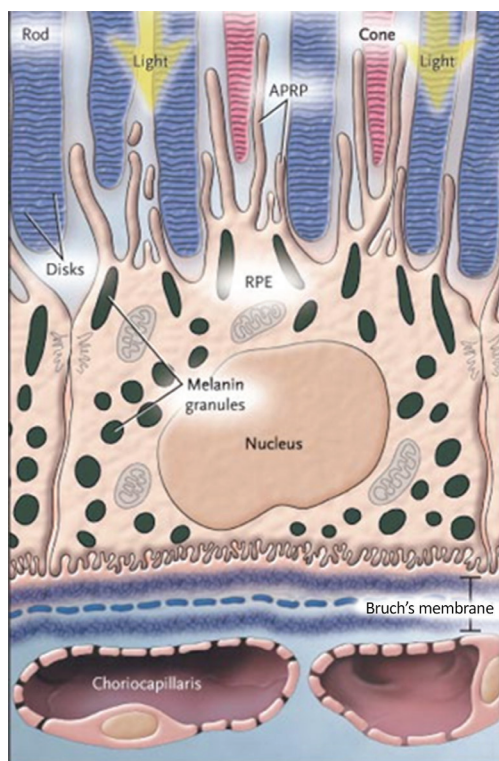
Figure 1.6. Schematic representation of the retinal pigment epithelium and its close relationship to the photoreceptors and choriocapillaris. (Source: de Jong et al, 2006.[56])

Like in the neuroretina, there are topographical differences in the RPE layer. For instance, the density of RPE cells is highest in the fovea and decreases eccentrically.[49,57,58] Additionally, macular RPE cells contain a larger number of melanosomes compared to peripheral RPE cells.[49] Macular RPE cells also are taller and have a smaller diameter,[49,57-59] which consequently leads to a lower number of photoreceptors per RPE cell.[60]

The choroid

The choroid consists of arterioles and venules that are connected by a meshwork of fenestrated capillaries. Blood enters the choroid through the posterior ciliary arteries. The large-caliber choroidal vessels are located in the outer layer, also known as the Haller layer.[61] The capillary meshwork, the choriocapillaris, is the most inner layer of the choroid located just outside Bruch membrane (Figure 1.6). The fenestrated capillaries of the choriocapillaris permit the extravasation of small molecules (e.g. fluorescein), while larger molecules (e.g. albumin) remain intravascular.[62,63] Blood from the choriocapillaris leaves the eye through four or five vortex veins that drain into the superior and inferior ophthalmic veins.

The blood flow rate in the choroid is highest of any tissue in the human body.[61,64] This is necessary to nourish the retina and remove lactic acid, since the retina has one of the highest metabolic rates per gram of tissue in the body.[65] The high choroidal blood flow rate also plays an important role in the drainage of thermal energy from light absorption.[61,66-68]

The choriocapillaris provides oxygen and nourishment to the retinal pigment epithelium (RPE) and the outer one-third of the retina, but 90% of the oxygen delivered to the retina by the choroid is consumed by photoreceptors.[61,64,69] The choriocapillaris depends on trophic factors produced by the RPE, among which factors that induce endothelial fenestration and vascular endothelial growth factors (VEGFs) necessary for the integrity of the choriocapillaris.[53,70-72] Atrophy of the choriocapillaris after degeneration of the RPE has been observed in animal studies,[73,74] as well as in patients with retinal dystrophies that primarily affect the RPE.

Physiology of vision

Vision is mediated by the phototransduction cascade, which takes place in the outer segment discs in both rod and cone photoreceptors. In this process, a light photon is captured by visual pigment and transduced into an electrical neuronal current. The visual (retinoid) cycle, the other vital cycle that partly takes place in the photoreceptor outer segments as well, recycles the vitamine A (retinoid) derivate 11-*cis*-retinal that converts into all-*trans*-retinal on photoactivation. Both the phototransduction cascade and the visual cycle are essential for vision and many of the underlying causes for inherited blindness can be found in defects in these complex systems.

The phototransduction cascade

The phototransduction system consists of a cascade of successive reactions following the excitation of rhodopsin with a photon (Figure 1.7). Rhodopsin is composed of the protein opsin and the chromophore 11-*cis*-retinal. Upon capture of a photon, 11-*cis*-retinal converts to its isomer all-*trans*-retinal, which subsequently transforms rhodopsin to the photoactive metarhodopsin II.[75] Metarhodopsin II degenerates through several intermediates, one of which activates the G-protein transducin, which on its turn activates a cyclic GMP (cGMP) phosphodiesterase that hydrolyses cGMP to 5'-GMP.[76] This leads to a decrease of the concentration of cGMP in the photoreceptor cytoplasm, which results in closure of the photoreceptor plasma membrane cGMP-gated cation channels. This in turn leads to a hyperpolarized plasma membrane caused by a significant drop in intracellular calcium levels. Hyperpolarization of the plasma membrane results in a decreased glutamate excretion at the photoreceptor's synapse.

After phototransduction, the recovery phase starts. In this phase, recovery of the pre-photoactivation situation occurs: (1) phosphorylation of metarhodopsin II by rhodopsin kinase and subsequent binding of arrestin, which stops the activation of transducin,[77,78] (2) dissociation of all-*trans*-retinal from the visual pigment, which is recycled to 11-*cis*-retinal via the visual (retinoid) cycle (see below), (3) inactivation of transducin by GTPase accelerating protein and thereby silencing the phosphodiesterase,[79,80] and (4) restoration of the intracellular cGMP levels by guanylate cyclase.[81] After all-*trans*-retinal has dissociated from the opsin, arrestin dissociates and the phosphates are removed. Regeneration of rhodopsin occurs when regenerated 11-*cis*-retinal binds to opsin.

The visual cycle

The vitamin A derivate 11-*cis*-retinal is crucial for the phototransduction cascade. Dietary vitamin A (all-*trans*-retinol) is absorbed from the blood and converted to 11-*cis*-retinal in the RPE. The visual cycle is a complex process that is focused on the regeneration of 11-*cis*-retinal from all-*trans*-retinal that is produced in the phototransduction cascade (Figure 1.7), and takes place simultaneously with the phototransduction process.
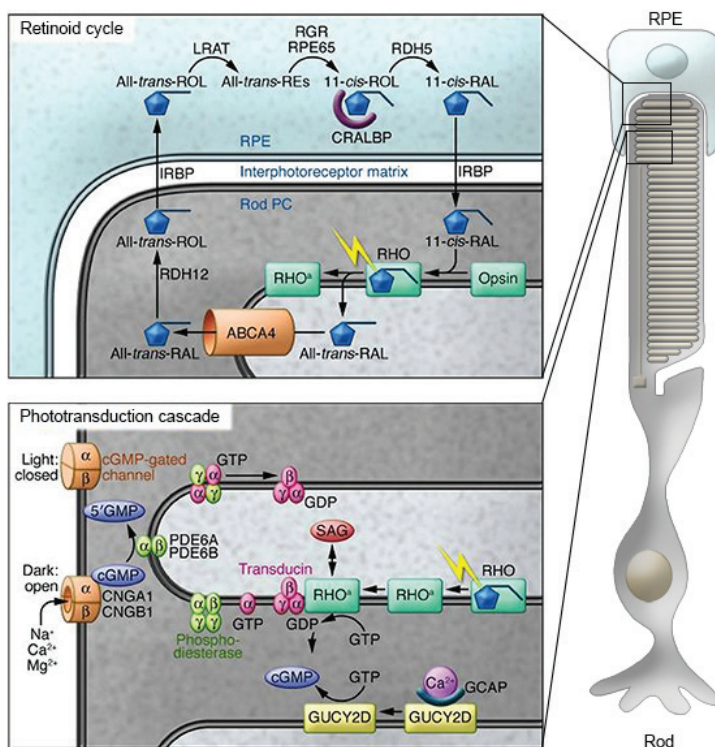
Figure 1.7. Schematic representation of the visual (retinoid) cycle (upper panel) and the phototransduction cascade (lower panel). Upper panel: The retinoid cycle regenerates 11-cis-retinal from all-trans-retinal. The process takes place in the outer segment discs, photoreceptor cytoplasma, interphotoreceptor matrix and cytoplasma of the RPE. Lower panel: The phototransduction cascade results in hyperpolarization of the photoreceptor's plasma membrane after activation of rhodopsin by a photon in the outer segment discs. ABCA4, ATP-binding cassette transporter type 4 (the gene underlying the ATP-binding cassette transporter ABCR); cGMP, cyclic guanosine monophosphate; CNGA1, cyclic nucleotide gated channel alpha 1; CNGB1, cyclic nucleotide gated channel beta 1; CRALBP, cellular retinaldehyde binding protein; GUCY2D, guanylate cyclase 2D; GCAP, guanylate cyclase activating protein 1A (official gene symbol: GUCA1A); GDP, Guanosine-5'-diphosphate; GTP, Guanosine-5'-triphosphate; IRBP, interphotoreceptor matrix retinal binding protein; LRAT, lecithin:retinol transferase; PDE6A, phosphodiesterase 6A; PDE6B, phosphodiesterase 6B; RAL, retinal; RDH5, 11-cis-retinol dehydrogenase; RE, retinyl esters; RGR, RPE-retinal G protein-coupled receptor; RHO, rhodopsin; RHO[a], photoactivated rhodopsin; ROL, retinol; RPE65, RPE specific protein 65 kDa; SAG, S-antigen (or Arrestin). (Adapted from: den Hollander AI et al, 2010.[92])

After photoactivation, all-*trans*-retinal is released from the activated visual pigment into the lumen of the outer segment discs. Here, it reacts with phosphatidylethanolamine and forms N-retinylidene-phosphatidylethanolamine (N-retinylidene-PE).[82] Through the flippase activity of the ABCR (ATP-binding cassette) transporter, the all-*trans*-retinal is released into the cytosol of the photoreceptor, where all-*trans*-retinal dehydrogenase (RDH) reduces all-*trans*-retinal to all-*trans*-retinol.[83,84] Subsequently, all-*trans*-retinol is transported into the interphotoreceptor space where it binds the interphotoreceptor matrix retinal binding protein (IRBP) that transports it into the RPE.[85] Once in the RPE's cytoplasm, all-*trans*-retinol

binds to cellular retinol binding protein (CRBP), after which all-*trans*-retinol is re-isomerized by a cascade involving lecithin:retinol acetyltransferase (LRAT), RPE specific protein 65 kDa (RPE65) and 11-*cis*-retinol dehydrogenase (RDH5).[86-90] The resulting 11-*cis*-retinal is transported into the interphotoreceptor matrix by cellular retinaldehyde binding protein (CRALBP) and subsequently transported back into the photoreceptor's cytosol by IRBP. Once in the photoreceptor, 11-*cis*-retinal binds opsin to form a new unexcited rhodopsin molecule. This pathway accounts for the re-isomerization of retinal in rods. Cones have a secondary visual cycle located in cone outer segments and Müller cells, which enables regeneration of 11-*cis*-retinal at a 20-fold faster rate.[91]

Clinical and functional assessment

Inherited retinal dystrophies (IRDs) display a wide spectrum of phenotypes. A diagnosis can often be made with a thorough history and ophthalmologic examination, including the age at onset, the severity and type of complaints, family history, retinal appearance and the progression over time. However, further clinical assessment may be necessary in the differential diagnostic track, evaluation of progression, and, in academic settings, for discovery of the molecular defect underlying the disorder. Additional functional evaluation of the retina includes visual acuity and visual field measurements, electrophysiological examinations, color vision tests and retinal imaging techniques, such as fundus autofluorescence (FAF) imaging, optical coherence tomography (OCT) and fluorescence angiography (FA). Nevertheless, identification of the correct diagnosis in patients with IRDs is often difficult due to the significant clinical overlap, and molecular genetic analyses are necessary.

Clinical ophthalmic examination

Visual acuity

Psychophysical testing measures the behavioral response to a stimulus, and includes visual acuity (VA) assessment, visual field measurements and color vision tests. VA is a measure for the keenness of sight, and was already performed by Egyptians 5000 years ago.[93] In the past few centuries, visual acuity has been well studied. Nowadays, we assess VA under standardized conditions with letters, numbers or figures of known visual angle at standard distances under standard illumination. The outcome is the quotient d/D, in which 'd' represents the distance at which the letter was read by the patient, and 'D' represents the distance from which a 'normal sighted' eye would be able to read that specific letter. Many different tests and notations are used, although the results often are interchangeable. In case other types of testing are required, e.g. in preverbal children, numerous age-adapted tests are available. In newborns, VA is not measurable, although fixation or fixing and following behavior can indicate the presence of vision.

Ophthalmoscopy

The easiest technique to visualize the posterior segment of the eye is direct ophthalmoscopy. The ophthalmoscope provides a monocular image of the retina at a high magnification (15x). More often used by ophthalmologists is indirect ophthalmoscopy, which includes the use of an additional lens between the observer and the patient. This provides a stereoptic view on

the retina with lower magnification (2-3x when 20, 28 or 30 diopter noncontact lenses are used). Indirect ophthalmoscopy using the slit-lamp microscope is preferred to evaluate the retina in more detail since the slit-lamp provides an additional magnification. For longitudinal follow-up of retinal abnormalities, color fundus photographs can be taken on regular intervals.

Perimetry

The assessment of the visual field, or perimetry, can be performed in a kinetic or static manner. The kinetic perimetry uses moving test light of standardized size and intensity. The lights are being moved within a ganzfeld dome to map the outer border of the area in which the spot of that specific size and intensity is seen by the patient (Figure 1.8A). Static perimetry uses test lights that have a fixed location in the visual field. During the test, lights appear and increase in strength. As soon as the patient observes the light, the sensitivity of that specific location in the visual field is known (Figure 1.8B). A proper fixation to a central spot is crucial in order to get reliable measurements.
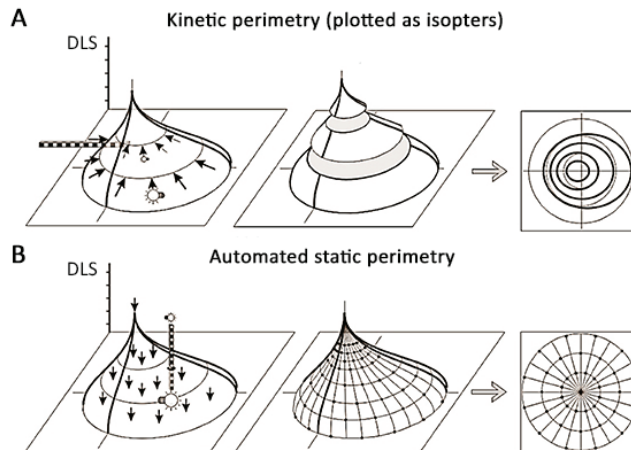
Figure 1.8. Schematic illustration of the kinetic and static approach to perform a perimetry. A, In a kinetic perimetry, the outer borders of stardardized sensitivities (called isopters) are determined. B, In static perimetry, the sensitivity of specific locations in the visual field are determined. DLS, differencial luminance sensitivity. (Source: Schiefer, Wilhelm, Hart (eds.). Clinical neuro-ophthalmology – A practical guide, Springer, Berlin/Heidelberg/New York, 2007.[94])

Color vision

Color vision tests have been used for many years to demonstrate abnormalities in retinal disorders with specific cone photoreceptor involvement. In the evaluation of IRDs, protanomaly, deutanomaly and tritanomaly correspond to abnormalities of the L ('red'), M ('green') and S ('blue') cones, respectively. Protanomaly and deutanomaly are more prominent in diseases involving the foveal cones, like for example achromatopsia and cone dystrophy, whereas tritanomalies are usually more prominent in generalized photoreceptor dystrophies. However, interpretation of the many different color vision tests that are available nowadays is difficult since color vision is not yet fully understood.

Dark adaptation

The dark adaptation test is performed to measure the thresholds of cone and rod sensitivity after exposure to light. The sensitivity to light recovers faster in cones than in rods. However, the absolute level of sensitivity to light is much higher in rod photoreceptors. During dark adaptation testing, the patient is initially exposed to light of standardized intensity. Subsequently, the light is turned off, and each one to two minutes a light of increasing intensity tests the patient's light sensitivity. The sensitivity measurements are plotted against time. In clinical practice, this examination can be used to objectify night blindness, especially in patients with scotopic full-field ERG responses within the normal limits, or minimal to no peripheral pathology on perimetry.

Electrophysiology

Electrophysiology provides objective data on retinal function. Most commonly used examinations include the full-field electroretinography (ERG) and multifocal ERG (mfERG). The ERG measures the mass response of the action potential produced by the photoreceptors in the retina after light flash stimulation. The examination is divided in a scotopic (dark-adapted) phase, and a photopic (light-adapted) phase. The scotopic responses are measured after a period of dark adaptation sufficient to reach maximal rod sensitivity to light. The photopic responses are measured after several minutes of light adaption to bleach out rod photoreceptors, which enables isolated measurement of cone photoreceptors.

During the scotopic phase isolated rod responses are measured with a light stimulus below the sensitivity threshold of cones. In addition, two more dark-adapted measurements are performed: the maximal (mixed) response, which includes the combined responses of rod and cones, and the oscillatory responses, which originates from photoreceptors, bipolar, amacrine and ganglion cells.[95-99] In the light-adapted phase, two measurements of the cone photoreceptors are performed, including isolated cone response and the 30Hz flicker response. Normal graphs of these five basic measurements are provided in Figure 1.9.

The mfERG provides a topographic measurement of retinal electrophysiological activity. Local ERG responses are calculated after pseudorandom stimulation of 61 or 103 hexagonal areas under light-adapted conditions. Local electrical responses are visualized in a graph pattern, and amplitudes can be plotted in a 3D map. In this manner, localized retinal damage that often is not visible in the panretinal responses of the full-field ERG can be objectified and quantified.

The electro-oculogram (EOG) measures the difference in electrical potential between the front and back of the eye (corneo-fundal potential). This potential is mainly derived from the RPE, and changes in response to retinal illumination. Like in full-field ERG testing, an EOG is tested in both a scotopic and photopic setting. The amplitude of the corneo-fundal potential is expressed as a ratio of the maximum (peak) amplitude in the photopic phase and the minimal (trough) amplitude during the scotopic phase, and is referred to as the light/dark ratio, or Arden ratio. To enhance comparison of electrophysiological examinations of studies, standard conditions have been published by the International Society for Clinical Electrophysiology of Vision (ISCEV).[100-102]

Retinal imaging

Confocal scanning laser ophthalmoscopy

In confocal scanning laser ophthalmoscopy (cSLO), a diode laser beam scans the retina rapidly in a raster fashion. A confocal photodiode that is conjugated to the retinal plane detects the backscattered light. The confocal filter provides a high resolution, since only light reflected from the narrow spot illuminated by the laser is recorded, and the out-of-focus light is suppressed. Different laser wavelengths provide evaluation of different tissues of the retina. For example, 488 nm wavelength cSLO is used for (blue-light) fundus autofluorescence imaging and fluorescein angiography, whereas 700-1400 nm wavelengths are used for infrared reflectance imaging. This technique provides *en face* imaging of the retina at a high magnification.
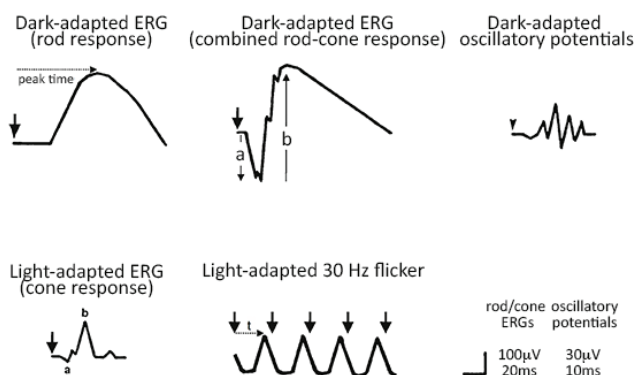
Figure 1.9. Diagram of the five basic ERG responses defined by the Standard. These waveforms are exemplary only, and are not intended to indicate minimum, maximum or even average values. Large arrowheads indicate the stimulus flash. Dotted arrows exemplify how to measure time-to-peak (t, implicit time), a-wave amplitude and b-wave amplitude. (Source: Marmor MF et al, 2008.[100])

Optical coherence tomography

Optical coherence tomography (OCT) is a noninvasive, noncontact imaging modality that provides a cross-sectional image of the retina, comparable to a histological section, with axial resolution that can be as high as 3 μm when Spectral-domain (SD) technology is used.[103] The image is based on the backscattered light from the different layers of the retina, comparable to ultrasound and radar imaging. Spectral-domain OCT provides A-scans (one-dimensional depth scans) of 2,048 pixels with a scan velocity of 18,000-55,000 A-scans per second.[103] This results in a two-dimensional image of the retina. Multiple OCT scans that are topographically orientated on cSLO *en face* infra-red images, allow three-dimensional reconstruction of the retina. SD-OCT imaging can be used to highlight subtle abnormalities in retinal structure.[104] On SD-OCT images 11 retinal layers can be recognized, in addition to the vitreous, Bruch membrane, choroid and the sclera (Figure 1.10).
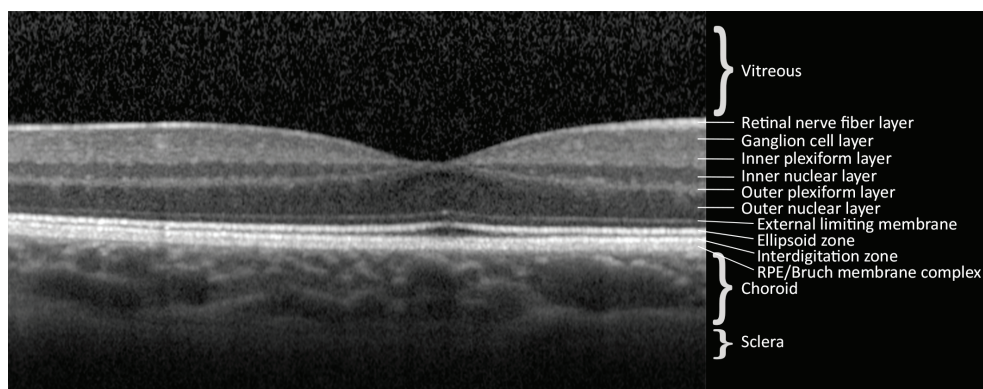
Figure 1.10. Optical coherence tomogram showing a cross-sectional scan of the normal retina and choroid at the level of the foveal depression.

Fundus autofluorescence imaging

Fundus autofluorescence (FAF) enables evaluation of the RPE function, and can be acquired in a rapid, noncontact, noninvasive manner. This technique uses the intrinsic autofluorescence that is emitted by a substance after being stimulated by excitation energy. Ocular tissues that autofluorescence include corneal epithelium and endothelium, lens tissue, macular and RPE pigments. In clinical practice, the autofluorescent characteristics of RPE pigments are most commonly used. FAF images can be acquired with a cSLO with a blue laser (488 nm) for excitation. Since the autofluorescence signal is much lower compared to fluorescein angiography and IR fundus reflectance, series of single FAF images are recorded that are subsequently averaged and normalized into a mean image.[43]

The autofluorescent compound in the RPE cells is lipofuscin.[105-107] When RPE cells phagocytize photoreceptor outer segments, and subsequently process the content of these outer segments, lipofuscin is formed as a by-product. N-retinylidene-N-retinylethanolamine (A2E) is the primary fluorophore of lipofuscin. High levels of lipofuscin, appear hyperautofluorescent on FAF images as observed in increased outer segment phagocytosis in photoreceptor degeneration, whereas a decrease in lipofuscin levels appear as hypoautofluorescence. Absence of autofluorescence can either be caused by the lack of lipofuscin, for example in case of RPE atrophy, or by blockage of the autofluorescence signal, as is observed at the blood vessels (Figure 1.11) and in case of preretinal hemorrhage.[106]

Fluorescein angiography

Fluorescein angiography (FA) allows examination of the retinal and choroidal circulation after intravenous injection or oral intake of sodium fluorescein, a molecule that fluoresces with green light (520-530 nm) when excited with blue light (465-490 nm). When the reflected blue and emitted green light exit the eye, the blue light is filtered out by a yellow-green barrier filter. This results in black and white images, where white represents high fluorescence, and black represents no fluorescence. Fluorescein normally does not pass the endothelium of the retinal vessels (the inner blood-retina barrier) or the RPE into the subretinal space

(outer blood-retinal barrier). In the choroid, due to the fenestrated vessels that leak the dye, fluorescein is diffusely present in the extravascular matrix, which causes diffuse background fluorescence on FA images.
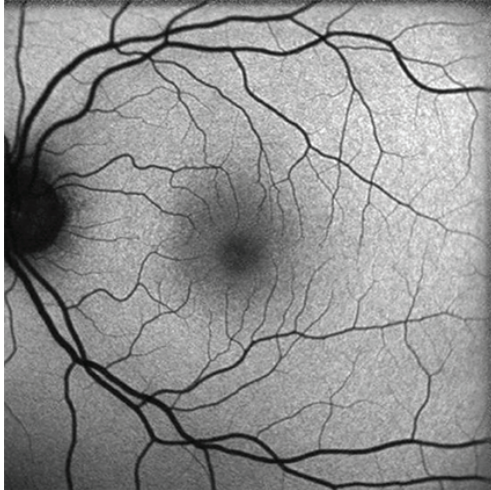
Figure 1.11. Fundus autofluorescence of a normal central retina. The retinal blood vessels appear black due to blockage of the autofluorescent signal. The fovea is darker because of the presence of macular pigment.

When pathology is present, leakage appears as local hyperfluorescence, just as local defects in the RPE layer that permit a direct view on the fluorescein present in the choroid (also known as 'window defect'). Hypofluorescence appears in vascular filling defects and blockage of fluorescence. In Stargardt disease, substantial blockage of the background fluorescence is caused by the accumulation of lipofuscin in the RPE cells, which causes the characteristic 'dark choroid' sign.

Clinical classification of selected inherited retinal dystrophies

It is challenging to provide a straightforward classification that compromises all inherited retinal dystrophies, since this group includes a wide spectrum of clinical phenotypes that show overlapping characteristics. However, retinal dystrophies can be stratified in stationary diseases, such as congenital stationary night blindness and achromatopsia, and progressive dystrophies. The latter is generally subdivided in peripheral (generalized) dystrophies that have early peripheral involvement, such as retinitis pigmentosa and choroideremia, and central degenerations. The central degenerations can be divided in those that affect the posterior pole, the macular dystrophies, and those that initiate in the macula and eventually affect the peripheral retina as well, e.g. cone dystrophy and cone-rod dystrophy. However, many macular dystrophies can be considered pan retinal disorders based on the molecular pathology, which makes this classification confusing.

This section provides the overall clinical features of the progressive dystrophies that are subject of this thesis: retinitis pigmentosa, cone-rod dystrophy, Stargardt disease, and dominant cystoid macular dystrophy.

Retinitis pigmentosa

Retinitis pigmentosa (RP) is a group of progressive retinal dystrophies in which the rod photoreceptors are more or equally affected than the cone photoreceptors (rod-cone dystrophies). RP is the most common retinal dystrophy with an incidence of approximately 1 in 4000,[25,108-110] and shows impressive variation in age of onset, progression rate, retinal appearance and visual function.

Despite this high variability, RP does have a set of characteristics that are generally preserved throughout all the RP phenotypes. These 'classic' RP symptoms include night blindness (nyctalopia) in the early phase of the disease, which is followed by relative defects in the midperipheral visual field. When the disease progresses, the peripheral visual field defects become more prominent and lead to tunnel vision, whereas central vision is often spared until end-stage disease.[25,111] The classic ophthalmoscopic features include intraretinal pigment deposits in a bone-spicule configuration that are mainly visible in the midperiphery, a waxy pale optic disc, and attenuated arterioles.[25,108,110] The bone-spicule pigmentation arises from RPE that migrates into the neuroretina in response to photoreceptor cell death,[112] whereas loss of ganglion cell axons after death of the parent cells causes the atrophic appearance of the optic disc.[113] The attenuation of the retinal vasculature is thought to arise from a decrease in metabolic demands.[113,114] In end-stage disease profound chorioretinal atrophy can be present in the (mid)periphery and sometimes the posterior pole as well. The ERG typically shows affected rod function that exceeds or is equal to cone dysfunction. However, the phenotype of RP is highly variable, and many forms of RP dissociate from the typical phenotype, as is highlighted in **chapters 2 and 3** of this thesis.

The vast majority of RP is restricted to the retina. However, 20-30% of RP forms also include symptoms in other tissue than the retina, which results in syndromic disease.[25] The most prevalent forms of syndromic RP include Usher syndrome (RP with variable degrees of neurosensory hearing loss) and Bardet-Biedl syndrome (RP with obesity, polydactyly, hypogonadism, renal failure, and cognitive impairment).[115,116] However, to what extend the various tissues are affected is highly variable, and can depend on the type of genetic defect. Indeed, some patients with mutations in the Bardet-Biedl genes only have retinal disease.[117]

Up to date, 84 genes are associated with nonsyndromic RP phenotype that cause disease in autosomal recessive, autosomal dominant and X-linked inheritance patterns when mutated (RetNet, available at https://sph.uth.edu/retnet/), and are involved in many different pathways (Appendix 1 and Table 1.1). In general, patients with X-linked RP exhibit more severe disease compared to autosomal recessive and dominant disease. Autosomal recessive inheritance is thought to account for 50-60% of RP patients, whereas the autosomal dominant and X-linked patterns are described in 30-40% and 5-15%, respectively. However, these proportions assume that all isolated cases are autosomal recessive, which is not the case since 15% of the isolated RP patients have mutations in X-linked RP genes *RPGR* and *RP2*.[118] Furthermore, these two genes also carry mutations in 8.5% of families that were initially thought to have autosomal dominant inheritance.[119] In only a few cases, mitochondrial and digenic inheritance are found.[120-122]

Table 1.1. Overview of the functional characteristics of the genes known up to date to cause non-syndromic retinitis pigmentosa.

Gene symbol	Protein	Function	Inheritance	Ref
Ciliary structure and transport				
ARL2BP	ADP-ribosylation factor-like 2 binding protein	May play a role in trafficking of ciliary proteins and factors	Recessive	[123]
BBS1*	BBS1 protein	Participates in the formation of a stable protein complex (the BBSome) involved in vesicular trafficking to the ciliary membrane	Recessive	[117,124]
C2orf71	Chromosome 2 open reading frame 71	The protein localizes to primary cilia, exact function unknown	Recessive	[125,126]
C8orf37	Chromosome 8 open reading frame 37	The protein localizes to the base of cilia in retinal photoreceptors and RPE cells; exact function unclear	Recessive	[127,128]
KIZ	Kizuna centrosomal protein	Stabilizes the ciliary centrosomes	Recessive	[129]
MAK	Male germ-cell associated kinase	Involved in regulation of retinal cilium and spermatogenesis	Recessive	[130-132]
RP1	Microtubule-associated protein	Ciliary microtubule formation and stabilisation	Recessive / Dominant	[133-135]
RP2	Plasma membrane associated protein	Photoreceptor ciliary transport, as well as in the interaction between plasma membrane and cytoskeleton	X-linked	[136]
RPGR	Retinitis pigmentosa GTPase regulator	Trafficking of proteins in the connecting cilium	X-linked	[137,138]
TOPORS	Topoisomerase I binding arginine/ serine rich protein	May play a key role in regulating primary cilia-dependent photoreceptor development and function	Dominant	[139,140]
TTC8	Tetratricopeptide repeat domain 8	Localizes to the connecting cilium in photoreceptors; interacts with PCM1, a protein involved in ciliogenesis	Recessive	[141,142]
TULP1	Tubby-like protein 1	Possibly involved in transport of rhodopsin from inner to outer segment	Recessive	[143-145]
Retinal development				
CRX*	Cone-rod otx-like photoreceptor homeobox transcription factor	Activator of retinal genes	Dominant	[146,147]
FAM161A	Family with sequence similarity 161 member A	Expressed in photoreceptors, involved in development of retinal progenitors during embryogenesis	Recessive	[148,149]
NEK2	NIMA (never in mitosis gene A)-related kinase 2	Plays an important role in regulation of cell cycle progression through localization to the centrosomes and interaction with microtubules	Recessive	[150]
NR2E3	Nuclear receptor subfamily 2	Ligand-dependent transcription factor	Recessive / Dominant	[151-153]

Gene symbol	Protein	Function	Inheritance	Ref
NRL	Neural retina lucine zipper	Retinal transcription factor which interacts with CRX, promotes transcription of rhodopsin and other retinal genes, and is required for rod photoreceptor development	Recessive / Dominant	[154,155]
SEMA4A	Semaphorin 4A (semaphorin B)	Involved in neuronal development and/ or immune response; enhances T-cell activation	Dominant	[156,157]
SLC7A14	Solute carrier family 7 member 14	Potential cationic transporter protein with an unknown ligand	Recessive	[158]
ZNF513	Zinc finger protein 513	Possible transcriptional regulator involved in retinal development	Recessive	[159]
Retinal homeostasis				
CA4	Carbonic anhydrase IV	pH regulation of retina and choriocapillaris	Dominant	[160]
CERKL	Ceramide kinase-like	Involved in neuronal cell survival and apopotosis in retinal ganglion cells	Recessive	[161]
KLHL7	Kelch-like 7 protein	Plays a role in the ubiquitin-proteasome pathway leading to protein degradation	Dominant	[162]
MERTK	Mer tyrosine kinase proto-oncogene	RPE receptor involved in outer segment phagocytosis	Recessive	[163]
MVK*	Mevalonate kinase	Peroxisomal enzyme; a key early enzyme in isoprenoid and sterol synthesis	Recessive	[164]
USH2A	Usherin	Basement membrane protein; may be important in development and homeostasis of the inner ear and retina	Recessive	[165-168]
RNA splicing				
DHX38*	DEAH (Asp-Glu-Ala-His) box polypeptide 38	Putative RNA helicase involved in pre-RNA splicing	Recessive	[169]
PRPF3	Precursor-mRNA processing factor 3	Member of the U4/U6-U5 tri-snRNP particle complex (spliceosome)	Dominant	[170,171]
PRPF31	Precursor-mRNA processing factor 31	Member of the U4/U6-U5 tri-snRNP particle complex (spliceosome)	Dominant	[172]
PRPF4	Precursor-mRNA processing factor 4	Member of the U4/U6-U5 tri-snRNP particle complex (spliceosome)	Dominant	[173]
PRPF6	Precursor-mRNA processing factor 6	Member of the U4/U6-U5 tri-snRNP particle complex (spliceosome)	Dominant	[174]
PRPF8	Precursor-mRNA processing factor 8	Member of the U4/U6-U5 tri-snRNP particle complex (spliceosome)	Dominant	[175]
RP9	PIM1-kinase associated protein 1	Has a role in pre-mRNA splicing and interacts with a U2-complex splice factor	Dominant	[176]
SNRNP200	Small nuclear ribonucleoprotein 200kDa (U5)	Member of the U4/U6-U5 tri-snRNP particle complex (spliceosome)	Dominant	[177,178]
Structure and cytoskeletal				
CRB1	Crumbs homologue 1	Transmembrane protein, adherent junctions	Recessive	[179]

Gene symbol	Protein	Function	Inheritance	Ref
EYS	Eyes shut/ spacemaker (Drosophila) homolog	Extracellular matrix protein; likely to have a role in the modeling of retinal architecture.	Recessive	[180]
FSCN2	Retinal fascin homolog 2	Photoreceptor-specific paralog of fascin which crosslinks and bundles f-actin; proposed to play a role in photoreceptor disk morphogenesis	Dominant	[181,182]
IMPG2	Interphotoreceptor matrix proteoglycan 2	Component of the retinal extracellular matrix; plays a role in the organization of the interphotoreceptor matrix and may promote the growth and maintenance of the light-sensitive photoreceptor outer segment	Recessive	[183]
PROM1	Prominin 1	5-transmembrane glycoprotein associated with plasma membrane evaginations in rod outer segments	Recessive	[184,185]
PRPH2	Peripherin-2	Outer disc segment membrane protein	Dominant / Digenic	[120,186,187]
ROM1*	Rod outer segment protein 1	Essential for disk morphogenesis; may also function as an adhesion molecule involved in stabilization and compaction of outer segment disks or in maintenance of rim curvature	Dominant / Digenic	[120,188]
Phototransduction				
CNGA1	Rod cGMP-gated cation channel α-subunit	α-subunit of the cGMP-gated cation channel that enables sodium, calcium and magnesium influx in photoreceptor cells	Recessive	[189]
CNGB1	Rod cGMP-gated cation channel β-subunit	β-subunit of the cGMP-gated cation channel that enables sodium, calcium and magnesium influx in photoreceptor cells	Recessive	[190-192]
DHDDS	Dehydrodolichyl diphosphate synthetase	Enzyme in the dolichol synthesis pathway and dolichol is involved in biosynthesis of N-linked oligosaccharide chains on proteins such as rhodopsin	Recessive	[193]
GUCA1B	Guanylate cyclase activating protein 1B	a calcium-binding protein that activates photoreceptor guanylate cyclases	Dominant	[194,195]
PDE6A	Rod cGMP-phosphodiesterase α-subunit	Rod cGMP-phosphodiesterase hydrolyses cGMP to 5'-GMP	Recessive	[196,197]
PDE6B	Rod cGMP-phosphodiesterase β-subunit	Rod cGMP-phosphodiesterase hydrolyses cGMP to 5'-GMP	Recessive	[196,197]
PDE6G	Rod cGMP-phosphodiesterase γ-subunit	Inhibitory subunit of cGMP phosphodiesterase	Recessive	[198]
RHO	Rhodopsin	G-protein coupled photon receptor; activation of transducin after photoactivation	Dominant	[199]
SAG	Arrestin	Arrestin binds to activated rhodopsin (metarhodopsin II) to stop the activation of transducin	Recessive	[77,199,200]

Gene symbol	Protein	Function	Inheritance	Ref
Retinoid metabolism				
ABCA4	ATP-binding cassette protein A4	Photoreceptor disc membrane flippase for all-trans-retinal	Recessive	[201-203]
LRAT*	Lecithin retinol acetyltransferase	Isomerization of all-trans-retinol to all-trans-retinylester	Recessive	[86,204]
RBP3	Retinol binding protein 3	Binds and transports retinoids in the interphotoreceptor matrix between the RPE and photoreceptors	Recessive	[205,206]
RDH11*	Retinol dehydrogenase 11	Oxidation 11-*cis*-retinol to 11-*cis*-retinal	Recessive	[207,208]
RDH12	Retinol dehydrogenase 12	Reduction of all-*trans*-retinal to all-*trans*-retinol	Dominant	[207,209]
RDH5*	11-*cis* retinol dehydrogenase 5	RPE microsomal enzyme involved in converting 11-*cis* retinol to 11-*cis* retinal	Recessive	[207,210,211]
RGR	RPE-vitamin A G-protein coupled receptor	Binds all-*trans* retinal which light converts to 11-*cis* retinal in the RPE	Recessive	[212]
RLBP1*	Retinaldehyde binding protein	11-cis-retinaldehyde carrier in visual cycle	Recessive	[90]
RPE65	Vitamin A trans-cis isomerase	Isomerization of all-trans-retinylester to 11-cis-retinol	Recessive	[204]
Other				
BEST1	Bestrophin 1	Transmembrane oligmeric chloride channel in the basolateral plasma membrane of the RPE	Recessive / Dominant	[213,214]
CLRN1	Clarin 1	4-transmembrane protein with a possible role in hair cell and photoreceptor synapses	Recessive	[215,216]
EMC1*	Endoplasmatic reticulum membrane protein complex subunit 1	Component of the endoplasmic reticulum; unknown function	Recessive	[217]
GPR125*	G protein-coupled receptor 125	Unknown function	Recessive	[217]
IDH3B	NAD(+)-specific isocitrate dehydrogenase 3 beta	Catalyzes conversion of isocitrate to α-ketogluterate in the citric acid cycle in mitochondria	Recessive	[218]
IMPDH1	Inosine-5' monophosphate dehydrogenase type I	Guanine nucleotide synthesis	Dominant	[219]
KIAA1549*	KIAA1549 protein	Unknown function	Recessive	[217]
PRCD	Progressive rod-cone degneration protein	Unknown function	Recessive	[220,221]
SPATA7*	Spermatogenesis associated protein 7	Localized in spermatocytes and multiple retinal layers; function unknown	Recessive	[222]

* Genes that have been described in non-syndromic RP, but that are not specified as a specific 'type' of RP. Therefore, these types are not included in Appendix 1.

Cone-rod dystrophy

In contrast to RP, patients with cone-rod dystrophy (CRD) reveal progressive photoreceptor degeneration in which cone dysfunction exceeds rod dysfunction. CRD occurs in approximately 1 in 30,000-40,000.[223-225] Symptoms generally initiate during childhood, and predominantly include decrease of visual acuity and central vision, photophobia and color vision abnormalities. Complaints of night blindness may develop later on in the disease.[225,226]

Retinal features may precede clinical symptoms, and include macular pigmentary changes that vary from mild granular pigment alterations to macular atrophy in a bull's eye-like pattern. In later stages of the disease macular intraretinal pigment deposits and attenuation of the arterioles can become apparent, as well as subtle bone spicule pigmentation in the periphery.[225] In this, the end-stage retinal abnormalities can mimic the retinal appearance of RP.

Perimetry examinations reveal central scotomas that enlarge with progression of the disease. Eventually concentric peripheral constriction may become apparent. ERG examination, crucial for the diagnosis of CRD, demonstrates a decrease of cone-driven responses that exceeds the decrease of rod-driven responses. Again, the difference between CRD and RP in end-stage disease can be difficult since ERG rod and cone responses may be non-recordable in both diseases. This highlights the importance of proper history taking in those cases that visit the ophthalmologist in the advanced disease stage.

Mutations in 26 genes have been associated with cone-rod dystrophies (RetNet, available at https://sph.uth.edu/retnet/), and include autosomal recessive, autosomal dominant and X-linked inheritance patterns, although CRD cases are often isolated.

Stargardt disease

Karl Stargardt described the first families with Stargardt disease (STGD1) in 1909.[5] STGD1 is the most common macular dystrophy with an incidence of 1 in approximately 10,000.[227] The disease typically presents within the first two decades of life,[5] but the disease may manifest in early childhood (< 5 years of age) to the elderly (60 years of age)) (see **chapters 8 and 9** of this thesis).[228] Patients with STGD1 usually note bilateral decrease in visual acuity that generally progresses to levels of 20/200. The fundoscopic features include irregular yellow-white fundus flecks, and macular atrophic lesions with a so-called 'beaten bronze' appearance or a bull's eye pattern.[229-231] In end-stage disease, intraretinal pigment depositions can be present. The ERG responses can be normal or reveal moderate to severe abnormalities of both cone- and rod-driven responses.[230] FA imaging reveals a darker appearance of the choroid ('dark choroid sign') that is thought to originate from the accumulation of lipofuscin in the RPE cells masking the background fluorescence from the choroid.[229,232,233]

STGD1 has been linked to mutations in the *ABCA4* gene, which encodes an adenosine triphosphate (ATP)-binding cassette transporter (ABCR) expressed specifically in the cones and rods of the retina.[201,234] Defects in ABCR function cause the accumulation of all-*trans*-retinal and its cytotoxic derivatives in photoreceptors and RPE cells, ultimately causing

RPE cell death and the subsequent loss of photoreceptors.[235] The inheritance follows the autosomal recessive pattern. Numerous mutations in *ABCA4* have been described, each with their own effect on the ABCR function. Based on this, Van Driel et al. and Maugeri et al. proposed a model that links phenotype severity to the degree of residual ABCR function.[236,237] Even within the STGD1 phenotype, a spectrum of disease severity has been observed, which also may relate to the residual ABCR function.

Dominant cystoid macular dystrophy
Dominant cystoid macular dystrophy (DCMD) is an autosomal dominant retinal dystrophy that has the hallmark feature of cystoid intraretinal fluid collections in the posterior pole, which appear before other retinal abnormalities become apparent.[238,239] The disease usually initiates in the first or second decade of life, and leads to progressive loss of central vision due to degeneration of the central retina. Patients with DCMD generally have moderate to high hyperopia.[240-242]

The disease is extremely rare. Up to now, only a limited number of patients have been described in literature, including one large Dutch family with a common ancestor that probably lived in the early 18th century,[240] one unrelated American family of Greek ancestry,[243] and one American and one Spanish patient.[244]

The causative gene has not been identified yet, but the disease has been linked to the locus (p15-p21) on chromosome 7.[245] Further details on the clinical phenotype and genetics of DCMD are provided in **chapter 10**.

Introduction in molecular genetics

Long before the discovery of deoxyribonucleic acid (DNA) and the modern dogmas of genetics, it was known that certain diseases, including retinal disease, run within families. Molecular genetics has been thriving over the last decades, and mutations in many different genes, more than 200 to date, have been associated with retinal disease. Thanks to our current understanding of molecular genetics and inheritance patterns, we are able to explain diseases up to the level of molecular pathways. The following section provides a basic overview of the structure and function of DNA, inheritance patterns, the different genetic assessment techniques and genetic context of retinal dystrophies.

DNA structure and function

The research of J. Watson, F. Crick, M. Wilkin and R. Franklin led to the discovery of the double helix structure of DNA.[246,247] The double helix is composed of two complementary strands build from 5-carbon sugar with attached phosphate groups that each carries a linear array of the purine bases guanine (G) and adenine (A), and of the pyrimidine bases cytosine (C) and thymine (T). A unit of a sugar with phosphate group and the base is called a nucleotide (Figure 1.12). A single DNA molecule (i.e. chromosome) can reach a length up to 250 million nucleotide pairs long.[248]
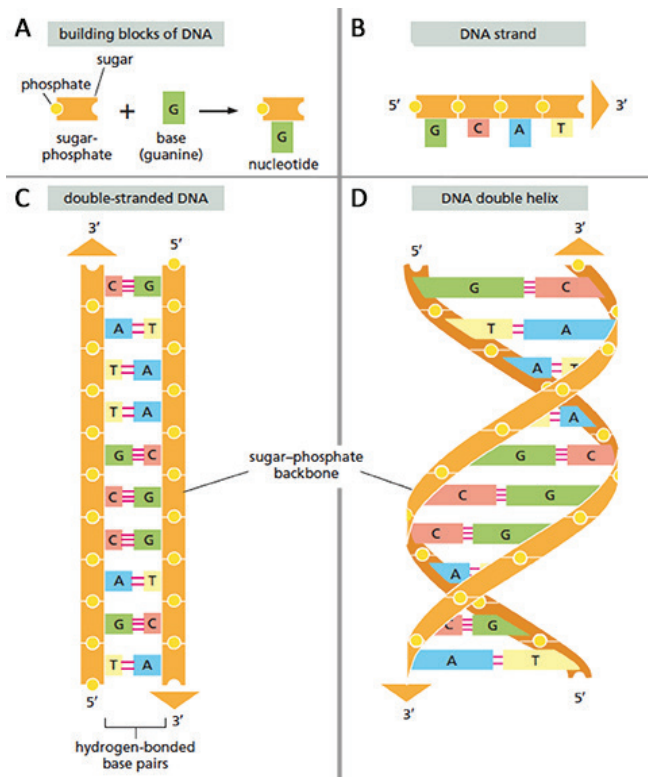
Figure 1.12. Schematic illustration of the molecular structure of DNA and its building blocks. A, The building blocks of DNA, called nucleotides, are composed of a sugarphosphate backbone and a base. B, The sugarphosphate backbone link to create a sequence of bases. C, Two strands of DNA with complementary bases are linked by hydrogen-bonds. This molecule has a double helix configuration as visualized in panel D. (Adapted from: Alberts et al. Essential Cell Biology, 4th edition, Garland Science, 2014.[249])

From DNA to protein

The genetic information is contained within the sequence of the nucleotides. Genes refer to the parts of the genetic code that are translated into proteins. The human genome contains approximately 25,000 genes, which together constitute 2% of the total DNA. The remaining 98% does not encode proteins, but does carry vital information for maintaining the structure of DNA, or for regulating gene expression.[250-254] Within each gene, the coding sequences, called the exons, are interrupted by sequences of noncoding DNA, the introns.

The process driving gene expression can roughly be divided in three steps: transcription, ribonucleic acid (RNA) splicing, and translation (Figure 1.13). *Transcription* is the process in which the DNA data is translated into RNA data. RNA is structurally similar to DNA, but is usually single-stranded, has a backbone made of ribose instead of deoxyribose, and contains the uracil pyrimidine base instead of thymine that is present in DNA.[255] During transcription, RNA polymerases create an RNA strand complementary to one of the DNA strands. In this process, the whole gene including both exons and introns is encoded into precursor messenger RNA (pre-mRNA).

Before the pre-mRNA molecule leaves the nucleus, a process of *RNA splicing* removes the intronic RNA from the molecule. The resulting RNA molecule only contains the information of
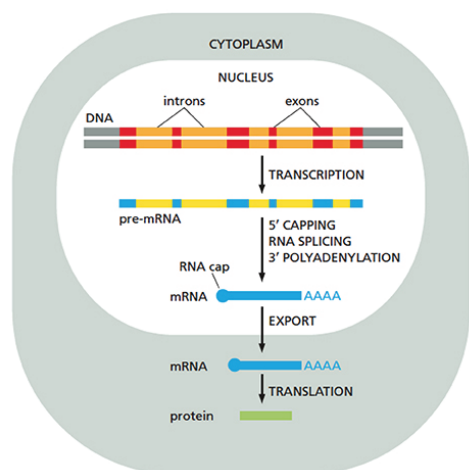
Figure 1.13. Schematic illustration of transcription, splicing and translation. The pre-mRNA contains data of the exons and introns of the transcripted gene. During the RNA splicing process, the intronic RNA is removed. Subsequently, the mRNA is exported to the cytoplasm, where the translation to a protein takes place. (Source: Alberts et al. Essential Cell Biology, 4th edition, Garland Science, 2014.[249])
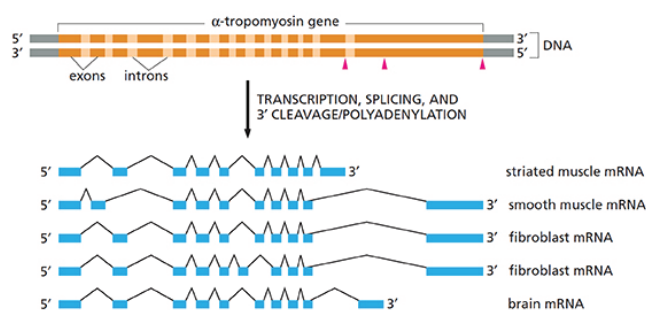
Figure 1.14. Schematized representation of alterative splicing of the α-tropomyosin gene. Each mRNA subtype leads to an isoform of the α-tropomyosin gene that are expressed in specific tissues. (Source: Alberts et al. Essential Cell Biology, 4th edition, Garland Science, 2014.[249])

the exons, and is referred to as messenger RNA (mRNA, Figure 1.13). The splicing process is not completely static: alternative splicing occurs in approximately 60% of genes.[248] In alternative splicing, specific exons are not included in the mRNA, and therefore lead to multiple different mRNA molecules from a single gene (Figure 1.14), which are translated into protein subtypes, called isoforms.

Isoforms can be either ubiquitously expressed, or tissue-specific. The process of alternative splicing provides the opportunity to further increase the already enormous coding potential of the human genome. To stabilize the molecule, promote export to the cytoplasm and mark the RNA molecule as a mRNA , the 5' end is capped with a guanine nucleotide bearing a methyl group, and the 3' end is elongated by a series of repeated adenine nucleotides that generally is a few hundred nucleotides long (poly-A-tail).[249]

The last step in the process from DNA to protein, *translation*, takes place in the cytoplasm, where ribosomes are located. The mRNA travels into the cytoplasm, where ribosomes bind to the molecule. These ribosomes enable transient binding of transport RNA (tRNA), which are special RNA molecules that carry amino acid, to the mRNA. The mRNA code is read in sequences of 3 nucleotides, called codons. When the ribosome encounters the start codon,

the tRNA molecules complementary to this codon binds. Subsequently, the ribosome reads the next codon and the complementary tRNA binds to this codon, after which the amino acid of the first tRNA is attached to the amino acid of the second tRNA (Figure 1.15). This process, creating a strain of amino acids, continues until a stop codon is encountered in the mRNA sequence. The stretch of amino acids subsequently is folded and finalized, which results in the newly produced protein.

Genetic defects

The genetic code directly determines the sequence of amino acids of a protein (see section above). Although the body has extremely efficient DNA repair mechanisms, changes in the genetic code occur. If changes in the genetic code are located in exons they may change the amino acid sequence, and with that the protein. Intronic changes are thought to be less pathogenic, although they may have effects on splicing and regulatory processes.

There are a wide variety of changes that can occur in the genetic code. Based on the frequency of the genetic change, the difference is made between polymorphisms (frequency >1% in the general population) and mutations (<1% in the general population). In monogenetic diseases, like the majority of IRDs, mutations are the underlying molecular cause leading to disease, although polymorphisms can be of influence on the clinical phenotype, e.g. modifier effects.

Mutations can either involve a single nucleotide (*point mutation*) or multiple nucleotides, which may extend up to large stretches of nucleotides or even whole exons. In this thesis, the mutations are often named after their effect on the protein instead of the specific genetic change. Examples are *silent mutations* (or *synonymous mutations*) that do not alter the amino acid sequence, *missense mutations* that cause a change of the amino acid, and *nonsense mutations* that result in a stop codon and cause a premature termination of the protein (Figure 1.16). *Insertions* and *deletions* (also abbreviated as 'indels') of one or multiple nucleotides result in a *frame shift* if the number of inserted or deleted nucleotides is not dividable by 3. This often results in a different stretch of amino acids and often a premature stop (Figure 1.16). *Splice site mutations* alter the sequence of the DNA in the exon-intron boundary area, affecting the location where the spliceosome adheres to initiate splicing. This often results in aberrant splicing.

The pathogenicity of a mutation is determined by its effect on the protein function. Nonsense mutations are generally considered to be pathogenic, since they cause a premature truncation of the protein, functional areas of the protein are often lost. Splice site mutations are also considered pathogenic, since altered splicing also often disrupts the correct composition of the mRNA molecule, and thus leads to the formation of no or a non-functional protein. Indels are considered pathogenic if a frame shift or a premature truncation of the protein occurs. Missense mutations, on the other hand, have a less clear-cut pathogenicity profile. Several factors are involved in the effects that missense mutations have on protein function, such as the differences in physical properties of the exchanged amino acids (Figure 1.16), the location of the amino acid change (whether it is located in a functional domain of the protein or not), and if the affected residue is conserved during evolution. For most of these factors computerized, or so-called *in silico*, prediction algorithms are available, e.g. the Polyphen-2 score, the Grantham score, SIFT and the PhyloP score.[256-259]
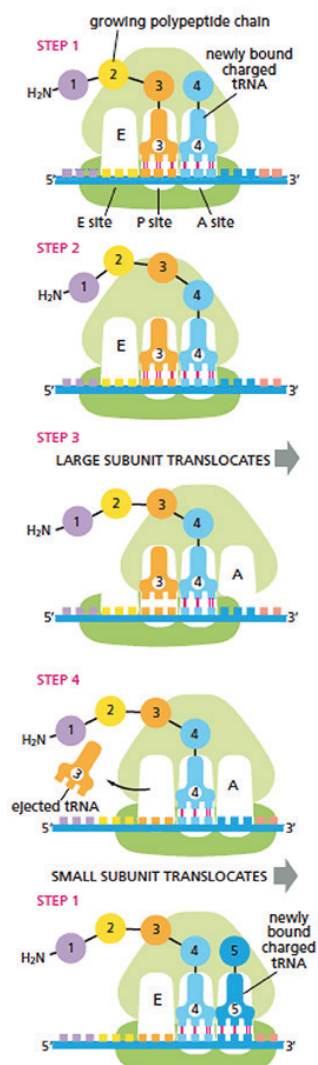
Figure 1.15. Schematic illustration of the translation process. The small and large ribosomal subunits bind to the mRNA, followed by the binding of tRNA molecules that carry an amino acid to the vacant A-site of the ribosome. The close relationship of the A and P sites only allow bondage of base pairs with codons that are contiguous, with no stray bases in between, which ensures preservation of the correct reading frame throughout the synthesis of the protein. Subsequently, the polypeptide chain (amino acid #3) is uncoupled from the tRNA at the P site and joined to the amino acid linked to the tRNA at the A site. Next, the ribosomal subunits translocate one codon, which ejects the tRNA at the E-site. This process is continued until a stop codon is encountered. (Source: Alberts et al. Essential Cell Biology, 4th edition, Garland Science, 2014.[249])

Inheritance patterns

The vast majority of the IRDs follow one of the Mendelian inheritance patterns. The *autosomal recessive* inheritance pattern is most common among IRDs. In this pattern both alleles, which are the maternal and paternal copies of the same gene, are affected. Mutations can be homozygous (both alleles carry the same mutation) or compound heterozygous (both alleles are affected but by different mutations). In the *autosomal dominant* inheritance pattern, a mutation on one of both alleles is sufficient to cause disease. Autosomal dominant diseases generally manifest in each generation of a pedigree, since the chance of passing on the mutated allele is 50%. In *X-linked* diseases, the mutation is located on the X-chromosome. These diseases generally behave like recessive disease: if one normal allele is present, no disease occurs. X-linked inherited diseases therefore generally only affect males, since males only carry one X-chromosome whereas females carry two. Female carriers usually have no complaints, although they may show subtle retinal changes. However, semi-dominant X-linked *RPGR*-associated RP cases have been described, in which female carriers were equally affected as the male patients.[260]

Other inheritance patterns that have been observed in IRDs are mitochondrial and digenic inheritance.[120-122]

Genetic heterogeneity

In the past few decades, many genetic causes of IRDs have been uncovered. In that time, the exceptional heterogeneity of the genetic background of IRDs became clear. Nowadays, over 200 genes have been known to carry mutations that lead to an IRD phenotype, where multiple genes can be involved in a single clinical subtype of IRD, for example 68 genes involved in non-syndromic RP. On the other hand, a single gene can cause different phenotypes depending of the mutation in that gene, for example *PRPH2* that can cause
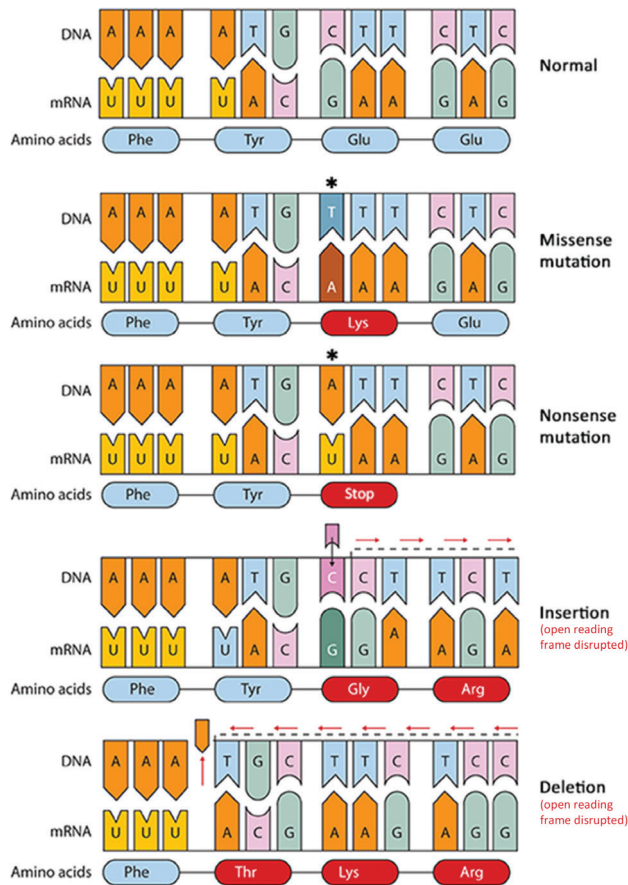
Figure 1.16. Illustration of the effects of missense and nonsense mutations, as well as insertions and deletions that often cause a shift of the reading frame. Arg, arginine; Glu, glutamic acid; Gly, glycine; Lys, lysine; Phe, phenylalanine; Thr, threonine; Tyr, tyrosine. The asterisk marks the mutated nucleotide.

autosomal dominant RP, as well as macular dystrophies such as central areolar choroidal dystrophy and various pattern dystrophies (Figure 1.17) (RetNet, available at https://sph.uth.edu/retnet/). In addition to the enormous number of genes involved in IRDs, the mutational variation is enormous. Only few more recurrently observed (founder) mutations are known. This extreme genetic heterogeneity complicates molecular genetic analyses in IRDs.

Genetic assessment techniques

Since the dawn of modern genetics, many techniques for genetic analysis have been developed. The most basic type of genetic analysis is Sanger sequencing, developed by two time Nobel price winner Frederik Sanger in 1977.[262] Sanger sequencing determines the sequence of nucleotides based on selective incorporation of chain-terminating
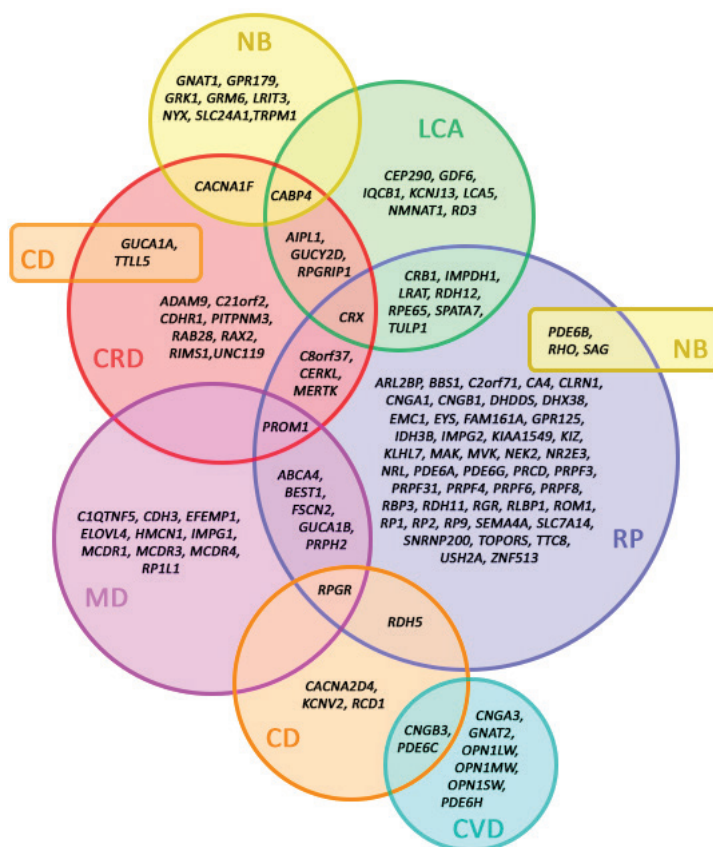
Figure 1.17. Clinical symptoms of non-syndromic monogenic retinal diseases and their causative genes. Clinical diagnoses are indicated by colored circles. Gene symbols in the overlapping areas show that mutations in the same gene can lead to different phenotypes. CD, cone dystrophy; CRD, cone-rod dystrophy; CVD, color vision defects; LCA, Leber congenital amaurosis; MD, macular dystrophy; NB, night blindness; RP, retinitis pigmentosa. (Adapted from Berger W, Kloeckener-Gruissem B, Neidhardt J. The molecular basis of human retinal and vitreoretinal diseases. Prog Retin Eye Res. 2010 Sep;29(5):335-75.[261])

dideoxynucleotides by DNA polymerase during in vitro DNA replication,[262,263] and is regarded as the golden standard in DNA sequencing. This method has been the main technique for DNA sequencing for over 25 years. In the past few years, however next-generation sequencing (NGS) techniques have supplanted Sanger sequencing, although the latter is still used to confirm mutations discovered with NGS technology.

Many different techniques are currently available for genetic analysis, each with its own advantages and disadvantages. Sanger sequencing is the most precise method available. However, it is costly, labor-intensive and time-consuming when used in sequencing of large numbers of genes. To analyze mutations in multiple genes in a cost-effective manner, the
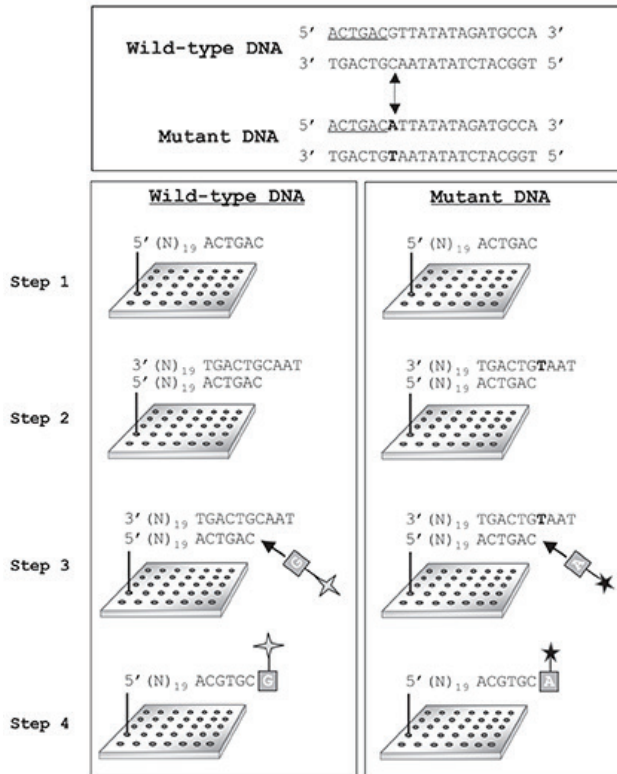
Figure 1.18. Outline of the arrayed primer extension (APEX) technique. Step 1: A primer of 25 nucleotides specific for a nucleotide sequence just next to the variant nucleotide of interest are linked to a glass slide. Step 2: hybridization of fractionated wild-type or mutant genomic sequences amplified by polymerase chain reaction (PCR). Step 3: primer-extension using fluorescently labeled dideoxynucleotides. Step 4: separation of template DNA and detection of specific fluorescent dye and thereby the variant nucleotide of interest.

micro-array chip was developed. This chip enabled screening of the presence (or absence) of specific mutations in different genes. In the field of IRDs, micro-array chips using the arrayed primer extension technique (Figure 1.18) are available for Stargardt disease (*ABCA4*), Leber congenital amaurosis (multiple genes) and autosomal recessive and dominant RP (multiple genes).[264-266] Whole exome sequencing is a new technique that enables sequencing of the exons of all genes in the human genome simultaneously. This had large consequences on the costs, labor and time necessary to perform genetic analysis in multiple genes, which all decreased tremendously.

In daily practice, Sanger sequencing is used if mutations in a specific gene are suspected. If the mutations causative to the phenotype could be situated in multiple genes, as is the case of most RP and CRD cases, high-throughput NGS techniques like whole exome sequencing are more adequate. Micro-array chips have been used to test the patient's DNA on certain specific mutations that are known to cause disease (Figures 1.18). However, since the number of genes and mutations in IRDs has grown significantly (Figures 1.19), this method has become inadequate and costly compared to NGS techniques (see **Chapter 7**).
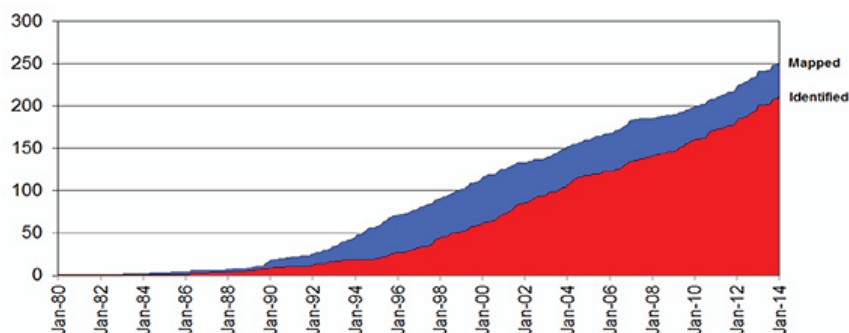
Figure 1.19. Impression of the number of IRD genes identified and IRD loci mapped over the last 34 years. (Source: RetNet, the Retinal Network, available at: https://sph.uth.edu/retnet/)

Aims and outline of this thesis

The growing number of genes involved in retinal dystrophies has increased our understanding of these diseases enormously. However, it also complicated the health care in these patients, especially for general ophthalmologist and geneticists. The main objective of this thesis was to improve our clinical and genetic knowledge on IRDs by providing detailed clinical descriptions of several subtypes of IRDs, as well as associate these phenotypic characteristics to the molecular genetic defects. This knowledge is important to counsel patients and their families, select the technique for genetic analysis, interpret molecular genetic findings, as well as to select patients amenable for future therapeutic trials.

Chapter 1 provides the basic aspects of the anatomy of the retina and choroid, as well as the physiologic processes that lead to vision. It discusses clinical tests and their value in clinical assessment of a patient. The reader is additionally introduced in the field of IRDs, and the general clinical aspects of the retinal dystrophies discussed in this thesis are considered. In addition, this chapter describes the basics of molecular genetics and the genetic context of IRDs.

The clinical characteristics of patients with RP associated to mutations in the *IMPG2* genes are discussed in **Chapter 2**. In this form of RP, the general symptoms of night blindness and tunnel vision are complicated with a decrease in central vision due to relatively early macular involvement. This macular disease often displays as a bull's eye maculopathy prior to further loss of macular tissue and a central atrophy becomes apparent. In this chapter we also discuss possible genotype-phenotype correlations.

Chapter 3 describes the clinical findings in *MAK*-associated RP, and also includes an overview of the retinal dystrophies caused by ciliary genes that cause both syndromic and nonsyndromic disease when mutated, and possible genotype-phenotype correlations. The *MAK* gene encodes a protein that plays a role in the connecting cilium of photoreceptor cells, and therefore defects in *MAK* are considered a form of ciliopathy. Ciliopathic disease can be

associated with syndromic disease, but *MAK*-associated RP appears not to be associated with syndromic symptoms.

In **Chapter 4**, the clinical characteristics of retinal disease caused by mutations in another ciliary gene, *C8orf37*, are discussed. Mutations in *C8orf37* can give rise to either a form of RP with macular atrophy during childhood or adolescence, or a rather classic form of CRD. Interestingly, in one family postaxial polydactyly has occurred, which may indicate that mutations in *C8orf37* may cause syndromic disease, and patients with this mutation should be carefully examined for extraocular abnormalities. Again, we provide possible correlations between the genetic and the phenotypic findings.

The clinical spectrum of disease caused by mutations in the *ABHD12* gene is represented in **Chapter 5**. Nonsense mutations in this gene causes the PHARC-syndrome, which includes polyneuropathy, hearing loss, ataxia, retinitis pigmentosa and cataract. The chapter describes missense mutations in *ABHD12*, as well as the clinical spectrum that ranges from the complete PHARC syndrome phenotype to non-syndromic retinal degeneration.

Chapter 6 evaluates the clinical spectrum of *USH1G*-associated disease. Mutations in this gene have been associated with Usher syndrome type 1, which is characterized by congenital neurosensory hearing loss, vestibular areflexia and RP. This study describes a Dutch family with sensorineural hearing loss caused by compound heterozygous missense and nonsense mutations in *USH1G* in absence of retinal degeneration.

The efficiency of the arrayed-primer extension (APEX) microarray screening for autosomal recessive RP is discussed in **Chapter 7**. Since the dawn of modern genetics, many genes involved in autosomal recessive RP have been described, which complicates genetic analysis. In 2006, APEX microarray screening was a cost-efficient technique to screening multiple genes for mutations simultaneously. However, better alternatives for genetic analysis of autosomal recessive RP became available with the dawn of NGS techniques.

In **Chapter 8,** we describe the clinical features of early-onset STGD1 patients that present with visual complaints before the age of 10. These patients often present with early foveal atrophy and progress to visual acuity levels of hand movements, in contrast to patients with a classic STGD1 phenotype that presents during adolescence or early adulthood and progress to visual acuity levels ranging from 20/200 to finger counting. The clinical characteristics and genetic findings of early-onset STGD1 are provided and discussed in this chapter.

Chapter 9 evaluates the clinical characteristics of the foveal sparing phenomenon in patients with STGD1. This phenomenon mainly occurs in late-onset Stargardt, and is characterized by a relative preservation of the visual acuity, although visual acuity ultimately deteriorates by the end-stage of the disease when the foveola degenerates. The clinical findings and natural history of foveal sparing in STGD1 provided in this study are clinically relevant to counsel

patients and their family members. Furthermore, this patient cohort may be promising candidates for future therapeutic trials.

The clinical phenotype of DCMD is presented in **Chapter 10**. It describes three grades of the disease based on the longitudinal data of multimodal imaging and electrophysiological findings in 97 Dutch patients, which is vital for counseling of patients and family members. In addition, therapeutic options in DCMD are discussed, as well as underlying pathophysiological processes.

Chapter 11 describes the set-up of the RD5000 database (RD5000db), the first multi-center, web-based database that includes anonymized detailed clinical data as well as selected genetic details in the Netherlands. The RD5000db has been created to enhance clinical and genetic studies on IRDs, as well as select patients for future clinical trials.

In **Chapter 12**, the studies described in this thesis are further discussed, integrated and place in a broader perspective.

References

1. von Helmholtz HL. Beschreibung eines Augenspiegels zu Untersuchung der Netzhaut im lebenden Auge. Berlin: A. Förster; 1851.
2. Van Trigt AC. De oogspiegel. *Nederlandsch Lancet* 1853:417-509.
3. Donders FC. Torpeur de la rétine congénital e héréditairie. *Ann ocul* 1855;34:270-3.
4. Ovelgün RF. Nyctalopia haereditaria. *Acta physico-medica Academiae Caesareae Leopoldino-Carolinae (Norimbergae)* 1744;7:76-7.
5. Stargardt K. Über familiäre, progressive Degeneration in der Maculagegend des Auges. *Graefe's Archive for Ophthalmology* 1909(71):534-50.
6. Franceschetti A. A special form of tapetoretinal degeneration: fundus flavimaculatus. *Trans Am Acad Ophthalmol Otolaryngol* 1965 Nov-Dec;69(6):1048-53.
7. Hadden OB, Gass JD. Fundus flavimaculatus and Stargardt's disease. *Am J Ophthalmol* 1976 Oct;82(4):527-39.
8. Rosehr K. Ueber dem weiteren Verlauf der von Stargardt und Behr beschriebenen familiaren Degeneration der Makula. *Klin Monbl Augenheilkd* 1954;124:171.
9. Cunier F. Histoire d'une hemeralopie hereditaire de puis deux siecles dans une famille de al commune de Vendemian pres Montpellier. *Ann soc med gand* 1838;4:385-95.
10. Nettleship E. A history of congenital stationary night-blindness in nine consecutive generations. *Trans Ophthal Soc UK* 1907;27:269-93.
11. Wilson E. The sex chromosomes. *Arch Mikrosk Anat Enwicklungsmech* 1911;77:249-71.
12. Bhattacharya SS, Wright AF, Clayton JF, et al. Close genetic linkage between X-linked retinitis pigmentosa and a restriction fragment length polymorphism identified by recombinant DNA probe L1.28. *Nat New Biol* 1984 May 17-23;309(5965):253-5.
13. Dryja TP, McGee TL, Reichel E, et al. A point mutation of the rhodopsin gene in one form of retinitis pigmentosa. *Nat New Biol* 1990 Jan 25;343(6256):364-6.
14. Cremers FP, van de Pol DJ, van Kerkhoff LP, Wieringa B, Ropers HH. Cloning of a gene that is rearranged in patients with choroideraemia. *Nat New Biol* 1990 Oct 18;347(6294):674-7.
15. Farrar GJ, Kenna P, Jordan SA, et al. A three-base-pair deletion in the peripherin-RDS gene in one form of retinitis pigmentosa. *Nat New Biol* 1991 Dec 12;354(6353):478-80.
16. Kajiwara K, Hahn LB, Mukai S, Travis GH, Berson EL, Dryja TP. Mutations in the human retinal degeneration slow gene in autosomal dominant retinitis pigmentosa. *Nat New Biol* 1991 Dec 12;354(6353):480-3.
17. Travis GH, Hepler JE. A medley of retinal dystrophies. *Nat Genet* 1993 Mar;3(3):191-2.
18. Hoyng CB, Heutink P, Testers L, Pinckers A, Deutman AF, Oostra BA. Autosomal dominant central areolar choroidal dystrophy caused by a mutation in codon 142 in the peripherin/RDS gene. *Am J Ophthalmol* 1996 Jun;121(6):623-9.
19. O'Rahilly RM, F. The Embryonic human brain: an atlas of developmental stages. New York: Wiley-Liss; 1994.
20. Woedeman WW. Experimentelle Untersuchungen uber Lage und Bau der augenbildeaden Bezirke in der Medullarplatte dem Axolotl. *Arch Entw Mech* 1929;116:220-41.
21. Marc RE. Functional neuroanatomy of the retina. 3rd ed. Albert DM, J., editor. New York: Elsevier; 2008.
22. Marc RE. Functional anatomy of the retina. Tasman WJ, E., editor. Philadelphia: Lippincott Williams & Wilkins; ; 2009.
23. Reichenbach A, Bringmann A. New functions of Muller cells. *Glia* 2013 May;61(5):651-78.
24. Metea MR, Newman EA. Glial cells dilate and constrict blood vessels: a mechanism of neurovascular coupling. *J Neurosci* 2006 Mar 15;26(11):2862-70.
25. Hartong DT, Berson EL, Dryja TP. Retinitis pigmentosa. *Lancet* 2006;368(9549):1795-809.
26. Satir P, Christensen ST. Structure and function of mammalian cilia. *Histochem Cell Biol* 2008 Jun;129(6):687-93.
27. Rosenbaum JL, Witman GB. Intraflagellar transport. *Nat Rev Mol Cell Biol* 2002 Nov;3(11):813-25.
28. Cruce M, Cruce R, Tanasescu D. [The molecular mechanism of visual transduction]. *Oftalmologia* 1996 Jul-Sep;40(3):201-9.
29. Dell'Orco D, Koch KW. A dynamic scaffolding mechanism for rhodopsin and transducin interaction in vertebrate vision. *Biochem J* 2011 Dec 1;440(2):263-71.
30. Anderson DH, Fisher SK, Steinberg RH. Mammalian cones: disc shedding, phagocytosis, and renewal. *Invest Ophthalmol Vis Sci* 1978 Feb;17(2):117-33.

31. Steinberg RH, Fisher SK, Anderson DH. Disc morphogenesis in vertebrate photoreceptors. *J Comp Neurol* 1980 Apr 1;190(3):501-8.

32. Wheway G, Parry DA, Johnson CA. The role of primary cilia in the development and disease of the retina. *Organogenesis* 2014 Jan 1;10(1):69-85.

33. Roorda A, Williams DR. The arrangement of the three cone classes in the living human eye. *Nat New Biol* 1999 Feb 11;397(6719):520-2.

34. Solomon SG, Lennie P. The machinery of colour vision. *Nat Rev Neurosci* 2007 Apr;8(4):276-86.

35. Curcio CA, Sloan KR, Kalina RE, Hendrickson AE. Human photoreceptor topography. *J Comp Neurol* 1990 Feb 22;292(4):497-523.

36. Ahnelt PK. The photoreceptor mosaic. *Eye (Lond)* 1998;12 (Pt 3b):531-40.

37. Curcio CA, Allen KA, Sloan KR, et al. Distribution and morphology of human cone photoreceptors stained with anti-blue opsin. *J Comp Neurol* 1991 Oct 22;312(4):610-24.

38. Osterberg GA. Topography of the layer of rods and cones in the human retina. *Acta Ophthalmol* 1935;13(supplement 6):1-97.

39. Lindsay PH, Norman DA. Human information processing : an introduction to psychology. 2d ed. New York: Academic Press; 1977.

40. Hollyfield JG, Varner HH, Rayborn ME, Osterfeld AM. Retinal attachment to the pigment epithelium. Linkage through an extracellular sheath surrounding cone photoreceptors. *Retina* 1989;9(1):59-68.

41. Hageman GS, Marmor MF, Yao XY, Johnson LV. The interphotoreceptor matrix mediates primate retinal adhesion. *Arch Ophthal* 1995 May;113(5):655-60.

42. Rattner A, Sun H, Nathans J. Molecular genetics of human retinal disease. *Annu Rev Genet* 1999;33:89-131.

43. Schmitz-Valckenberg S, Holz FG, Bird AC, Spaide RF. Fundus autofluorescence imaging: review and perspectives. *Retina* 2008 Mar;28(3):385-409.

44. Hughes BAG, R.P.; Miller, S.S. Transport mechanisms in the retinal pigment epithelium. In: Marmor MFW, T.J., editor. The retinal pigment epithelium: function and disease. New York: Oxford University Press; 1998.

45. Negi A, Marmor MF. Quantitative estimation of metabolic transport of subretinal fluid. *Invest Ophthalmol Vis Sci* 1986 Nov;27(11):1564-8.

46. Tsuboi S, Pederson JE. Volume flow across the isolated retinal pigment epithelium of cynomolgus monkey eyes. *Invest Ophthalmol Vis Sci* 1988 Nov;29(11):1652-5.

47. Frambach DA, Marmor MF. The rate and route of fluid resorption from the subretinal space of the rabbit. *Invest Ophthalmol Vis Sci* 1982 Mar;22(3):292-302.

48. Sarna T. Properties and function of the ocular melanin--a photobiophysical view. *J Photochem Photobiol B* 1992 Feb 28;12(3):215-58.

49. Boulton M, Dayhaw-Barker P. The role of the retinal pigment epithelium: topographical variation and ageing changes. *Eye (Lond)* 2001 Jun;15(Pt 3):384-9.

50. Rozanowska M, Korytowski W, Rozanowski B, et al. Photoreactivity of aged human RPE melanosomes: a comparison with lipofuscin. *Invest Ophthalmol Vis Sci* 2002 Jul;43(7):2088-96.

51. Hollyfield JG, Rayborn ME, Tammi M, Tammi R. Hyaluronan in the interphotoreceptor matrix of the eye: species differences in content, distribution, ligand binding and degradation. *Exp Eye Res* 1998 Feb;66(2):241-8.

52. Adamis AP, Shima DT, Yeo KT, et al. Synthesis and secretion of vascular permeability factor/vascular endothelial growth factor by human retinal pigment epithelial cells. *Biochem Biophys Res Commun* 1993 Jun 15;193(2):631-8.

53. Blaauwgeers HG, Holtkamp GM, Rutten H, et al. Polarized vascular endothelial growth factor secretion by human retinal pigment epithelium and localization of vascular endothelial growth factor receptors on the inner choriocapillaris. Evidence for a trophic paracrine relation. *Am J Pathol* 1999 Aug;155(2):421-8.

54. Qi JH, Ebrahem Q, Moore N, et al. A novel function for tissue inhibitor of metalloproteinases-3 (TIMP3): inhibition of angiogenesis by blockage of VEGF binding to VEGF receptor-2. *Nat Med* 2003 Apr;9(4):407-15.

55. Ruiz A, Brett P, Bok D. TIMP-3 is expressed in the human retinal pigment epithelium. *Biochem Biophys Res Commun* 1996 Sep 13;226(2):467-74.

56. de Jong PT. Age-related macular degeneration. *N Engl J Med* 2006 Oct 5;355(14):1474-85.

57. Strauss O. The retinal pigment epithelium in visual function. *Physiol Rev* 2005 Jul;85(3):845-81.

58.   Dorey CK, Wu G, Ebenstein D, Garsd A, Weiter JJ. Cell loss in the aging retina. Relationship to lipofuscin accumulation and macular degeneration. *Invest Ophthalmol Vis Sci* 1989 Aug;30(8):1691-9.

59.   Weiter JJ, Delori FC, Wing GL, Fitch KA. Retinal pigment epithelial lipofuscin and melanin and choroidal melanin in human eyes. *Invest Ophthalmol Vis Sci* 1986 Feb;27(2):145-52.

60.   Snodderly DM, Sandstrom MM, Leung IY, Zucker CL, Neuringer M. Retinal pigment epithelial cell distribution in central retina of rhesus monkeys. *Invest Ophthalmol Vis Sci* 2002 Sep;43(9):2815-8.

61.   Parver LM, Auker C, Carpenter DO. Choroidal blood flow as a heat dissipating mechanism in the macula. *Am J Ophthalmol* 1980 May;89(5):641-6.

62.   Pino RM. Restriction to endogenous plasma proteins by a fenestrated capillary endothelium: an ultrastructural immunocytochemical study of the choriocapillary endothelium. *Am J Anat* 1985 Apr;172(4):279-89.

63.   Tornquist P, Alm A, Bill A. Permeability of ocular vessels and transport across the blood-retinal-barrier. *Eye (Lond)* 1990;4 (Pt 2):303-9.

64.   Guyer DRS, A.P.; Green, W.R. The choroid: structural considerations. Schachat AP, editor. Philadelphia: Mosby; 2008.

65.   Wangsa-Wirawan ND, Linsenmeier RA. Retinal oxygen: fundamental and clinical aspects. *Arch Ophthal* 2003 Apr;121(4):547-57.

66.   Bill A, Sperber G, Ujiie K. Physiology of the choroidal vascular bed. *Int Ophthalmol* 1983 Feb;6(2):101-7.

67.   Parver LM, Auker CR, Carpenter DO. The stabilizing effect of the choroidal circulation on the temperature environment of the macula. *Retina* 1982;2(2):117-20.

68.   Parver LM, Auker CR, Carpenter DO, Doyle T. Choroidal blood flow II. Reflexive control in the monkey. *Arch Ophthal* 1982 Aug;100(8):1327-30.

69.   Ahmed J, Braun RD, Dunn R, Jr., Linsenmeier RA. Oxygen distribution in the macaque retina. *Invest Ophthalmol Vis Sci* 1993 Mar;34(3):516-21.

70.   Burns MS, Hartz MJ. The retinal pigment epithelium induces fenestration of endothelial cells in vivo. *Curr Eye Res* 1992 Sep;11(9):863-73.

71.   Marneros AG, Fan J, Yokoyama Y, et al. Vascular endothelial growth factor expression in the retinal pigment epithelium is essential for choriocapillaris development and visual function. *Am J Pathol* 2005 Nov;167(5):1451-9.

72.   Henkind P, Gartner S. The relationship between retinal pigment epithelium and the choriocapillaris. *Trans Ophthalmol Soc U K* 1983;103 (Pt 4):444-7.

73.   Korte GE, Reppucci V, Henkind P. RPE destruction causes choriocapillary atrophy. *Invest Ophthalmol Vis Sci* 1984 Oct;25(10):1135-45.

74.   Neuhardt T, May CA, Wilsch C, Eichhorn M, Lutjen-Drecoll E. Morphological changes of retinal pigment epithelium and choroid in rd-mice. *Exp Eye Res* 1999 Jan;68(1):75-83.

75.   Wald G. The molecular basis of visual excitation. *Nat New Biol* 1968 Aug 24;219(5156):800-7.

76.   Stryer L. Cyclic GMP cascade of vision. *Annu Rev Neurosci* 1986;9:87-119.

77.   Gurevich VV, Gurevich EV, Cleghorn WM. Arrestins as multi-functional signaling adaptors. *Handb Exp Pharmacol* 2008(186):15-37.

78.   Palczewski K. Structure and functions of arrestins. *Protein Sci* 1994 Sep;3(9):1355-61.

79.   Krispel CM, Chen D, Melling N, et al. RGS expression rate-limits recovery of rod photoresponses. *Neuron* 2006 Aug 17;51(4):409-16.

80.   Pugh EN, Jr. RGS expression level precisely regulates the duration of rod photoresponses. *Neuron* 2006 Aug 17;51(4):391-3.

81.   Koch KW, Stryer L. Highly cooperative feedback control of retinal rod guanylate cyclase by calcium ions. *Nat New Biol* 1988 Jul 7;334(6177):64-6.

82.   Liu J, Itagaki Y, Ben-Shabat S, Nakanishi K, Sparrow JR. The biosynthesis of A2E, a fluorophore of aging retina, involves the formation of the precursor, A2-PE, in the photoreceptor outer segment membrane. *J Biol Chem* 2000 Sep 22;275(38):29354-60.

83.   Haeseleer F, Huang J, Lebioda L, Saari JC, Palczewski K. Molecular characterization of a novel short-chain dehydrogenase/reductase that reduces all-trans-retinal. *J Biol Chem* 1998 Aug 21;273(34):21790-9.

84. Rattner A, Smallwood PM, Nathans J. Identification and characterization of all-trans-retinol dehydrogenase from photoreceptor outer segments, the visual cycle enzyme that reduces all-trans-retinal to all-trans-retinol. *J Biol Chem* 2000 Apr 14;275(15):11034-43.

85. Gonzalez-Fernandez F. Evolution of the visual cycle: the role of retinoid-binding proteins. *J Endocrinol* 2002 Oct;175(1):75-88.

86. Saari JC, Bredberg DL. Lecithin:retinol acyltransferase in retinal pigment epithelial microsomes. *J Biol Chem* 1989 May 25;264(15):8636-40.

87. Trehan A, Canada FJ, Rando RR. Inhibitors of retinyl ester formation also prevent the biosynthesis of 11-cis-retinol. *Biochemistry* 1990 Jan 16;29(2):309-12.

88. Deigner PS, Law WC, Canada FJ, Rando RR. Membranes as the energy source in the endergonic transformation of vitamin A to 11-cis-retinol. *Science (80-)* 1989 May 26;244(4907):968-71.

89. Moiseyev G, Chen Y, Takahashi Y, Wu BX, Ma JX. RPE65 is the isomerohydrolase in the retinoid visual cycle. *Proc Natl Acad Sci U S A* 2005 Aug 30;102(35):12413-8.

90. Saari JC, Nawrot M, Kennedy BN, et al. Visual cycle impairment in cellular retinaldehyde binding protein (CRALBP) knockout mice results in delayed dark adaptation. *Neuron* 2001 Mar;29(3):739-48.

91. Mata NL, Radu RA, Clemmons RC, Travis GH. Isomerization and oxidation of vitamin a in cone-dominant retinas: a novel pathway for visual-pigment regeneration in daylight. *Neuron* 2002 Sep 26;36(1):69-80.

92. den Hollander AI, Black A, Bennett J, Cremers FP. Lighting a candle in the dark: advances in genetics and gene therapy of recessive retinal dystrophies. *J Clin Invest* 2010 Sep 1;120(9):3042-53.

93. Wade NJ. Image, eye, and retina (invited review). *J Opt Soc Am A Opt Image Sci Vis* 2007 May;24(5):1229-49.

94. Schiefer U, Wilhelm H, Hart WM. Clinical neuro-ophthalmology : a practical guide. Berlin ; New York: Springer; 2007.

95. Brown KT. The electroretinogram: its components and their origins. *Vision Res* 1968 Jun;8(6):633-77.

96. Ogden TE. The oscillatory waves of the primate electroretinogram. *Vision Res* 1973 Jun;13(6):1059-74.

97. Rangaswamy NV, Hood DC, Frishman LJ. Regional variations in local contributions to the primate photopic flash ERG: revealed using the slow-sequence mfERG. *Invest Ophthalmol Vis Sci* 2003 Jul;44(7):3233-47.

98. Moller A, Eysteinsson T. Modulation of the components of the rat dark-adapted electroretinogram by the three subtypes of GABA receptors. *Vis Neurosci* 2003 Sep-Oct;20(5):535-42.

99. Dong CJ, Agey P, Hare WA. Origins of the electroretinogram oscillatory potentials in the rabbit retina. *Vis Neurosci* 2004 Jul-Aug;21(4):533-43.

100. Marmor MF, Fulton AB, Holder GE, Miyake Y, Brigell M, Bach M. ISCEV Standard for full-field clinical electroretinography (2008 update). *Doc Ophthalmol* 2009;118(1):69-77.

101. Hood DC, Bach M, Brigell M, et al. ISCEV standard for clinical multifocal electroretinography (mfERG) (2011 edition). *Doc Ophthalmol* 2012 Feb;124(1):1-13.

102. Marmor MF, Brigell MG, McCulloch DL, Westall CA, Bach M, International Society for Clinical Electrophysiology of V. ISCEV standard for clinical electro-oculography (2010 update). *Doc Ophthalmol* 2011 Feb;122(1):1-7.

103. Kiernan DF, Mieler WF, Hariprasad SM. Spectral-domain optical coherence tomography: a comparison of modern high-resolution retinal imaging systems. *Am J Ophthalmol* 2010 Jan;149(1):18-31.

104. Spaide RF, Curcio CA. Anatomical correlates to the bands seen in the outer retina by optical coherence tomography: literature review and model. *Retina* 2011 Sep;31(8):1609-19.

105. Kitagawa K, Nishida S, Ogura Y. In vivo quantitation of autofluorescence in human retinal pigment epithelium. *Ophthalmologica Journal international d'ophtalmologie International journal of ophthalmology Zeitschrift fur Augenheilkunde* 1989;199(2-3):116-21.

106. Delori FC, Dorey CK, Staurenghi G, Arend O, Goger DG, Weiter JJ. In vivo fluorescence of the ocular fundus exhibits retinal pigment epithelium lipofuscin characteristics. *Invest Ophthalmol Vis Sci* 1995 Mar;36(3):718-29.

107. von Ruckmann A, Fitzke FW, Bird AC. Distribution of fundus autofluorescence with a scanning laser ophthalmoscope. *Br J Ophthalmol* 1995 May;79(5):407-12.

108. Berson EL. Retinitis pigmentosa. The Friedenwald Lecture. *Invest Ophthalmol Vis Sci* 1993;34(5):1659-76.

109. Bunker CH, Berson EL, Bromley WC, Hayes RP, Roderick TH. Prevalence of retinitis pigmentosa in Maine. *Am J Ophthalmol* 1984;97(3):357-65.

110. Hamel C. Retinitis pigmentosa. *Orphanet J Rare Dis* 2006;1:40.

111. Grover S, Fishman GA, Brown J, Jr. Patterns of visual field progression in patients with retinitis pigmentosa. *Ophthalmology* 1998 Jun;105(6):1069-75.

112. Li ZY, Possin DE, Milam AH. Histopathology of Bone Spicule Pigmentation in Retinitis-Pigmentosa. *Ophthalmology* 1995 May;102(5):805-16.

113. Milam AH, Li ZY, Fariss RN. Histopathology of the human retina in retinitis pigmentosa. *Prog Retin Eye Res* 1998 Apr;17(2):175-205.

114. Ma Y, Kawasaki R, Dobson LP, et al. Quantitative analysis of retinal vessel attenuation in eyes with retinitis pigmentosa. *Invest Ophthalmol Vis Sci* 2012;53(7):4306-14.

115. Pennings RJ, Te Brinke H, Weston MD, et al. USH2A mutation analysis in 70 Dutch families with Usher syndrome type II. *Hum Mutat* 2004 Aug;24(2):185.

116. Mockel A, Perdomo Y, Stutzmann F, Letsch J, Marion V, Dollfus H. Retinal dystrophy in Bardet-Biedl syndrome and related syndromic ciliopathies. *Prog Retin Eye Res* 2011 Jul;30(4):258-74.

117. Estrada-Cuzcano A, Koenekoop RK, Senechal A, et al. BBS1 mutations in a wide spectrum of phenotypes ranging from nonsyndromic retinitis pigmentosa to Bardet-Biedl syndrome. *Arch Ophthalmol* 2012 Nov;130(11):1425-32.

118. Branham K, Othman M, Brumm M, et al. Mutations in RPGR and RP2 account for 15% of males with simplex retinal degenerative disease. *Invest Ophthalmol Vis Sci* 2012 Dec;53(13):8232-7.

119. Churchill JD, Bowne SJ, Sullivan LS, et al. Mutations in the X-linked retinitis pigmentosa genes RPGR and RP2 found in 8.5% of families with a provisional diagnosis of autosomal dominant retinitis pigmentosa. *Invest Ophthalmol Vis Sci* 2013 Feb;54(2):1411-6.

120. Dryja TP, Hahn LB, Kajiwara K, Berson EL. Dominant and digenic mutations in the peripherin/RDS and ROM1 genes in retinitis pigmentosa. *Invest Ophthalmol Vis Sci* 1997;38(10):1972-82.

121. Kajiwara K, Berson EL, Dryja TP. Digenic retinitis pigmentosa due to mutations at the unlinked peripherin/RDS and ROM1 loci. *Science (80-)* 1994;264(5165):1604-8.

122. Schrier SA, Falk MJ. Mitochondrial disorders and the eye. *Curr Opin Ophthalmol* 2011 Sep;22(5):325-31.

123. Davidson AE, Schwarz N, Zelinger L, et al. Mutations in ARL2BP, Encoding ADP-Ribosylation-Factor-Like 2 Binding Protein, Cause Autosomal-Recessive Retinitis Pigmentosa. *Am J Hum Genet* 2013 Jul 10.

124. Nachury MV, Loktev AV, Zhang Q, et al. A core complex of BBS proteins cooperates with the GTPase Rab8 to promote ciliary membrane biogenesis. *Cell* 2007 Jun 15;129(6):1201-13.

125. Collin RW, Safieh C, Littink KW, et al. Mutations in C2ORF71 cause autosomal-recessive retinitis pigmentosa. *Am J Hum Genet* 2010 May 14;86(5):783-8.

126. Nishimura DY, Baye LM, Perveen R, et al. Discovery and functional analysis of a retinitis pigmentosa gene, C2ORF71. *Am J Hum Genet* 2010 May 14;86(5):686-95.

127. Estrada-Cuzcano A, Neveling K, Kohl S, et al. Mutations in C8orf37, encoding a ciliary protein, are associated with autosomal-recessive retinal dystrophies with early macular involvement. *Am J Hum Genet* 2012 Jan 13;90(1):102-9.

128. van Huet RA, Estrada-Cuzcano A, Banin E, et al. Clinical characteristics of rod and cone photoreceptor dystrophies in patients with mutations in the C8orf37 gene. *Invest Ophthalmol Vis Sci* 2013 Jul;54(7):4683-90.

129. El Shamieh S, Neuille M, Terray A, et al. Whole-exome sequencing identifies KIZ as a ciliary gene associated with autosomal-recessive rod-cone dystrophy. *Am J Hum Genet* 2014 Apr 3;94(4):625-33.

130. Omori Y, Chaya T, Katoh K, et al. Negative regulation of ciliary length by ciliary male germ cell-associated kinase (Mak) is required for retinal photoreceptor survival. *Proc Natl Acad Sci U S A* 2010 Dec 28;107(52):22671-6.

131. Ozgul RK, Siemiatkowska AM, Yucel D, et al. Exome sequencing and cis-regulatory mapping identify mutations in MAK, a gene encoding a regulator of ciliary length, as a cause of retinitis pigmentosa. *Am J Hum Genet* 2011 Aug 12;89(2):253-64.

132. Stone EM, Luo X, Heon E, et al. Autosomal recessive retinitis pigmentosa caused by mutations in the MAK gene. *Invest Ophthalmol Vis Sci* 2011 Dec;52(13):9665-73.

133. Pierce EA, Quinn T, Meehan T, McGee TL, Berson EL, Dryja TP. Mutations in a gene encoding a new oxygen-regulated photoreceptor protein cause dominant retinitis pigmentosa. *Nat Genet* 1999 Jul;22(3):248-54.

134. Liu Q, Zhou J, Daiger SP, et al. Identification and subcellular localization of the RP1 protein in human and mouse photoreceptors. *Invest Ophthalmol Vis Sci* 2002 Jan;43(1):22-32.

135. Liu Q, Zuo J, Pierce EA. The retinitis pigmentosa 1 protein is a photoreceptor microtubule-associated protein. *J Neurosci* 2004 Jul 21;24(29):6427-36.

136. Veltel S, Gasper R, Eisenacher E, Wittinghofer A. The retinitis pigmentosa 2 gene product is a GTPase-activating protein for Arf-like 3. *Nat Struct Mol Biol* 2008 Apr;15(4):373-80.

137. Hong DH, Pawlyk B, Sokolov M, et al. RPGR isoforms in photoreceptor connecting cilia and the transitional zone of motile cilia. *Invest Ophthalmol Vis Sci* 2003 Jun;44(6):2413-21.

138. Khanna H, Hurd TW, Lillo C, et al. RPGR-ORF15, which is mutated in retinitis pigmentosa, associates with SMC1, SMC3, and microtubule transport proteins. *J Biol Chem* 2005 Sep 30;280(39):33580-7.

139. Chakarova CF, Papaioannou MG, Khanna H, et al. Mutations in TOPORS cause autosomal dominant retinitis pigmentosa with perivascular retinal pigment epithelium atrophy. *Am J Hum Genet* 2007 Nov;81(5):1098-103.

140. Chakarova CF, Khanna H, Shah AZ, et al. TOPORS, implicated in retinal degeneration, is a cilia-centrosomal protein. *Hum Mol Genet* 2011 Mar 1;20(5):975-87.

141. Ansley SJ, Badano JL, Blacque OE, et al. Basal body dysfunction is a likely cause of pleiotropic Bardet-Biedl syndrome. *Nat New Biol* 2003 Oct 9;425(6958):628-33.

142. Blacque OE, Reardon MJ, Li C, et al. Loss of C. elegans BBS-7 and BBS-8 protein function results in cilia defects and compromised intraflagellar transport. *Genes Dev* 2004 Jul 1;18(13):1630-42.

143. Ajmal M, Khan MI, Micheal S, et al. Identification of recurrent and novel mutations in TULP1 in Pakistani families with early-onset retinitis pigmentosa. *Mol Vis* 2012;18:1226-37.

144. den Hollander AI, van Lith-Verhoeven JJ, Arends ML, Strom TM, Cremers FP, Hoyng CB. Novel compound heterozygous TULP1 mutations in a family with severe early-onset retinitis pigmentosa. *Arch Ophthal* 2007 Jul;125(7):932-5.

145. Xi Q, Pauer GJ, Marmorstein AD, Crabb JW, Hagstrom SA. Tubby-like protein 1 (TULP1) interacts with F-actin in photoreceptor cells. *Invest Ophthalmol Vis Sci* 2005 Dec;46(12):4754-61.

146. Sohocki MM, Sullivan LS, Mintz-Hittner HA, et al. A range of clinical phenotypes associated with mutations in CRX, a photoreceptor transcription-factor gene. *Am J Hum Genet* 1998 Nov;63(5):1307-15.

147. Swaroop A, Wang QL, Wu W, et al. Leber congenital amaurosis caused by a homozygous mutation (R90W) in the homeodomain of the retinal transcription factor CRX: direct evidence for the involvement of CRX in the development of photoreceptor function. *Hum Mol Genet* 1999 Feb;8(2):299-305.

148. Bandah-Rozenfeld D, Mizrahi-Meissonnier L, Farhy C, et al. Homozygosity mapping reveals null mutations in FAM161A as a cause of autosomal-recessive retinitis pigmentosa. *Am J Hum Genet* 2010 Sep 10;87(3):382-91.

149. Langmann T, Di Gioia SA, Rau I, et al. Nonsense mutations in FAM161A cause RP28-associated recessive retinitis pigmentosa. *Am J Hum Genet* 2010 Sep 10;87(3):376-81.

150. Nishiguchi KM, Tearle RG, Liu YP, et al. Whole genome sequencing in patients with retinitis pigmentosa reveals pathogenic DNA structural changes and NEK2 as a new disease gene. *Proc Natl Acad Sci U S A* 2013 Oct 1;110(40):16139-44.

151. Coppieters F, Leroy BP, Beysen D, et al. Recurrent mutation in the first zinc finger of the orphan nuclear receptor NR2E3 causes autosomal dominant retinitis pigmentosa. *Am J Hum Genet* 2007 Jul;81(1):147-57.

152. Escher P, Gouras P, Roduit R, et al. Mutations in NR2E3 can cause dominant or recessive retinal degenerations in the same family. *Hum Mutat* 2009 Mar;30(3):342-51.

153. Gire AI, Sullivan LS, Bowne SJ, et al. The Gly56Arg mutation in NR2E3 accounts for 1-2% of autosomal dominant retinitis pigmentosa. *Mol Vis* 2007;13:1970-5.

154. Farjo Q, Jackson A, Pieke-Dahl S, et al. Human bZIP transcription factor gene NRL: structure, genomic sequence, and fine linkage mapping at 14q11.2 and negative mutation analysis in patients with retinal degeneration. *Genomics* 1997 Oct 15;45(2):395-401.

155. Rehemtulla A, Warwar R, Kumar R, Ji X, Zack DJ, Swaroop A. The basic motif-leucine zipper transcription factor Nrl can positively regulate rhodopsin gene expression. *Proc Natl Acad Sci U S A* 1996 Jan 9;93(1):191-5.

156. Rice DS, Huang W, Jones HA, et al. Severe retinal degeneration associated with disruption of semaphorin 4A. *Invest Ophthalmol Vis Sci* 2004 Aug;45(8):2767-77.
157. Abid A, Ismail M, Mehdi SQ, Khaliq S. Identification of novel mutations in the SEMA4A gene associated with retinal degenerative diseases. *J Med Genet* 2006 Apr;43(4):378-81.
158. Jin ZB, Huang XF, Lv JN, et al. SLC7A14 linked to autosomal recessive retinitis pigmentosa. *Nat Commun* 2014;5:3517.
159. Li L, Nakaya N, Chavali VR, et al. A mutation in ZNF513, a putative regulator of photoreceptor development, causes autosomal-recessive retinitis pigmentosa. *Am J Hum Genet* 2010 Sep 10;87(3):400-9.
160. Yang Z, Alvarez BV, Chakarova C, et al. Mutant carbonic anhydrase 4 impairs pH regulation and causes retinal photoreceptor degeneration. *Hum Mol Genet* 2005 Jan 15;14(2):255-65.
161. Bornancin F, Mechtcheriakova D, Stora S, et al. Characterization of a ceramide kinase-like protein. *Biochimica et biophysica acta* 2005 Feb 21;1687(1-3):31-43.
162. Friedman JS, Ray JW, Waseem N, et al. Mutations in a BTB-Kelch protein, KLHL7, cause autosomal-dominant retinitis pigmentosa. *Am J Hum Genet* 2009 Jun;84(6):792-800.
163. Vollrath D, Feng W, Duncan JL, et al. Correction of the retinal dystrophy phenotype of the RCS rat by viral gene transfer of Mertk. *Proc Natl Acad Sci U S A* 2001 Oct 23;98(22):12584-9.
164. Siemiatkowska AM, van den Born LI, van Hagen PM, et al. Mutations in the mevalonate kinase (MVK) gene cause nonsyndromic retinitis pigmentosa. *Ophthalmology* 2013 Dec;120(12):2697-705.
165. Rivolta C, Sweklo EA, Berson EL, Dryja TP. Missense mutation in the USH2A gene: association with recessive retinitis pigmentosa without hearing loss. *Am J Hum Genet* 2000 Jun;66(6):1975-8.
166. Dreyer B, Tranebjaerg L, Rosenberg T, Weston MD, Kimberling WJ, Nilssen O. Identification of novel USH2A mutations: implications for the structure of USH2A protein. *Eur J Hum Genet* 2000 Jul;8(7):500-6.
167. Bernal S, Meda C, Solans T, et al. Clinical and genetic studies in Spanish patients with Usher syndrome type II: description of new mutations and evidence for a lack of genotype--phenotype correlation. *Clin Genet* 2005 Sep;68(3):204-14.
168. Baux D, Larrieu L, Blanchet C, et al. Molecular and in silico analyses of the full-length isoform of usherin identify new pathogenic alleles in Usher type II patients. *Hum Mutat* 2007 Aug;28(8):781-9.
169. Ajmal M, Khan MI, Neveling K, et al. A missense mutation in the splicing factor gene DHX38 is associated with early-onset retinitis pigmentosa with macular coloboma. *J Med Genet* 2014 Jul;51(7):444-8.
170. Lauber J, Plessel G, Prehn S, et al. The human U4/U6 snRNP contains 60 and 90kD proteins that are structurally homologous to the yeast splicing factors Prp4p and Prp3p. *RNA* 1997 Aug;3(8):926-41.
171. Wang A, Forman-Kay J, Luo Y, et al. Identification and characterization of human genes encoding Hprp3p and Hprp4p, interacting components of the spliceosome. *Hum Mol Genet* 1997 Nov;6(12):2117-26.
172. Zhou Z, Licklider LJ, Gygi SP, Reed R. Comprehensive proteomic analysis of the human spliceosome. *Nat New Biol* 2002 Sep 12;419(6903):182-5.
173. Chen X, Liu Y, Sheng X, et al. PRPF4 mutations cause autosomal dominant retinitis pigmentosa. *Hum Mol Genet* 2014 Jun 1;23(11):2926-39.
174. Tanackovic G, Ransijn A, Ayuso C, Harper S, Berson EL, Rivolta C. A missense mutation in PRPF6 causes impairment of pre-mRNA splicing and autosomal-dominant retinitis pigmentosa. *Am J Hum Genet* 2011 May 13;88(5):643-9.
175. Umen JG, Guthrie C. Prp16p, Slu7p, and Prp8p interact with the 3' splice site in two distinct stages during the second catalytic step of pre-mRNA splicing. *RNA* 1995 Aug;1(6):584-97.
176. Keen TJ, Hims MM, McKie AB, et al. Mutations in a protein target of the Pim-1 kinase associated with the RP9 form of autosomal dominant retinitis pigmentosa. *Eur J Hum Genet* 2002 Apr;10(4):245-9.
177. Benaglio P, McGee TL, Capelli LP, Harper S, Berson EL, Rivolta C. Next generation sequencing of pooled samples reveals new SNRNP200 mutations associated with retinitis pigmentosa. *Hum Mutat* 2011 Jun;32(6):E2246-58.
178. Zhao C, Bellur DL, Lu S, et al. Autosomal-dominant retinitis pigmentosa caused by a mutation in SNRNP200, a gene required for unwinding of U4/U6 snRNAs. *Am J Hum Genet* 2009 Nov;85(5):617-27.

179. Pellikka M, Tanentzapf G, Pinto M, et al. Crumbs, the Drosophila homologue of human CRB1/RP12, is essential for photoreceptor morphogenesis. *Nat New Biol* 2002 Mar 14;416(6877):143-9.

180. Collin RW, Littink KW, Klevering BJ, et al. Identification of a 2 Mb human ortholog of Drosophila eyes shut/spacemaker that is mutated in patients with retinitis pigmentosa. *Am J Hum Genet* 2008 Nov;83(5):594-603.

181. Saishin Y, Ishikawa R, Ugawa S, et al. Retinal fascin: functional nature, subcellular distribution, and chromosomal localization. *Invest Ophthalmol Vis Sci* 2000 Jul;41(8):2087-95.

182. Tubb BE, Bardien-Kruger S, Kashork CD, et al. Characterization of human retinal fascin gene (FSCN2) at 17q25: close physical linkage of fascin and cytoplasmic actin genes. *Genomics* 2000 Apr 15;65(2):146-56.

183. Bandah-Rozenfeld D, Collin RW, Banin E, et al. Mutations in IMPG2, encoding interphotoreceptor matrix proteoglycan 2, cause autosomal-recessive retinitis pigmentosa. *Am J Hum Genet* 2010;87(2):199-208.

184. Maw MA, Corbeil D, Koch J, et al. A frameshift mutation in prominin (mouse)-like 1 causes human retinal degeneration. *Hum Mol Genet* 2000 Jan 1;9(1):27-34.

185. Zhang Q, Zulfiqar F, Xiao X, et al. Severe retinitis pigmentosa mapped to 4p15 and associated with a novel mutation in the PROM1 gene. *Hum Genet* 2007 Nov;122(3-4):293-9.

186. Connell G, Bascom R, Molday L, Reid D, McInnes RR, Molday RS. Photoreceptor peripherin is the normal product of the gene responsible for retinal degeneration in the rds mouse. *Proc Natl Acad Sci U S A* 1991 Feb 1;88(3):723-6.

187. Travis GH, Sutcliffe JG, Bok D. The retinal degeneration slow (rds) gene product is a photoreceptor disc membrane-associated glycoprotein. *Neuron* 1991 Jan;6(1):61-70.

188. Clarke G, Goldberg AF, Vidgen D, et al. Rom-1 is required for rod photoreceptor viability and the regulation of disk morphogenesis. *Nat Genet* 2000 May;25(1):67-73.

189. Dhallan RS, Macke JP, Eddy RL, et al. Human rod photoreceptor cGMP-gated channel: amino acid sequence, gene structure, and functional expression. *J Neurosci* 1992 Aug;12(8):3248-56.

190. Batra-Safferling R, Abarca-Heidemann K, Korschen HG, et al. Glutamic acid-rich proteins of rod photoreceptors are natively unfolded. *J Biol Chem* 2006 Jan 20;281(3):1449-60.

191. Korschen HG, Beyermann M, Muller F, et al. Interaction of glutamic-acid-rich proteins with the cGMP signalling pathway in rod photoreceptors. *Nat New Biol* 1999 Aug 19;400(6746):761-6.

192. Poetsch A, Molday LL, Molday RS. The cGMP-gated channel and related glutamic acid-rich proteins interact with peripherin-2 at the rim region of rod photoreceptor disc membranes. *J Biol Chem* 2001 Dec 21;276(51):48009-16.

193. Zelinger L, Banin E, Obolensky A, et al. A missense mutation in DHDDS, encoding dehydrodolichyl diphosphate synthase, is associated with autosomal-recessive retinitis pigmentosa in Ashkenazi Jews. *Am J Hum Genet* 2011 Feb 11;88(2):207-15.

194. Payne AM, Downes SM, Bessant DA, et al. Genetic analysis of the guanylate cyclase activator 1B (GUCA1B) gene in patients with autosomal dominant retinal dystrophies. *J Med Genet* 1999 Sep;36(9):691-3.

195. Sato M, Nakazawa M, Usui T, Tanimoto N, Abe H, Ohguro H. Mutations in the gene coding for guanylate cyclase-activating protein 2 (GUCA1B gene) in patients with autosomal dominant retinal dystrophies. *Graefes Arch Clin Exp Ophthalmol* 2005 Mar;243(3):235-42.

196. Fung BK, Young JH, Yamane HK, Griswold-Prenner I. Subunit stoichiometry of retinal rod cGMP phosphodiesterase. *Biochemistry* 1990 Mar 20;29(11):2657-64.

197. Koutalos Y, Nakatani K, Yau KW. The cGMP-phosphodiesterase and its contribution to sensitivity regulation in retinal rods. *J Gen Physiol* 1995 Nov;106(5):891-921.

198. Dvir L, Srour G, Abu-Ras R, Miller B, Shalev SA, Ben-Yosef T. Autosomal-recessive early-onset retinitis pigmentosa caused by a mutation in PDE6G, the gene encoding the gamma subunit of rod cGMP phosphodiesterase. *Am J Hum Genet* 2010 Aug 13;87(2):258-64.

199. Hargrave PA. Rhodopsin structure, function, and topography the Friedenwald lecture. *Invest Ophthalmol Vis Sci* 2001 Jan;42(1):3-9.

200. Nakazawa M, Wada Y, Tamai M. Arrestin gene mutations in autosomal recessive retinitis pigmentosa. *Arch Ophthal* 1998 Apr;116(4):498-501.

201. Allikmets R, Singh N, Sun H, et al. A photoreceptor cell-specific ATP-binding transporter gene (ABCR) is mutated in recessive Stargardt macular dystrophy. *Nat Genet* 1997 Mar;15(3):236-46.

202. Weng J, Mata NL, Azarian SM, Tzekov RT, Birch DG, Travis GH. Insights into the function of Rim protein in photoreceptors and etiology of Stargardt's disease from the phenotype in abcr knockout mice. *Cell* 1999 Jul 9;98(1):13-23.

203. Sun H, Nathans J. Mechanistic studies of ABCR, the ABC transporter in photoreceptor outer segments responsible for autosomal recessive Stargardt disease. *J Bioenerg Biomembr* 2001 Dec;33(6):523-30.

204. Xue L, Gollapalli DR, Maiti P, Jahng WJ, Rando RR. A palmitoylation switch mechanism in the regulation of the visual cycle. *Cell* 2004 Jun 11;117(6):761-71.

205. den Hollander AI, McGee TL, Ziviello C, et al. A homozygous missense mutation in the IRBP gene (RBP3) associated with autosomal recessive retinitis pigmentosa. *Invest Ophthalmol Vis Sci* 2009 Apr;50(4):1864-72.

206. Valverde D, Vazquez-Gundin F, del Rio E, Calaf M, Fernandez JL, Baiget M. Analysis of the IRBP gene as a cause of RP in 45 ARRP Spanish families. Autosomal recessive retinitis pigmentosa. Interstitial retinol binding protein. Spanish Multicentric and Multidisciplinary Group for Research into Retinitis Pigmentosa. *Ophthalmic Genet* 1998 Dec;19(4):197-202.

207. Parker RO, Crouch RK. Retinol dehydrogenases (RDHs) in the visual cycle. *Exp Eye Res* 2010 Dec;91(6):788-92.

208. Xie YA, Lee W, Cai C, et al. New syndrome with retinitis pigmentosa is caused by nonsense mutations in retinol dehydrogenase RDH11. *Hum Mol Genet* 2014 Jun 10.

209. Fingert JH, Oh K, Chung M, et al. Association of a novel mutation in the retinol dehydrogenase 12 (RDH12) gene with autosomal dominant retinitis pigmentosa. *Arch Ophthal* 2008 Sep;126(9):1301-7.

210. Cideciyan AV, Haeseleer F, Fariss RN, et al. Rod and cone visual cycle consequences of a null mutation in the 11-cis-retinol dehydrogenase gene in man. *Vis Neurosci* 2000 Sep-Oct;17(5):667-78.

211. Yamamoto H, Simon A, Eriksson U, Harris E, Berson EL, Dryja TP. Mutations in the gene encoding 11-cis retinol dehydrogenase cause delayed dark adaptation and fundus albipunctatus. *Nat Genet* 1999 Jun;22(2):188-91.

212. Chen P, Hao W, Rife L, et al. A photic visual cycle of rhodopsin regeneration is dependent on Rgr. *Nat Genet* 2001 Jul;28(3):256-60.

213. Davidson AE, Millar ID, Urquhart JE, et al. Missense mutations in a retinal pigment epithelium protein, bestrophin-1, cause retinitis pigmentosa. *Am J Hum Genet* 2009 Nov;85(5):581-92.

214. Marmorstein AD, Marmorstein LY, Rayborn M, Wang X, Hollyfield JG, Petrukhin K. Bestrophin, the product of the Best vitelliform macular dystrophy gene (VMD2), localizes to the basolateral plasma membrane of the retinal pigment epithelium. *Proc Natl Acad Sci U S A* 2000 Nov 7;97(23):12758-63.

215. Adato A, Vreugde S, Joensuu T, et al. USH3A transcripts encode clarin-1, a four-transmembrane-domain protein with a possible role in sensory synapses. *Eur J Hum Genet* 2002 Jun;10(6):339-50.

216. Joensuu T, Hamalainen R, Yuan B, et al. Mutations in a novel gene with transmembrane domains underlie Usher syndrome type 3. *Am J Hum Genet* 2001 Oct;69(4):673-84.

217. Abu-Safieh L, Alrashed M, Anazi S, et al. Autozygome-guided exome sequencing in retinal dystrophy patients reveals pathogenetic mutations and novel candidate disease genes. *Genome Res* 2013 Feb;23(2):236-47.

218. Hartong DT, Dange M, McGee TL, Berson EL, Dryja TP, Colman RF. Insights from retinitis pigmentosa into the roles of isocitrate dehydrogenases in the Krebs cycle. *Nat Genet* 2008 Oct;40(10):1230-4.

219. Bowne SJ, Sullivan LS, Blanton SH, et al. Mutations in the inosine monophosphate dehydrogenase 1 gene (IMPDH1) cause the RP10 form of autosomal dominant retinitis pigmentosa. *Hum Mol Genet* 2002 Mar 1;11(5):559-68.

220. Nevet MJ, Shalev SA, Zlotogora J, Mazzawi N, Ben-Yosef T. Identification of a prevalent founder mutation in an Israeli Muslim Arab village confirms the role of PRCD in the aetiology of retinitis pigmentosa in humans. *J Med Genet* 2010 Aug;47(8):533-7.

221. Zangerl B, Goldstein O, Philp AR, et al. Identical mutation in a novel retinal gene causes progressive rod-cone degeneration in dogs and retinitis pigmentosa in humans. *Genomics* 2006 Nov;88(5):551-63.

222. Wang H, den Hollander AI, Moayedi Y, et al. Mutations in SPATA7 cause Leber congenital amaurosis and juvenile retinitis pigmentosa. *Am J Hum Genet* 2009 Mar;84(3):380-7.

223. Hamel CP. Cone rod dystrophies. *Orphanet J Rare Dis* 2007;2:7.

224. Hamel CP, Griffoin JM, Bazalgette C, et al. [Molecular genetics of pigmentary retinopathies: identification of mutations in CHM, RDS, RHO, RPE65, USH2A and XLRS1 genes]. *Journal francais d'ophtalmologie* 2000 Dec;23(10):985-95.

225. Roosing S, Thiadens AA, Hoyng CB, Klaver CC, den Hollander AI, Cremers FP. Causes and consequences of inherited cone disorders. *Prog Retin Eye Res* 2014 May 22.

226. Thiadens AA, Phan TM, Zekveld-Vroon RC, et al. Clinical course, genetic etiology, and visual outcome in cone and cone-rod dystrophy. *Ophthalmology* 2012 Apr;119(4):819-26.

227. Blacharski PA. Fundus flavimaculatus. New York: Raven Press; 1988.

228. Westeneng-van Haaften SC, Boon CJ, Cremers FP, Hoefsloot LH, den Hollander AI, Hoyng CB. Clinical and genetic characteristics of late-onset Stargardt's disease. *Ophthalmology* 2012 Jun;119(6):1199-210.

229. Fishman GA, Stone EM, Grover S, Derlacki DJ, Haines HL, Hockey RR. Variation of clinical expression in patients with Stargardt dystrophy and sequence variations in the ABCR gene. *Arch Ophthal* 1999 Apr;117(4):504-10.

230. Lois N, Holder GE, Bunce C, Fitzke FW, Bird AC. Phenotypic subtypes of Stargardt macular dystrophy-fundus flavimaculatus. *Arch Ophthal* 2001 Mar;119(3):359-69.

231. Lois N, Holder GE, Fitzke FW, Plant C, Bird AC. Intrafamilial variation of phenotype in Stargardt macular dystrophy-Fundus flavimaculatus. *Invest Ophthalmol Vis Sci* 1999 Oct;40(11):2668-75.

232. Fish G, Grey R, Sehmi KS, Bird AC. The dark choroid in posterior retinal dystrophies. *Br J Ophthalmol* 1981 May;65(5):359-63.

233. Armstrong JD, Meyer D, Xu S, Elfervig JL. Long-term follow-up of Stargardt's disease and fundus flavimaculatus. *Ophthalmology* 1998 Mar;105(3):448-57; discussion 57-8.

234. Molday LL, Rabin AR, Molday RS. ABCR expression in foveal cone photoreceptors and its role in Stargardt macular dystrophy. *Nat Genet* 2000 Jul;25(3):257-8.

235. Sparrow JR, Wu Y, Kim CY, Zhou J. Phospholipid meets all-trans-retinal: the making of RPE bisretinoids. *J Lipid Res* 2010 Feb;51(2):247-61.

236. Maugeri A, van Driel MA, van de Pol DJ, et al. The 2588G-->C mutation in the ABCR gene is a mild frequent founder mutation in the Western European population and allows the classification of ABCR mutations in patients with Stargardt disease. *Am J Hum Genet* 1999 Apr;64(4):1024-35.

237. van Driel MA, Maugeri A, Klevering BJ, Hoyng CB, Cremers FP. ABCR unites what ophthalmologists divide(s). *Ophthalmic Genet* 1998 Sep;19(3):117-22.

238. Deutman AF, Pinckers AJ, Aan de Kerk AL. Dominantly inherited cystoid macular edema. *Am J Ophthalmol* 1976 Oct;82(4):540-8.

239. Notting JG, Pinckers JL. Dominant cystoid macular dystrophy. *Am J Ophthalmol* 1977 Feb;83(2):234-41.

240. Pinckers A, Deutman AF, Lion F, Aan de Kerk AL. Dominant cystoid macular dystrophy (DCMD). *Ophthalmic Paediatr Genet* 1983;3(3):11.

241. Pinckers A, Deutman AF, Notting JG. Retinal functions in dominant cystoid macular dystrophy (DCMD). *Acta Ophthalmol* 1976 Oct;54(5):579-90.

242. Pinckers A, Notting JG, Lion F. [Dominant cystoid macular dystrophy (author's transl)]. *Journal francais d'ophtalmologie* 1978 Feb;1(2):107-10.

243. Fishman GA, Goldberg MF, Trautmann JC. Dominantly inherited cystoid macular edema. *Ann Ophthalmol* 1979 Jan;11(1):21-7.

244. Schadlu R, Shah GK, Prasad AG. Optical coherence tomography findings in autosomal dominant macular dystrophy. *Ophthalmic Surg Lasers Imaging* 2008 Jan-Feb;39(1):69-72.

245. Kremer H, Pinckers A, van den Helm B, Deutman AF, Ropers HH, Mariman EC. Localization of the gene for dominant cystoid macular dystrophy on chromosome 7p. *Hum Mol Genet* 1994 Feb;3(2):299-302.

246. Watson JD, Crick FH. Molecular structure of nucleic acids; a structure for deoxyribose nucleic acid. *Nat New Biol* 1953 Apr 25;171(4356):737-8.

247. Watson JD, Crick FH. The structure of DNA. *Cold Spring Harb Symp Quant Biol* 1953;18:123-31.

248. Alberts B, Bray D, Hopkin K, et al. Essential Cell Biology, Fourth Edition. New York: Taylor & Francis Group; 2013.

249. Alberts B. Essential cell biology. Fourth edition. ed.

250. Consortium EP, Bernstein BE, Birney E, et al. An integrated encyclopedia of DNA elements in the human genome. *Nat New Biol* 2012 Sep 6;489(7414):57-74.

251. Consortium EP, Birney E, Stamatoyannopoulos JA, et al. Identification and analysis of functional elements in 1% of the human genome by the ENCODE pilot project. *Nat New Biol* 2007 Jun 14;447(7146):799-816.
252. Djebali S, Davis CA, Merkel A, et al. Landscape of transcription in human cells. *Nat New Biol* 2012 Sep 6;489(7414):101-8.
253. Gerstein MB, Kundaje A, Hariharan M, et al. Architecture of the human regulatory network derived from ENCODE data. *Nat New Biol* 2012 Sep 6;489(7414):91-100.
254. Sanyal A, Lajoie BR, Jain G, Dekker J. The long-range interaction landscape of gene promoters. *Nat New Biol* 2012 Sep 6;489(7414):109-13.
255. Berg JM, Stryer L, Tymoczko JL. Biochemistry. Fifth ed. La Jolla: Granite Hill Publishers; 2002.
256. Adzhubei IA, Schmidt S, Peshkin L, et al. A method and server for predicting damaging missense mutations. *Nat Methods* 2010 Apr;7(4):248-9.
257. Grantham R. Amino acid difference formula to help explain protein evolution. *Science (80-)* 1974 Sep 6;185(4154):862-4.
258. Ng PC, Henikoff S. Predicting deleterious amino acid substitutions. *Genome Res* 2001 May;11(5):863-74.
259. Cooper GM, Stone EA, Asimenos G, et al. Distribution and intensity of constraint in mammalian genomic sequence. *Genome Res* 2005 Jul;15(7):901-13.
260. Banin E, Mizrahi-Meissonnier L, Neis R, et al. A non-ancestral RPGR missense mutation in families with either recessive or semi-dominant X-linked retinitis pigmentosa. *Am J Med Genet A* 2007 Jun 1;143A(11):1150-8.
261. Berger W, Kloeckener-Gruissem B, Neidhardt J. The molecular basis of human retinal and vitreoretinal diseases. Prog Retin Eye Res 2010;29:335-375.
262. Sanger F, Nicklen S, Coulson AR. DNA sequencing with chain-terminating inhibitors. *Proc Natl Acad Sci U S A* 1977 Dec;74(12):5463-7.
263. Sanger F, Coulson AR. A rapid method for determining sequences in DNA by primed synthesis with DNA polymerase. *J Mol Biol* 1975 May 25;94(3):441-8.
264. Jaakson K, Zernant J, Kulm M, et al. Genotyping microarray (gene chip) for the ABCR (ABCA4) gene. *Hum Mutat* 2003 Nov;22(5):395-403.
265. Clark GR, Crowe P, Muszynska D, et al. Development of a diagnostic genetic test for simplex and autosomal recessive retinitis pigmentosa. *Ophthalmology* 2010 Nov;117(11):2169-77 e3.
266. Blanco-Kelly F, Garcia-Hoyos M, Corton M, et al. Genotyping microarray: mutation screening in Spanish families with autosomal dominant retinitis pigmentosa. *Mol Vis* 2012;18:1478-83.

Authors

Ramon A.C. van Huet,[1] Rob W.J. Collin,[2, 3] Anna M. Siemiatkowska,[2, 3] Caroline C.W. Klaver,[4] Carel B. Hoyng,[1] Francesca Simonelli,[5] Muhammad I. Khan,[2, 6] Raheel Qamar,[6, 7] Eyal Banin,[8] Frans P.M. Cremers,[2, 3] Thomas Theelen,[1] Anneke I. Den Hollander,[1] L. Ingeborgh van den Born,[9] B. Jeroen Klevering[1]

Affiliations

[1]the Department of Ophthalmology, Radboud university medical center, Nijmegen, The Netherlands;
[2]the Department of Human Genetics, Radboud university medical center, Nijmegen, The Netherlands;
[3]Radboud Institute for Molecular Life Sciences, Radboud university medical center, Nijmegen, The Netherlands;
[4]the Erasmus University Rotterdam Medical Center, Rotterdam, The Netherlands
[5]the Department of Ophthalmology, Seconda Università degli Studi di Napoli, Naples, Italy;
[6]the Department of Biosciences, COMSATS Institute of Information Technology, Islamabad, Pakistan;
[7]Shifa College of Medicine, Islamabad, Pakistan;
[8]the Department of Ophthalmology, Hadassah-Hebrew University Medical Center, Jerusalem, Israel;
[9]The Rotterdam Eye Hospital, Rotterdam, The Netherlands.

IMPG2-associated retinitis pigmentosa displays relatively early macular involvement

2

Abstract

Purpose. To provide the first detailed clinical description in patients with retinitis pigmentosa (RP) caused by recessive mutations in *IMPG2*.

Methods. This international collaborative study includes 17 RP patients with inherited retinal disease caused by mutations in *IMPG2*. The patients were clinically (re-)examined, including extensive medical history taking, slit-lamp biomicroscopy, ophthalmoscopy, perimetry, electroretinography (ERG), optical coherence tomography (OCT), fundus autofluorescence (FAF) imaging, fundus photography, and color vision tests. The main outcome measures included mean age at onset, initial symptom, best-corrected visual acuity, fundus appearance, perimetry results, ERG responses, OCT images, FAF imaging, color vision test reports and DNA sequence variants.

Results. The mean age at onset was 10.5 years (range: 4–20 years). Initial symptoms included night blindness in 59% of patients, a decreased visual acuity in 35% and visual field loss in 6%. Fundus abnormalities were typical of RP: optic disc pallor, attenuated vessels, bone spicules and generalized atrophy of the retina and choriocapillaris. Additionally, we observed macular abnormalities in all patients, ranging from subtle mottling of the macular pigment epithelium (two patients), a bull's eye maculopathy (7 patients) to macular chorioretinal atrophy (7 patients).

Conclusions. Mutations in *IMPG2* cause a severe form of RP with symptoms manifesting in the first two decades of life. *IMPG2*-associated RP is frequently accompanied by macular involvement, ranging from mild pigment alterations to profound chorioretinal atrophy. The resulting decrease in central vision in combination with the severe tunnel vision leads to severe visual impairment in patients with *IMPG2*-associated RP.

Introduction

Retinitis pigmentosa (RP) is a group of diseases featuring progressive degeneration of rod and cone photoreceptor cells and retinal pigment epithelium (RPE), and is considered the most commonly inherited retinal dystrophy with an estimated prevalence of approximately 1:4000.[1-3] RP typically starts with night blindness followed by loss of the peripheral visual field that leads to tunnel vision, whereas visual acuity often remains normal until the late stages.[3, 4] Hallmark fundus abnormalities in RP are bone-spicule pigmentation, a waxy pale optic disc and attenuation of retinal vessels. Electroretinography (ERG) responses reveal rod and cone dysfunction, where rod abnormalities often are observed earlier in the course of the disease. However, wide variability in terms of disease onset, progression rate and degeneration patterns are observed in RP.[4, 5]

The genetic background underlying RP is also very heterogeneous. Inheritance modes observed in RP include autosomal-recessive (30% of patients), autosomal-dominant (20%), X-linked (10%), mitochondrial (<1%) patterns, and few cases of digenic RP.[6-9] However, the remaining 40% of patients are isolated cases.[10] Autosomal recessive RP is currently associated with mutations in 42 different genes (RetNet, https://sph.uth.edu/retnet/), which provide a molecular genetic explanation for approximately 50% of all recessive RP cases.[11] The proteins encoded by these genes are involved in a broad range of cellular functions, including phototransduction, the visual (retinoid) cycle, transport along the connecting cilium, cell to cell signaling or synaptic interaction, gene regulation, cell- or cytoskeletal structure, cell-cell interactions and outer segment phagocytosis.[4, 10, 12]

Recently, mutations in the *IMPG2* gene have been implicated in autosomal recessive RP.[13] This gene encodes the interphotoreceptor matrix proteoglycan-2 (IMPG2), formerly known as IPM 200 or SPACRCAN,[14] which is localized in the retinal extracellular matrix (also known as the interphotoreceptor matrix, IPM). The IPM is a viscous substance mainly composed of glycoproteins and proteoglycans that fills the space between individual photoreceptor cells and between photoreceptors and the RPE.[15, 16] For many years the IPM was considered merely a fixating medium,[17] but in the last few decades multiple functions of the IPM have been reported, including important functions in intercellular communication, regulation of neovascularisation, cell survival, membrane turnover, photoreceptor differentiation and maintenance, retinoid transport, matrix turnover and the precise alignment of the photoreceptor cells to the optical light path.[14, 18, 19] Both rod and cone photoreceptor cells synthesize IMPG2 and secrete the protein into the IPM,[20] where it binds to other proteins like hyaluronan, and also seems to be anchored in the plasma membrane of the photoreceptor cells, thereby fixating the photoreceptors in the IPM.[21] Additionally, IMPG2 is thought to have calcium binding potential, which suggests it has an important role in sequestering extracellular calcium released by photoreceptors in response to light.[21]

Knowledge of the natural course of *IMPG2*-related RP is of significant importance for prognosis counseling as well as genetic counseling. Furthermore, this knowledge is vital in the view of emerging therapy trials, in terms of patient selection as well as the assessment of treatment effects. In this international collaborative study, we aim to provide a detailed overview of the clinical findings in patients with *IMPG2*-associated RP.

Methods and patients

Subjects and genetic analysis

The specialized ophthalmogenetic centers of the Radboud university medical center (RACvH, CBH and BJK), the Rotterdam Eye Hospital (LIvdB), the Erasmus University Medical Center Rotterdam (CCWK), the Hadassah-Hebrew University Medical Center in Jerusalem (EB), the Seconda Università degli Studi di Napoli (FS) and the Shifa College of Medicine in Islamabad (RQ) participated in this study. As described previously,[13] six families of Israeli, Palestinian, Pakistani, Italian or Dutch origin were found to carry causative mutations in *IMPG2* (families A-F, Figure 2.1). Additionally, we selected four more families after identification of causative *IMPG2* mutations in a targeted next-generation sequencing experiment in 100 Dutch RP probands (family G),[22] or whole exome sequencing (families H, J, K, Figure 2.1).
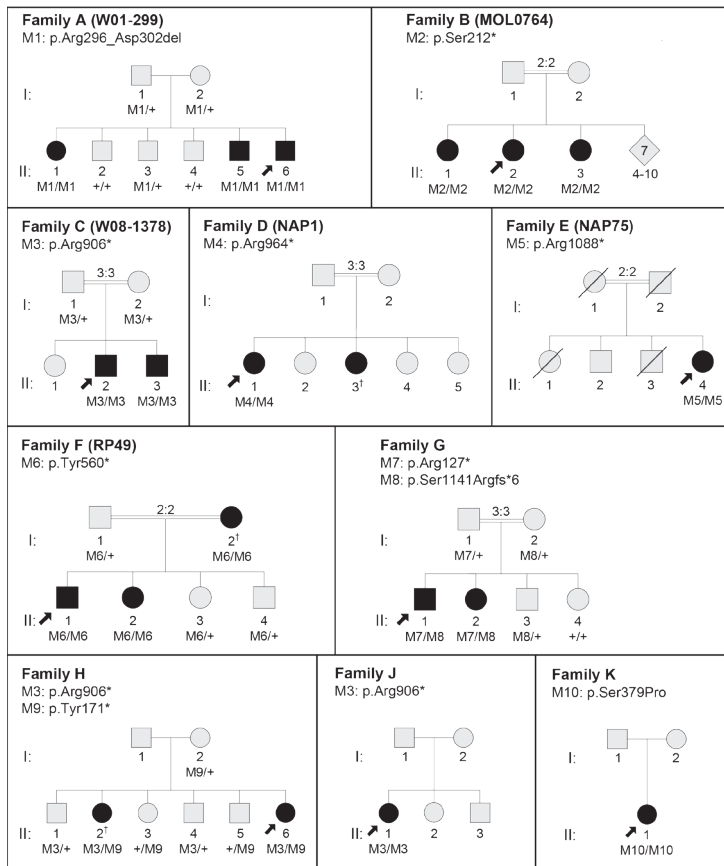
Figure 2.1. Pedigrees of the families that were included in this study. Where relatives were available (families A, B, C, F, G, and H),the mutation segregates with the disease. Plus signs denote the wild type allele, square boxes indicate men, circles indicate women, and affected individuals are pointed out in black. The arrows indicate the probands. Double lines point out consanguineous marriages, the numbers indicate the degree of consanguinity. The dagger(†) indicates the patients diagnosed with RP not included in this study, due the lack of clinical data.

Exome sequencing was performed using the 5500xl Genetic Analyzer of Life Technologies™ (Life Technologies, Applied Biosystems, Foster City, CA, U.S.A.) and the Agilent SureSelectXT Human All Exon 50Mb amplification kit (Agilent Technologies Inc., Santa Clara, CA, U.S.A.). Data was analyzed with LifeScope™ software (version 2.1; Life Technologies, Applied Biosystems, Foster City, CA, U.S.A.). All mutations were confirmed with Sanger sequencing.

We adhered to the tenets of the Declaration of Helsinki and obtained approval for this study from the Institutional Ethics Committee from the Radboud university medical center. Approval included permission to use the documented medical data and, when indicated, clinically re-assess affected individuals and to obtain blood for the purposes of DNA extraction and genetic analysis. We obtained informed consent from all participants prior to the collection of blood samples and additional ophthalmologic examinations.

Clinical analysis

We collected the available clinical data from the medical files of all patients. Nine patients were clinically re-evaluated after the identification of causative *IMPG2* mutations. Medical history was registered with a focus on the age at onset, initial symptoms and the overall course of the retinal disorder. The age at onset was defined as the age at which the initial symptom was noticed by the patient. Additionally, we questioned patients about the presence of syndromic features, which generally occur in 20-30% of RP patients.[4] This questionnaire included the presence of hearing and balance abnormalities, renal failure, cardiac and respiratory anomalies, polydactyly, obesity, cognitive impairment, fertility disorders, hypogonadism and dental anomalies.

Clinical examination included best-corrected visual acuity (BCVA), slit-lamp biomicroscopy, and ophthalmoscopy. Additional examinations were performed if feasible. Goldmann (kinetic) perimetry was performed in 11 patients using targets V-4e, III-4e, I-4e, I-3e, I-2e and I-1e. In two patients (F-II:1 and F-II:2) perimetry was restricted to analysis of the central 30 degrees of the visual field with the Humphrey perimeter (Carl Zeiss Meditec, Jena, Germany). In all but one patient (F-II:2), full-field ERG was performed according the guidelines of the Internationals Society for Clinical Electrophysiology of Vision (ISCEV).[23] Results were compared to the local reference values. We evaluated color vision in six patients using the Farnsworth Dichotomous Test (Panel D-15) and/or the Hardy-Rand-Rittlers (HRR) test. Fundus photographs of the central retina (Topcon TRC50IX, Topcon Corporation, Tokyo, Japan) were obtained in 15 patients. Fundus autofluorescence images (Spectralis™, Heidelberg Engineering, Heidelberg, Germany) of the central retina were acquired in eight patients using a confocal scanning laser ophthalmoscope (cSLO) with an optically pumped solid state laser (488 nm) for excitation. Spectral-domain optical coherence tomography (SD-OCT, Spectralis™, Heidelberg Engineering, Heidelberg, Germany) could be performed in 13 patients. In three patients a high resolution OCT was not available and a time-domain OCT (Stratus, Carl Zeiss Meditec, Jena, Germany) was obtained. No OCT images were available for the remaining 4 patients. In eight Dutch patients with high-resolution SD-OCT images (mean age: 51 years, range: 23-67 years), we quantified thickness of the total retina at the foveola and at 0.25, 0.5, 1, 1.5, 2 and 2.5 mm eccentricity from the foveola in the right eye using the thickness graphs in the Heidelberg Eye Explorer Software (version 1.6.4.0;

Heidelberg Engineering, Heidelberg, Germany). In seven of these patients, we quantified the foveal volume by measuring the retinal volume within the central 3 mm^2 using the thickness map in the Heidelberg Eye Explorer Software (version 1.6.4.0; Heidelberg Engineering, Heidelberg, Germany). A normal dataset of retinal thickness and foveal volume in individuals without (vitreo)retinal disease was obtained from 25 age-matched Dutch individuals (mean age: 46 years, range: 27-62 years) for reference purposes.

Results

Ten families with a total of 17 affected individuals were included in this study. The pedigrees of all families are depicted in Figure 2.1. An overview of the clinical findings in all 17 patients is provided in Table 2.1.

Clinical evaluation

The most recent examination of the 17 RP patients was performed at a mean age of 49 years (range: 23-67 years). The mean age at onset was 10.5 years (range: 4–20 years), and night blindness was the most frequent initial symptom occurring in 10 patients (59%). Other initial symptoms were decrease in visual acuity (35%) and loss of visual field (6%). In the patients who initially revealed a decreased visual acuity, normal BCVA were measured prior to the decrease in visual acuity, which excludes refractive amblyopia. In one patient (A-II:6), the diagnosis of RP was made during a routine ophthalmologic consultation when he was 12 years old. At that time, he had not noticed any symptoms associated with RP, but later in the course of the dystrophy night blindness manifested as the first symptom at age 24. In eight patients, an extended clinical follow-up period varying from 14 to 48 years was available (mean: 29 years). The course of the BCVA for each of these patients during follow-up is represented in Figure 2.2. None of the patients showed extra-ocular abnormalities that are indicative of syndromic RP.

Refractive errors included mild to high myopia (range of spherical equivalents: plan to -12.00D; Table 2.1). Significant lens opacities were observed in 13 patients, most often subcapsular posterior cataracts (seven patients (41%), Table 2.1). Six patients had experienced cataract surgery, most often in the fourth decade (5 of 6 patients). Ophthalmoscopy revealed the classic RP features, including bone spicule pigmentation at the (mid)periphery, attenuated vessels, waxy pallor of the optic disc and atrophy of the RPE and choriocapillaris in all RP patients. In one patient (A-II:5) marked sheathing of the peripheral retinal vessels was noted (Figure 2.3A). In addition, all patients revealed macular abnormalities ranging from subtle changes, such as mottling of the macular RPE as observed in C-II:2 and J-II:1, to profound macular atrophy as was observed in seven patients (mean age: 57 years, range: 36-66, Figure 2.3B). A bull's eye maculopathy (BEM) was a distinctive ophthalmoscopic feature in six patients, which mainly was observed during the fifth and sixth decades of life (mean age: 51 years, range: 32-67 years, Figures 2.3C, 2.3D, and 2.4A). Since the exact onset of

Course of the visual acuity
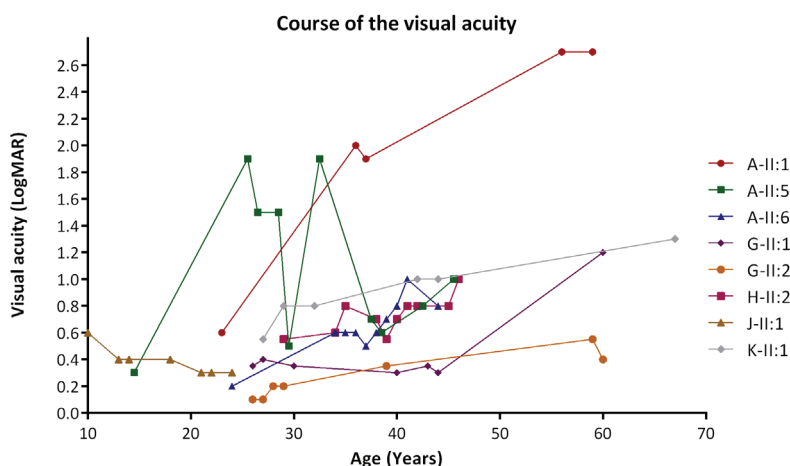
Figure 2.2. Graph showing the change in visual acuity (y-axis) related to the age in years (x-axis) in patients carrying mutations in the IMPG2 gene. Snellen visual acuity was transformed into logarithm of the minimal angle of resolution (logMAR) for visualisation purposes. A logMAR value of 1.9 was assigned to counting fingers (CF), 2.3 to hand movements (HM) and 2.7 to light perception (LP). When the visual acuity differed in both eyes, the visual acuity of the best eye was used. The improvement in visual acuity in patient A-II:5 was seen after cataract surgery; subsequently, the decrease in visual acuity was probably due to cystoid macular edema, which was successfully treated. The cause of the improvement in patient J-II:1 is unclear, since refractive, optical or retinal causes seemed absent.

the BEM could not be ascertained, we were unable to define the interval in which the BEM had been present in these patients. Progression of a BEM to atrophy covering the whole fovea was observed in the follow-up data of patient G-II:1.

Perimetry revealed visual field constriction resulting in tunnel vision of 20° or less in nine patients (mean age: 48 years, range: 23-66 years; Figure 2.5). Macular involvement was apparent by a gradual decrease in central sensitivity, which we observed in 10 patients (mean age: 40 years, range: 23-66 years). We observed paracentral scotomas in two patients (C-II:2 and C-II:3) with a relatively intact (mid)peripheral visual field (Figure 2.5C). Additionally, paracentral scotomas were present in patients F-II:1 and F-II:2, in whom only the central 30° were analyzed with the more sensitive static perimeter (Table 2.1). ERG responses were nonrecordable in 11 patients (mean age: 51 years). In five patients (mean age: 31 years) a severely reduced photoreceptor dysfunction was seen in a rod-cone pattern. Evaluation of color vision resulted in an isolated tritan defect in patients A-II:6, G-II:1 and G-II:2 at age 24, 40 and 39, respectively, whereas patients C-II:2 and C-II:3 demonstrated strong protan, deutan and tritan defects at age 33 and 36, respectively. In patient A-II:5 we did not detect color vision defects.

Table **2.1.** Clinical findings in patients with IMPG2-associated retinitis pigmentosa at their most recent visit.

Family*	Patient ID/AaO (y)/Age(y)/Sex	Initial symptom	Visual Acuity† OD	OS	SER (D)‡ OD	OS	Lens Status	Ophthalmoscopy Results	ERG Results Scotopic	Photopic
A (W01-299)	A-II:1/8/59/F	Decrease in visual acuity	LP (2.7)	LP (2.7)	-4.00	-4.00	PSC cataract; extracted at 37y (RE) and 38y (LE)	BEM, optic disc paleness, peripapillary atrophy, vessel attenuation, RPE atrophy and bone spicule pigmentations in the periphery.	NR (age 8 and 27)	NR (age 8 and 27)
A (W01-299)	A-II:5/14/45/M	Loss of visual field	20/200 (1.0)	LP (2.7)	-0.25	-0.25	PSC cataract; extracted at 24y (LE) and 32y (RE)	Subtle BEM, ERM, peripapillary atrophy, optic disc pallor, attenuated vessels. Periphery: sheating of the vessels, RPE atrophy and bone spicule pigmentations.	SR (age 14 and 30)	SR (age 14 and 30)
A (W01-299)	A-II:6/12/44/M	None, after diagnosis night blindness	20/120 (0.8)	20/400 (1.3)	plan	-0.25	PSC cataract; extracted at 32y (both eyes)	BEM, peripapillary atrophy, pale optic disc, attenuated vessels, RPE atrophy and bone spicule pigmentations in the periphery.	SR (age 12 and 23)	SR (age 12 and 23)
B (MOLO764)	B-II:1/ Child-hood/66/F	Decrease in visual acuity	LP (2.7)	LP (2.7)	-12.00	-11.75	PSC and nuclear cataract	Posterior staphyloma, macular atrophy, optic disc paleness, attenuated vessels, RPE atrophy with bone spicules in periphery	NR	NR
B (MOLO764)	B-II:2/ Child-hood/60/F	Decrease in visual acuity	HM (2.3)	HM (2.3)	-8.25	-5.50	PSC cataract	Myopic changes, RPE atrophy in posterior pole, optic disc pallor, attenuated vessels, RPE atrophy and bone spicules in periphery.	NR	NR
B (MOLO764)	B-II:3/ Child-hood/52/F	Decrease in visual acuity	CF (1.9)	CF (1.9)	-3.00	-3.25	Mild PSC cataract	RPE atrophy in posterior pole, pallor of the optic disc, attenuated vessels, RPE atrophy and bone spicules in the periphery.	NR	NR

| Family* | Patient ID/AaO (y)/Age(y)/Sex | Initial symptom | Visual Acuity† | | SER (D)‡ | | Lens Status | Ophthalmoscopy Results | ERG Results | |
			OD	OS	OD	OS			Scotopic	Photopic
C (W08-1378)	C-II:2/8/33/M	Night blindness	20/50 (0.4)	20/50 (0.4)	-5.50	-7.00	Clear	Mottling of macular RPE, optic disc pallor, subtle peripapillary atrophy, vessel attenuation, midperipheral bone spicules.	NR	NR
C (W08-1378)	C-II:3/8/36/M	Night blindness and decreased color vision	20/50 (0.4)	CF (1.9)	-4.00	-4.50	Small opacities	Macular atrophy with pigment changes, peripapillary atrophy, waxy optic disc, bone spicule pigmentations in the midperiphery.	NR	NR
D (NAP1)	D-II:1/20/65/F	Night blindness	HM (2.3)	HM (2.3)	NP	NP	PSC cataract	Macular atrophy, pallor of the optic disc, attenuation of the vessels, RPE atrophy and bone spicule in the periphery.	NR	NR

Table 2.1. Clinical findings in patients with IMPG2-associated retinitis pigmentosa at their most recent visit. (continued)

Goldmann Perimetry	OCT Results	Autofluorescence Results	Follow-up (y)
NP	Severely thinned retina, generalized loss of the outer retina, central RPE residue with parafoveal RPE atrophy	NP	48
Constricted to 10° with moderately sensitivity loss.	Generalized loss of reflectance of the outer retinal layers, irregular reflective spots just above the RPE reflective band, lowered parafoveal RPE reflectance, ERM with minimal traction inferior of the fovea.	Irregular hypoAF in the macula, normofluorescent aspect surrounding the macula giving the impression of a hyperAF ring, mottled aspect of hypoAF in the midperiphery.	28
Constricted to 10° with moderately sensitivity loss.	Generalized loss of the outer retinal layers, RPE reflectance fairly intact, expect for in the temporal parafovea.	Granular hypoAF aspect of the macula, perifoveal deep hypoAF signal giving the impression of a bull's eye-like aspect, normofluorescent aspect surrounding the macula giving the impression of a hyperAF ring, mottled aspect of hypoAF and larger hypoAF lesions in the midperiphery.	19
Constricted VF up to less than 5°.	Severely thinned central retina.	NP	0
Constricted VF up to 5°.	Severe thinning of central retina, atrophy of the choriocapillaris.	HypoAF macula and peripapillary region, granular hypoAF aspect of midperiphery.	0
Peripheral island	NP	NP	0
Mildly decreased sensitivity with absolute nasal paracentral scotomas	NP	NP	0
Mildly decreased sensitivity, relative and absolute scotomas in the midperiphery, temporal paracentral scotoma.	NP	NP	0
NP	NP	NP	0

Table 2.1. Clinical findings in patients with IMPG2-associated retinitis pigmentosa at their most recent visit. (continued)

Family*	Patient ID/AaO (y)/Age(y)/Sex	Initial symptom	Visual Acuity† OD	OS	SER (D)‡ OD	OS	Lens Status	Ophthalmoscopy Results	ERG Results Scotopic	Photopic
F (RP49)	F-II:1/12/23/M	Night blindness	20/120 (0.8)	20/40 (0.3)	-1.00	-3.00	Clear	Parafoveal atrophy, the optic disc pallor (LE > RE), narrow vessels, few bone spicules in the midperiphery.	NR	NR
F (RP49)	F-II:2/10/32/F	Night blindness	20/120 (0.8)	20/100 (0.7)	-5.75	-6.50	Clear	BEM, ERM, waxy pallor of the optic disc, vessel attenuation (RE > LE), bone spicule pigmentations, generalized retinal degeneration.	NP	NP
G	G-II:1/17/60/M	Night blindness	20/300 (1.2)	20/300 (1.2)	-2.00	-3.00	Clear	Macular atrophy, peripapillary atrophy, bone spicule pigmentations, waxy optic disc, narrow vessels, generalized chorioretinal atrophy.	NR	SR
G	G-II:2/16/59/F	Night blindness	20/30 (0.2)	20/40 (0.3)	-6.00	-7.00	CN cataract	BEM, peripapillary atrophy, waxy optic disc, narrow vessels. Periphery: bone spicule pigmentations and chorioretinal atrophy.	NR (age 37)	NR (age 37)
H	H-II:6/17/46/F	Night blindness	CF (1.9)	20/200 (1.0)	-5.00	-3.75	Cataract extracted at age 35 (RE) and 39 (LE)	Small central area with spared RPE, fovea dark compared to perifovea, but no evident bull's eye, moderate/severe pallor optic disc, severely attenuated vessels, Periphery: bone spicules and drusenoid deposits.	NR (age 34)	NR (age 34)
J	J-II:1/4/23/F	Decrease in visual acuity	20/40 (0.3)	20/40 (0.3)	Plan	Plan	Mild cortical opacities	Mottled macula, moderate pallor, moderate attenuated vessels, RPE atrophy and bone spicules anterior of vascular arcades.	SR (age 18)	SR (age 18)
K	K-II:1/4/67/F	Decrease in visual acuity	20/400 (1.3)	20/400 (1.3)	-4.25	-3.50	Pseudophakia in RE, mild cataract in LE	BEM, pallor of the optic disc, peripapillary pigmentation, severely attenuated vessels, RPE atrophy and intraretinal bone spicule pigmentations in the midperiphery.	SR (age 24)	WNL (age 24)

2

Table 2.1. Clinical findings in patients with IMPG2-associated retinitis pigmentosa at their most recent visit. (continued)

Goldmann Perimetry	OCT Results	Autofluorescence Results	Follow-up (y)
Constricted to 20° with residue inferior. Sensitivity very mildly decreased.	Fairly intact foveal laminar retinal architecture, confluence of the bands corresponding to the ellipsoid inner segments and the RPE, ELM reflectance is only present in the fovea, thinned ONL outside the fovea, minimal CME in the LE, the RPE seems fairly intact except for irregular thinning the fovea and RPE loss in the peripapillary region; profound loss of the outer retinal, RPE and choriocapillaris reflectance in the midperiphery.	Two small hypoAF spots in the otherwise hyperAF macula, subtle hyperAF ring around macula, granular aspect with sporadic hypoAF lesion just anterior of the vascular arcades, prominent blockage of AF by bone spicules.	34
Constricted to <10°, moderately decreased central sensitivity, small inferotemporal residues	Severely thinned central retina, small central residue of the ONL, fairly intact RPE reflectance in the fovea.	HyperAF macula, mottled aspect of hypoAF and larger hypoAF lesions just anterior of the vascular arcades, peripapillary hypoAF.	16
Constricted to 40° with temporal residual VF, mildly decreased central sensitivity in RE, severely decreased central sensitivity in LE	Loss of the bands corresponding the photoreceptor inner and outer segments, severely thinned ONL outside the fovea, irregular reflectance of presumably the ELM in the foveola. RPE reflectance intact in central retina.	Irregular hyperAF in macula (LE>RE), sporadic small hypoAF spots just anterior of the vascular arcades	14
NP	Loss of the bands corresponding the photoreceptor inner and outer segments, severely thinned ONL in the central retina, RPE reflectance intact except for in the parafovea.	Mottled hypoAF aspect of the perifoveal region, hyperAF in the fovea, mottled hypoAF aspect just anterior of the vascular arcades.	41

AaO = Age at onset; BEM = bull's eye maculopathy; CF = counting fingers; CME = cystoid macular edema; CN = corticonuclear; D = diopters; ELM = external limiting membrane; ERG = electroretinogram; ERM = epiretinal membrane; F = female HM = hand movements; IS = inner segments; LE = left eye; LP = light perception; M = male; MR = moderately reduced; NP = not performed; NR = nonrecordable; OCT = optical coherence tomography; ONL = outer nuclear layer; OS = outer segments; PSC = posterior subcapsular; RE = right eye; RPE = retinal pigment epithelium; SER = spherical equivalent refraction; SR = severely reduced; TD = time-domain; VF = visual field; y = years. *The family ID between brackets are those used before in reference 13. For readability issues, we preferred one letter family IDs. †The visual acuity is in noted in both Snellen visual acuity and logMAR visual acuity (between brackets). ‡If cataract surgery have been performed, the pre-surgery SER was noted.
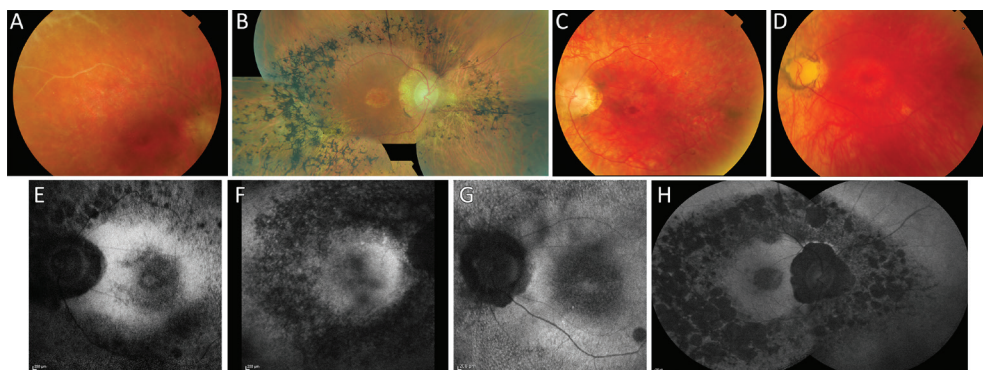
Figure 2.3. Fundus photographs (FP) and fundus autofluorescence (FAF) imaging of patients carrying mutations in IMPG2. **A/F,** FP of temporal superior region of the retina (A), showing sheating of the retinal vessels, and FAF imaging of the central retina (F), revealing irregular FAF signal in the macula and a granular hypoautofluorescent aspect of the RPE surrounding the posterior pole, in patient A-II:5 (age 45). **B/H,** FP composition (B), showing macular atrophy, and FAF images (H), revealing a hypoautofluorescent macula, a granular aspect with large confluent hypoautofluorescent lesions in the midperiphery, and peripapillary hypoautofluorescence, of patient G-II:1 (age 60). **C/E**, FP (C) and FAF image (E) of the central retina in patient A-II:6 (age 44). The FP reveals a bull's eye maculopathy (BEM). The FAF image shows granular aspect of the macula, whereas deeper perifoveal hypoautofluorescence gives the impression of a BEM, mottled aspect of midperiphery with larger hypoautofluorescent lesions. **D/G**, FP (D) and FAF image (G) of the central retina in patient K-II:1 (age 67). The FP shows a BEM, whereas FAF reveals a mottled hypoautofluorescent aspect of the perifoveal region, hyperautofluorescence in the fovea, as well as a mottled aspect just anterior of the vascular arcades.

FAF images revealed macular involvement in all eight patients of whom FAF imaging was available. The macular aspects varied from hyperautofluorescence to profound hypoautofluorescent RPE lesions (mean age: 51 years, range: 23-67 years, Figures 2.3E-G, 2.3I, 2.4B). Midperipheral changes include granular or mottled hypoautofluorescent changes that are spread to the vascular arcades. In some patients, large (confluent) hypoautofluorescent lesions were observed just anterior of the vascular arcades (Figures 2.3E, 2.3H). Evaluation of the central retinal structure with SD-OCT revealed loss of photoreceptors prior to RPE cell loss, which eventually result in moderate to severe retinal thinning (Figure 2.6A). The foveal volume in seven Dutch RP patients (mean age: 49 years, range: 23-67) was significantly lower compared to the foveal volume in 25 age-matched Dutch healthy controls (p<0.0001; Figure 2.6B). In all patients with high-resolution SD-OCT except in G-II:2, the bands corresponding to the photoreceptor inner and outer segments were lost.[24] The outer nuclear layer, containing the photoreceptor cell bodies, was concentrically lost and severely thinned where present. We observed concentric atrophy of the layer that corresponds to the RPE cells that progressed from the midperiphery. The central abnormalities in the RPE layer started in the parafoveal region, as was observed in four patients who also revealed a BEM (Figure 2.6D). In patient J-II:1, who displayed mottling in the macula, the RPE appeared normal on SD-OCT (Figure 6E). In later stages of the disease, we observed loss of the foveal RPE layer, which was highlighted by a increased beam penetration and choroidal reflection in patient E-II:4 and G-II:1 (Figure 2.6F). SD-OCT scans in the midperiphery revealed loss of the photoreceptor-RPE complex and intraretinal pigment deposits in patients G-II:1 and G-II:2 at age 60 and 59, respectively (Figure 6G), whereas patient J-II:1 at the age of 23 only revealed photoreceptor loss (Figure 2.6H).
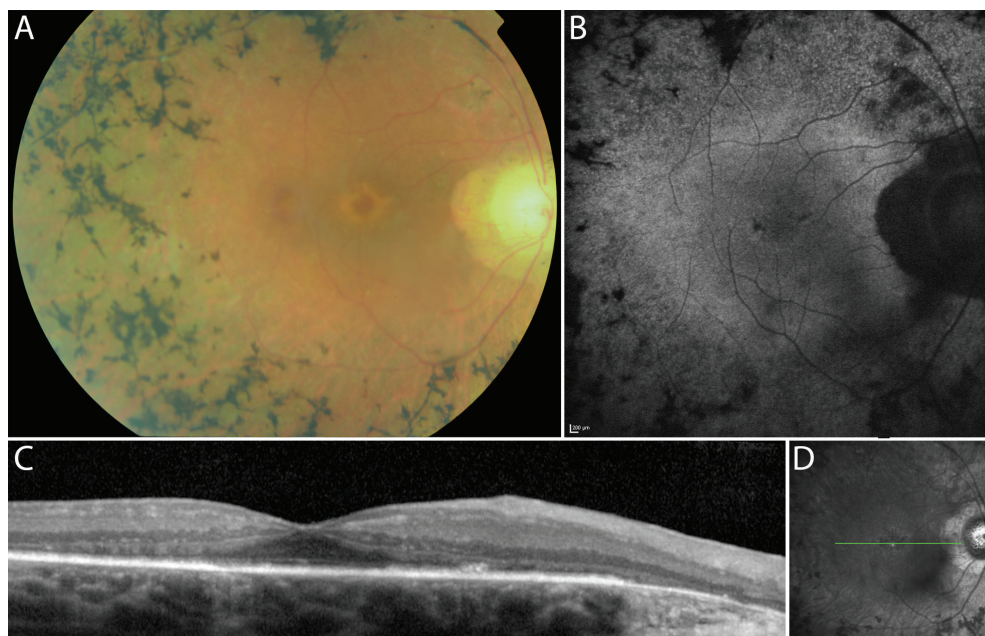
Figure 2.4. Multimodal imaging of the central retina in patient G-II:2 at the age of 59. **A,** Fundus photograph showing a bull's eye maculopathy, attenuated vessels, peripapillary atrophy, pale optic disc, bone-spicule pigmentations and chorioretinal atrophy in the midperiphery. **B,** Autofluorescence imaging shows a subtle hyperautofluorescent ring around the macula, spots of decreased macular and peripheral autofluorescence and absence of autofluorescence corresponding with the peripapillary atrophy. **C,** SD-OCT reveals loss of the bands corresponding to the photoreceptor inner and outer segments in the macula. The external limiting membrane (ELM) is only present in the fovea. The RPE layer seems fairly intact, except for irregular thinning in the fovea and loss of RPE in the peripapillary region. **D,** Infrared en face image reveals the location of the SD-OCT image (green line).

Mutation analysis

A description of the molecular genetic findings in families A-F were reported earlier.[13] In summary, sequence analysis of all 19 coding exons of *IMPG2* led to the identification of 10 different pathogenic variants in these 17 patients (Table 2.2). In the families with available family members, the homozygous or compound heterozygous mutations segregated completely with the RP phenotype (Figure 2.1).[13]

In addition to the mutations described earlier,[13] four new pathogenic variants in *IMPG2* were identified. In family G, a targeted next generation sequencing approach that covered 111 blindness genes resulted in two compound heterozygous mutations: a nonsense mutation (p.Arg127*), which is predicted to cause premature truncation of the IMPG2 protein, and a 4-base-pair deletion (c.3423-8_c.3423-5del) that affects the splice acceptor site (Table 2.2).[22] Reverse transcriptase polymerase chain reaction analysis on RNA isolated from patient's lymphoblastoid cells revealed that, instead of the regular splice acceptor site, a second splice site located upstream in the same intron is used that results in the inclusion of 80 additional nucleotides to *IMPG2* mRNA, subsequently leading to a frameshift
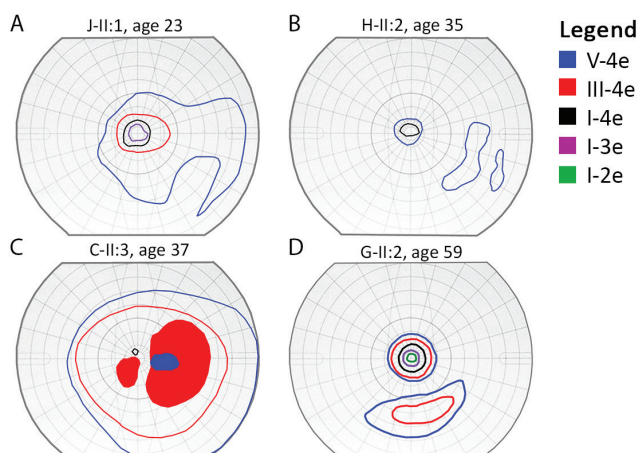
Figure 2.5. Goldmann perimetry findings in the right eyes of patients J-II:1 (age 23, A), H-II:2 (age 35, B) C-II:3 (age 37, C) and G-II:2 (age 59, D). The colored lines indicate the outer borders of the isopters. The filled areas indicate scotomas for the isopter of that color.

and premature termination of IMPG2 (Figure 2.7). cDNA products generated from RNAs isolated from cells grown under nonsense-mediated decay (NMD) suppressing conditions show subtle differences compared to those generated from RNAs isolated from cells grown under normal conditions. Growing cells under NMD-suppressing conditions did not yield an obvious difference in the amount of aberrantly spliced IMPG2, indicating that a truncated protein may be produced. The other novel mutations include a nonsense mutation (p.Tyr171*) and a missense mutation (p.Ser379Pro). The nonsense mutation is predicted to cause a premature truncation of IMPG2. The p.Ser379Pro missense mutation changes a highly conserved amino acid and is unanimously predicted to be pathogenic by multiple *in silico* prediction tools (SIFT: deleterious [score: 0], Polyphen-2: probably damaging [score: 1.000], Align GVGD: Class C65, MutationTaster: disease causing [probability: 0.994], Grantham score: 74, PROVEAN prediction: deleterious [score: -2.972]).

Discussion

The phenotype of IMPG2-associated RP

In this study we provide a detailed clinical description of the RP associated with mutations in *IMPG2,* a gene that recently was added to the long list of genes that may cause autosomal recessive RP when mutated.[13] Most of the patients with *IMPG2*-associated RP demonstrated the classic RP symptoms: night blindness and progressive concentric loss of the visual field. However, six out of 17 patients mentioned a decrease in BCVA as the initial symptom, that could not be attributed to amblyopia. Loss of vision as initial symptom is not just a result of our electrically illuminated night-time environment that compensates for an impaired night vision,[4, 5] but a consequence of macular abnormalities that are a prominent feature of this type of RP. Overall, the BCVA progressively decreased during the first four decades of life,
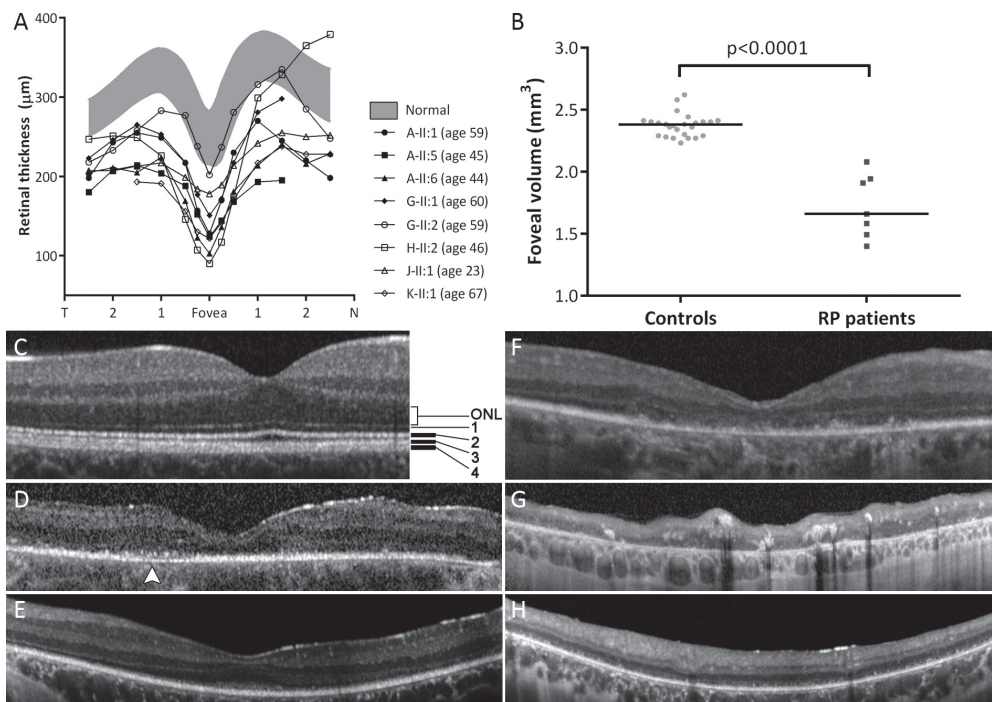
Figure 2.6. OCT examinations in patients with IMPG2-associated RP. **A,** Thickness of the total retina in eight Dutch patients (mean age: 49 years, range: 23-67). Shaded areas: normal limits (mean ± 2 standard deviations) as measured in 25 controls (mean age: 46 year). **B**, Foveal volume (mm^3) measured in the central 3 mm^2 in these patients except patient A-II:1. The foveal volume in seven Dutch IMPG2-associated RP patients (mean age: 49 years, range: 23-67) was significantly lower than in 25 age-matched healthy Dutch controls (p<0.0001). The horizontal bars indicate the median of the corresponding cohort. **C,** SD-OCT scan of a normal central retina (age: 25). The hyperreflective bands correspond to the external limiting membrane (1), the ellipsoid photoreceptor inner segments (2), the photoreceptor outer segment/RPE contact cylinder region (3) and the RPE (4).[24] **D**, SD-OCT of patient A-II:6 (age 44) that reveals generalized loss of the outer retinal layers, whereas the RPE reflectance is fairly intact expect for the irregular signal and thinning in the temporal parafovea (white arrowhead). **E/H**, SD-OCT in patient J-II:1 (age 23). The central retina (E) revealed normal bands corresponding to the RPE, whereas the photoreceptor bands are absent outside the fovea. The midperipheral retina (H) reveals loss of the photoreceptor inner and outer segments bands. However, no profound RPE atrophy or intraretinal pigment deposits were observed yet. **F/G**, SD-OCT of patient G-II:1 (age 60). The central retina (F) reveals generalized loss of photoreceptor inner and outer segments, a thinned ONL, and patchy loss/thinning of the foveal RPE. The midperipheral retina (G) shows profound loss of the outer retinal layers, RPE and choriocapillaris reflectance, as well as intraretinal pigment deposits. ONL, outer nuclear layer.

and subsequently deteriorates to levels lower than 20/300 during the fifth and sixth decade of life. The only exception was patient G-II:2, who still enjoyed a BCVA of 20/30 at the age of 59.

Thirteen of the 17 RP patients included in this study showed significant macular abnormalities: a BEM was observed in six patients (mean age: 51 years) and profound macular atrophy

Figure 2.7. Reverse transcription-PCR of IMPG2 mRNA of affected individuals of family G. Reverse transcription (RT)-PCR analysis of IMPG2 amplicon containing exons 16 and 17 in family G showing the consequence of the c.3423-8_3423-5del mutation. An extra band containing 80 additional nucleotides is visible in cDNA samples of both affected siblings (G-II:1 and G-II:2). To rule out the possibility of aberrant transcripts undergoing nonsense-mediated decay (NMD), part of the cells from each individual was cultured with cycloheximide (CH), an NMD-blocking agent. The amount of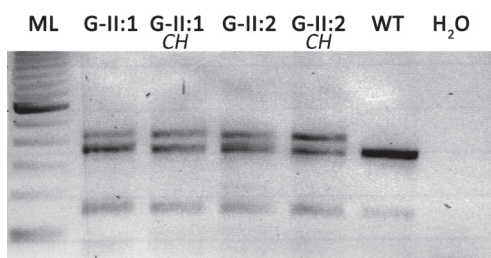 aberrant cDNA splice products generated from cells grown under NMD-suppressing conditions (G-II:1 CH and G-II:2 CH) show a slight increase compared to the products generated without NMD-suppressing conditions (G-II:1 and G-II:2). ML, 100-bp ladder; WT, wild-type control cDNA; H_2O, negative control (water).

in seven patients (mean age: 57 years). We hypothesize that the perifoveal atrophy, manifesting as a bull's eye pattern, eventually progresses to macular atrophy with profound degeneration of photoreceptors and RPE, although this was only observed in patient G-II:1 since longitudinal data of the other patients with macular atrophy were not available. The 13 patients with macular involvement displayed a decreased central sensitivity and/or paracentral scotomas on visual field examination in addition to the concentric constriction that is typically seen in RP (Table 2.1, Figure 2.5). SD-OCT of the macula showed early loss of photoreceptor inner and outer segments prior to loss of the RPE layer in the central retina. On FAF imaging, macular hypoautofluorescence was observed, whereas hypoautofluorescence in the midperiphery generally had a granular aspect. In contrast to the significant macular involvement that was observed in the majority of patients, subtle macular FAF abnormalities appeared in patients C-II:2 and J-II:1. However, subtle macular FAF abnormalities have been observed in other forms of RP with intact central vision and therefore do not automatically predate loss of macular function.[25]

A BEM is a non-specific reaction of the posterior pole, which can occur in various diseases affecting the bipolar cell layer, photoreceptor cell layer or RPE.[26] It is not often observed in RP, but has been reported in some specific forms of syndromic and nonsyndromic RP,[27-31] and is associated with a faster deterioration of the visual acuity compared to RP without specific macular lesions.[32] Concerning the BEM in *IMPG2*-associated RP, multimodal imaging revealed abnormalities in the photoreceptor and RPE cell layers. However, it is unclear why RPE abnormalities initially predominate in the perifoveal region, since the preceding abnormalities in the photoreceptor layer are ubiquitously present. Possible explanations may include topographical differences in metabolism and cell densities,[33] the higher vulnerability of S ('blue') cone photoreceptors to retinal disease compared to M and L cones,[34] and the higher vulnerability of parafoveal rods to aging and light-induced damage.[35-37] In patient G-II:2 (age 59), we observed a prominent BEM due to hypopigmentation rather than atrophy of the

Table 2.2 Mutations identified in the *IMPG2* genes in the patients with inherited retinal disease included in this study.

ID	Inheritance	Origin	Allele 1		Allele 2		Type of mutations	Consanguinity
			cDNA variant	Effect	cDNA variant	Effect		
A-II:1	AR	Dutch	c.888-1554_908+274del	p.Arg296_Asp302 del	c.888-1554_908+274del	p.Arg296_Asp302 del	Deletion	None
A-II:5	AR	Dutch	c.888-1554_908+274del	p.Arg296_Asp302 del	c.888-1554_908+274del	p.Arg296_Asp302 del	Deletion	None
A-II:6	AR	Dutch	c.888-1554_908+274del	p.Arg296_Asp302 del	c.888-1554_908+274del	p.Arg296_Asp302 del	Deletion	None
B-II:1	AR	Iraqi Jew	c.635C→G	p.Ser212*	c.635C→G	p.Ser212*	Nonsense	First cousins
B-II:2	AR	Iraqi Jew	c.635C→G	p.Ser212*	c.635C→G	p.Ser212*	Nonsense	First cousins
B-II:3	AR	Iraqi Jew	c.635C→G	p.Ser212*	c.635C→G	p.Ser212*	Nonsense	First cousins
C-II:2	AR	Dutch	c.2716C→T	p.Arg906*	c.2716C→T	p.Arg906*	Nonsense	Second cousins
C-II:3	AR	Dutch	c.2716C→T	p.Arg906*	c.2716C→T	p.Arg906*	Nonsense	Second cousins
D-II:1	AR	Italian	c.2890C→T	p.Arg964*	c.2890C→T	p.Arg964*	Nonsense	Second cousins
E-II:4	Isolated	Italian	c.3262C→T	p.Arg1088*	c.3262C→T	p.Arg1088*	Nonsense	First cousins
F-II:1	AR	Pakistan	c.1680T→A	p.Tyr560*	c.1680T→A	p.Tyr560*	Nonsense	First cousins
F-II:2	AR	Pakistan	c.1680T→A	p.Tyr560*	c.1680T→A	p.Tyr560*	Nonsense	First cousins
G-II:1	AR	Dutch	c.379G→A	p.Arg127*	c.3423-8_c.3423-5del	Splicing	Nonsense / Deletion	Second cousins
G-II:2	AR	Dutch	c.379G→A	p.Arg127*	c.3423-8_c.3423-5del	Splicing	Nonsense / Deletion	Second cousins
H-II:2	AR	Dutch	c.513T→G	p.Tyr171*	c.2716C→T	p.Arg906*	Nonsense	None
J-II:1	Isolated	Dutch	c.2716C→T	p.Arg906*	c.2716C→T	p.Arg906*	Nonsense	None
K-II:1	Isolated	Dutch	c.1135T→C	p.Ser379Pro	c.2716C→T	p.Arg906*	Nonsense	None

AR = autosomal recessive; NI = not identified; del = deletion, * = premature stop.

Nonsense mutations change a DNA codon for an amino acid in a stop codon, inducing a premature truncation of the protein. Deletions remove one or more nucleotides from the DNA, which can alter the reading frame. In these cases, the deletions cause frameshifts and prematurely truncated proteins. Missense mutations change a DNA codon for an amino acid in a codon for another amino acid. These mutations can have structural or functional effects on the protein depending on the domain the mutation occurs in. Missense mutations generally have less severe effects on protein function when compared to nonsense mutations or frameshift-inducing deletions. The p.Arg906* mutation was identified frequently in the Dutch patients included in this study (9/22 alleles, 41%) and may be a Dutch founder mutation.

perifoveal RPE, since there were only minor RPE changes on FAF imaging (Figure 2.4B) and mild changes of the band corresponding to the photoreceptor outer segment-RPE complex (Figure 2.4C). By contrast, other patients with BEM revealed perifoveal hypoautofluorescence indicating perifoveal RPE atrophy (Figure 2.3E and 2.3G). In late stages of the disease, profound macular hypoautofluorescence developed, which is indicative of RPE atrophy (Figure 2.3H). In the light of future therapeutic options for retinal dystrophies, knowledge of the natural course of *IMPG2*-associated retinal disease is necessary to select patients amenable for treatment and to correctly interpret the effect of therapeutic intervention.

Genotype-phenotype correlation

Bandah-Rozenfeld *et al.* only identified mutations with severe effects on the IMPG2 protein in RP patients, whereas a homozygous mild missense mutation was identified in one patient with a mild maculopathy.[13] In families G-K, we identified two novel truncating nonsense mutations (families G and H), a deletion causing a splice defect (family G) and a missense mutation that is unanimously predicted to be pathogenic (family K). The function of IMPG2 is vital for retinal survival and function, since the majority of *IMPG2* mutations that are identified in our patients can be considered true loss-of-function alleles. Until now only one homozygous mild (missense) mutation in *IMPG2* has been described in a single patient with an isolated maculopathy and a mildly affected visual function.[13] This might indicate that a minimal loss of function of the IMPG2 protein may result in mild or even absent retinal disease.

Each of the seven nonsense mutations lead to either mRNA breakdown because of nonsense-mediated decay, or predicted truncated IMPG2 proteins that all lack the transmembrane domain and the cytoplasmic tail. The in-frame deletion identified in family A (c.888-1554_908+274del; absence of 7 amino acids) is thought to result in a nonfunctional IMPG2 protein, as in a cellular transfection assay this mutant protein was retained in the endoplasmic reticulum, while IMPG2 is physiologically located in the cell membrane.[13] The 4-base-pair deletion of the splice acceptor site in family G (c.3423-8_c.3423-5del) was found to result in the use of an alternative splice acceptor site, and thereby also predict to result in the generation of a truncated protein that most likely has reduced or no remaining function. Interestingly, the p.Arg906* was present in 8 of 20 alleles (40%) in 10 Dutch patients, which may imply a founder mutation in the Dutch population.

Since the identified mutations cause (near-)complete loss of IMPG2 function, the clinical variation is limited in *IMPG2*-associated RP. The patients in family G, however, retained slightly better visual acuity and visual field compared to the other patients (Figure 2.2, Table 2.1). This could imply that the splice defect in this family results in an IMPG2 protein with some residual function. However, functional assays are needed to reveal the true effect of the c.3423-8_c.3423-5 deletion, since there also is evidence of modifying factors in this family (Table 2.1; Figures 2.2, 2.3B, 2.3H, and 2.4) that influence the intrafamilial differences.

The IMPG2 protein (SPACRCAN) is highly homologous to SPACR, the product of the interphotoreceptor matrix proteoglycan 1 (*IMPG1*) gene, which has been linked to benign concentric annular macular dystrophy (BCAMD) and vitelliform macular dystrophy (VMD).[38,][39] Interestingly, BCAMD includes parafoveal hypopigmentation and RP-like fundoscopic changes in the end-stage disease, although visual acuity is generally better preserved

than in the *IMPG2*-associated RP patients in this report.[38] The *IMPG1*-associated vitelliform dystrophy is also associated with macular pathology, although this is characterized by accumulation of lipofuscin rather than a BEM.[39]

In conclusion, severe mutations in *IMPG2* are the cause of an autosomal recessive RP phenotype that manifests in the early teens and is accompanied by atrophic maculopathy often in a bull's eye pattern. In early disease stages, the maculopathy is characterized by mild RPE alterations, but in later stages of the disease a BEM and profound macular chorioretinal atrophy may occur. In most patients, the RP phenotype arising from mutations in the *IMPG2* gene is severe, because of the unfortunate combination of progressive constriction of the visual fields and maculopathy that occurs relatively early in the course of the disease.

References

1. Bunker CH, Berson EL, Bromley WC, Hayes RP, Roderick TH. Prevalence of retinitis pigmentosa in Maine. Am J Ophthalmol 1984;97:357-365.
2. Rosenberg T. Epidemiology of hereditary ocular disorders. Dev Ophthalmol 2003;37:16-33.
3. Berson EL. Retinitis pigmentosa. The Friedenwald Lecture. Invest Ophthalmol Vis Sci 1993;34:1659-1676.
4. Hartong DT, Berson EL, Dryja TP. Retinitis pigmentosa. Lancet 2006;368:1795-1809.
5. Hamel C. Retinitis pigmentosa. Orphanet J Rare Dis 2006;1:40.
6. Dryja TP, Hahn LB, Kajiwara K, Berson EL. Dominant and digenic mutations in the peripherin/RDS and ROM1 genes in retinitis pigmentosa. Invest Ophthalmol Vis Sci 1997;38:1972-1982.
7. den Hollander AI, Roepman R, Koenekoop RK, Cremers FP. Leber congenital amaurosis: genes, proteins and disease mechanisms. Prog Retin Eye Res 2008;27:391-419.
8. Schrier SA, Falk MJ. Mitochondrial disorders and the eye. Curr Opin Ophthalmol 2011;22:325-331.
9. Kajiwara K, Berson EL, Dryja TP. Digenic retinitis pigmentosa due to mutations at the unlinked peripherin/RDS and ROM1 loci. Science (80-) 1994;264:1604-1608.
10. den Hollander AI, Black A, Bennett J, Cremers FP. Lighting a candle in the dark: advances in genetics and gene therapy of recessive retinal dystrophies. J Clin Invest 2010;120:3042-3053.
11. Neveling K, Feenstra I, Gilissen C, et al. A post-hoc comparison of the utility of sanger sequencing and exome sequencing for the diagnosis of heterogeneous diseases. Hum Mutat 2013;34:1721-1726.
12. Berger W, Kloeckener-Gruissem B, Neidhardt J. The molecular basis of human retinal and vitreoretinal diseases. Prog Retin Eye Res 2010;29:335-375.
13. Bandah-Rozenfeld D, Collin RW, Banin E, et al. Mutations in IMPG2, encoding interphotoreceptor matrix proteoglycan 2, cause autosomal-recessive retinitis pigmentosa. Am J Hum Genet 2010;87:199-208.
14. Inatani M, Tanihara H. Proteoglycans in retina. Prog Retin Eye Res 2002;21:429-447.
15. Adler AJ, Klucznik KM. Proteins and glycoproteins of the bovine interphotoreceptor matrix: composition and fractionation. Exp Eye Res 1982;34:423-434.
16. Hageman GS, Johnson LV. Structure, composition and function of the retinal interphotoreceptor matrix. In: Osborne N, Chader G (eds), Retinal Research. New York: Pergamon Press; 1991:207-249.
17. Berman ER. Mucopolysaccharides (glycosaminoglycans) of the retina: identification, distribution and possible biological role. Bibl Ophthalmol 1969;79:5-31.
18. Hewit AT, Adler R. The retinal pigment epithelium and interphotoreceptor matrix: structure and specialized function. In: Ryan SJ (ed), Retina. St. Louis: CV Mosby Co; 1989:57-64.
19. Enoch JM, Laties AM. An analysis of retinal receptor orientation. II. Predictions for psychophysical tests. Invest Ophthalmol 1971;10:959-970.
20. Acharya S, Foletta VC, Lee JW, et al. SPACRCAN, a novel human interphotoreceptor matrix hyaluronan-binding proteoglycan synthesized by photoreceptors and pinealocytes. J Biol Chem 2000;275:6945-6955.
21. Chen Q, Cai S, Shadrach KG, Prestwich GD, Hollyfield JG. Spacrcan binding to hyaluronan and other glycosaminoglycans. Molecular and biochemical studies. J Biol Chem 2004;279:23142-23150.
22. Neveling K, Collin RW, Gilissen C, et al. Next Generation Genetic Testing for Retinitis Pigmentosa. Hum Mutat 2012.
23. Marmor MF, Fulton AB, Holder GE, Miyake Y, Brigell M, Bach M. ISCEV Standard for full-field clinical electroretinography (2008 update). Doc Ophthalmol 2009;118:69-77.
24. Spaide RF, Curcio CA. Anatomical correlates to the bands seen in the outer retina by optical coherence tomography: literature review and model. Retina 2011;31:1609-1619.
25. Makiyama Y, Ooto S, Hangai M, et al. Macular cone abnormalities in retinitis pigmentosa with preserved central vision using adaptive optics scanning laser ophthalmoscopy. PLoS One 2013;8:e79447.
26. Pinckers A, Cruysberg JR, aan de Kerk AL. Main types of bull's eye maculopathy. Functional classification. Doc Ophthalmol 1984;58:257-267.

27. Campo RV, Aaberg TM. Ocular and systemic manifestations of the Bardet-Biedl syndrome. Am J Ophthalmol 1982;94:750-756.

28. Koenekoop RK, Loyer M, Hand CK, et al. Novel RPGR mutations with distinct retinitis pigmentosa phenotypes in French-Canadian families. Am J Ophthalmol 2003;136:678-687.

29. Kikawa E, Nakazawa M, Chida Y, Shiono T, Tamai M. A novel mutation (Asn244Lys) in the peripherin/RDS gene causing autosomal dominant retinitis pigmentosa associated with bull's-eye maculopathy detected by nonradioisotopic SSCP. Genomics 1994;20:137-139.

30. Demirci FY, Gupta N, Radak AL, et al. Histopathologic study of X-linked cone-rod dystrophy (CORDX1) caused by a mutation in the RPGR exon ORF15. Am J Ophthalmol 2005;139:386-388.

31. Michaelides M, Gaillard MC, Escher P, et al. The PROM1 mutation p.R373C causes an autosomal dominant bull's eye maculopathy associated with rod, rod-cone, and macular dystrophy. Invest Ophthalmol Vis Sci 2010;51:4771-4780.

32. Flynn MF, Fishman GA, Anderson RJ, Roberts DK. Retrospective longitudinal study of visual acuity change in patients with retinitis pigmentosa. Retina 2001;21:639-646.

33. Curcio CA, Sloan KR, Kalina RE, Hendrickson AE. Human photoreceptor topography. J Comp Neurol 1990;292:497-523.

34. Greenstein VC, Hood DC, Ritch R, Steinberger D, Carr RE. S (blue) cone pathway vulnerability in retinitis pigmentosa, diabetes and glaucoma. Invest Ophthalmol Vis Sci 1989;30:1732-1737.

35. Curcio CA. Photoreceptor topography in ageing and age-related maculopathy. Eye (Lond) 2001;15:376-383.

36. Curcio CA, Millican CL, Allen KA, Kalina RE. Aging of the human photoreceptor mosaic: evidence for selective vulnerability of rods in central retina. Invest Ophthalmol Vis Sci 1993;34:3278-3296.

37. Okano K, Maeda A, Chen Y, et al. Retinal cone and rod photoreceptor cells exhibit differential susceptibility to light-induced damage. J Neurochem 2012;121:146-156.

38. van Lith-Verhoeven JJ, Hoyng CB, van den Helm B, et al. The benign concentric annular macular dystrophy locus maps to 6p12.3-q16. Invest Ophthalmol Vis Sci 2004;45:30-35.

39. Manes G, Meunier I, Avila-Fernandez A, et al. Mutations in IMPG1 cause vitelliform macular dystrophies. Am J Hum Genet 2013;93:571-578.

Authors

Ramon A.C. van Huet,[1] Anna M. Siemiatkowska,[2] Riza Köksal Özgül,[3] Didem Yücel,[3] Carel B. Hoyng,[1]
Eyal Banin,[4] Anat Blumenfeld,[4] Ygal Rotenstreich,[5] Frans C.C. Riemslag,[6,7] Anneke I. den Hollander,[1,2,8]
Thomas Theelen,[1] Rob W.J. Collin,[2,8] L. Ingeborgh van den Born,[6] B. Jeroen Klevering[1]

Affiliations

[1]Department of Ophthalmology, Radboud University Medical Center, Nijmegen, The Netherlands;
[2]Department of Human Genetics, Radboud University Medical Center, Nijmegen, The Netherlands;
[3]Institute of Child Health and Metabolism Unit, Department of Pediatrics, Hacettepe University, Ankara,
Turkey;
[4]Department of Ophthalmology, Hadassah-Hebrew University Medical Center, Jerusalem, Israel;
[5]Electrophysiology Clinic, Goldschleger Eye Research Institute, Tel Aviv University, Sheba Medical
Centre, Israel;
[6]The Rotterdam Eye Hospital, Rotterdam, The Netherlands;
[7]Bartiméus, Institute for the visually handicapped, Zeist, The Netherlands;
[8]Nijmegen Center for Molecular Life Sciences, Radboud University Medical Center, Nijmegen,
The Netherlands.

Retinitis pigmentosa caused by mutations in the ciliary *MAK* gene is relatively mild and is not associated with apparent extra-ocular features

3

Abstract

Purpose. Defects in MAK, encoding a protein localized to the photoreceptor connecting cilium, have recently been associated with autosomal recessive retinitis pigmentosa (RP). The aim of this study is to describe our detailed clinical observations in patients with MAK-associated RP, including an assessment of syndromic symptoms frequently observed in ciliopathies.

Methods. In this international collaborative study, 11 patients carrying nonsense or missense mutations in MAK were clinically evaluated, including extensive assessment of the medical history, slit-lamp biomicroscopy, ophthalmoscopy, kinetic perimetry, electroretinography (ERG), spectral-domain optical coherence tomography (SD-OCT), autofluorescence imaging, and fundus photography. Additionally, we used a questionnaire to evaluate the presence of syndromic features and tested the olfactory function.

Results. MAK-associated RP is not associated with syndromic features, not even with subclinical dysfunction of the olfactory apparatus. All patients experienced typical RP symptoms of night blindness followed by visual field constriction. Symptoms initiated between childhood and the age of 43 (mean: 23 years). Although some patients experienced vision loss, the visual acuity remained normal in most patients. ERG and ophthalmoscopy revealed classic RP characteristics, and SD-OCT demonstrated thinning of the overall retina, outer nuclear layer and photoreceptor-pigment epithelium complex.

Conclusion. Nonsense and missense mutations in MAK give rise to a non-syndromic recessive RP phenotype without apparent extra-ocular features. When compared to other retinal ciliopathies, MAK-associated RP appears to be relatively mild and shows remarkable resemblance to RP1-associated RP, which could be explained by the close functional relation of these proteins.

Introduction

Retinitis pigmentosa (RP) comprises a group of inherited retinal dystrophies that share clinical characteristics but display an impressive heterogeneity in phenotype and genotype. Symptoms include progressive loss of night vision and peripheral visual field loss that results in tunnel vision. Eventually patients may lose central vision.[1,2] Although normal in early stages, the fundus appearance in advanced RP reveals attenuated retinal vessels, waxy pallor of the optic disc, retinal pigment epithelium (RPE) atrophy and bone spicule pigmentations.[1,2] Full-field electroretinography (ERG) typically shows reduced responses, where rod-driven responses generally are equally or more affected than cone-driven responses.

Mutations in the *MAK* gene, which encodes male germ cell-associated kinase, have recently been associated with retinal degeneration in mice and autosomal recessive RP in humans.[3-5] The MAK protein is involved in regulating ciliary length in many species,[3,6,7] and non-functional MAK results in elongation of the photoreceptor connecting cilium, diminished ciliary transport (intraflagellar transport, IFT) and subsequent photoreceptor degeneration in mice.[3]

Diseases that involve dysfunction of the cilium are generally referred to as ciliopathies.[8] They include multi-organ syndromic phenotypes, since the mutated ciliary genes are expressed in multiple tissues,[9-11] although mutations in ubiquitously expressed ciliary genes may also result in single-organ disease.[12] Expression of *MAK* was first identified in murine testicular germ cells.[13] Subsequently, expression in photoreceptors, olfactory receptors and in the epithelium of the respiratory tract and choroid plexus has been shown in mice.[14,15] Nevertheless, no syndromic features have been observed in Mak^{-/-} mice.[3]

In a recent study, Stone and colleagues described the ophthalmic features observed in 24 *MAK*-associated RP patients. In that study, all but one patient were from Ashkenazi Jewish origin and carried a homozygous 353-base pair insertion in exon 9, which results in loss of the retina-specific isoform of MAK.[16] Although the *MAK* exon 9 insertion is the most frequent cause of RP in Ashkenazi Jews, this insertion has so far not been identified in individuals from other origins.[4,16] Detailed clinical features of RP patients carrying missense or nonsense mutations in *MAK* have not been described yet. In addition, the presence of syndromic features has thus far not been evaluated in any *MAK*-related RP patient.

In this report, we describe the clinical results of an international collaborative study that investigated the clinical characteristics and possible syndromic associations of 11 patients with RP caused by nonsense or missense mutations in *MAK*.

Patients and Methods

Patients

Eleven RP patients with mutations in *MAK* from 7 families were studied at Hacettepe University in Ankara, Turkey (by RKÖ, family A); the Radboud University Medical Centre in Nijmegen, the Netherlands (by RACvH, CBH and BJK, families B-D); the Rotterdam Eye Hospital in Rotterdam, the Netherlands (by LIvdB and FCCR, family E); the Hadassah-Hebrew University Medical Center in Jerusalem, Israel (by EB, family F) and the Goldschleger Eye Research Institute in Sheba Medical Center, Israel (by YR, family G).

This study adhered to the tenets of the Declaration of Helsinki and informed consent was obtained from all participating patients prior to blood withdrawal and additional ophthalmologic examinations. Prior to this study, we obtained institutional review board approvals.

Genetic analysis

In six families (families A-F), *MAK* mutations were identified as described previously.[4] Genetic analysis using Sanger sequencing of all exons and intron-exon boundaries of *MAK* in the probands of five genetically unsolved families of Iraqi origin resulted in the identification of a homozygous mutation in one family, which was included in this study. The most recent human genome variation society (HGVS) nomenclature was used (http://www.hgvs.org/mutnomen/).

Clinical analysis

Clinical data were collected from the medical records of these patients. Following the identification of causative *MAK* mutations, six patients (families B, C, D and E) were re-evaluated in addition to the data collected during routine visits over the years. Medical history was registered with a focus on age of onset, initial symptoms and overall course of the retinal disorder. Age of onset was defined as the age at which the initial symptom was first noticed by the patient. The initial symptom was defined as the first symptom noted by the patient.

The ophthalmic clinical examination included best-corrected visual acuity (BCVA), slit-lamp biomicroscopy, ophthalmoscopy, and fundus photography. Goldmann perimetry was performed using targets V-4e, III-4e, I-4e, I-3e, I-2e and I-1e in all but two patients: patient A-IV:1 underwent a full-field 120 point screening test using the Humphrey Field Analyser II (Carl Zeiss, Dublin, CA, USA); perimetry was unavailable in case F-II:2. Fundus autofluorescence (FAF; Spectralis™, Heidelberg Engineering, Heidelberg, Germany) was performed in six patients with a confocal scanning laser ophthalmoscope. FAF images with a view of 30˚ and 55˚ on the central retina were acquired using a confocal scanning laser ophthalmoscope (cSLO) with an optically pumped solid state laser (488 nm) for excitation. All patients underwent a full-field ERG except for patient F-II:2. We performed ERG according the guidelines of the International Society for Clinical Electrophysiology of Vision (ISCEV).[17] Responses were evaluated using local reference values.

Retinal structure. We obtained cross-sectional images along the horizontal meridian of the central retina with commercially available Spectral-domain optical coherence tomography (SD-OCT) instruments (Spectralis™, Heidelberg Engineering, Heidelberg, Germany) in 8 patients using a 20° single line scan covering the fovea. We quantified thickness of the total retina, the outer nuclear layer (ONL) and photoreceptor-RPE complex (PR+RPE) in 4 *MAK*-related RP patients. For reference purposes, a normal dataset for the thickness of all three layers on SD-OCT was obtained from 25 age-matched individuals (mean age: 46 years, range 27-62 years) without retinal or vitreoretinal disease. Thickness measurements of the ONL and the PR+RPE were performed at the foveola and at 0.25, 0.5, 1, 1.5, 2 and 2.5 mm eccentricity from the foveola using the thickness graphs in Heidelberg Eye Explorer software (Heidelberg Engineering, Heidelberg, Germany). The ONL was measured from the outer plexiform layer to the external limiting membrane (ELM); the RP+RPE thickness was

measured from the ELM to the Bruch membrane; and the total retinal thickness was measured from vitreous-retinal interface to the Bruch membrane complex (Figure 3.1). The reference lines that demarcate the layers were manually set and verified; all thickness measurements were performed by the same operator (R.A.C.v.H.). Postacquisition interpolation of normal data was performed with custom programs using MatLab (Version R2011a, The MathWorks Incorporated, Natick, MA, USA).
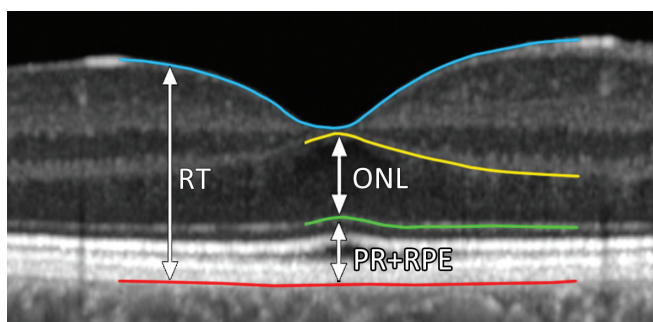
Figure 3.1. Illustration of the measured parameters on optical coherence tomography images. The outer nuclear layer (ONL) was measured from the outer border of plexiform layer (yellow line) to the external limiting membrane (ELM, green line). The thickness of the photoreceptor-RPE complex (PR+RPE) was measured from the ELM (green line) to the Bruch membrane (red line), and the total retinal thickness (RT) was measured from the vitreous-retinal interface (blue line) to the Bruch membrane (red line).

Evaluation of extra-ocular symptoms. To evaluate presence of syndromic features in the patients with *MAK* mutations, we questioned all patients about the presence of various extra-ocular manifestations covering deficiencies in most tissues that are usually involved in syndromic ciliopathies.[10] This questionnaire investigated hearing and balance abnormalities, renal failure or anomalies, cardiac and respiratory anomalies, olfactory deficiencies, polydactyly, obesity, cognitive impairment, fertility disorders, hypogonadism and dental anomalies. Additionally, we assessed olfactory function in 6 patients using the University of Pennsylvania Smell Identification Test (UPSIT; Sensonics Inc, Haddon Heights, New Jersey, USA), because olfactory deficiencies frequently go unnoticed by patients and olfactory functioning might be affected based on the expression of *MAK* in murine olfactory receptors.[14,18] UPSIT-scores were evaluated using the age-matched gender-stratified scoring keys provided in the manual.[19]

We avoided further invasive procedures to assess the testicular function, as spermatogenesis was normal in *MAK* knock-out mice, and sperm motility and male-derived litter sizes were only mildly reduced.[20]
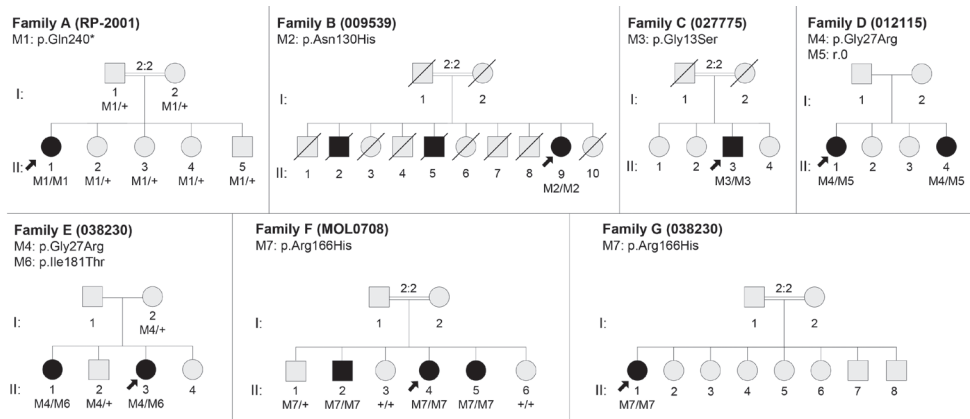
Figure 3.2. Revised pedigrees of six families included in this study. Where relatives were available (families A, D and E),the mutation segregates with the disease. Plus signs denote the wild type allele, square boxes indicate men, circles indicate women, and affected individuals are pointed out in black. An arrow indicates the proband. Double lines point out consanguineous marriages, the numbers above the double lines indicate the degree of consanguinity.

Results

Clinical characteristics

This study included a total of 11 patients (mean age: 50 years) from 7 families (Figure 3.2). Longitudinal data were available for seven patients (mean duration: 9.3 years). The mean age at onset was 30 years and ranged from childhood to the age of 54, but could not be reliably determined in three patients. The age at diagnosis (mean age: 38 years, range: 20-57 years, *n*=10) was generally within the first decade after the onset of the disease. All patients noticed night blindness as initial symptom of their disease. In one patient (E-II:1), the molecular diagnosis preceded the visual symptoms after segregation analysis in her family. One year later, she noticed a slightly prolonged adaptation to darkness and minor constriction of her temporal visual field.

An overview of the clinical findings in these patients at the most recent examination is provided in Table 3.1. The course of the BCVA in the cases with follow-up data is shown in Figure 3.3. The mean BCVA was approximately 20/40 at a mean age of 50. BCVA was ≥20/50 in at least one eye of 9 patients and ≥20/25 in 6 of these cases, including individuals in their seventh or eighth decade of life. We observed a vision impairing stromal haze, which was already reported at the age of 57, in the cornea of the right eye of patient B-II:9. The origin of this haze was not clear. Lens opacities were observed in patient C-II:3 (polar posterior cataract) and patient E-II:3 (mild posterior subcapsular cataract), whereas patients B-II:9, D-II:1 and F-II:4 underwent cataract extraction, the latter patient due to congenital cataract.

Table 3.1. Clinical features at most recent examination in patients carrying mutations in *MAK*.

ID/Age of onset (y)/Age/Sex	Initial symptom	Visual Acuity		Lens Status	Ophthalmoscopy Results	ERG Results		Goldmann Perimetry
		RE	LE			Scot.	Phot.	
A-IV:1/~20/33/F	Night blindness	20/25	20/25	Clear	Scattered pigment accumulations	SR	SR	Constricted VF, central residue: 25°
B-II:9/~57/74/F	Night blindness	HM	HM	Pseudophakia	Large parafoveal lesions of RPE atrophy, RPE changes in remaining posterior pole, attenuated vessels, waxy pallor of the optic disc, bone spicules in midperiphery, RPE atrophy anterior of vascular arcades	NR	NR	Constricted VF, central residue: 20°, severe central sensitivity loss
C-II:3/17/41/M	Night blindness	20/125	20/200	Polar posterior cataract	Severely attenuated vessels, waxy pallor of the optic disc, sporadic bone spicules in superotemporal and superonasal midperiphery, RPE atrophy anterior of the vascular arcades, wrinkling of ILM just nasal of fovea	NR	NR	Constricted VF, central residue: 20°, moderate central sensitivity loss
D-II:1/45/72/F	Night blindness	20/25	20/25	Pseudophakia	RPE alterations in the macula, attenuated arterioles, pallor of the optic disc, bone spicules in midperiphery (less densely packed in temporal quadrant compared to the other quadrants), RPE atrophy anterior of vascular arcade	NR	NR	Constricted VF, central residue: 20°, mild central sensitivity loss in LE
D-II:4/43/63/F	Night blindness	20/15	20/20	Clear	Normal macula, attenuated arterioles, waxy pallor of the optic disc, bone spicules in nasal midperiphery, RPE atrophy anterior of the vascular arcades	NR	NR	Mild relative constriction of VF, no absolute constriction, normal central sensitivity
E-II:1/53/55/F	Night blindness	20/15	20/22	Clear	Normal macula, mildly attenuated vessels, normal optic disc, mild RPE alterations and sporadic bone spicules in midperiphery. A small region of lattice degeneration in far periphery and laser scars in far periphery.	WNL	WNL	Mild relative constricted VF, normal central sensitivity

3

Table 3.1. Continued

| ID/Age of onset (y)/Age/ Sex | Initial symptom | Visual Acuity | | Lens Status | Ophthalmoscopy Results | ERG Results | | Goldmann Perimetry |
		RE	LE			Scot.	Phot.	
E-II:3 childhood/ 49/F	Night blindness	20/200	20/22	RE: Mild PSC LE: Clear	Normal macula (apart from wrinkling of ILM in the RE), attenuated vessels, normal optic disc, bone spicule pigmentations in nasal and inferior midperiphery, RPE atrophy anterior of vascular arcade.	SR (age 43)	WNL (age 43)	Constricted VF, central residue: 10°, sensitivity, mild sensitivity loss in LE
F-II:2/NA/33/M	Night blindness	20/63	20/50	NA	NA	NA	NA	NA
F-II:4/NA/57/F	Night blindness	20/50	20/32	Aphakic after congenital cataract	Mild pigmentary changes around arcades	SR	SR	Midperipheral scotomas, temporal VF more affect than nasal VF
F-II:5/NA/49/F	Night blindness	20/32	20/25	NA	Posterior pole normal, mild changes in nasal retina	SR	MR	Midperipheral temporal scotoma
G-II:1/6/32/F	Night blindness	20/25	20/25	Clear	Normal posterior pole, mild attenuation of the vessels, mild waxy pallor of the optic disc, RPE atrophy and bone spicules in the periphery.	SR (age 28)	SR (age 28)	Constricted VF, central residue: 20°, mild central sensitivity loss

Table **3.1.** Clinical features at most recent examination in patients carrying mutations in *MAK*.(continued)

OCT Results	Autofluorescence Results	Non-ocular findings	Dx	Follow-up (y)
Irregular foveal photoreceptor reflectance. Otherwise normal.	Hypoautofluorescent lesions in midperiphery,	None	RP	0
Severely loss of photoreceptor-RPE complex. Central photoreceptor residue. Diffuse thinning of central retina.	Large hypoautofluorescent lesions and diffuse hyperautofluorescence in posterior pole. Multiple hypoautofluorescent lesions in midperiphery	None	RP	17
Loss of photoreceptor reflectance peripheral of fovea. ERM with retinal wrinkling.	Parafoveal hyperautofluorescent ring. Hypoautofluorescent lesions in posterior pole, midperiphery and peripapillary region.	None	RP	18.5
Loss of photoreceptor reflectance peripheral of fovea. Atrophy of choriocapillaris, especially in peripapillary region. IS+OS: 65μm (RE), 71 μm (LE)	Diffuse hypoautofluorescent lesions and blockage of signal by bone spicules in midperiphery.	None	RP	16
Loss of photoreceptor reflectance peripheral of macula. IS+OS: 82 μm (RE), 79 μm (LE)	Hyperautofluorescent ring within vascular arcades. Diffuse small hypoautofluorescent spots in nasal midperiphery. Hypoautofluorescent peripapillary lesion.	None	RP	1
Normal	Normal	None	RP	2
Loss of photoreceptor reflectance peripheral of macula. Diffuse atrophy of choriocapillaris.	Only LE: Hyperautofluorescent ring within vascular arcades. Diffuse hypoautofluorescent spots in midperiphery.	None	RP	6.5
NA	NA	None	RP	0
NA	NA	None	RP	0
NA	NA	None	Sectorial RP	0
Loss of photoreceptor reflectance peripheral of macula. Diffuse atrophy of choriocapillaris.	NA	None	RP	4

All features are present symmetrically, unless mentioned otherwise. Dx = final diagnosis; ERG = electroretinography; ERM = epiretinal membrane; HM = Hand movements; ILM = internal limiting membrane; LE = Left eye; MR = moderately reduced; NA = not available; NR = nonrecordable; Ph = photopic responses; PSC: posterior subcapsular cataract; RE = right eye; RPE = retinal pigment epithelium; Sc: scotopic responses; SR = severely reduced; VF = visual field; WNL = within normal limits
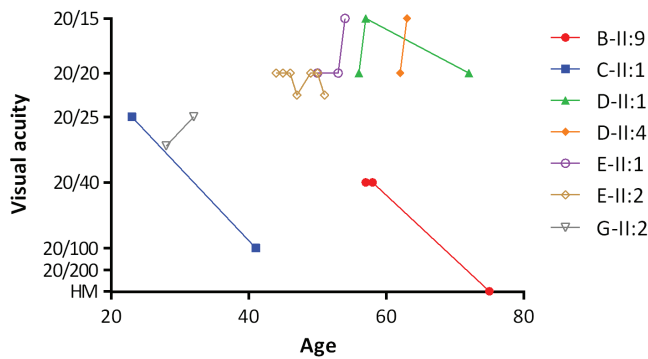
Figure 3.3. Best corrected visual acuity (y-axis) related to age (x-axis) in seven patients with MAK-related retinitis pigmentosa. If visual acuity differed between both eyes, the best visual acuity was used. Small variability in visual acuity was observed in the patients of families D and E. HM, hand movements.

Ophthalmoscopy revealed typical RP features including vessel attenuation, waxy pallor of the optic disc and bone spicules in all patients (Figure 3.4A-E). In early stages, the nasal and inferior quadrants were predominantly affected, whereas in later stages the retina in the superior quadrant became affected in a likewise fashion. The temporal retina showed less densely packed bone spicules in end-stage disease (Figure 3.4A-B and 3.4D-E). The macular region was unaffected in all patients except for patient B-II:9, who, at the age of 74, showed large atrophic chorioretinal lesions (Figure 3.4F) with a corresponding low visual acuity of hand movements in both eyes. An earlier examination, at the age of 57, revealed a bull's eye maculopathy.

Autofluorescence imaging (mean age: 51, range: 41-63 years) revealed typical RP features (Figure 3.4G-H), including the hyperautofluorescent ring associated with the transitional zone where photoreceptor inner and outer segments are lost (Figure 3.4I-J),[21,22] and hypoautofluorescent lesions in the midperiphery. Electrophysiological rod- and cone-driven responses were either severely reduced or non-recordable (Figure 3.5). In patients E-II:3 and F-II:5, the responses showed a rod-cone pattern, where rod-driven responses were more severely affected than cone-driven responses. ERG responses within the normal limits were obtained in patient E-II:1, although scotopic minimal responses were at the lower end of the normal spectrum.

Perimetric testing revealed that tunnel vision was a prominent feature in 6 patients (55%): constricted visual fields up to 10° were observed (Table 3.1). Visual field loss followed the patterns reported earlier,[16] where no or minor temporal field defects are present in early stages of the disease, whereas in more advanced stages the field is constricted to a central residue. However, the course of visual field loss was highly variable: patients C-II:3, G-II:1 and E-II:3 had an isolated central residual field (pattern 5) at age 25, 28 and 49, respectively, whereas E-II:1, D-II:1 and D-II:4 had a nearly complete visual field (pattern 1) at age 54, 55 and 63, respectively. Details of visual fields are depicted in Figure 3.6. Central sensitivity remained relatively spared in 7 patients, which is in accordance with the observed visual acuity (Table 3.1).
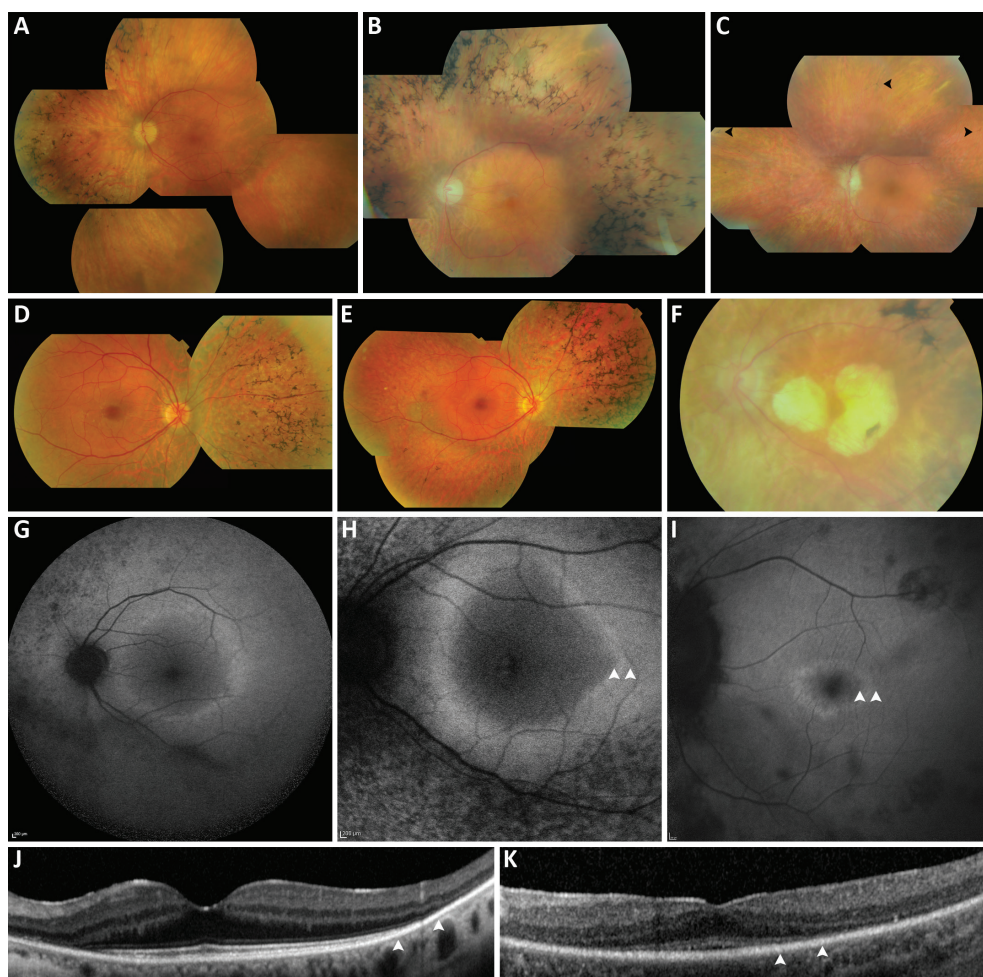
Figure 3.4. Fundus photographs and autofluorescence imaging in patients with MAK-related retinitis pigmentosa. **A,** Composition fundus photograph of the left eye of case D-II:4 (age 63) illustrating attenuated vessels, waxy pallor of the optic disc and bone spicule pigmentations in the nasal-superior midperiphery. **B,** Composition photograph of the left fundus in patient D-:II:1 (age 72) showing attenuated vessels, pallor of the optic disc and bone spicules in the midperiphery. **C,** Composition fundus photograph of the left eye in patient C-II:3 (age 41) revealing severely attenuated vessels, a pale optic disc amd sporadic bone spicules in superotemporal and superonasal midperiphery (black arrows heads). **D/E,** Composition fundus photos of the right eye in patient E-II:3 at age 44 (D) and age 46 (E) highlighting the increase in bone spicule pigmentations in the nasal and inferior quadrants as well as the progression in atrophy of the RPE. **F,** Photograph of the left fundus in patient B-II:9 (age 74) showing large RPE lesions surrounding the fovea, as well as attenuated vessels, waxy pallor of the optic disc and bones spicule pigmentations. **G/H,** FAF images of the left fundi in patients D-II:4 at age 63 (G) and E-II:3 at age 46 (H) revealing a hyperautofluorescent ring surrounding the normal appearing macula and fine hypoautofluorescent spots in the nasal and superior midperiphery. **I,** FAF image of the left fundus of case C-II:3 (age 43) revealing a hyperautofluorescent ring around the fovea and irregular hypoautofluorescent spots scattered throughout the posterior pole. **J/K,** OCT scans along the horizontal meridian of the central retina in patients D-II:4 at age 63 (J) and E-II:3 at age 46 (K) highlighting the remaining photoreceptors and the transitional zone (marked by white arrow heads).

Retinal Structure

We observed profound loss of photoreceptor layer structure in the perimacular zone in six patients (mean age: 57; range: 28-74 years). In accordance to the findings at ophthalmoscopy and perimetry, photoreceptor loss was more advanced towards the fovea in the nasal retina compared to the temporal retina (Figure 3.4J). In later stages, loss of the photoreceptor layer temporal to the fovea occurred (Figure 3.4K).
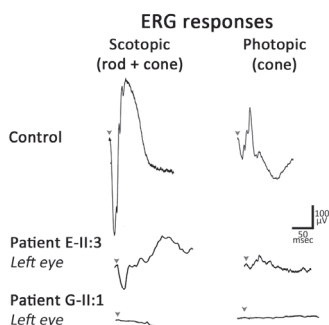
Figure 3.5 ERG recordings of two patients with recordable responses. (patient E-II:3 at age 43 and G-II:1 at age 28). Only scotopic mixed (rod + cone) responses and photopic (cone) responses are depicted. Arrowheads indicate the moment of the light flash. Control shows normal responses of individuals with healthy retinas. Patient E-II:3 has severely reduced scotopic responses and photopic responses just within normal limits. Both dark-adapted and light-adapted responses of patient G-II:1 show barely detectable responses of <10 microvolts. ERG, electroretinography; msec, millisecond; µV, microvolts.
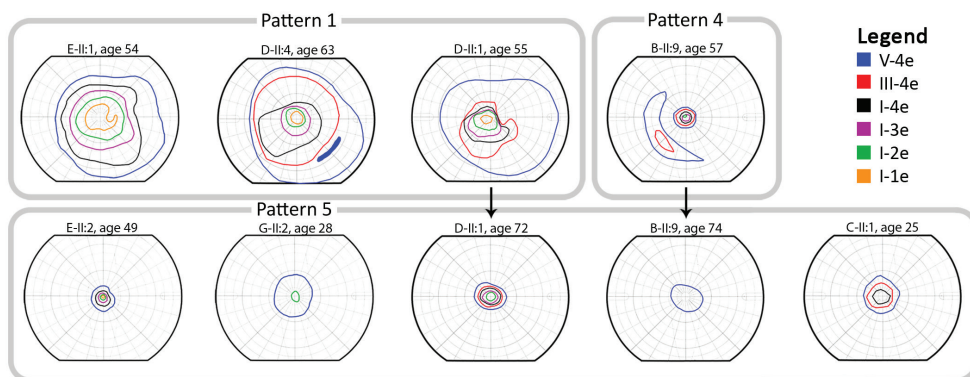
Figure 3.6. Patterns of visual field loss by Goldmann kinetic perimetry. All fields are depicted as right eyes. Patterns are numbered according to Stone et al. (Stone et al. 2011). Pattern 1: Field show nearly full extent with the V-4e isopter and absolute scotoma, if present, are situated in the superotemporal quadrant. Pattern 4: isolation of the central field from the residual nasal field by a complete midperipheral scotoma. Pattern 5: only a residual small central island with V-4e and even smaller with I-4e. Fields are grouped by pattern. Patient ID and age are at the top of each map. Solid areas: absolute scotoma.

Thickness measurements are plotted in Figure 3.7; normal data were plotted (mean ± 2 SD) as reference for the data from the patients. The overall retina became thinned beyond the fovea in 3 RP patients, of which 2 patients also showed a thinned foveal retina. The OCT scan in patient D-II:4 was acquired slightly superior to the foveal dip, resulting in the thickened foveal retina depicted in Figure 3.7 (top panel). The other values in this patient were within the normal range due to the early stage of disease. Both ONL and PR+RPE layers were thinned beyond the fovea, except for patient C-II:3 in whom the foveal ONL and PR+RPE thinned as well. Thinning of the retinal, ONL and PR+RPE thickness in the fovea correlated with a decrease in visual acuity. We did not observe thickening of the ONL or PR+RPE layer.
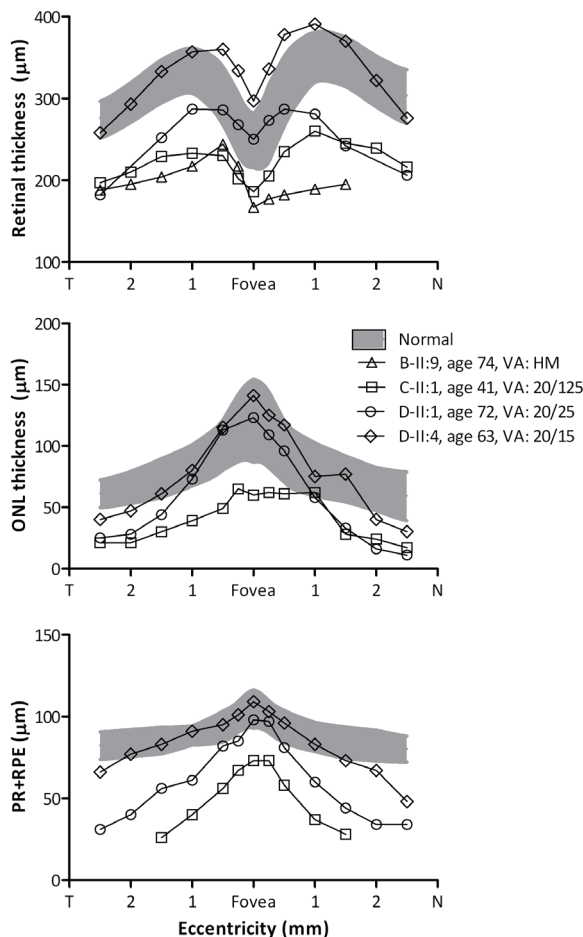
Figure 3.7. Retinal laminar architecture by OCT in MAK-related RP. Thickness of the overall retina, ONL and photoreceptor-RPE (PR+RPE) complex along the horizontal meridian in 4 patients. In patient B-II:9 only the retinal thickness could be measured as unstable fixation led to low scan quality. Shaded areas: normal limits (mean ± 2 standard deviations) as measured in 25 individuals without vitreoretinal and retinal disease (mean age: 46 year). VA, visual acuity; HM, hand movements.

Evaluation of extra-ocular features

All patients were in good general health. No extra-ocular manifestations were reported in the questionnaire and, more specifically, no history of sub- or infertility was reported in both males included in this study. In the six patients tested with the UPSIT, the absolute ability to smell varied from complete loss (anosmia, patient B-II:9) to normal olfactory function (normosmia, patient D-II:4). However, the absolute ability to smell decreases with age in normal individuals while variance of olfactory function widens, and anosmia is observed in a portion of the normal elderly above the age of 60.[19] Compared to age-matched controls, the olfactory function of the six patients tested in this study were all within the normal limits, although often at the lower end (Table 3.2). None of the patients complained about loss of their ability to smell or taste.

Table 3.2. UPSIT-scores and interpretation of 6 patients with *MAK*-associated RP.

Patient	Age	UPSIT-score	Percentile*	Absolute olfactory function corrected for age and gender
B-II:9	74	15/40	7th	Anosmia
C-II:3	41	32/40	13nd	Mild microsmia
D-II:1	72	26/40	17th	Moderate microsmia
D-II:4	63	36/40	53rd	Normosmia
E-II:1	54	33/40	17th	Mild microsmia
E-II:3	49	33/40	6th	Mild microsmia

* = percentiles indicate the percentage of normal individuals that reach an equal or lower score as the patient. UPSIT, University of Pennsylvania Smell Identification Test.

Discussion

MAK has recently been added to the expanding list of genes associated with autosomal recessive RP.[4,5] Pathologic mutations in *MAK* cause abnormal elongation of the cilium, which eventually results in photoreceptor cell death.[3] Defects in genes involved in ciliary structure or transport are known to cause syndromes that include retinal dystrophy.[10,23-25] The exclusion of syndromic abnormalities in *MAK*-associated RP is therefore important. Previously, Stone and co-workers described the retinal phenotype in a genetically homogeneous group of almost exclusively Ashkenazi Jewish patients.[16] The RP patients in this study carry causative mutations different from the specific insertion described in *MAK,* and were not of Ashkenazi Jewish ancestry.

The MAK-associated retinal phenotype
The retinal phenotype of the patients in this study is typical for RP and starts with night blindness and subsequent progressive constriction of the visual field. Visual acuity can remain relatively normal up to late age due to prolonged survival of the central retina, as was observed by Stone and colleagues.[16] However, in cases B-II:9, C-II:3 and F-II:2, visual acuity decreased to 20/50 or less in both eyes at the age of respectively 74, 41 and 57 years, although in case of C-II:3 this may also be explained by visually disturbing cataracts.

In *MAK*-associated RP, visual field loss was initially restricted to the temporal field that gradually progressed to loss of the entire (mid)peripheral field, and ends with a isolated central residue. These perimetric findings correlate with the patterns described earlier in *MAK*-related RP by Stone et al, although we observed only three of five patterns and end-stage pattern 5 was reached at an earlier age by patients C-II:3 and G-II:1 (Figure 3.6).[16]

SD-OCT imaging clearly demonstrated the overall thinning of the retina, as well as thinning of the ONL and PR+RPE, whereas foveal thickness initially is spared. PR+RPE thickening that could accompany the elongation of the connecting cilium to twice its normal length, which was present in rod photoreceptors of *MAK* knock-out mice,[3] was not observed in our patients. This absence of retinal thickening may signify the absence of these structural abnormalities in human photoreceptors, although it cannot be excluded that such thickening lies beyond the resolution of current OCT systems.

Genotype-phenotype analysis
All but one (B-II:9) patients demonstrated the slowly progressive, central-preserving retinal phenotype. Accordingly, the mutations identified in our patients (Table 3.3) all affect the kinase activity that is crucial for normal functioning of the MAK protein.[4] Nonsense mutations, which are generally assumed to have more detrimental effects on protein function than missense changes, were identified in family A. However, the phenotype in patient A-IV:1 did not significantly differ from that in the other families. The p.Asn130His and p.Gly13Ser mutations, identified in B-II:9 and C-II:3 respectively, alter amino acids that are universally conserved across all known kinases,[26] and these mutant forms of MAK show virtually no kinase activity in vitro.[4] However, the distinct retinal differences between these two patients suggest differences in the total mutational load elsewhere in the genome.

Variants in other retinal genes may have modified the phenotype in patient B-II:9. Prior to the identification of *MAK* mutations in patient B-II:9, targeted next generation sequencing in 111 known blindness genes had been performed (individual 9535 in this study).[27] A heterozygous genetic variant was found in *GPR98*, which might have a modifying effect on the disease. Alternatively, modifier effects from variants in other (retinal) genes that were not analyzed in the targeted next generation sequencing approach might be involved in the phenotype in patient B-II:9 since the atrophic macular phenotype deviates significantly from the relative preservation of macular function observed in the other patients. Additional genetic analysis with e.g. whole exome sequencing may reveal pathologic mutations other than those present in *MAK*.

Although the absence of syndromic features is not uncommon in ciliary retinal disorders,[12] the question remains why syndromic features are absent while multiple tissues express *MAK*. Tissue-specific isoforms can result in disease features in only one tissue, and a retina-specific isoform of MAK, which includes an extra exon (exon 12 in that transcript) that is regulated by exon 9, has been described.[5] However, none of the *MAK* mutations identified in our patients were located in either exon 9 or 12. Other explanations may include variance in levels of gene expression among tissues and the high metabolic rate of the retina compared to other tissues, potentially making the retina more prone to disruptive processes. Alternatively, we cannot completely rule out that we missed very subtle extra-ocular features.

Table 3.3. Genetic findings in the patients included in this study.

Patient ID	Allele 1		Allele 2		Exon	Consanguinity
	Mutation	*Effect*	*Mutation*	*Effect*		
A-IV:1	c.718C→T	p.Gln240*	c.718C→T	p.Gln240*	8	First cousins
B-II:9	c.388A→C	p.Asn130His	c.388A→C	p.Asn130His	6	First cousins
C-II:3	c.37G→A	p.Gly13Ser	c.37G→A	p.Gly13Ser	2	First cousins
D-II:1	c.79G→A	p.Gly27Arg	NI	r.0	2	No
D-II:4	c.79G→A	p.Gly27Arg	NI	r.0	2	No
E-II:1	c.79G→C	p.Gly27Arg	c.542T→C	p.Ile181Thr	2, 7	No
E-II:3	c.79G→C	p.Gly27Arg	c.542T→C	p.Ile181Thr	2, 7	No
F-II:2	c.497G→A	p.Arg166His	c.497G→A	p.Arg166His	7	Yes
F-II:4	c.497G→A	p.Arg166His	c.497G→A	p.Arg166His	7	Yes
F-II:5	c.497G→A	p.Arg166His	c.497G→A	p.Arg166His	7	Yes
G-II:1	c.497G→A	p.Arg166His	c.497G→A	p.Arg166His	7	First cousins

NI, not identified.

MAK-related RP vs. ciliopathies
To date, mutations in 34 ciliary genes have been associated with both syndromic and non-syndromic retinal disease (RetNet, available at https://sph.uth.edu/retnet/). Non-syndromic retinal disease is caused by defects in twenty-four of these genes and the associated retinal phenotypes are summarized in Table 3.4 (except for the *MAK*-associated phenotype). Besides

MAK, 13 ciliary genes are exclusively associated with non-syndromic retinal disease, without being associated with syndromic disease as well. Although detailed descriptions of most phenotypes associated with ciliary gene defects are lacking, we observed a remarkable clinical variability among non-syndromic ciliary retinal disease, ranging from relatively mild phenotypes like pericentral retinal dystrophy and occult macular dystrophy, to severe early-onset retinal degeneration phenotypes such as Leber congenital amaurosis (Table 3.4).

Non-syndromic RP forms caused by ciliary genes generally initiate during the first two decades of life and demonstrate reduced visual acuity as an early feature. Accordingly, profound macular atrophy is observed in a subset of these RP forms (Table 3.4). Mild RP phenotypes without early macular involvement are observed in retinal disease associated with mutations in *RP1*, *RP1L1*, *TOPORS* or *C2orf71*,[28-33] which generally are adult-onset and characterized by a slow decline in visual acuity. Since *RP1*, *RP1L1* and *TOPORS* are the only ciliary genes that cause non-syndromic dominant RP known to date, the classic dogma that dominantly inherited RP is milder compared to recessive and X-linked RP also applies when only ciliary RP is considered.[2]

Like these dominantly inherited phenotypes, *MAK*-associated recessively inherited RP resides at the mild end of the spectrum of diseases caused by ciliary genes. It shows remarkable resemblance to the phenotype observed in patients with *RP1* mutations in respect to the course of visual acuity loss, the patterns of retinal degeneration and visual field loss as described by Jacobson and colleagues.[28] Underlying mechanisms for the regional retinal variations have been optioned to lie in topographic characteristics in gene expression,[34-37] but further studies are necessary on this subject. The resemblance in phenotypes is especially intriguing as RP1 and MAK are functionally related: both proteins localize to the outer segment axoneme in murine photoreceptors and RP1 is a phosphorylation target of MAK.[3] Omori et al. suggested that phosphorylation of RP1 may influence microtubule stability and regulation of ciliary length.[3] Moreover, if lack of RP1 phosphorylation is the direct cause of *MAK*-associated RP, this would also be in accordance with the absence of syndromic features, since *RP1* is expressed in the retina only.[38]

In conclusion, we observed slowly progressive, autosomal recessive RP without syndromic features in patients with various nonsense or missense mutations in *MAK*. Visual acuity usually remains intact, although modifier effects may have negative consequences on central vision. *MAK*-associated RP is at the mild end of the ciliopathic RP phenotypes and shows remarkable resemblance to the retinal phenotype observed in *RP1*-related RP. Thus, defects in proteins that act in the pathway that involves MAK and RP1, may lead to relatively mild retinal phenotypes.

Table 3.4. General phenotypic features of non-syndromic ciliopathic retinal dystrophies.

Gene name	Pattern of inheritance	Associated syndromes	Non-syndromic retinal phenotype					Associated extra-ocular features*	Reference
			Phenotype	Onset	Retinal features	Visual function	Full-field ERG		
ARL2BP	AR	None	RP	Third decade of life	pallor of the optic discs, bone-spicule pigmentation, attenuated vessels, macular atrophic lesions	Fast deterioration of visual acuity. Constriction of VF up to ~10°	NR	Situs inversus, PCD, including recurrent infections of ear and sinorespiratory tract	39
ARL6	AR	BBS	RP	NS	NS	NS	NS	None	40,41
BBS1	AR	BBS	RP	First two decades of life	Typical RP features, macular atrophy is common	Early deterioration of visual acuity in some patients Central residue of ~10°	Rod-cone pattern, often NR	Obesity	42,43
BBS9	AR	BBS	RP	NS	NS	NS	NS	None	44
C2orf71	AR	None	RP	Mainly adult-onset, two early-onset (<5y) described	Bone spicule deposits, attenuated vessels Severe generalized degeneration in early-onset disease	Night blindness, mild visual acuity loss Ring scotomas in 4th-5th decade of life.	Rod-cone pattern, often NR	None	30,31
C8orf37	AR	None	CRD	First two decades of life	Macular pigmentary changes and atrophy, attenuated vessels, sporadic bone spicule pigmentation in midperiphery	Early decrease of visual acuity Relative or absolute central scotoma	Cone-rod pattern	Polydactyly	45,46
			RP	First two decades of life	Midperipheral bone-spicule pigmentations, waxy pallor of the optic disc, attenuated vessels, macular atrophy	Night blindness, early decrease in visual acuity Central residue on VF	Rod-cone pattern, but often NR	None	

Gene name	Pattern of inheritance	Associated syndromes	Non-syndromic retinal phenotype					Associated extra-ocular features*	Reference
			Phenotype	Onset	Retinal features	Visual function	Full-field ERG		
CEP290	AR	BBS, JBTS, SLS, MKS	LCA	At birth or within a few months after birth	Pink optic disc, attenuated vessels (mild-moderate), preserved RPE in posterior pole, dot-like pigmentation, sporadic bone spicules. Cystoid macular edema in some patients	Early deterioration of visual acuity, although cases with relatively preserved visual acuity	Cone-rod pattern, generally NR	Hypotonia, ataxia and mentral retardation, infertility, poor olfactory function	47-52
			EOSRD	Within 6 months after birth	Pink optic discs, attenuated vessels, and subtle RPE changes in the macular region	Decreased visual acuity from birth, although less fulminant as in the CEP290-LCA phenotype. Constriction of the VF	Initial rod-cone pattern (age 2y), later NR	None	53
CLRN1	AR	Usher syndrome type 3	RP	NS	Attenuation of the retinal vessels, waxy appearance of the optic disc and bone spicule pigmentation in the periphery	NS	Rod-cone pattern	None	54
FAM161A	AR	None	RP	During first three decades of life	Attenuated arteries, bone spicules and optic atrophy although only to a limited degree	Severe visual handicap and legal blind in fifth and sixth decade of life, respectively. Tunnel vision up to 10°	NR	None	55,56

Table 3.4. General phenotypic features of non-syndromic ciliopathic retinal dystrophies. (continued)

Gene name	Pattern of inheritance	Associated syndromes	Non-syndromic retinal phenotype				Full-field ERG	Associated extra-ocular features*	Reference
			Phenotype	Onset	Retinal features	Visual function			
IQCB1	AR	SLS	LCA	At birth or within first years of life	Early changes: 'lobular' pattern of hypo- and hyperpigmentation outside the retinal arcades. Later on, hypopigmentation outside the arcades and diffuse RPE atrophy with intraretinal pigment changes	Severely affected visual acuity of most often light perception (range 20/80-light perception)	NR	None	[57,58]
LCA5	AR	None	LCA	From birth	very thin vessels, salt and pepper pigmentation, some bone-spicule pigments in the peripheral region and an atrophic aspect of the macular area	Night blindness, photoaversion, congenital visual loss.	NR	None	[59-61]
NEK2	AR	None	RP	NS	NS	NS	NS	NS	[62]
OFD1	XL	JBTS, OFD, SGBS2	RP	Before age of 2y	Grayish spots at the level of the RPE, which confluent later on causing an overall appearance of the retina, small patches of RPE atrophy in the midperiphery, granularity of macular RPE	Early loss of central vision Only temporal and inferior VF residues	NR	None	[63,64]

Non-syndromic retinal phenotype									
Gene name	Pattern of inheritance	Associated syndromes	Pheno-type	Onset	Retinal features	Visual function	Full-field ERG	Associated extra-ocular features*	Refer-ence
RAB28	AR	None	CRD	Second decade of life	Foveal hyperpigmentation	Central scotoma, color defects in all three axis	Cone-rod pattern	NS	65
RP1	AD, AR	None	RP	Second or third decade of life	Narrowed retinal vessels, pale discs, and pigmentary changes in the periphery, inferonasal retina most vulnerable, whereas central and superotemporal retina was better preserved	Night blindness, visual acuity was normal or moderately impaired Severely constricted VF	Rod-cone pattern	None	28,32
RP1L1	OMD: AD with reduced penetrance	None	OMD	Very broad range (6-81y)	Normal ophthalmoscopic appearance	Decrease in visual acuity	ffERG: normal mfERG: significantly reduced	None	66
	RP: AR		RP	Third decade of life	Bone spicule deposits and RPE atrophy in the midperiphery, attenuated vessels	Moderately reduced visual acuity Constricted visual field up to 10°	NS	None	33
RP2	XL	None	RP	Mainly before age of 10y, but onset during adolescence or 20s observed as well	Macular abnormalities including granularity, bull's eye or RPE atrophy, periphery show pigmentary retinopathy and atrophic lesions, sometimes choroideremia-like degeneration	Night blindness, early loss of central vision Severely constricted VF in patients <16y, central scotoma in 50% of patients	Rod-cone pattern	None	67-70

Table 3.4. General phenotypic features of non-syndromic ciliopathic retinal dystrophies. (continued)

Gene name	Pattern of inheritance	Associated syndromes	Non-syndromic retinal phenotype					Associated extra-ocular features*	Reference
			Pheno-type	Onset	Retinal features	Visual function	Full-field ERG		
RPGR	XL	Usher syndrome	RP	First two decades of life	Bone spicule pigmentations, attenuated vessels, pallor of the optic disc, macular involvement variable ranging from no abnormalities to atrophic lesions	Night blindness, Early loss of central vision with median age to reach legal blindness: 45y, annual loss of 4-8%, Midperipheral annular scotomas progressing to a isolated central residue or isolated peripheral islands, annual loss VF: 4.7-9%	Rod-cone pattern, often NR	PCD, including recurrent infections of ear and sinorespiratory tract	25,71-74
			CRD	First two decades of life	(Bull's eye) atrophic appearance of the macula, attenuated vessels	Eearly decrease in visual acuity Sensitivity loss or central scotoma	Cone-rod pattern	None	74,75
			CD	Mean: 36y	Progressive macular deterioration ranging from no abnormalities to a bull's eye maculopathy or atrophy	Hemeralopia Central sensitivity loss or absolute central scotoma on VF examination	SR or NR photopic responses, normal scotopic responses	None	76
RPGRIP1	AR	None	LCA	From birth	Posterior pole normal, mild vascular attenuation, RPE changes in periphery (range, hypopigmentation to bone spicules)	Severely decreased visual acuity beginning within the first year of life	Cone-rod pattern, generally NR	None	61,77,78
			CRD	First two decades of life	Macular granularity and atrophy. Bull's eye maculopathy observed	Rapid loss of vision between 14-16y	Cone-rod pattern	None	79

3

Gene name	Pattern of inheritance	Associated syndromes	Non-syndromic retinal phenotype						Reference
			Phenotype	Onset	Retinal features	Visual function	Full-field ERG	Associated extra-ocular features*	
TOPORS	AD	None	RP	Second to fifth decade of life	Perivascular RPE atrophy, which progresses to a diffuse pigmentary retinopathy with choroidal sclerosis	Visual acuity is maintained in most patients VF demonstrates constriction (range 80-10°)	Rod-cone pattern, but much variation in amplitudes	None	[29]
			PRD	Third decade of life or later	Pericentral abnormalities sparing the macula, periphery essentially normal, advanced stage disease indistinguishable from end-stage RP	Night blindness, relatively preserved visual function Pericentral scotoma	ffERG: normal mfERG: subnormal	None	[80]
TTC8	AR	BBS	RP	First decade of life (2-4y)	Attenuated arteries, bone spicule pigmentations	NS	NR	None	[81]
TULP1	AR	None	LCA	Few months after birth	Carpet-like retinal degeneration, macular atrophy, nummular pigmentation and bone spicule pigmentations are common	Nystagmus, poor vision	NR	None	[61,82]
	AR		RP	First decade of life	Attenuated retinal vessels, waxy pale appearance of the optic disc, bone spicule pigmentations and RPE atrophy extending to the macula. A yellow perifoveal annular ring in some RP patients with TULP1 mutations	Early deterioration of central vision General and central decline in sensitivity with progression to a constricted VF of 10°	NR	None	[83-85]

Table 3.4. General phenotypic features of non-syndromic ciliopathic retinal dystrophies. (continued)

Gene name	Pattern of inheritance*	Associated syndromes	Non-syndromic retinal phenotype					Associated extra-ocular features*	Reference
			Phenotype	Onset	Retinal features	Visual function	Full-field ERG		
			CD	Third to fifth decade of life	Bull's eye maculopathy, bone spicule pigmentations, pallor of the optic discs and attenuation of the retinal vessels may be present	Rapid decrease in visual acuity Central scotoma, periphery may show constriction	Within normal limits, although cone response at lower end	None	86
USH2A	AR	Usher syndrome	RP	Highly variable, generally during or after puberty	Highly variable, ranging from normal function in some retinal regions to severely degenerated retinas	Moderately reduced visual acuity VF findings highly variable, ranging from near normal to constriction up to 10°	Rod-cone pattern	None	87,88

*This column include the extra-ocular signs observed in patients with a phenotype that does not fall in one of the recognized syndromes.

AD, autosomal dominant; AR, autosomal recessive; BBS, Bardet-Biedl syndrome; CD, cone dystrophy; CRD, cone-rod dystrophy; EOSRD, early-onset severe retinal dystrophy; ffERG, full-field electroretinography; JBTS, Joubert syndrome; LCA, Leber congenital amaurosis; mfERG, multifocal electroretinography; MKS, Meckel-Gruber syndrome; NS, not specified; NR, non-recordable; OFD, orofaciodigital syndrome; OMD, occult macular dystrophy; PCD, primary cilia dyskinesia; PRD, pericentral retinal dystrophy; RP, retinitis pigmentosa; SGBS2, Simpson-Golabi-Behmel syndrome type 2; SLS, Senior-Løken syndrome; SR, severely reduced; VF, visual field; XL, X-linked; y, years.

3

References

1. Berson EL. Retinitis pigmentosa. The Friedenwald Lecture. *Invest Ophthalmol Vis Sci*. 1993;34(5):1659-76.
2. Hartong DT, Berson EL, Dryja TP. Retinitis pigmentosa. *Lancet*. 2006;368(9549):1795-809.
3. Omori Y, Chaya T, Katoh K, et al. Negative regulation of ciliary length by ciliary male germ cell-associated kinase (Mak) is required for retinal photoreceptor survival. *Proc Natl Acad Sci U S A*. 2010 Dec 28;107(52):22671-6.
4. Ozgul RK, Siemiatkowska AM, Yucel D, et al. Exome sequencing and cis-regulatory mapping identify mutations in MAK, a gene encoding a regulator of ciliary length, as a cause of retinitis pigmentosa. *Am J Hum Genet*. 2011 Aug 12;89(2):253-64.
5. Tucker BA, Scheetz TE, Mullins RF, et al. Exome sequencing and analysis of induced pluripotent stem cells identify the cilia-related gene male germ cell-associated kinase (MAK) as a cause of retinitis pigmentosa. *Proc Natl Acad Sci U S A*. 2011 Aug 23;108(34):E569-76.
6. Berman SA, Wilson NF, Haas NA, Lefebvre PA. A novel MAP kinase regulates flagellar length in Chlamydomonas. *Curr Biol*. 2003 Jul 1;13(13):1145-9.
7. Bengs F, Scholz A, Kuhn D, Wiese M. LmxMPK9, a mitogen-activated protein kinase homologue affects flagellar length in Leishmania mexicana. *Mol Microbiol*. 2005 Mar;55(5):1606-15.
8. Hildebrandt F, Benzing T, Katsanis N. Ciliopathies. *N Engl J Med*. 2011 Apr 21;364(16):1533-43.
9. Nigg EA, Raff JW. Centrioles, centrosomes, and cilia in health and disease. *Cell*. 2009 Nov 13;139(4):663-78.
10. Mockel A, Perdomo Y, Stutzmann F, Letsch J, Marion V, Dollfus H. Retinal dystrophy in Bardet-Biedl syndrome and related syndromic ciliopathies. *Prog Retin Eye Res*. 2011 Jul;30(4):258-74.
11. Novarino G, Akizu N, Gleeson JG. Modeling human disease in humans: the ciliopathies. *Cell*. 2011 Sep 30;147(1):70-9.
12. Estrada-Cuzcano A, Roepman R, Cremers FP, den Hollander AI, Mans DA. Non-syndromic retinal ciliopathies: translating gene discovery into therapy. *Hum Mol Genet*. 2012 Jul 26.
13. Matsushime H, Jinno A, Takagi N, Shibuya M. A novel mammalian protein kinase gene (mak) is highly expressed in testicular germ cells at and after meiosis. *Mol Cell Biol*. 1990 May;10(5):2261-8.
14. Bladt F, Birchmeier C. Characterization and expression analysis of the murine rck gene: a protein kinase with a potential function in sensory cells. *Differentiation*. 1993 Jun;53(2):115-22.
15. Blackshaw S, Harpavat S, Trimarchi J, et al. Genomic analysis of mouse retinal development. *PLoS Biol*. 2004 Sep;2(9):E247.
16. Stone EM, Luo X, Heon E, et al. Autosomal recessive retinitis pigmentosa caused by mutations in the MAK gene. *Invest Ophthalmol Vis Sci*. 2011 Dec;52(13):9665-73.
17. Marmor MF, Fulton AB, Holder GE, Miyake Y, Brigell M, Bach M. ISCEV Standard for full-field clinical electroretinography (2008 update). *Doc Ophthalmol*. 2009;118(1):69-77.
18. Hoffman HJ, Cruickshanks KJ, Davis B. Perspectives on population-based epidemiological studies of olfactory and taste impairment. *Ann N Y Acad Sci*. 2009 Jul;1170:514-30.
19. Doty RL. The Smell Identification Test Administration Manual (3rd ed.). Haddon Heights, NJ: Sensonics, Inc.; 1995.
20. Shinkai Y, Satoh H, Takeda N, et al. A testicular germ cell-associated serine-threonine kinase, MAK, is dispensable for sperm formation. *Mol Cell Biol*. 2002 May;22(10):3276-80.
21. Popovic P, Jarc-Vidmar M, Hawlina M. Abnormal fundus autofluorescence in relation to retinal function in patients with retinitis pigmentosa. *Graefes Arch Clin Exp Ophthalmol*. 2005 Oct;243(10):1018-27.
22. Greenstein VC, Duncker T, Holopigian K, et al. Structural and functional changes associated with normal and abnormal fundus autofluorescence in patients with retinitis pigmentosa. *Retina*. 2012 Feb;32(2):349-57.
23. Campo RV, Aaberg TM. Ocular and systemic manifestations of the Bardet-Biedl syndrome. *Am J Ophthalmol*. 1982 Dec;94(6):750-6.
24. Eudy JD, Weston MD, Yao S, et al. Mutation of a gene encoding a protein with extracellular matrix motifs in Usher syndrome type IIa. *Science (80-)*. 1998 Jun 12;280(5370):1753-7.
25. Zito I, Downes SM, Patel RJ, et al. RPGR mutation associated with retinitis pigmentosa, impaired hearing, and sinorespiratory infections. *J Med Genet*. 2003 Aug;40(8):609-15.
26. Hanks SK, Hunter T. Protein kinases 6. The eukaryotic protein kinase superfamily: kinase (catalytic) domain structure and classification. *FASEB J*. 1995 May;9(8):576-96.

27. Neveling K, Collin RW, Gilissen C, et al. Next-generation genetic testing for retinitis pigmentosa. *Hum Mutat*. 2012 Jun;33(6):963-72.

28. Jacobson SG, Cideciyan AV, Iannaccone A, et al. Disease expression of RP1 mutations causing autosomal dominant retinitis pigmentosa. *Invest Ophthalmol Vis Sci*. 2000 Jun;41(7):1898-908.

29. Chakarova CF, Papaioannou MG, Khanna H, et al. Mutations in TOPORS cause autosomal dominant retinitis pigmentosa with perivascular retinal pigment epithelium atrophy. *Am J Hum Genet*. 2007 Nov;81(5):1098-103.

30. Collin RW, Safieh C, Littink KW, et al. Mutations in C2ORF71 cause autosomal-recessive retinitis pigmentosa. *Am J Hum Genet*. 2010 May 14;86(5):783-8.

31. Nishimura DY, Baye LM, Perveen R, et al. Discovery and functional analysis of a retinitis pigmentosa gene, C2ORF71. *Am J Hum Genet*. 2010 May 14;86(5):686-95.

32. Audo I, Mohand-Said S, Dhaenens CM, et al. RP1 and autosomal dominant rod-cone dystrophy: novel mutations, a review of published variants, and genotype-phenotype correlation. *Hum Mutat*. 2012 Jan;33(1):73-80.

33. Davidson AE, Sergouniotis PI, Mackay DS, et al. RP1L1 variants are associated with a spectrum of inherited retinal diseases including retinitis pigmentosa and occult macular dystrophy. *Hum Mutat*. 2013 Mar;34(3):506-14.

34. Sakuta H, Suzuki R, Takahashi H, et al. Ventroptin: a BMP-4 antagonist expressed in a double-gradient pattern in the retina. *Science (80-)*. 2001 Jul 6;293(5527):111-5.

35. Sharon D, Blackshaw S, Cepko CL, Dryja TP. Profile of the genes expressed in the human peripheral retina, macula, and retinal pigment epithelium determined through serial analysis of gene expression (SAGE). *Proc Natl Acad Sci U S A*. 2002 Jan 8;99(1):315-20.

36. Cornish EE, Madigan MC, Natoli R, Hales A, Hendrickson AE, Provis JM. Gradients of cone differentiation and FGF expression during development of the foveal depression in macaque retina. *Vis Neurosci*. 2005 Jul-Aug;22(4):447-59.

37. Tanito M, Kaidzu S, Ohira A, Anderson RE. Topography of retinal damage in light-exposed albino rats. *Exp Eye Res*. 2008 Sep;87(3):292-5.

38. Sullivan LS, Heckenlively JR, Bowne SJ, et al. Mutations in a novel retina-specific gene cause autosomal dominant retinitis pigmentosa. *Nat Genet*. 1999 Jul;22(3):255-9.

39. Davidson AE, Schwarz N, Zelinger L, et al. Mutations in ARL2BP, Encoding ADP-Ribosylation-Factor-Like 2 Binding Protein, Cause Autosomal-Recessive Retinitis Pigmentosa. *Am J Hum Genet*. 2013 Jul 10.

40. Aldahmesh MA, Safieh LA, Alkuraya H, et al. Molecular characterization of retinitis pigmentosa in Saudi Arabia. *Mol Vis*. 2009;15:2464-9.

41. Abu Safieh L, Aldahmesh MA, Shamseldin H, et al. Clinical and molecular characterisation of Bardet-Biedl syndrome in consanguineous populations: the power of homozygosity mapping. *J Med Genet*. 2010 Apr;47(4):236-41.

42. Cannon PS, Clayton-Smith J, Beales PL, Lloyd IC. Bardet-biedl syndrome: an atypical phenotype in brothers with a proven BBS1 mutation. *Ophthalmic Genet*. 2008 Sep;29(3):128-32.

43. Estrada-Cuzcano A, Koenekoop RK, Senechal A, et al. BBS1 mutations in a wide spectrum of phenotypes ranging from nonsyndromic retinitis pigmentosa to Bardet-Biedl syndrome. *Arch Ophthalmol*. 2012 Nov;130(11):1425-32.

44. Abu-Safieh L, Al-Anazi S, Al-Abdi L, et al. In search of triallelism in Bardet-Biedl syndrome. *Eur J Hum Genet*. 2012 Apr;20(4):420-7.

45. Estrada-Cuzcano A, Neveling K, Kohl S, et al. Mutations in C8orf37, encoding a ciliary protein, are associated with autosomal-recessive retinal dystrophies with early macular involvement. *Am J Hum Genet*. 2012 Jan 13;90(1):102-9.

46. van Huet RA, Estrada-Cuzcano A, Banin E, et al. Clinical characteristics of rod and cone photoreceptor dystrophies in patients with mutations in the C8orf37 gene. *Invest Ophthalmol Vis Sci*. 2013 Jul;54(7):4683-90.

47. McEwen DP, Koenekoop RK, Khanna H, et al. Hypomorphic CEP290/NPHP6 mutations result in anosmia caused by the selective loss of G proteins in cilia of olfactory sensory neurons. *Proc Natl Acad Sci U S A*. 2007 Oct 2;104(40):15917-22.

48. Perrault I, Delphin N, Hanein S, et al. Spectrum of NPHP6/CEP290 mutations in Leber congenital amaurosis and delineation of the associated phenotype. *Hum Mutat*. 2007 Apr;28(4):416.

49. Frank V, den Hollander AI, Bruchle NO, et al. Mutations of the CEP290 gene encoding a centrosomal protein cause Meckel-Gruber syndrome. *Hum Mutat*. 2008 Jan;29(1):45-52.

50. Coppieters F, Casteels I, Meire F, et al. Genetic screening of LCA in Belgium: predominance of CEP290 and identification of potential modifier alleles in AHI1 of CEP290-related phenotypes. *Hum Mutat*. 2010 Oct;31(10):E1709-66.

51. Alazami AM, Alshammari MJ, Salih MA, et al. Molecular characterization of Joubert syndrome in Saudi Arabia. *Hum Mutat*. 2012 Oct;33(10):1423-8.

52. Yzer S, Hollander AI, Lopez I, et al. Ocular and extra-ocular features of patients with Leber congenital amaurosis and mutations in CEP290. *Mol Vis*. 2012;18:412-25.

53. Littink KW, Pott JW, Collin RW, et al. A novel nonsense mutation in CEP290 induces exon skipping and leads to a relatively mild retinal phenotype. *Invest Ophthalmol Vis Sci*. 2010 Jul;51(7):3646-52.

54. Khan MI, Kersten FF, Azam M, et al. CLRN1 mutations cause nonsyndromic retinitis pigmentosa. *Ophthalmology*. 2011 Jul;118(7):1444-8.

55. Bandah-Rozenfeld D, Mizrahi-Meissonnier L, Farhy C, et al. Homozygosity mapping reveals null mutations in FAM161A as a cause of autosomal-recessive retinitis pigmentosa. *Am J Hum Genet*. 2010 Sep 10;87(3):382-91.

56. Langmann T, Di Gioia SA, Rau I, et al. Nonsense mutations in FAM161A cause RP28-associated recessive retinitis pigmentosa. *Am J Hum Genet*. 2010 Sep 10;87(3):376-81.

57. Estrada-Cuzcano A, Koenekoop RK, Coppieters F, et al. IQCB1 mutations in patients with leber congenital amaurosis. *Invest Ophthalmol Vis Sci*. 2011 Feb;52(2):834-9.

58. Stone EM, Cideciyan AV, Aleman TS, et al. Variations in NPHP5 in patients with nonsyndromic leber congenital amaurosis and Senior-Loken syndrome. *Arch Ophthal*. 2011 Jan;129(1):81-7.

59. den Hollander AI, Koenekoop RK, Mohamed MD, et al. Mutations in LCA5, encoding the ciliary protein lebercilin, cause Leber congenital amaurosis. *Nat Genet*. 2007 Jul;39(7):889-95.

60. Gerber S, Hanein S, Perrault I, et al. Mutations in LCA5 are an uncommon cause of Leber congenital amaurosis (LCA) type II. *Hum Mutat*. 2007 Dec;28(12):1245.

61. McKibbin M, Ali M, Mohamed MD, et al. Genotype-phenotype correlation for leber congenital amaurosis in Northern Pakistan. *Arch Ophthal*. 2010 Jan;128(1):107-13.

62. Nishiguchi KM, Tearle RG, Liu YP, et al. Whole genome sequencing in patients with retinitis pigmentosa reveals pathogenic DNA structural changes and NEK2 as a new disease gene. *Proc Natl Acad Sci U S A*. 2013 Oct 1;110(40):16139-44.

63. Hardcastle AJ, Thiselton DL, Zito I, et al. Evidence for a new locus for X-linked retinitis pigmentosa (RP23). *Invest Ophthalmol Vis Sci*. 2000 Jul;41(8):2080-6.

64. Webb TR, Parfitt DA, Gardner JC, et al. Deep intronic mutation in OFD1, identified by targeted genomic next-generation sequencing, causes a severe form of X-linked retinitis pigmentosa (RP23). *Hum Mol Genet*. 2012 Aug 15;21(16):3647-54.

65. Roosing S, Rohrschneider K, Beryozkin A, et al. Mutations in RAB28, encoding a farnesylated small GTPase, are associated with autosomal-recessive cone-rod dystrophy. *Am J Hum Genet*. 2013 Jul 11;93(1):110-7.

66. Akahori M, Tsunoda K, Miyake Y, et al. Dominant mutations in RP1L1 are responsible for occult macular dystrophy. *Am J Hum Genet*. 2010 Sep 10;87(3):424-9.

67. Ponjavic V, Andreasson S, Abrahamson M, et al. Clinical expression of X-linked retinitis pigmentosa in a Swedish family with the RP2 genotype. *Ophthalmic Genet*. 1998 Dec;19(4):187-96.

68. Rosenberg T, Schwahn U, Feil S, Berger W. Genotype-phenotype correlation in X-linked retinitis pigmentosa 2 (RP2). *Ophthalmic Genet*. 1999 Sep;20(3):161-72.

69. Jayasundera T, Branham KE, Othman M, et al. RP2 phenotype and pathogenetic correlations in X-linked retinitis pigmentosa. *Arch Ophthalmol*. 2010;128(7):915-23.

70. De Lin W, Wang CH, Chou IC, Tsai FJ. A novel one-base insertion mutation in the retinitis pigmentosa 2 gene in a large X-linked Taiwanese family. *Acta Ophthalmol*. 2014 Mar;92(2):e161-2.

71. Fishman GA, Grover S, Jacobson SG, et al. X-linked retinitis pigmentosa in two families with a missense mutation in the RPGR gene and putative change of glycine to valine at codon 60. *Ophthalmology*. 1998 Dec;105(12):2286-96.

72. Iannaccone A, Breuer DK, Wang XF, et al. Clinical and immunohistochemical evidence for an X linked retinitis pigmentosa syndrome with recurrent infections and hearing loss in association with an RPGR mutation. *J Med Genet*. 2003 Nov;40(11):e118.

73. Moore A, Escudier E, Roger G, et al. RPGR is mutated in patients with a complex X linked phenotype combining primary ciliary dyskinesia and retinitis pigmentosa. *J Med Genet*. 2006 Apr;43(4):326-33.

74. Sandberg MA, Rosner B, Weigel-DiFranco C, Dryja TP, Berson EL. Disease course of patients with X-linked retinitis pigmentosa due to RPGR gene mutations. *Invest Ophthalmol Vis Sci.* 2007 Mar;48(3):1298-304.

75. Huang WC, Wright AF, Roman AJ, et al. RPGR-associated retinal degeneration in human X-linked RP and a murine model. *Invest Ophthalmol Vis Sci.* 2012;53(9):5594-608.

76. Thiadens AA, Soerjoesing GG, Florijn RJ, et al. Clinical course of cone dystrophy caused by mutations in the RPGR gene. *Graefes Arch Clin Exp Ophthalmol.* 2011 Oct;249(10):1527-35.

77. Walia S, Fishman GA, Jacobson SG, et al. Visual acuity in patients with Leber's congenital amaurosis and early childhood-onset retinitis pigmentosa. *Ophthalmology.* 2010 Jun;117(6):1190-8.

78. Khan AO, Abu-Safieh L, Eisenberger T, Bolz HJ, Alkuraya FS. The RPGRIP1-related retinal phenotype in children. *Br J Ophthalmol.* 2013 Jun;97(6):760-4.

79. Hameed A, Abid A, Aziz A, Ismail M, Mehdi SQ, Khaliq S. Evidence of RPGRIP1 gene mutations associated with recessive cone-rod dystrophy. *J Med Genet.* 2003 Aug;40(8):616-9.

80. Selmer KK, Grondahl J, Riise R, et al. Autosomal dominant pericentral retinal dystrophy caused by a novel missense mutation in the TOPORS gene. *Acta Ophthalmol.* 2010 May;88(3):323-8.

81. Riazuddin SA, Iqbal M, Wang Y, et al. A splice-site mutation in a retina-specific exon of BBS8 causes nonsyndromic retinitis pigmentosa. *Am J Hum Genet.* 2010 May 14;86(5):805-12.

82. Chen Y, Zhang Q, Shen T, et al. Comprehensive mutation analysis by whole-exome sequencing in 41 Chinese families with Leber congenital amaurosis. *Invest Ophthalmol Vis Sci.* 2013 Jun;54(6):4351-7.

83. den Hollander AI, van Lith-Verhoeven JJ, Arends ML, Strom TM, Cremers FP, Hoyng CB. Novel compound heterozygous TULP1 mutations in a family with severe early-onset retinitis pigmentosa. *Arch Ophthal.* 2007 Jul;125(7):932-5.

84. den Hollander AI, Lopez I, Yzer S, et al. Identification of novel mutations in patients with Leber congenital amaurosis and juvenile RP by genome-wide homozygosity mapping with SNP microarrays. *Invest Ophthalmol Vis Sci.* 2007 Dec;48(12):5690-8.

85. Ajmal M, Khan MI, Micheal S, et al. Identification of recurrent and novel mutations in TULP1 in Pakistani families with early-onset retinitis pigmentosa. *Mol Vis.* 2012;18:1226-37.

86. Roosing S, van den Born LI, Hoyng CB, et al. Maternal uniparental isodisomy of chromosome 6 reveals a TULP1 mutation as a novel cause of cone dysfunction. *Ophthalmology.* 2013 Jun;120(6):1239-46.

87. Bernal S, Ayuso C, Antinolo G, et al. Mutations in USH2A in Spanish patients with autosomal recessive retinitis pigmentosa: high prevalence and phenotypic variation. *J Med Genet.* 2003 Jan;40(1):e8.

88. Schwartz SB, Aleman TS, Cideciyan AV, et al. Disease expression in Usher syndrome caused by VLGR1 gene mutation (USH2C) and comparison with USH2A phenotype. *Invest Ophthalmol Vis Sci.* 2005 Feb;46(2):734-43.

Authors

Ramon. A.C. van Huet,[1] Alejandro Estrada-Cuzcano,[2,3] Eyal Banin,[4] Ygal Rotenstreich,[5] Stephanie Hipp,[6] Susanne Kohl,[7] Carel B. Hoyng,[1] Anneke I. den Hollander,[1,2] Rob W.J. Collin,[2,3] B. Jeroen Klevering,[1]

Affiliations

[1]Department of Ophthalmology, Radboud University Nijmegen Medical Centre, Nijmegen, The Netherlands;

[2]Department of Human Genetics, Radboud University Nijmegen Medical Centre, Nijmegen, The Netherlands;

[3]Nijmegen Center for Molecular Life Sciences, Radboud University Nijmegen Medical Centre, Nijmegen, The Netherlands;

[4]Department of Ophthalmology, Hadassah-Hebrew University Medical Center, Jerusalem, Israel;

[5]Electrophysiology Clinic, Goldschleger Eye Research Institute, Tel Aviv University, Sheba Medical Centre, Israel;

[6]Institute for Ophthalmic Research, Centre for Ophthalmology, 72076 Tuebingen, Germany;

[7]Molecular Genetics Laboratory, Institute for Ophthalmic Research, Centre for Ophthalmology, 72076 Tuebingen, Germany

Clinical characteristics of rod and cone photoreceptor dystrophies in patients with mutations in the *C8orf37* gene

4

Abstract

Purpose. To provide the clinical features in patients with retinal disease caused by *C8orf37* gene mutations.

Methods. Eight patients – four diagnosed with retinitis pigmentosa (RP) and four with cone-rod dystrophy (CRD) – carrying causal *C8orf37* mutations were clinically evaluated, including extensive medical history taking, slit-lamp biomicroscopy, ophthalmoscopy, kinetic perimetry, electroretinography (ERG), spectral-domain optical coherence tomography (SD-OCT), fundus autofluorescence imaging (FAF) and fundus photography.

Results. In families A and D, respectively, one and three patients showed a classic RP phenotype with night blindness followed by concentric loss of visual field. Severe visual loss to light perception occurred early in the course of the disease. The symptoms initiated during infancy (family A) or adolescence (family D). Ophthalmoscopy revealed macular atrophy, bone spicules, attenuated vessels and waxy pale optic discs. SD-OCT showed profound photoreceptor degeneration and FAF demonstrated atrophy of the retinal pigment epithelium (RPE). ERG responses were non-recordable in these patients.

In families B and C, the patients were diagnosed with CRD. Initial symptoms were photophobia or loss of visual acuity and occurred during infancy (family B) or adolescence (family C). Ophthalmoscopy and FAF revealed profound macular RPE atrophy, SD-OCT demonstrated macular photoreceptor degeneration. ERG responses were severely reduced in a cone-rod pattern or non-recordable. Interestingly, both patients in family B demonstrated polydactyly.

Conclusions: Mutations in *C8orf37* give rise to an early or adolescent-onset autosomal recessive CRD or RP phenotype with early macular atrophy. The occurrence of postaxial polydactyly in one family suggests a syndromic phenotype, which may indicate C8orf37 has a ciliary function.

Introduction

Retinitis pigmentosa (RP) and cone-rod dystrophy (CRD) are inherited photoreceptor dystrophies, which are genetically and clinically highly heterogeneous. RP is the most common photoreceptor dystrophy with a prevalence of approximately 1 in 4,000 individuals,[1-3] whereas CRD is less frequent with an estimated prevalence of 1 in 40,000 individuals.[4, 5] Both conditions are characterized by progressive degeneration of photoreceptors, although in different patterns. In RP, rod photoreceptor degeneration usually starts prior to the loss of the cone photoreceptors, causing primary symptoms like night blindness and peripheral visual field loss. Ophthalmoscopic characteristics include attenuated vessels, peripheral bone spicule pigmentation, waxy pallor of the optic disc and peripheral chorioretinal atrophy.[3, 6] In CRD, the cone photoreceptors usually degenerate prior to the rod photoreceptors, which the patients perceives as photophobia, loss of visual acuity and central scotomas. Ophthalmoscopic features initially include macular retinal atrophy and pigment deposits, whereas in later stages mild attenuated vessels and bone spicule pigmentations in the periphery may be present, mimicking RP. These two photoreceptor degeneration patterns can be distinguished by performing an electroretinography (ERG). In RP, the rod-driven (scotopic) responses are equally or more severely reduced than cone-driven (photopic) responses,[7, 8] whereas in early CRD there are normal rod responses and substantially reduced cone responses, although rod responses will deteriorate as the disease progresses.

Mutations in many different genes have been associated with either CRD or RP. CRD as well as RP display all Mendelian modes of inheritance.[6] Also, digenic and mitochondrial inheritance have been described for RP.[9-11] Until now, mutations in 36 genes have been associated with non-syndromic autosomal recessive (ar) RP.[12] Proteins of these genes are involved in phototransduction, retinoid (vitamin A) metabolism, transport along the connecting cilium, intercellular signaling or synaptic interaction, interphotoreceptor matrix, gene regulation and phagocytosis,[6, 11, 13] which emphasizes that RP should be defined as a spectrum of dystrophies with a similar phenotype. For CRD, mutations in six genes have been described to date.[12] Mutations in two of these genes (*ABCA4* and *CERKL*) can also cause autosomal recessive RP.[14, 15] Taken together, it is estimated that mutations in these 40 genes are causative for ~ 50-60% of all autosomal recessive RP and CRD cases,[13] but new genes are still being discovered.

Recently, causative mutations in the *C8orf37* gene have been described in both autosomal recessive RP and CRD patients.[16] Sequence analysis of all six coding exons of the *C8orf37* gene led to the identification of four different pathogenic variants in these eight affected individuals.[16] *C8orf37* is ubiquitously expressed in adult human tissues, but is highly expressed in brain, heart and retinal tissues. The function of the C8orf37 protein is not known yet, but immunolocalization studies showed that it is localized at the base of the connecting cilium, suggesting a ciliary function.[16]

Mutations in *C8orf37* are known to cause CRD or RP, but specific clinical features have not yet been described. A detailed clinical description of the patients with mutations in *C8orf37* may help to provide insight into the gene's function and improve patient counseling on the prognosis of the disease. Furthermore, this type of knowledge is crucial to the emerging new

field of gene therapy, not only to select patients amenable for treatment, but also to determine the effects of the treatment they may receive.

Methods

Subjects and genetic analysis

Patients with inherited photoreceptor dystrophies were referred to specialized ophthalmic centers and examined at the Radboud University Nijmegen Medical Centre (by CBH and BJK), Hadassah-Hebrew University Medical Center in Jerusalem, Israel (by EB), the Goldschleger Eye Research Institute (by YR) or the Institute for Ophthalmic Research in Tuebingen, Germany (by SH).

Subsequently, genetic analysis was performed in all cases. After the discovery of a causative homozygous *C8orf37* mutation using homozygosity mapping and targeted next generation sequencing (NGS) in a German RP patient (A-IV:1), further genetic analysis was performed in ~400 families with autosomal recessive RP, CRD, or Leber congenital amaurosis. This resulted in three more families from the Netherlands or Israel with causative mutations in *C8orf37*.[16] In total, four families including eight affected individuals were selected for this clinical study (Table 4.1).

We adhered to the tenets of the Declaration of Helsinki and informed consent was obtained from all participating patients prior to the collection of a blood sample and additional ophthalmologic examinations. Prior to this study, we obtained approval from the Institutional Ethics Committee from the Radboud University Nijmegen Medical Centre.

Clinical analysis

Clinical data were collected from the medical records of these patients. Following the identification of causative *C8orf37* mutations, all patients were re-evaluated in addition to the data accumulated over the years. Medical history was registered with a focus on age of onset, initial symptoms and overall course of the retinal disorder. Age of onset was defined as the age at which the initial symptom was first noticed by the patient. We asked all patients about the presence of syndromic features, which are generally present in 20-30% of retinal dystrophy patients. These questions concerned the presence of hearing and balance abnormalities, renal failure, cardiac and respiratory anomalies, polydactyly, obesity, cognitive impairment, fertility disorders, hypogonadism and dental anomalies. The clinical examination included best-corrected visual acuity (BCVA), slit-lamp biomicroscopy, ophthalmoscopy and fundus photography. Goldmann (kinetic) perimetry was performed in 6 patients. In patients A-IV:1 and D-IV:4 perimetry proved impossible due to severe visual impairment. Cross-sectional images of the central retina were obtained with a commercially available Spectral-domain optical coherence tomography (SD-OCT) instrument (Spectralis, Heidelberg Engineering, Heidelberg, Germany; Cirrus, Carl Zeiss Meditec, Jena, Germany) by performing a volume scan (15° x 20°) through the fovea. Central foveal thickness was measured at the foveola using Heidelberg Eye Explorer software (version 1.6.4.0, Heidelberg Engineering, Heidelberg, Germany) or the Cirrus Software (version 5.1.1.6, Carl Zeiss Meditec, Jena, Germany). Fundus autofluorescence (FAF; Spectralis, Heidelberg Engineering, Heidelberg, Germany) could be performed in six patients. A full-field ERG was performed in all patients except patient D-IV:4.

ERGs were performed using Dawson-Trick-Litzkow (DTL) electrodes and the Espion Visual Electrophysiology System (Diagnosys, LLC, Lowell, USA) in the Institute for Ophthalmic Research Tuebingen, Germany; DTL-electrodes and the RETI-port system (Roland Consults, Stasche & Finger GmbH, Brandenburg an der Hazel, Germany) in the Radboud University Nijmegen Medical Centre, The Netherlands; Bipolar Burien Allen electrodes and the UTAS SunBurst™ Color LED Ganzfeld (LKC technologies, Gaithersburg, MD) in Goldschleger Eye Research Institute, Israel; and monopolar corneal electrodes (Henkes-type, Medical Workshop B.V., Groningen, The Netherlands) and the computerized UTAS 3000 system (LKC technologies, Gaithersburg, MD) in the Hadassah-Hebrew University Medical Center, Israel. ERGs were assessed according to local standard values. All centers followed the guidelines of the International Society for Clinical Electrophysiology of Vision (ISCEV).[17]

Results

We included a total of eight patients from four families in this study. An overview of the clinical findings in these patients is provided in Table 4.1. In families A and D, the affected individuals were diagnosed with RP, whereas in the other families (B and C) the patients were diagnosed with CRD. Additionally, both patients from family B mentioned postaxial polydactyly in their medical history, including one additional finger and toe on the right hand and foot respectively. In the other families, no extra-ocular abnormalities suggesting syndromic RP or CRD were observed.

In the RP families (A and D), the mean age of onset was approximately 12 years and ranged from infancy to the age of 18. The initial symptom in these patients was either loss of visual acuity (n=2) or night blindness (n=1) in these patients, although both symptoms occurred within a year after the onset of the disease in these patients. In one patient (D-IV:1), the exact initial symptom could not be determined as night blindness and visual acuity loss occurred simultaneously. After the onset of the disease, visual acuity deteriorated to hand movements or light perception within the following two decades (range: 8-17 years). No nystagmus was observed. Early stages of posterior subcapsular cataract were present in the patients of family D, whereas the lens of patient A-IV:1 was clear. Ophthalmoscopy displayed the classic RP features of bone spicule pigmentation, attenuated vessels and pallor of the optic disc as well as profound atrophic lesions in the macular RPE, along the vascular arcades and peripapillary region (mean age 40 years; Figure 4.1A and D). Correspondingly, autofluorescence imaging showed hypoautofluorescent lesions in these areas (Figure 4.2A and G), whereas OCT examination showed generalized loss of the photoreceptor-retinal pigment epithelium (RPE) complex (Figure 4.2B and H).

Table 4.1. Clinical features at most current examination in patients carrying mutations in *C8orf37*.

Patient-ID/Age of onset(y)/Age/Sex	Initial symptom	Visual Acuity*	Lens Status	Ophthalmoscopy Results	ERG Results†	Goldmann Perimetry
A-IV:1/Infancy/ 37/M	Night blindness/ loss of visual acuity	LP LP	Clear	Profound panretinal chorioretinal atrophy, waxy pallor of the optic disc, severely attenuated vessels, irregular pigment clumps, bone spicules in the midperiphery	NR‡ NR‡	UTP
B-V:1/17/41/F	Photophobia	CF CF	Clear	Severe atrophy with RPE alterations and gliosis in the macula, normal aspect of the optic disc, mild attenuation of peripheral retinal vessels only, peripheral pigmentations (both bone spicule-like as well as round), chorioretinal atrophy in the midperiphery.	NR§ NR§	LE: Central scotoma RE: not reliable. Progressive constriction of VF‖
B-V:7/10/26/M	Photophobia	20/125 20/125	Clear	RPE alterations, atrophy and gliosis in the macula. Normal aspect of vasculature and optic disc. Sporadic round pigmentations in periphery.	NR NR	Unreliable. BE: Constricted VF
C-II:1/Infancy/ 36/M	Loss of visual acuity	20/250 20/345	Clear	Macular atrophy with intraretinal pigment clumping, peripapillary atrophy, temporal optic disc pallor, attenuation of the retinal vessels.	SR# NR	NP
C-II:2/Infancy/ 30/M	Loss of visual acuity	20/60 20/400	Clear	Macular atrophy, peripapillary atrophy, temporal optic disc pallor, attenuated vessels, RPE changes in the RE following extra-ocular surgery for retinal detachment.	SR# NR	NP
D-IV:1/18/38/F	Night blindness/ loss of visual acuity	HM HM	Very mild PSC cataract in BE	Yellow-brown atrophic lesion in the macula with pigment clumps, waxy optic disc pallor, attenuated vessels, gray atrophy along the vascular arcades, heavy bone spicule pigmentations in mid-periphery.	NR NR	LE performed only; remaining VF of 5° with severe sensitivity loss.
D-IV:3/17/43/F	Loss of visual acuity	LP LP	Very mild PSC cataract in BE	Yellow-brown atrophic lesion in the macula with pigment clumps, pallor optic disc with peripapillary atrophy, attenuated vessels; gray atrophic lesions with pigmentation along the vascular arcades, heavy bone spicules pigmentation in mid-periphery.	NR NR	LE performed only; remaining VF of 5° with severe sensitivity loss.
D-IV:4/10/40/F	Loss of visual acuity	LP LP	Mild PSC cataract in BE	Brown atrophic lesion in the macula with pigment clumps, waxy optic disc pallor and peripapillary atrophy, attenuated vessels; grayish atrophic changes in the perimacular region, heavy bone spicule pigmentation in the mid-periphery.	NP NP	UTP

Table 4.1. Clinical features at most current examination in patients carrying mutations in *C8orf37*. (continued)

Patient-ID/Age of onset(y)/Age/Sex	Initial symptom	Visual Acuity*	Lens Status	Ophthalmoscopy Results	ERG Results†	Goldmann Perimetry
A-IV:1/Infancy/ 37/M	Night blindness/ loss of visual acuity	LP / LP	Clear	Profound panretinal chorioretinal atrophy, waxy pallor of the optic disc, severely attenuated vessels, irregular pigment clumps, bone spicules in the midperiphery	NR‡ / NR‡	UTP
B-V:1/17/41/F	Photophobia	CF / CF	Clear	Severe atrophy with RPE alterations and gliosis in the macula, normal aspect of the optic disc, mild attenuation of peripheral retinal vessels only, peripheral pigmentations (both bone spicule-like as well as round), chorioretinal atrophy in the midperiphery.	NR§ / NR§	LE: Central scotoma RE: not reliable. Progressive constriction of VF∥
B-V:7/10/26/M	Photophobia	20/125 / 20/125	Clear	RPE alterations, atrophy and gliosis in the macula. Normal aspect of vasculature and optic disc. Sporadic round pigmentations in periphery.	NR / NR	Unreliable. BE: Constricted VF
C-II:1/Infancy/ 36/M	Loss of visual acuity	20/250 / 20/345	Clear	Macular atrophy with intraretinal pigment clumping, peripapillary atrophy, temporal optic disc pallor, attenuation of the retinal vessels.	SR# / NR	NP
C-II:2/Infancy/ 30/M	Loss of visual acuity	20/60 / 20/400	Clear	Macular atrophy, peripapillary atrophy, temporal optic disc pallor, attenuated vessels, RPE changes in the RE following extra-ocular surgery for retinal detachment.	SR# / NR	NP
D-IV:1/18/38/F	Night blindness/ loss of visual acuity	HM / HM	Very mild PSC cataract in BE	Yellow-brown atrophic lesion in the macula with pigment clumps, waxy optic disc pallor, attenuated vessels, gray atrophy along the vascular arcades, heavy bone spicule pigmentations in mid-periphery.	NR / NR	LE performed only: remaining VF of 5° with severe sensitivity loss.
D-IV:3/17/43/F	Loss of visual acuity	LP / LP	Very mild PSC cataract in BE	Yellow-brown atrophic lesion in the macula with pigment clumps, pallor optic disc with peripapillary atrophy, attenuated vessels; gray atrophic lesions with pigmentation along the vascular arcades, heavy bone spicules pigmentation in mid-periphery.	NR / NR	LE performed only: remaining VF of 5° with severe sensitivity loss.

4

Table 4.1. Clinical features at most current examination in patients carrying mutations in *C8orf37*. (continued)

Patient-ID/Age of onset(y)/Age/Sex	Initial symptom	Visual Acuity*	Lens Status	Ophthalmoscopy Results	ERG Results†	Goldmann Perimetry
D-IV:4/10/40/F	Loss of visual acuity	LP LP	Mild PSC cataract in BE	Brown atrophic lesion in the macula with pigment clumps, waxy optic disc pallor and peripapillary atrophy, attenuated vessels; grayish atrophic changes in the perimacular region, heavy bone spicule pigmentation in the mid-periphery.	NP NP	UTP

BE = both eyes; CF = counting fingers; CFT = central foveal thickness; Dx = diagnosis; ERG = electroretinogram; F = Female; HM = hand movements; LE = left eye; LP = light perception; M = Male; NP = not performed; NR = nonrecordable; OCT = optical coherence tomography; PIS = photoreceptor inner segment; POS = photoreceptor outer segments; PSC = posterior subcapsulary cataracts; RE = right eye; SR = severely reduced; UTP = unable to perform test, due to severe of vision loss; VF = visual field. * = The upper line represents the right eye, the lower line represents the left eye. † = The upper line represents the scotopic results, the lower line represents the photopic results. ‡ = ERG performed at the age of 19 and 37. Both rod and cone responses were nonrecordable at age of 19. § = ERG performed at the age of 29 and 41. Scotopic responses were severely reduced and photopic responses were nonrecordable at age of 29. ‖ = Goldmann perimetry performed at age of 29 and 41. At an age of 29, there was no constriction of the visual field. # = Negative scotopic ERG.
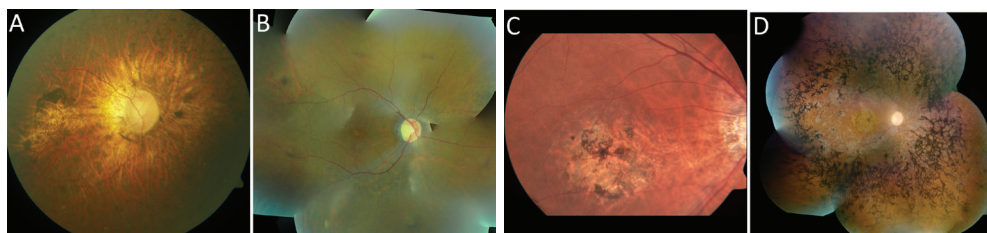
Figure 4.1. Fundus photographs of patients carrying mutations in C8orf37. **A,** Fundus photograph of the central retina in the right eye of patient A-IV:1 (age 37) showing profound retinal degeneration, waxy pallor of the optic disc, attenuated vessels, irregular pigmentations in the macula, as well as bone spicule-like pigmentation in the mid-periphery. **B,** Fundus photograph composition of right eye of patient B-V:7, aged 26, revealing macular atrophy as well as slightly attenuated arterioles and areas of ongoing chorioretinal atrophy. One round pigmentation can be found along the inferior vascular arcade. **C,** Fundus photograph of the central retina in the right eye of patient C-II:1 (age 36) showing profound macular atrophy and intraretinal irregular pigmentation, as well as attenuated arterioles. **D,** Fundus photograph composition of patient D-IV:1 at age 39 (right eye) reveals macular atrophy and pigmentation clumps, as well as pallor of the optic disc, attenuated vessels, paravascular atrophy of the retinal pigment epithelium and abundant bone spicules.

On ERG examination, both rod- and cone-driven responses were nonrecordable in all patients (mean age 33 years). Perimetry (patients D-IV:1 and D-IV:3) showed a severely constricted visual field with approximately 5° remaining using target V-4e (mean age 41 years).

In the two CRD families (B and C), the mean age of onset was approximately seven years and, like in the RP patients, ranged from infancy to the age of 18. Either photophobia (n=2) or loss of visual acuity (n=2) was mentioned as initial symptom. In the three decades following the onset of the disease, all four CRD patients developed loss of visual acuity that gradually decreased to low vision levels of 20/60 to counting fingers. These patients showed eccentral fixation, no nystagmus or nystagmoid wandering eye movements were present. Biomicroscopy revealed no cataract was present in these patients. Ophthalmoscopy revealed macular RPE atrophy as well as (mild) attenuation of the vessels (mean age 33 years; Figure 4.1B and C). In patient C-II:2, pigment changes due to extra-ocular surgery for retinal detachment were observed. Autofluorescence imaging showed focal hypoautofluorescent lesions in the macula (Figure 4.2C and E), whereas OCT examination showed generalized photoreceptor degeneration (Figure 4.2D and F). Initially, cone-driven responses were more severely affected than the rod-driven responses, which were nonrecordable and severely reduced respectively. In the affected individuals of family C, the mixed dark-adapted recordings showed negative waveforms. In later stages, rod-driven responses also became nonrecordable in the patients from family B (mean age 34 years). Perimetry was difficult to perform, but concentric restriction of the visual field was present (mean age 34 years). A central scotoma was found in only one patient (B-V:1).

Thinning of the central neuroretina was observed in all patients, except for A-IV:1 and C-II:1. The central foveal thickness (CFT) was 74 micron on average (mean age 36 years; Table 4.1), whereas CFT generally is ~230 micron in healthy individuals as found by Tick and colleagues.[18]

Discussion

Inherited retinal dystrophies are highly variable in their clinical presentation, even when more or less specific phenotypes such as RP and CRD are considered. This clinical heterogeneity is for a large part the result of the many different genes and mutations that are involved. In addition, incompletely understood genetic and environmental modifying factors influence the disease phenotype. Recently, mutations in the *C8orf37* gene have been linked to an autosomal recessive retinal dystrophy.[16] This report provides an overview of the clinical features of the *C8orf37*-associated retinal dystrophy.

The eight patients in this study presented either with a CRD phenotype or an RP phenotype with early macular involvement. Macular atrophy is an early feature of CRD. It usually does not occur in classic RP until the very end stage of disease, although it is observed in some specific forms of RP.[19-22] The RP patients in our study demonstrated a profound loss of vision in an early stage of the disease, and some even mentioned loss of visual acuity as initial symptom, although night blindness followed visual loss only by a couple of months. Ophthalmoscopy, OCT and FAF examination revealed profound atrophy of the photoreceptor-RPE complex in the maculae of the RP patients. Contrary to the CRD patients, RP patients developed tunnel vision. Perimetry examination in patients D-IV:1 and D-IV:3 did not show an absolute central scotoma, but a remaining central visual field residue of 5° with decreased sensitivity.

The disease progression rate was high in all patients in this study: end stage disease was reached within two decades after the onset in the RP patients and within three decades in the CRD patients. Presently, at a mean age of 36 years, most CRD and RP patients demonstrate severely atrophic retinas as a final common end stage. In the light of gene therapy development, knowledge about the natural course of *C8orf37*-associated diseases is important. When available, early treatment before severe damage to the retinal architecture occurs, is essential in these patients.[23] The high rate of disease progression makes early evaluation of treatment effect possible. Unfortunately, gene therapy will probably not be developed in the near future, as the estimated frequency of *C8orf37* mutations as a cause of RP/CRD is low (<1%), and a suitable (animal) model is lacking.

Interestingly, *C8orf37* is one of few genes that can cause both autosomal recessive RP and CRD. Until now, this has only been described in two other genes: *ABCA4* and *CERKL*. For *ABCA4*, it is hypothesized that the level of dysfunctional ABCA4 protein is instrumental in the degeneration pattern, causing either Stargardt disease, CRD or RP.[24-26] Although the phenotype associated with *CERKL* mutations was originally characterized as RP,[15, 27] most patients that have been described until now are diagnosed with CRD.[28-31] This is in accordance with the observation that the CERKL protein is mainly localized in cone photoreceptors of mouse retinae.[32] The *C8orf37* gene is expressed in both rod and cone photoreceptors.[16] This fits with the involvement of both types of photoreceptors, but does not explain the pattern of photoreceptor degeneration. Within the 4 families, we did not observe differences in degeneration patterns. This suggests a connection between the degeneration pattern and a genetic cause, as family members carry identical *C8orf37* mutations and are likely to share modifier alleles as well. Here, the correlation between phenotype and genotype is mainly
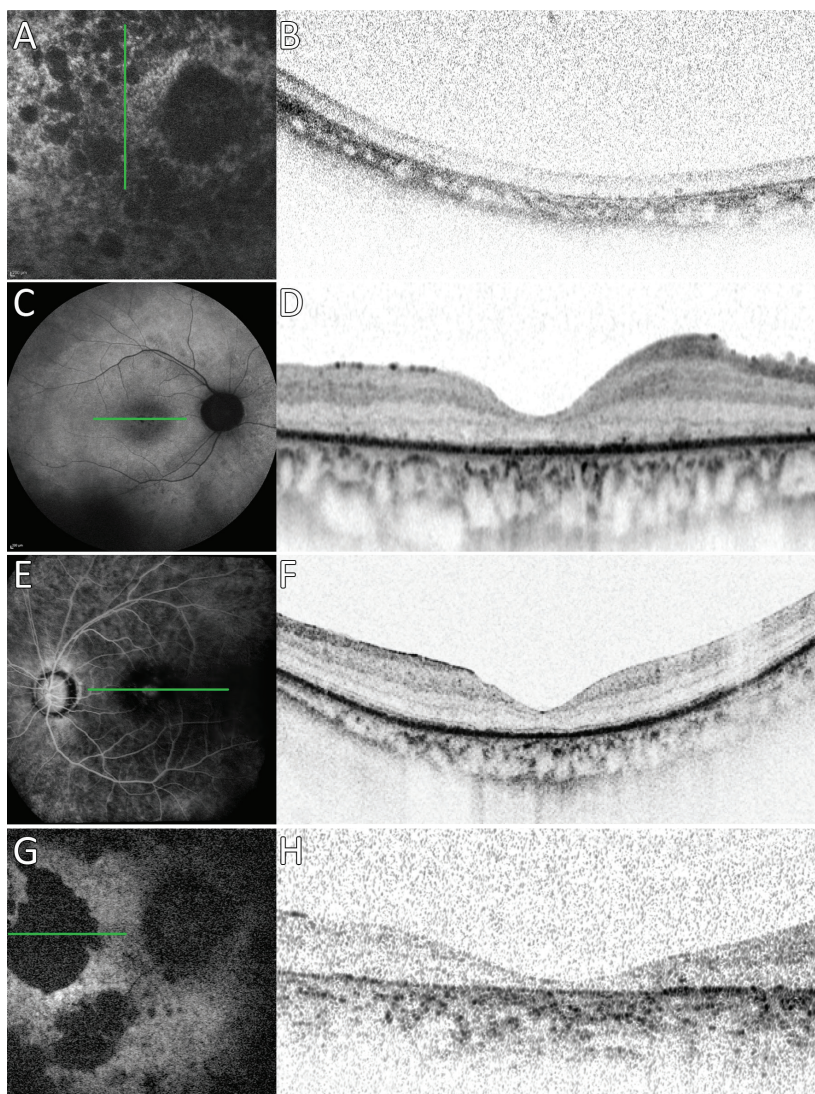
Figure 4.2. (Auto)fluorescence imaging and corresponding SD-OCT examinations in patients with mutations in C8orf37. **A, B.** Autofluorescence (A) and SD-OCT (B) image of the right eye of patient A-IV:1 (age 37) showing macular hypoautofluorescence and numerous hypoautofluorescent lesions in the perimacular region (A), as well as severe thinning of the retina temporal of the macula (B). **C, D.** Autofluorescence (C) and SD-OCT (D) imaging of the right eye of patient B-V:7 (age 26) reveals foveal hypoautofluorescence, parafoveal hyperautofluorescence, numerous irregular hypoautofluorescent spots in the perimacular region (C), and severe thinning of the foveal thickness and profound loss of the photoreceptor layer with preservation of the RPE cells (D). **E, F.** Fluorescence angiography (E) and OCT (F) image of the central retina in the left eye of patient C-II:2 at the age of 30 (no autofluorescence was performed) showing hypofluorescence in the macula (E), and loss of photoreceptor outer segments, thinning of the retina and atrophy of the choriocapillaris (F). **G, H.** Autofluorescence (G) and OCT (H) image of the central retina in the right eye of patient D-IV:1 (age 39) reveals hypoautofluorescence in macula indicating atrophy as well as atrophic lesions along the vascular arcades (G) and severe thinning of the retina with profound loss of the photoreceptor-RPE complex (H). Green lines indicate the location of the corresponding OCT examination. Image quality varies as result of unstable eccentric fixation.

theoretical as the exact effects of the mutations on the C8orf37 protein and its function are not known. However, our previous study localized the protein to the ciliary rootlet of the connecting cilia in mouse photoreceptors and to the base of the primary cilia of human RPE cells, indicating a ciliary function.[16]

Ciliopathies are diseases characterized by the dysfunction of the cilium,[33] which may lead to either multi-organ syndromic phenotypes or to single organ diseases.[34] The presence of postaxial polydactyly in patients B-V:1 and B-V:7 is interesting in view of the probable ciliary function of C8orf37, as it is one of the cardinal features of Bardet-Biedl syndrome (BBS), a ciliopathy characterized by retinal degeneration, obesity, polydactyly, hypogonadism, renal dysfunction and cognitive impairment.[34] Retinal degeneration is a hallmark of many syndromic ciliopathies,[35, 36] although mutations in retina-specific ciliary genes may also lead to non-syndromic RP.[37, 38] One-third of non-syndromic retinal dystrophies involve defects in a ciliary protein.[38] Ubiquitously expressed ciliary genes, like *C8orf37* and for example *RPGR*, are more likely to cause syndromic phenotypes. Also in *RPGR*-associated disease, most of the patients demonstrate isolated RP,[39] although systemic symptoms have been identified occasionally.[40, 41]

ERG responses

Scotopic (rod + cone)   Photopic (cone)

Control

100 µV
50 msec

Patient C-II:1
Left eye

Right eye
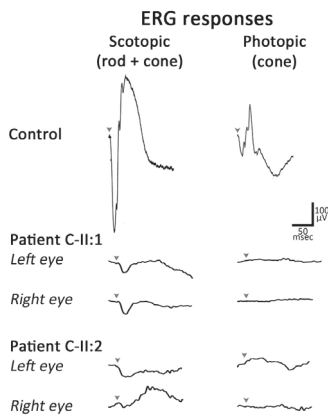
Patient C-II:2
Left eye

Right eye

Figure 4.3 ERG recordings of all patients with recordable responses. (patient C-II:1 at age 36 and C-II:2 at age 30). Only scotopic mixed (rod + cone) responses and photopic (cone) responses are depicted. Arrowheads indicate the moment of the light flash. Control shows normal responses of individuals with healthy retinas. Both patients have severely reduced scotopic responses and nonrecordable photopic responses. The dark-adapted responses of patient C-II:1 show negative ERG waveforms. The dark-adapted responses of patient C-II:2 only show a negative ERG waveform in the left eye. ERG, electroretinography; msec, millisecond; µV, microvolts.

Besides the postaxial polydactyly in individuals B-V:1 and B-V:7, we did not identify other syndromic features in these individuals. In the other patients no syndromic abnormalities were observed, although we could not perform detailed additional examinations to exclude subclinical symptoms. Polydactyly generally occurs in 5 to 19 per 10000 live births.[42] We cannot exclude coincidental co-existence but the polydactyly in this family only occurred in the siblings affected with CRD. This strengthens the hypothesis of associations between the retinal phenotype and polydactyly. In the remaining patients, we could identify other features previously linked to ciliopathies: electronegative ERG waveforms in patients C-II:1 and C-II:2 (Figure 4.3), which have been described in *BBS1*-associated BBS,[43, 44] and the early occurrence of macular atrophy.[21, 22, 43-46] These data indicate that mutations in *C8orf37* may be able to cause both syndromic and non-syndromic phenotype, similar to other ciliary genes such as *USH2A*,[47] *BBS1*,[48] and *RPGR*.[39-41]

In conclusion, mutations in *C8orf37* cause autosomal recessive CRD or RP with early macular involvement. The dystrophies start in the first two decades of life and progress relatively fast to a common phenotype of end-stage retinal degeneration. Although the exact function of C8orf37 is not known yet, its immunolocalization, associations and interactions with other proteins and presence of polydactyly in one of our families suggest a ciliary function.

References

1. Bunker CH, Berson EL, Bromley WC, Hayes RP, Roderick TH. Prevalence of retinitis pigmentosa in Maine. *Am J Ophthalmol* 1984;97:357-365.
2. Rosenberg T. Epidemiology of hereditary ocular disorders. *Dev Ophthalmol* 2003;37:16-33.
3. Berson EL. Retinitis pigmentosa. The Friedenwald Lecture. *Invest Ophthalmol Vis Sci* 1993;34:1659-1676.
4. Michaelides M, Hunt DM, Moore AT. The cone dysfunction syndromes. *Br J Ophthalmol* 2004;88:291-297.
5. Hamel CP. Cone rod dystrophies. *Orphanet J Rare Dis* 2007;2:7.
6. Hartong DT, Berson EL, Dryja TP. Retinitis pigmentosa. *Lancet* 2006;368:1795-1809.
7. Deutman AF (ed) *Rod-cone dystrophy, hereditary, pigmentary retinopathy, retinitis pigmentosa.* Hagerstown: Harper & Row Publishers, Inc; 1977:479-576.
8. Gouras P, Carr RE. Electrophysiological Studies in Early Retinitis Pigmentosa. *Arch Ophthalmol* 1964;72:104-110.
9. Kajiwara K, Berson EL, Dryja TP. Digenic retinitis pigmentosa due to mutations at the unlinked peripherin/RDS and ROM1 loci. *Science* 1994;264:1604-1608.
10. Dryja TP, Hahn LB, Kajiwara K, Berson EL. Dominant and digenic mutations in the peripherin/RDS and ROM1 genes in retinitis pigmentosa. *Invest Ophthalmol Vis Sci* 1997;38:1972-1982.
11. Berger W, Kloeckener-Gruissem B, Neidhardt J. The molecular basis of human retinal and vitreoretinal diseases. *Prog Retin Eye Res* 2010;29:335-375.
12. Daiger SP, Rossiter BJF, Greenberg J, Christoffels A, Hide W. RetNet, the Retinal Information Network.Accessed on: 26 Feb 2013. http://www.sph.uth.tmc.edu/RetNet/
13. den Hollander AI, Black A, Bennett J, Cremers FP. Lighting a candle in the dark: advances in genetics and gene therapy of recessive retinal dystrophies. *J Clin Invest* 2010;120:3042-3053.
14. Cremers FP, van de Pol DJ, van Driel M, et al. Autosomal recessive retinitis pigmentosa and cone-rod dystrophy caused by splice site mutations in the Stargardt's disease gene ABCR. *Hum Mol Genet* 1998;7:355-362.
15. Tuson M, Marfany G, Gonzalez-Duarte R. Mutation of CERKL, a novel human ceramide kinase gene, causes autosomal recessive retinitis pigmentosa (RP26). *Am J Hum Genet* 2004;74:128-138.
16. Estrada-Cuzcano A, Neveling K, Kohl S, et al. Mutations in C8orf37, encoding a ciliary protein, are associated with autosomal-recessive retinal dystrophies with early macular involvement. *Am J Hum Genet* 2012;90:102-109.
17. Marmor MF, Fulton AB, Holder GE, Miyake Y, Brigell M, Bach M. ISCEV Standard for full-field clinical electroretinography (2008 update). *Doc Ophthalmol* 2009;118:69-77.
18. Tick S, Rossant F, Ghorbel I, et al. Foveal shape and structure in a normal population. *Invest Ophthalmol Vis Sci* 2011;52:5105-5110.
19. Avila-Fernandez A, Riveiro-Alvarez R, Vallespin E, et al. CERKL mutations and associated phenotypes in seven Spanish families with autosomal recessive retinitis pigmentosa. *Invest Ophthalmol Vis Sci* 2008;49:2709-2713.
20. Mackay DS, Henderson RH, Sergouniotis PI, et al. Novel mutations in MERTK associated with childhood onset rod-cone dystrophy. *Mol Vis* 2010;16:369-377.
21. Koenekoop RK, Loyer M, Hand CK, et al. Novel RPGR mutations with distinct retinitis pigmentosa phenotypes in French-Canadian families. *Am J Ophthalmol* 2003;136:678-687.
22. Campo RV, Aaberg TM. Ocular and systemic manifestations of the Bardet-Biedl syndrome. *Am J Ophthalmol* 1982;94:750-756.
23. Maguire AM, High KA, Auricchio A, et al. Age-dependent effects of RPE65 gene therapy for Leber's congenital amaurosis: a phase 1 dose-escalation trial. *Lancet* 2009;374:1597-1605.
24. Allikmets R, Singh N, Sun H, et al. A photoreceptor cell-specific ATP-binding transporter gene (ABCR) is mutated in recessive Stargardt macular dystrophy. *Nat Genet* 1997;15:236-246.
25. Klevering BJ, Yzer S, Rohrschneider K, et al. Microarray-based mutation analysis of the ABCA4 (ABCR) gene in autosomal recessive cone-rod dystrophy and retinitis pigmentosa. *Eur J Hum Genet* 2004;12:1024-1032.
26. Klevering BJ, Deutman AF, Maugeri A, Cremers FP, Hoyng CB. The spectrum of retinal phenotypes caused by mutations in the ABCA4 gene. *Graefes Arch Clin Exp Ophthalmol* 2005;243:90-100.
27. Bayes M, Goldaracena B, Martinez-Mir A, et al. A new autosomal recessive retinitis pigmentosa locus maps on chromosome 2q31-q33. *J Med Genet* 1998;35:141-145.

28.   Ali M, Ramprasad VL, Soumittra N, et al. A missense mutation in the nuclear localization signal sequence of CERKL (p.R106S) causes autosomal recessive retinal degeneration. *Mol Vis* 2008;14:1960-1964.

29.   Auslender N, Sharon D, Abbasi AH, Garzozi HJ, Banin E, Ben-Yosef T. A common founder mutation of CERKL underlies autosomal recessive retinal degeneration with early macular involvement among Yemenite Jews. *Invest Ophthalmol Vis Sci* 2007;48:5431-5438.

30.   Tang Z, Wang Z, Ke T, Wang QK, Liu M. Novel compound heterozygous mutations in CERKL cause autosomal recessive retinitis pigmentosa in a nonconsanguineous Chinese family. *Arch Ophthalmol* 2009;127:1077-1078.

31.   Avila-Fernandez A, Cantalapiedra D, Aller E, et al. Mutation analysis of 272 Spanish families affected by autosomal recessive retinitis pigmentosa using a genotyping microarray. *Mol Vis* 2010;16:2550-2558.

32.   Vekslin S, Ben-Yosef T. Spatiotemporal expression pattern of ceramide kinase-like in the mouse retina. *Mol Vis* 2010;16:2539-2549.

33.   Hildebrandt F, Benzing T, Katsanis N. Ciliopathies. *N Engl J Med* 2011;364:1533-1543.

34.   Mockel A, Perdomo Y, Stutzmann F, Letsch J, Marion V, Dollfus H. Retinal dystrophy in Bardet-Biedl syndrome and related syndromic ciliopathies. *Prog Retin Eye Res* 2011;30:258-274.

35.   Gerdes JM, Davis EE, Katsanis N. The vertebrate primary cilium in development, homeostasis, and disease. *Cell* 2009;137:32-45.

36.   Badano JL, Mitsuma N, Beales PL, Katsanis N. The ciliopathies: an emerging class of human genetic disorders. *Annu Rev Genomics Hum Genet* 2006;7:125-148.

37.   Koenekoop RK. RPGRIP1 is mutated in Leber congenital amaurosis: a mini-review. *Ophthalmic Genet* 2005;26:175-179.

38.   Estrada-Cuzcano A, Roepman R, Cremers FP, den Hollander AI, Mans DA. Non-syndromic retinal ciliopathies: translating gene discovery into therapy. *Hum Mol Genet* 2012.

39.   Hosch J, Lorenz B, Stieger K. RPGR: role in the photoreceptor cilium, human retinal disease, and gene therapy. *Ophthalmic Genet* 2011;32:1-11.

40.   Zito I, Downes SM, Patel RJ, et al. RPGR mutation associated with retinitis pigmentosa, impaired hearing, and sinorespiratory infections. *J Med Genet* 2003;40:609-615.

41.   Iannaccone A, Breuer DK, Wang XF, et al. Clinical and immunohistochemical evidence for an X linked retinitis pigmentosa syndrome with recurrent infections and hearing loss in association with an RPGR mutation. *J Med Genet* 2003;40:e118.

42.   Zguricas J, Heus H, Morales-Peralta E, et al. Clinical and genetic studies on 12 preaxial polydactyly families and refinement of the localisation of the gene responsible to a 1.9 cM region on chromosome 7q36. *J Med Genet* 1999;36:32-40.

43.   Azari AA, Aleman TS, Cideciyan AV, et al. Retinal disease expression in Bardet-Biedl syndrome-1 (BBS1) is a spectrum from maculopathy to retina-wide degeneration. *Invest Ophthalmol Vis Sci* 2006;47:5004-5010.

44.   Cox KF, Kerr NC, Kedrov M, et al. Phenotypic expression of Bardet-Biedl syndrome in patients homozygous for the common M390R mutation in the BBS1 gene. *Vision Res* 2012;75:77-87.

45.   Jayasundera T, Branham KE, Othman M, et al. RP2 phenotype and pathogenetic correlations in X-linked retinitis pigmentosa. *Arch Ophthalmol* 2010;128:915-923.

46.   Lorenz B, Andrassi M, Kretschmann U. Phenotype in two families with RP3 associated with RPGR mutations. *Ophthalmic Genet* 2003;24:89-101.

47.   Rivolta C, Sweklo EA, Berson EL, Dryja TP. Missense mutation in the USH2A gene: association with recessive retinitis pigmentosa without hearing loss. *Am J Hum Genet* 2000;66:1975-1978.

48.   Estrada-Cuzcano A, Koenekoop RK, Senechal A, et al. BBS1 mutations in a wide spectrum of phenotypes ranging from nonsyndromic retinitis pigmentosa to Bardet-Biedl syndrome. *Arch Ophthalmol* 2012;130:1425-1432.

Authors

Koji M. Nishiguchi,[1]* Almudena Avila-Fernandez,[2]* Ramon A. C. van Huet,[3]* Marta Corton,[2] Raquel Pérez-Carro,[2] Esther Martín-Garrido,[2] María Isabel López-Molina,[4] Fiona Blanco-Kelly,[2] Lies H. Hoefsloot,[5] Wendy A. van Zelst-Stams,[5] Pedro J. García-Ruiz,[6] Javier del Val,[6] Silvio Alessandro Di Gioia,[1] B. Jeroen Klevering,[3,7] Bart P. C. van de Warrenburg,[8,9] Carlos Vazquez,[10] Frans P. M. Cremers,[5,11] Blanca García-Sandoval,[4] Carel B. Hoyng,[3] Rob W. J. Collin,[5,7,11]* Carlo Rivolta,[1]* Carmen Ayuso[2]*

Affiliations

[1]Department of Medical Genetics, University of Lausanne, Lausanne, Switzerland.

[2]Department of Genetics, IIS-Fundación Jiménez Díaz, CIBERER, Madrid, Spain.

[3]Department of Ophthalmology, Radboud University Medical Center, Nijmegen, The Netherlands.

[4]Department of Ophthalmology, Fundación Jiménez Díaz, Madrid, Spain.

[5]Department of Human Genetics, Radboud University Medical Center, Nijmegen, The Netherlands.

[6]Department of Neurology, Fundación Jiménez Díaz, Madrid, Spain.

[7]Institute for Genetic and Metabolic Disease, Radboud University Medical Center, Nijmegen, The Netherlands.

[8]Department of Neurology, Radboud University Medical Center, Nijmegen, The Netherlands.

[9]Donders Institute for Brain, Cognition, and Behaviour, Radboud University Medical Center, Nijmegen, The Netherlands.

[10]Department of Genetics, Insular-Materno Infantil University Hospital, Las Palmas de Gran Canaria, Spain.

[11]Nijmegen Center for Molecular Life Sciences, Radboud University Medical Center, Nijmegen, The Netherlands.

*These authors contributed equally as first authors.

Exome sequencing extends the phenotypic spectrum for *ABHD12* mutations

From Syndromic to Nonsyndromic Retinal Degeneration

5

Abstract

Objective. To identify the genetic causes underlying autosomal recessive retinitis pigmentosa (arRP) and to describe the associated phenotype.

Design. Case series.

Participants. Three hundred forty-seven unrelated families affected by arRP and 33 unrelated families affected by retinitis pigmentosa (RP) plus noncongenital and progressive hearing loss, ataxia, or both, respectively.

Methods. A whole exome sequencing (WES) analysis was performed in 2 families segregating arRP. A mutational screening was performed in 378 additional unrelated families for the exon-intron boundaries of the ABHD12 gene. To establish a genotype-phenotype correlation, individuals who were homozygous or compound heterozygotes of mutations in ABHD12 underwent exhaustive clinical examinations by ophthalmologists, neurologists, and otologists.

Main Outcome Measures. DNA sequence variants, best-corrected visual acuity, visual field assessments, electroretinogram responses, magnetic resonance imaging, and audiography.

Results. After a WES analysis, we identified 4 new mutations (p.Arg107Glufs*8, p.Trp159*, p.Arg186Pro, and p.Thr202Ile) in *ABHD12* in 2 families (RP-1292 and W08-1833) previously diagnosed with nonsyndromic arRP, which cosegregated with the disease among the family members. Another homozygous mutation (p.His372Gln) was detected in 1 affected individual (RP-1487) from a cohort of 378 unrelated arRP and syndromic RP patients. After exhaustive clinical examinations by neurologists and otologists, the 4 affected members of the RP-1292 had no polyneuropathy or ataxia, and the sensorineural hearing loss and cataract were attributed to age or the normal course of the RP, whereas the affected members of the families W08-1833 and RP-1487 showed clearly symptoms associated with polyneuropathy, hearing loss, cerebellar ataxia, RP, and early-onset cataract (PHARC) syndrome.

Conclusions. Null mutations in the *ABHD12* gene lead to PHARC syndrome, a neurodegenerative disease including polyneuropathy, hearing loss, cerebellar ataxia, RP, and early-onset cataract. Our study allowed us to report 5 new mutations in *ABHD12*. This is the first time missense mutations have been described for this gene. Furthermore, these findings are expanding the spectrum of phenotypes associated with *ABHD12* mutations ranging from PHARC syndrome to a nonsyndromic form of retinal degeneration.

Introduction

Retinitis pigmentosa (RP; Mendelian Inheritance in Man, 268000) is the most common form of inherited retinal dystrophies affecting 1 in 4000 persons.[1] Symptoms include night blindness in the early phase of the disease, the development of tunnel vision, and a slowly progressive decrease in central vision.[2] On examination, patients have decreased visual acuity and constricted visual fields accompanied by the classic fundus appearance with dark pigmentary clumps in the midperiphery and perivenous areas, attenuated retinal vessels, and waxy optic disc pallor. However, the disease onset, progression, retinal appearance, and visual function may vary significantly among patients and even within a family.

Retinitis pigmentosa usually is restricted to the eye; however, in 20% to 30% of cases, it is associated with nonocular signs leading to more than 30 different syndromes.[3] The most frequent syndromic RP form is Usher syndrome, in which retinal degeneration is associated with hearing impairment, accounting for approximately 10% to 20% of all RP cases.

Retinitis pigmentosa is also a very heterogeneous genetic disorder; the disease can be inherited as an autosomal dominant trait (approximately 20% of cases), as an autosomal recessive trait (30% of cases), or as an X-linked trait (10% of cases). Approximately 40% of patients with RP are isolated cases, although this percentage varies when considering different populations.[1,4] Non-Mendelian inheritance patterns such as digenic, mitochondrial, or de novo mutations have been reported, accounting for a small proportion of cases.[3] To date, mutations in 41 genes have been described as causing nonsyndromic autosomal recessive RP (arRP), and mutations in 56 genes have been identified as being responsible for autosomal recessive syndromic retinal dystrophy, including Bardet-Biedl and Usher syndromes.[5] However, mutations in these genes account for the disease in little more than half of all patients.[1,6] Although the functions of some of these genes have been studied extensively, it is difficult to establish a precise genotype phenotype correlation because mutations in different RP genes can cause overlapping clinical phenotypes.[7]

Recently, a novel form of syndromic RP, a neurodegenerative disease including polyneuropathy, hearing loss, cerebellar ataxia, retinitis pigmentosa, and early-onset cataract (PHARC; Mendelian Inheritance in Man, 612674), has been described.[8] Manifesting typically in the late teens, PHARC syndrome is an autosomal recessive progressive and degenerative disease. Although the phenotype is quite variable, even within a family, it is observed that the hearing loss, the cataract, and the RP are presented in all adult patients described so far.[8-10] Null mutations in the *ABHD12* gene, encoding α-β hydrolase 12 protein, have been associated with this syndrome in a total of 12 unrelated families,[9,10] as well as with a less aggressive phenotype without polyneuropathy that was considered to be a variant of PHARC syndrome in a single family.[11] In this study, after a whole exome sequencing (WES) analysis, we identified 5 new mutations in *ABHD12* in 3 families affected with arRP, one of hich did not present any systematic abnormalities, after careful evaluation of neurologic and auditory function. In addition, this is the first report of missense mutations in *ABHD12*, thereby expanding the spectrum of mutations and phenotypes that range from PHARC syndrome to a nonsyndromic form of retinal degeneration.

Methods

Patient Recruitment

Patients diagnosed with RP were recruited from the Biobank of the Fundación Jiménez Díaz Hospital, Madrid, Spain, and from the department of Ophthalmology, Radboud University Medical Center, Nijmegen, The Netherlands. Diagnostic criteria of RP included night blindness, peripheral visual loss, or both, with visual field loss and poor visual acuity in advanced stages of the disease.

A total of 347 unrelated families with arRP or sporadic RP (346 Spanish families and 1 Dutch family) and 33 unrelated families affected with RP plus noncongenital and progressive hearing loss, ataxia, or both were selected. Informed consent was obtained from all patients and family members or their legal guardians involved in the study. All procedures were reviewed and approved by the ethics committees of our institutions and adhered to the tenets of the Declaration of Helsinki.

One hundred seventy-six unrelated individuals of Spanish origin without RP family history were screened as controls to evaluate the frequency of the missense mutations p.Thr202Ile and p.His372Gln found in these studied Spanish families. The occurrence of the missense variant that was identified in a Dutch family (p.Arg186Pro) was assessed in an in-house exome database consisting of more than 500 unrelated individuals.

Peripheral blood samples of index cases and their family members were collected in EDTA (ethylenediaminetetraacetic acid) tubes. DNA was extracted from peripheral blood leukocytes with an automated DNA extractor (model BioRobotEZ1; Qiagen, Hilden, Germany) following the manufacturer's instructions, or with a standard salting out procedure.

Genetic Analysis

Next Generation Sequencing. Whole exome sequencing was performed in the index cases of the RP-1292 and the W08-1833 families as previously described.[12,13]

Sanger Sequencing Analysis. Bidirectional automatic sequencing was performed to confirm and segregate the obtained results by WES in the RP-1292 and W08-1833 families, to screen the *ABHD12* gene for mutations in a total of 378 additional arRP families, and to determine the frequency of one of the missense variations in the control population. Exons and exon-intron boundaries of the *ABHD12* gene (RefSeq NM_001042472) were analyzed using 14 oligonucleotide primer pairs designed using Primer3 software (available at: www.cgi.com; accessed July 13, 2012). Sequences and annealing temperatures are available from the authors on request.

Sequencing results were analyzed by using Staden Package software version 1.7.0 (available at: staden.sourceforge.net; accessed February 4, 2014) by assembling the sequenced contigs and then visualizing the aligned sequences of the exons. High-Resolution Melting Analysis. High-resolution melting analysis was developed specifically and optimized for the mutational scanning of one of the new missense mutations to evaluate the frequency of the missense variation in the control population. The methodological optimization was performed as described previously.[14] Polymerase chain reaction conditions are available from the authors by request. The high-resolution melting (HRM) curve analysis was performed using the LightCycler 480 Gene Scanning Software (Hoffmann-La Roche,

Basel, Switzerland). Melting curves were normalized and temperature adjusted, and finally, a difference plot was generated.

Prediction of the Pathogenic Effect of the Missense Variations. The pathogenicity of the new variants found in this study was established by the following criteria:
1. Cosegregation in the family.
2. Absence in 176 Spanish healthy control individuals.
3. Amino acid conservation for the missense mutations, which was determined using 31 orthologs of the ABHD12 protein belonging to different evolutionary branches. The BLINK tool (available at: http://www.ncbi.nlm.nih.gov/sutils/blink/; accessed February 4, 2014) and the Jalview Alignment Editor program (available at: http://www.jalview.org; accessed February 4, 2014) were used to analyze the multiple sequence alignments. If a residue did not change throughout the species, it was considered highly conserved; if the variant residue was present in fewer than 3 species, the change was considered moderately conserved; if it was present in 3 to 5 ortholog proteins, it was considered to be weakly conserved; otherwise, it was classified as nonconserved.
4. Pathogenicity prediction with in silico tools, including PolyPhen-2 (Polymorphism Phenotyping version 2; available at: http://genetics.bwh.harvard.edu/pph2/; accessed February 4, 2014), SIFT (available at: http://sift.jcvi.org/; accessed February 4, 2014), and Mutation Taster (available at: http://www.mutationtaster.org/; accessed February 4, 2014) bioinformatics programs.
5. Three-dimensional structure prediction to determine the possible structural changes in the mutant ABHD12 protein. The structure prediction was performed using Project HOPE (available at: http://www.cmbi.ru.nl/hope/home/; accessed February 4, 2014) taking the protein sequencing Q8N2K0 providing by UniprotKB (Universal Protein Resource) database.[15]

Clinical Examination

Ophthalmic Evaluation. Ophthalmic examinations were performed including visual acuity, intraocular pressure, ocular motility, pupillary reaction, biomicroscopic slit-lamp examination, and dilated fundus examination. Visual function was evaluated by static perimetry and Ganzfeld electroretinography according to the International Society for Clinical Electrophysiology of Vision.[16]

Hearing Evaluation. Hearing assessment was performed by pure tone audiometry, speech-audiometry, and otoscopic examination.

Neurologic Evaluation. A complete neurologic examination was carried out including cranial nerves, mental status examination, sensory system, extrapyramidal and pyramidal system, cerebellum, peripheral nervous system, individual muscle testing, and evaluation of speech and language. To determine if the patients had cerebellar atrophy, magnetic resonance imaging was performed.
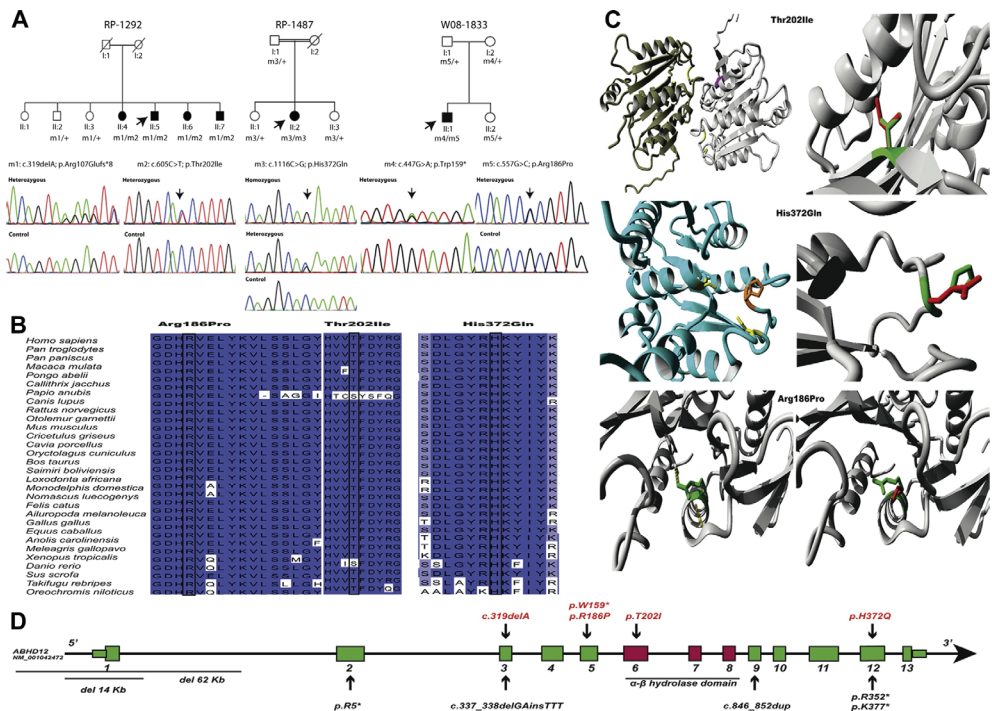
Figure 5.1. A, Pedigrees of the 3 studied families with *ABHD12* mutations. The index case is indicated with an arrow. Sanger sequencing confirmed the mutations identified by whole exome sequencing (WES) and revealed their complete cosegregation with the disease. The chromatograms of a mutant and a control individual are depicted for each variant (arrows). **B**, Cross-species comparison of 3 regions of *ABHD12* indicates that the 3 identified missense mutations affect highly conserved residues. **C**, Three-dimensional structural model of *ABHD12*. The Ile amino acid residue at position 202 (purple) may lead to distortion of the active site (yellow) of the other monomer. For variant p.His372Gln, the Gln amino acid residue at position 372 (red) does not seem to impair the predicted structure of the protein. The His residue is shown in orange. For variant p.Arg186Pro, the change, Arg (green) to Pro (red), seems to disturb the predicted structure of the protein. The hydrogen bonds and hydrophobic interactions are shown in yellow. **D**, Intron-exon structure of *ABHD12* and location of all mutations identified so far. Mutations previously associated with polyneuropathy, hearing loss, cerebellar ataxia, retinitis pigmentosa, and early-onset cataract (PHARC) syndrome or PHARC-like syndrome are shown in black. Red exons indicate the α-β hydrolyze domain of the protein. The mutations identified in this study and associated with PHARC syndrome or nonsyndromic retinitis pigmentosa are shown in red.

Results

Genetic Analysis

A Spanish family with 4 affected siblings (Figure 5.1A) with arRP was recruited. Previously, known mutations associated with arRP were discarded using a commercial genotyping microarray (AsperBiotech AS; Tartu, Estonia). In addition, whole genome homozygosity mapping using a 6.0 Affymetrix SNP array (Affymetrix AS; Santa Clara, CA) excluded the presence of IBD regions. To identify the genetic defect underlying the arRP in this family, a WES analysis was performed. The WES analysis, after sequencing on a HiSeq2000 platform (Illumina Inc., San Diego, CA) for the index case of the RP-1292 family (Figure 1A) yielded total of approximately 7254 Mb (raw data), among which approximately 4298 Mb were mapped to

the target region with a mean depth of x114.4. As a result, 98.7% of the target regions were covered at least x4, with 92.0% covered at least x20. After the WES analysis, 65,444 variants were identified after mapping the reads to the human genome reference sequence (National Center for Biotechnology Information build 36.1). Prioritization of possibly pathogenic changes was performed as follows. We first selected 138 nonsynonymous variants comprised within the coding sequence of 160 known genes associated with hereditary retinal degenerations and then excluded DNA variants that had more than 2% frequency within the general population (dbSNP version 130; database http://www.ncbi.nlm.nih.gov/SNP/) resulting in 30 variants. Notably, among the variants identified in the known retinal degeneration genes, a missense change (p.Leu1970Phe; c.5908C/T) in the *ABCA4* gene previously associated with both Stargardt disease[17] and age-related macular degeneration[18] was identified as heterozygous. However, no other mutation in this gene that could account for the autosomal recessive mode of inheritance was found. Then, we considered only 15 variants in genes carrying 2 such changes within their sequence (1 homozygous variant or 2 compound heterozygous variants) and cross-checked our results manually with the literature, newest single nucleotide polymorphism databases, and so forth. After applying these filters, we were left 1 novel homozygous mutation (p.Val349Asp) in the NPHP4 gene, previously associated with Senior-Loken syndrome,[19] and 1 novel homozygous mutation (p.Glu224*) in the *GPR98* gene, underlying Usher syndrome type 2.[20] Both homozygous variants in the *NPHP4* and *GRP98* genes were false positives after their confirmation by Sanger sequencing. For the *ABHD12* gene, one of them was a 1-base pair deletion (c.319delA) in exon 3, resulting in a frameshift and a stop codon after 8 residues (p.Arg107Glufs*8). The other one was a C-to-T substitution at nucleotide 605 in exon 6 (c.605C→T) causing an amino acid change at codon 202 (p.Thr202Ile).

In parallel, a sporadic Dutch case of the family W08-1833 (Figure 5.1A), which initially was considered to have nonsyndromic retinal degeneration, was analyzed by WES in a molecular diagnostic setting.[13] Only variants in genes in which mutations previously were described to be causative for inherited retinal dystrophies were analyzed. In the index case, this prefiltering step yielded 724 variants. After the removal of variants present in more than 1% of our in-house exome sequencing database and including only those variants that affect exons or canonical splice sites, only 12 variants were left. Two compound heterozygous variants in *ABHD12* (p.Trp159* and p.Arg186Pro) were the only 2 variations that were in line with an autosomal recessive mode of inheritance, and thus were considered to be the prime candidates underlying retinal dystrophy in this family. One of them was a G-to-A substitution at nucleotide 447 in exon 4 (c.447G→A) resulting in a stop codon (p.Trp159*), and the other one was a G-to-A substitution at nucleotide 557 (c.557G→A) causing an amino acid change at codon 186 (p.Arg186Pro).

Sanger sequencing of the specific regions confirmed the presence of the variants identified by WES in both index cases and affected members, which cosegregated with the disease in the families according to a recessive pattern of inheritance (Figure 5.1A). After this finding, a mutation analysis of the *ABHD12* gene was performed by Sanger sequencing in 345 additional Spanish patients affected with nonsyndromic arRP. The study of all the exons and intron-exon boundaries (RefSeq NM_001042472) was performed in the index cases. Family RP-1487 carried a novel homozygous missense mutation (c.1116C→G) in exon

12, leading to an amino acid change at codon 372 (p.His372Gln). Sanger sequencing in all family members of pedigree RP-1487 confirmed that inheritance of this mutation was compatible with that of a pathogenic recessive allele (Figure 5.1B).

Throughout this study, we identified 3 novel missense variants. Pathogenicity of these variants first was assessed by cosegregation with the disease in the families and by their absence in a total of more than 500 Dutch individuals for c.557G→A and in 352 healthy control Spanish chromosomes in the case of thec.605C→T and c.1116C→G variations. We also considered amino acid conservation in 31 different ABHD12 proteins across evolution in combination with a functional prediction in silico analysis. The 3 variants, p.Arg186Pro, p.Thr202Ile, and p.His372Gln, accordingly were classified as most likely damaging by 3 bioinformatic prediction tools (Table 5.1).

The mutation p.Arg186Pro changes a highly conserved and positively charged amino acid (arginine) into a neutral residue (proline; Figure 5.1B). As shown in Figure 5.1C, the R168 is located in one of the central helices in the protein. The 3-dimensional structure analyses showed that when the arginine residue changes to a proline, the hydrogen bonds and the hydrophobic interactions are lost. Besides that, the proline disturbs the helix, which may affect other residues. This means that the mutation severely affects the structure.

The mutation p.Thr202Ile changes a small, hydrophilic, and highly conserved residue (threonine; Figure 5.1C) into a bigger and hydrophobic one (isoleucine). A 3-dimensional structure analysis by Project HOPE showed, after analyzing multiple different models, that the best model seems to be in a dimer conformation. As shown in Figure 5.1C, the mutation is located far away from the putative active site in its own monomer. However, it is located close to the active site in the other monomer, and therefore it could prevent dimerization or interactions with other proteins.

The variant p.His372Gln changes a highly conserved and positively charged amino acid (histidine) into a neutral residue (glutamine; Figure 5.1C). However, possibly in virtue of the similar sizes of histidine and glutamine, the change did not seem to impair the predicted structure of the protein (Figure 5.1D). Nevertheless, the p.His372 involves 1 of the 3 charge-relay residues in ABHD12 supporting the hypothesis that p.His372Gln is functionally deleterious. Moreover, a recent study has shown that site-directed mutagenesis of residues of the catalytic triad abolished the enzymatic activity of ABHD12.21

Table 5.1. In Silico Predictions of Novel Missense Variants.

Exon No.	Nucleotide Change	AA Change	Conser-vation	Polyphen Prediction	SIFT Prediction	Mutation Taster Prediction
5	c.557G/A	p.Arg186Pro	HC	Probably damaging	Deleterious	Disease causing
6	c.605C/T	p.Thr202Ile	HC	Probably damaging	Affects protein function	Disease causing
12	c.1116C/G	p.His372Gln	HC	Probably damaging	Affects protein function	Disease causing

AA = amino acid; HC = highly conserved, considering 31 orthologs of the ABHD12 protein belonging to different evolutionary branches; SIFT = sorting tolerant from intolerant.

Novel variants described in this study. Nucleotide numbering is based on RefSeq DNA accession number NM_001042472

Table 5.2. Clinical features of patients with mutation in the ABHD12 gene.

Family	Patient ID	Age (yr)	Retinal Degeneration			Fundus Aspect	BMC
			First symptoms and course	Visual Field	ERG		
RP-1292	II:4	78	NB (38yr), field constriction and progressive loss of VA	Absolute scotoma except some peripheral islands	NR	Pale optic disc, retina vessels attenuation and bone spicule pigmentation (paravascular and mild periphery), perifoveal atrophy LE and choriocapillaris atrophy	PSC (77yr)
	II:5	75	NB (thirties), field constriction and progressive loss of VA	Restricted to 5° central field (65yr)	NR	Pale optic disc, narrowed vessels and diffuse bone spicule pigmentation	PSC (63yr)
	II:6	72	NB (thirties), field constriction and progressive loss of VA	Temporal islands RE; paracentral and nasal islands LE	NR	Pale optic disc, retina vessels attenuation, bone spicule pigmentation (paravascular and mild periphery), macular RPE alteration	PSC (71yr)
	II:7	66	NB (thirties), field constriction and progressive loss of VA	Central scotoma	Diminished	Pale optic disc, narrowed vessels, bone spicule pigmentation (paravascular and mild periphery) with macular preservation	PSC (65yr)
RP-1487	II:2	38	NB (22yr), field constriction and progressive loss of VA	Restricted to 10° central field	Diminished	Typical RP	PSC (21yr)
W08-1833	II:1	34	NB, progressive loss of VA	Decreased central sensitivity	Scotopic: Severely reduced (~1-percentile) Photopic: Normal (29yr) Scotopic: Severely reduced (~1-percentile) Photopic: Moderately reduced (~5th-percentile) (31yr)	Parafoveal atrophy, bull's eye appearance, attenuation of the arterioles and pallor of the optic disc	Mild PSC

5

Sensory and Motor Neuropathy	Pyramidal Tract Signs	Sensorineural Hearing Loss	Ataxia	MRI of brain
Preserved strength; present tendon reflexes; decreased vibration sense in lower limbs; no paresthesia	Normal flexor and extensor plantar response; preserved reflexes	Age-related BE (Presbyacusis)	Normal gait; no dysmetria and dysarthria	Normal cerebellum and brainstem; minimal cerebral atrophy
Preserved sensitivity; slightly loss of strength right upper limb; present tendon reflexes; no paresthesia	Normal flexor and extensor plantar response; preserved reflexes	Age-related RE (Presbyacusis)	Dysmetria in lower limbs; gait with a slightly wide base	Normal except for some minimal old residual ischemic injuries in semovial centers and left cerebellum hemisphere
Preserved strength and sensitivity; present tendon reflexes; no paresthesia	Flexor and extensor plantar response; preserved reflexes	Not referred NCD	Gait somewhat unstable without a wide base; no adiadocokinesia	NCD
Preserved strength and sensitivity; present reflexes; no paresthesia	Normal flexor and extensor plantar response; preserved reflexes	Age-related BE (Presbyacusis)	Normal gait with a normal base width; slight dysarthria; no dysmetria; mild distal postural tremor	Normal except for some minimal residual ischemic injuries in white matter
No tremor; no pes cavus; Hypoesthesia distal symmetric to touch and pain	No hyperreflexia; Achilles reflex abolished	Sensorineural hearing loss BE (37y)	Normal gait; no dysmetria and dysarthria.	Cerebral and cerebellar atrophy
Preserved strengths, decreased peripheral sensitivity; no achilles tendon reflex, low arm reflexes, normal knee tendon reflex	Normal plantar response	Decreased sensitivity in 1500-8000 Hz range to levels of ~40dB.	Wide based gait. Heel-knee sign clearly atactic, stuttering speech. No dysmetria.	Normal cerebellum

ID, identification; YR, years; ERG, electroretinogram; BMC, biomicroscopy; MRI, magnetic resonance imaging; NB, night blindness; VA visual acuity; NR, non recordable; LE, left eye; PSC, posterior subcapsular cataract; BE, both ears; RE, right ear; RE, right eye; RPE, retinal pigment epithelium; NCD, no clinical data.

Clinical Examination

Three of the 4 affected individuals of family RP-1292 (II:4, II:5, and II:7) and the index cases of the families RP-1487 (II:2) and W08-1833 (II:1) were examined comprehensively

by ophthalmologists, otologists, and neurologists. The clinical features of the patients are summarized in Table 5.2. All of the affected individuals presented with an RP phenotype characterized by a symptom-free period in the first 2 decades of life. Night blindness was the first symptom, followed by central visual field loss and reduction of visual acuity.

At the time of the last ophthalmologic examination, in all mutated cases, visual fields were reduced symmetrically from 10° to absolute scotoma and the visual acuity varied depending on the different stages of macular involvement. Posterior subcapsular cataract was found in all the affected individuals carrying ABHD12 mutations. Fundi showed changes typical of RP with pale disc, narrowed vessels, and bone spicule pigmentation, although the latter were absent in individual II:1 of family W08-1833. In addition, some patients had macular retinal pigment epithelium degeneration of various degrees (Figure 5.2A). Full-field electroretinography was nonrecordable or substantially reduced in all cases.

For family RP-1292, patient II:4 reported recent hypoacusis (a 78-year-old woman), whereas siblings II:6 (a 72-year-old woman) and II:7 (a 66-year-old man) did not report hearing loss. The II:5 individual (a 75-year-old man) had severe hearing loss in the left ear because of the presence of a cholesteatoma. Audiograms of the patients II:4 and II:7 showed sensorineural hearing loss of both ears for higher frequencies (>2000 Hz), whereas patient II:5 had hearing loss only in the right ear (Figure 5.2B). After clinical examination, the diagnosis for the 4 patients was an age-related hearing loss or presbyacusis.

Neurologic examination of the 4 affected individuals of the RP-1292 family revealed no signs of peripheral polyneuropathy or ataxia. None of the patients showed pes cavus or hammertoes. The strength and sensitivity were preserved in every case. All the reflexes were present and the gait was normal, except for individual II:5. None of them reported balance problems. Magnetic resonance imaging scans did not show an indication of cerebellar atrophy in any case, except for individual II:5, who showed a localized abnormality in the left cerebellum interpreted to be caused by a previous ischemic event (Figure 5.2C). No patient showed evidence of polyneuropathy or ataxia.

After an exhaustive clinical examination at 38 years of age, the index case of the RP-1487 family was found to have bilateral hearing loss. An audiogram of the patient showed slight hearing loss for low frequencies (<1000 Hz) and moderate hearing loss for median and higher frequencies (>2000 Hz) for the right ear and moderate hearing loss in all frequencies for the left ear. Currently, she is wearing a hearing aid. Bilateral cataract surgery was performed at 21 years of age. She also demonstrated some features of motor and sensory peripheral neuropathy. The electroneurographic study was consistent with a moderate demyelinating sensorimotor polyneuropathy in the upper and lower limbs. Cerebral and cerebellar atrophy were observed on magnetic resonance imaging (image not available).

Patient II:1 from family W08-1833 did not report any neurologic symptoms, but a detailed neurologic examination revealed a wide-based gait, peripheral sensitivity loss at the lower extremities, and low tendon reflexes. Signs of ataxia were observed in stuttering speech, an ataxic heel-knee sign, and intentional tremor at the finger-to-nose test, although no structural abnormalities of the cerebellum were observed on magnetic resonance imaging examination (Figure 5.2C). Audiography revealed significantly decreased sensitivity of frequencies higher than 1500 Hz to levels of 40 dB or lower in both ears (Figure 5.2B).
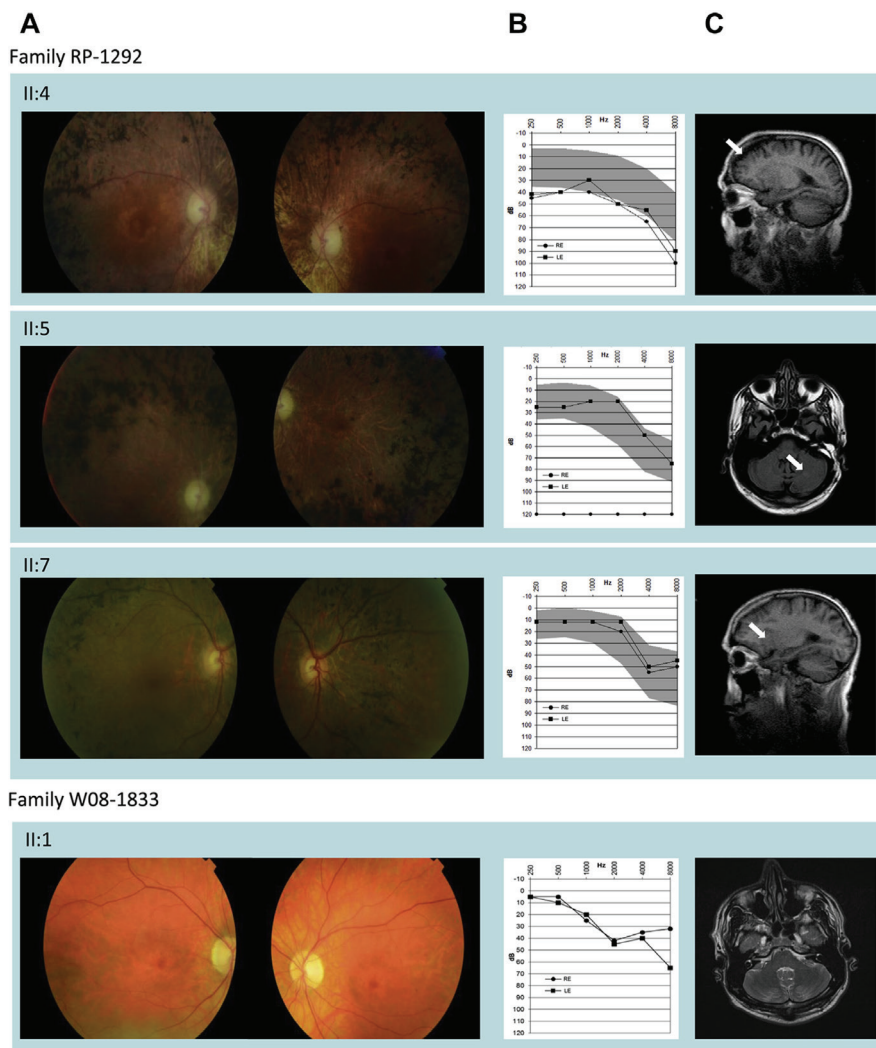
Figure 5.2. Phenotype of patients from the RP-1292 and W08-1833 families with mutations in the ABHD12 gene. A, Spectrum of fundus findings in different individuals. Funduscopy of 3 patients of the RP-1292 family (II:4, II:5, and II:7) shows pale optic discs, attenuation of retinal vessels, and bone spicule pigmentation. Funduscopy of patient II:1 of the W08-1833 family shows pallor of the optic disc, attenuation of the arterioles, and parafoveal atrophy with bull's-eye appearance B, Pure-tone air conduction audiograms of the patients. The grey areas are the hearing ranges for normal individual at 70 to 79 years of age (women), 70 to 79 years of age (men), and 60 to 69 years of age (men), respectively, as reported by Cruickshanks et al.32 Family RP-1292: for patients II:4 (female) and II:7 (male), the audiogram shows age-related hearing loss. Audiogram of the patient II:5 (male) shows hearing loss of the right ear. Family W08-1833: audiogram of the patient II:1 shows sensorineural hearing loss of both eyes. C, Magnetic resonance imaging (MRI) scans. Family RP-1292: for patient II:4, MRI scan shows minimal cerebral atrophy (white arrow), whereas in patient II:5, some injuries in the left cerebellum hemisphere consistent with the consequence of an ischemic event (white arrow) are present. Patient II:7 has a minimal abnormality probably resulting from an ischemic injury (white arrow). Family W08-1833: for patient II:1, no structural abnormalities of the cerebellum are observed.

Discussion

The *ABHD12* gene is located on chromosome 20p11.21 and contains 13 exons, encoding a protein of 398 amino acids. The protein includes 1 α-β hydrolase domain that spans amino acids 171 to 335 and contains 3 active sites located in residues 246, 333, and 372. In vitro, the ABHD12 enzyme hydrolyzes 2-arachidonoyl glycerol, the main endocannabinoid, by converting it into metabolites arachidonate and glycerol.[21,22] However, in vivo it is only responsible for a small fraction of the 2-arachidonoyl glycerol hydrolase activity in mouse brain, showing that in the mouse brain, ABHD12 is a major lysophosphatidylserine lipase.

In Abhd12 knockout mice, auditory and motor defects and neuroinflammatory responses develop. These results suggested that the accumulation of the lysophosphatidylserine could contribute to the PHARC phenotype.[23] *ABHD12* is differentially expressed in various cell types and cellular compartments,[23-25] being highly expressed in microglia. Endocannabinoids are implicated in microglia-mediated neuroinflammation, and the dysregulated lysophosphatidylserine metabolism produces microglial and neurobehavioral abnormalities.[23] Moreover, microglia dysfunction is known to be involved in neurodegenerative diseases[26] and in retinal dystrophies,[27] although further studies are mandatory to elucidate how the loss of the ABHD12 function results in the wide spectrum of phenotypes we are describing here.

After an exhaustive review of the literature (PubMed: abhd12; accessed January 17, 2014; http://www.ncbi.nlm.nih.gov/pubmed/?term=abhd12) and consultation of the databases (HGMD Professional 2013.4 and Eye Diseases-LOVD version 2.0; both accessed January 17, 2014) available for mutations in the *ABHD12* gene, it has been observed that a total of 7 different mutations in the *ABHD12* gene have been identified so far as causes of PHARC syndrome.[9,10,11] All of them are interpreted as null mutations leading to an abolished or a severely reduced activity of the encoded enzyme. In our study, we identified 5 new mutations in the ABHD12 gene. Two of them were null mutations (p.Arg107Glufs*8 and p.Trp159*). As is the case with the previously described mutations, these changes also may result in a null allele, whereas the 3 novel missense changes, p.Arg186Pro, p.Thr202Ile, and p.His372Gln, may result in a reduced, although not completely abolished, activity of the ABHD protein. Taking this hypothesis into account and considering what is known about other retinal dystrophies, it is reasonable to expect that mutations in the *ABHD12* gene may result in a range of disease, from lethal multisystem disorders associated with null alleles to a milder spectrum of manifestations from mutations with a hypomorphic character.[28,29] However, after a thorough clinical examination of the patients with mutations in the *ABHD12* gene identified in this study, we could not establish a clear genotype-phenotype correlation.

Although the affected members of the RP-1487 and W08-1388 families showed a moderate form of PHARC syndrome including sensorineural hearing loss, cataract, RP, and polyneuropathy, none of the patients from the RP-1292 family demonstrated symptoms that are distinctive of PHARC, and all of them indeed maintained the initial diagnosis of nonsyndromic RP even at later stages of life.

All the modest nonocular abnormalities, such as cataract, hearing loss, and ischemic injury, detected in the patients of the RP-1292 family were not debilitating and could be attributed to other age-related complications. It is well known that the development of the

cataract, most prevalent being the posterior subcapsular cataract, in the RP population is more frequent than in the general population and also that the age of onset is earlier. However, this is usually present at mid stage in the progression of the disease.[2,30,31] The affected individuals from families RP-1487 and W08-1388 demonstrated a cataract at the same age or earlier than they demonstrated RP, whereas all affected members of the RP-1292 family demonstrated posterior subcapsular cataract at a very advanced age, an occurrence that is compatible with the natural course of RP or with the age of the patients.

Coinciding with the features described in PHARC syndrome, the patients II:2 (RP1487) and II:1 (W08-1388) showed a sensorineural hearing loss in the twenties and early thirties, respectively. However, in accordance with the report by Cruickshanks et al,[32] where it was demonstrated that hearing loss is a very common problem affecting older adults, 3 of 4 affected individuals for the RP-1292 family showed hearing loss that was diagnosed as age related (presbyacusis) by the clinical specialists. However, the gait with a slightly wide base present in individual II:5 of the RP-1292 family is most likely the consequence of ischemic injuries in the left cerebellum.

Based on these results, it is not possible to establish a clear genotype-phenotype correlation for *ABHD12* mutations, and it is not clear if less detrimental mutations cause a less severe phenotype. Alternatively, the highly heterogeneous clinical differences observed in the patients with mutations in the *ABHD12* gene may suggest the involvement of genetic modifiers, as has been described previously in other cases for retinal dystrophies.[33-36] However, because one of the families presented in this study carries a missense mutation in the *ABHD12* gene and has members with nonsyndromic RP, we could not completely deny the possibility that hypomorphic mutations lead to milder disease. Overall, a larger number of patients with missense mutations in this gene need to be assessed clinically, which should be coupled further with functional analysis of the mutant proteins to draw definitive conclusions on the genotype-phenotype correlation.

In conclusion, this study allowed us to report 5 new variations in the *ABHD12* gene, representing the first time missense mutations have been described. We have determined, using a WES analysis followed by an exhaustive clinical examination, that mutations in the *ABHD12* gene can cause a wide spectrum of phenotypes ranging from PHARC syndrome to a nonsyndromic form of retinal degeneration.

References

1. Den Hollander AI, Black A, Bennett J, Cremers FP. Lighting a candle in the dark: advances in genetics and gene therapy of recessive retinal dystrophies. J Clin Invest 2010;120: 3042–53.
2. Hamel C. Retinitis pigmentosa. Orphanet J Rare Dis 2006; 1:40.
3. Hartong DT, Berson EL, Dryja TP. Retinitis pigmentosa. Lancet 2006;368:1795–809.
4. Ayuso C, Garcia-Sandoval B, Najera C, et al. Retinitis pigmentosa in Spain. The Spanish Multicentric and Multidisciplinary Group for Research into Retinitis Pigmentosa. Clin Genet 1995;48:120–2.
5. Retinal Information Network (RetNet). Number of Genes and Loci by Disease Category (One Disease per Gene/Locus). Available at: https://sph.uth.edu/retnet/sum-dis.htm#A-genes. Accessed February 4, 2014.
6. Wright AF, Chakarova CF, Abd El-Aziz MM, Bhattacharya SS. Photoreceptor degeneration: genetic and mechanistic dissection of a complex trait. Nat Rev Genet 2010;11:273–84.
7. Berger W, Kloeckener-Gruissem B, Neidhardt J. The molecular basis of human retinal and vitreoretinal diseases. Prog Retin Eye Res 2012;29:335–75.
8. Fiskerstrand T, Knappskog P, Majewski J, et al. A novel Refsum-like disorder that maps to chromosome 20. Neurology 2009;72:20–7.
9. Fiskerstrand T, H'mida-Ben Brahim D, Johansson S, et al. Mutations in ABHD12 cause the neurodegenerative disease PHARC: An inborn error of endocannabinoid metabolism. Am J Hum Genet 2010;87:410–7.
10. Chen DH, Naydenov A, Blankman JL, et al. Two novel mutations in ABHD12: expansion of the mutation spectrum in PHARC and assessment of their functional effects. Hum Mutat 2013;7:410–7.
11. Eisenberger T, Slim R, Mansour A, et al. Targeted nextgeneration sequencing identifies a homozygous nonsense mutation in ABHD12, the gene underlying PHARC, in a family clinically diagnosed with Usher syndrome type 3. Orphanet J Rare Dis 2012;7:59.
12. Corton M, Nishiguchi KM, Avila-Fernández A, et al. Exome sequencing of index patients with retinal dystrophies as a tool for molecular diagnosis. PLoS One 2013;8:e65574.
13. Neveling K, Feenstra I, Gilissen C, et al. A post-hoc comparison of the utility of Sanger sequencing and exome sequencing for the diagnosis of heterogeneous diseases. Hum Mutat 2013;34:1721–6.
14. Corton M, Tatu SD, Avila-Fernandez A, et al. High frequency of CRB1 mutations as cause of Early-Onset Retinal Dystrophies in the Spanish population. Orphanet J Rare Dis 2013;8:20.
15. UniProtKB. Uniprot (Universal Protein Resource) database. Available at: http://www.uniprot.org. Accessed February 4, 2014.
16. Marmor MF, Fulton AB, Holder GE, et al. International Society for Clinical Electrophysiology of Vision. ISCEV Standard for full-field clinical electroretinography. Doc Ophthalmol 2009;118:69–77.
17. Allikmets R, Singh N, Sun H, et al.Aphotoreceptor cell-specific ATP-binding transporter gene (ABCR) is mutated in recessive Stargardt macular dystrophy. Nat Genet 1997;15:236–46.
18. Allikmets R. Further evidence for an association of ABCR alleles with age-related macular degeneration. The International ABCR Screening Consortium. Am J Hum Genet 2000;67:487–91.
19. Schuermann MJ, Otto E, Becker A, et al. Mapping of gene loci for nephronophthisis type 4 and Senior-Løken syndrome, to chromosome 1p36. Am J Hum Genet 2002;70:1240–6.
20. Hmani M, Ghorbel A, Boulila-Elgaied A, et al. A novel locus for Usher syndrome type II, USH2B, maps to chromosome 3 at p23-24.2. Eur J Hum Genet 1999;7:363–7.
21. Navia-Paldanius D, Savinainen JR, Laitinen JT. Biochemical and pharmacological characterization of human α-β hydrolase domain containing 6 (ABHD6) and 12 (ABHD12). J Lipid Res 2013;53:2413–24.
22. Blankman JL, Simon GM, Cravatt BF. A comprehensive profile of brain enzymes that hydrolyze the endocannabinoid 2-arachidonoylglycerol. Chem Biol 2007;14:1347–56.
23. Blankman JL, Long JZ, Trauger SA, et al. ABHD12 controls brain lysophosphatidylserine pathways that are deregulated in a murine model of the neurodegenerative disease PHARC. Proc Natl Acad Sci U S A 2013;110:1500–5.
24. Marrs W, Stella N. Measuring endocannabinoid hydrolysis: refining our tools and understanding. AAPS J 2009;11:307–11.

25. Muccioli GG, Xu C, Odah E, et al. Identification of a novel endocannabinoid-hydrolyzing enzyme expressed by microglial cells. J Neurosci 2007;27:2883–9.
26. Landreth GE. Microglia in central nervous system diseases. J Neuroimmune Pharmacol 2009;4:369–70.
27. Ebert S, Weigelt K, Walczak Y, et al. Docosahexaenoic acid attenuates microglial activation and delays early retinal degeneration. J Neurochem 2009;110:1863–75.
28. Littink KW, Pott JW, Collin RW, et al. A novel nonsense mutation in CEP290 induces exon skipping and leads to a relatively mild retinal phenotype. Invest Ophthalmol Vis Sci 2010;51:3646–52.
29. Khan MI, Kersten FF, Azam M, et al. CLRN1 mutations cause nonsyndromic retinitis pigmentosa. Ophthalmology 2011;118: 1444–8.
30. Pruett RC. Retinitis pigmentosa: clinical observations and correlations. Trans Am Ophthalmol Soc 1983;81:693–735.
31. Lee SH, Yu HG, Seo JM, et al. Hereditary and clinical features of retinitis pigmentosa in Koreans. J Korean Med Sci 2010;25: 918–23.
32. Cruickshanks KJ, Wiley TL, Tweed TS, et al. Prevalence of hearing loss in older adults in Beaver Dam, Wisconsin: The Epidemiology of Hearing Loss Study. Am J Epidemiol 1998;148:879–86.
33. Coppieters F, Casteels I, Meire F, et al. Genetic screening of LCA in Belgium: predominance of CEP290 and identification of potential modifier alleles in AHI1 of CEP290-related phenotypes. Hum Mutat 2010;31:E1709–66.
34. Khanna H, Davis EE, Murga-Zamalloa CA, et al. A common allele in RPGRIP1L is a modifier of retinal degeneration in ciliopathies. Nat Genet 2009;41:739–45.
35. Fahim AT, Bowne SJ, Sullivan LS, et al. Allelic heterogeneity and genetic modifier loci contribute to clinical variation in males with X-linked retinitis pigmentosa due to RPGR mutations. PLoS One 2011;6:e23021.
36. Estrada-Cuzcano A, Koenekoop RK, Senechal A, et al. BBS1 mutations in a wide spectrum of phenotypes ranging from nonsyndromic retinitis pigmentosa to Bardet-Biedl syndrome. Arch Ophthalmol 2012;130:1425–32.

Authors

A.M.M. Oonk[1,2], R.A.C. van Huet[3], J.M. Leijendeckers[1,2], J.Oostrik[1,2,4], H. Venselaar[5], E. van Wijk[1,2,4], A. Beynon[1,2], H.P.M. Kunst[1,2], C.B. Hoyng[3], H. Kremer[1,2,4,6], M. Schraders[1,2,4], R.J.E. Pennings[1,2]

Affiliations

[1]Department of Otorhinolaryngology, Hearing & Genes, Radboud university medical center, Nijmegen, the Netherlands.

[2]Radboud university medical center, Donders Institute for Brain, Cognition and Behavior, Nijmegen, the Netherlands.

[3]Department of Ophthalmology, Radboud university medical center, Nijmegen, the Netherlands.

[4]Nijmegen Centre for Molecular Life Sciences, Radboud university medical center, Nijmegen, the Netherlands.

[5]Centre for Molecular and Biomolecular Informatics, Radboud university medical center, Nijmegen, the Netherlands.

[6]Department of Human Genetics, Radboud University Nijmegen Medical Centre, Nijmegen, the Netherlands.

Nonsyndromic hearing loss caused by *USH1G* mutations: widening the *USH1G* disease spectrum

6

Abstract

Currently, six genes are known to be associated with Usher syndrome type I and mutations in most of these genes can also cause nonsyndromic hearing loss. The one exception is USH1G, which is currently only known to be involved in Usher syndrome type I and atypical Usher syndrome.

Here we present clinical and genetic data of a Dutch family with autosomal recessively inherited hearing loss. The hearing loss had an early onset with a downsloping audiogram configuration. Slight progression of the hearing loss was seen in both affected individuals. Compound heterozygous mutations in USH1G were found to segregate with the hearing loss in this family, a missense (c.310A→G, p.Met104Val) and a frameshift mutation (c.780insGCAC, p.Tyr261Alafs*96). Extensive ophthalmic and vestibular examinations demonstrated no abnormalities that are usually associated with Usher syndrome type I.

This is the first family presented with nonsyndromic hearing loss caused by mutations in USH1G. Our findings expand the phenotypic spectrum of mutations in USH1G.

Introduction

Usher syndrome is the most common cause of combined hereditary hearing and vision loss.[1] It is clinically and genetically heterogeneous, but it is mainly characterized by bilateral sensorineural hearing loss and retinitis pigmentosa (RP). Vestibular dysfunction is seen in part of the cases. Based on severity of hearing loss and presence or absence of vestibular dysfunction, Davenport and Omenn distinguished three types in 1977.[2] Type I is characterized by congenital, stable, severe to profound hearing loss, vestibular areflexia and RP that has an onset before puberty. Type II can be distinguished from type I based on severity of hearing loss (moderate - severe), absence of vestibular dysfunction and a later onset of RP. Type III is characterized by progressive hearing loss, variable vestibular dysfunction and variable onset of RP.[1,3] Up to now, twelve loci are known for Usher syndrome and for ten of these loci the involved genes have been identified. Eight loci are known for Usher syndrome type I and the six causative genes are: *MYO7A, CDH23, USH1C, PCDH15, USH1G* and *CIB2*.[4]

Like in Usher syndrome, clinical and genetic heterogeneity are also seen in autosomal recessive nonsyndromic hearing loss, for which 49 genes have been identified so far.[4] Interestingly, five genes known to be involved in Usher syndrome type I, *MYO7A, CDH23, USH1C, PCDH15* and *CIB2*, are also involved in nonsyndromic hearing loss: DFNB2, DFNB12, DFNB18A, DFNB23, and DFNB48, respectively. These DFNB phenotypes are generally characterized by prelingual, severe to profound hearing loss, occasionally including minor retinal abnormalities not typical for RP.[5-8] Exceptions are DFNB2, which is reported to have a more variable onset age,[9,10] and DFNB12 which can also present with moderate hearing loss, but with a progressive nature.[11,12]

USH1G is located at chromosome 17q25.1 and encodes the protein SANS. Mutations in this gene have, up to now, only been described to cause Usher syndrome type I or atypical Usher syndrome.[13-15] The latter is characterized as atypical since the patients did not suffer from visual problems. Ophthalmic examination, however, revealed bone spicules and atrophy of the retinal pigment epithelium (RPE), which was characterized as late-onset RP.[13,14] To our knowledge there are no reports that describe hereditary non-syndromic sensorineural hearing loss caused by mutations in *USH1G*. In this study, we report a Dutch family with nonsyndromic sensorineural hearing loss caused by compound heterozygous missense and frameshift mutations in *USH1G*.

Material and methods

Clinical examinations

A non-consanguineous Dutch family (W08-2221) was studied. The pedigree demonstrates that hearing loss is present in only one generation, which may indicate an autosomal recessive inheritance pattern (Figure 1). This study was approved by the local medical ethics committee. All participants signed an informed consent, which additionally was used to retrieve relevant data from other medical centers. All family members of the second generation completed a questionnaire on hearing and balance. Hearing impaired participants underwent complete ear, nose and throat examination including otoscopy and external ear inspection to exclude

external ear deformities, previous surgery and other possible causes of hearing impairment. A computed tomography (CT) scan of the temporal bone was performed in individual II.1 in order to exclude cochlear malformations.

Genetic analyses and molecular modeling
Peripheral blood was drawn from all family members for genetic analysis. Genomic DNA was isolated from lymphocytes according to standard procedures. Single Nucleotide Polymorphism (SNP) genotypes of individuals II.1 and II.4 were determined by use of the Affymetrix® Genome-Wide Human SNP Array 6.0. All SNP array experiments were performed and data was analyzed according to the manufacturer's protocol. Genotype calling and calculation of the regions of homozygosity was performed with the Affymetrix® Genotype Console Software v2.1 with use of default settings. The segregation of the genotypes for each previously reported nonsyndromic, recessive deafness gene was visually evaluated.

Haplotype analysis of Variable Number Tandem Repeat (VNTR) markers was used to evaluate the family for involvement of *OTOGL, PTPRQ, STRC, GJB3* and *SYNE4.* VNTR marker analysis was performed as described before by Schraders et al.[16]

We performed Sanger sequence analysis for genes associated with autosomal recessive hearing impairment in shared genotype regions, *TRIOBP, SOX10, GIPC3, MSRB3, TECTA, BSND, WHRN, TPRN, SLC26A4, SLC26A5, GRXCR1, PJVK, TMC1* and *USH1G*. The effect of the missense mutation on the surface and structure of the SANS protein was predicted by using a hybrid model of the protein constructed by the automatic script in YASARA.[17] The structure of the area surrounding amino acid residue 104 is based on the Protein Data Bank file 1n0r, which has a sequence identity of 41% with SANS.

Audiometry
Pure tone audiometry was performed, according to current standards to determine hearing thresholds at frequencies of 0.25, 0.5, 1, 2, 4 and 8 kHz. To exclude conductive hearing impairment, both air and bone conduction thresholds were determined. Speech recognition scores were measured by using standard Dutch phonetically balanced consonant-vowel-consonant word lists. The maximum phoneme recognition score (mean value of both ears) was obtained from monaural performance versus intensity curves. The mean value of both ears was plotted against age and mean pure tone average (PTA) at 1, 2 and 4 kHz. These curves were compared to the curves of presbyacusis patients.[18]

We additionally tested acoustic reflexes, as well as loudness scaling and speech perception thresholds in individual II.1. Acoustic reflexes were measured at the contralateral ear as well as at the ipsilateral ear at 0.5, 1, 2 and 4 kHz up to the loudness discomfort level. Loudness scaling and speech perception thresholds in noise were evaluated as described before.[19,20] The results of these examinations were compared to those of normal hearing individuals, retrieved from our own clinic, and to those of presbyacusis patients.[19]

Prism 5.0 (Graphpad Software Inc., San Diego, CA, USA) was used to evaluate progression of hearing loss, speech recognition scores and loudness scaling by means of regression analysis.

Vestibular examination

Vestibular function was evaluated by electronystagmography in individual II.1. This involved calorisation and a rotary chair testing using the velocity-step test. A smooth pursuit, a gaze, an optokinetic test and saccadic tests were performed to confirm normal vestibule-oculomotor function and to exclude the presence of possible central lesions. To determine the reactivity and possible vestibular preponderance of both individual vestibuli bithermal (30 and 44˚C) water irrigation of the external auditory canal was used for calorisation. For the velocity step test, the patient was seated in a rotary chair with the head ante-flexed at 30˚ to obtain a horizontal position of the horizontal semicircular canals. The chair was accelerated and when the rotatory nystagmus had subsided during constant rotation, the chair was suddenly stopped. This was done for both directions in order to calculate the possible presence of directional preponderance (asymmetry). Analyses were performed as described previously.[21]

Ophthalmic evaluation

Retinal function was evaluated in detail in individual II.1. We performed history taking and standard ophthalmic examination including best-corrected visual acuity (BCVA), slit-lamp biomicroscopy and ophthalmoscopy. Goldmann perimetry was performed using targets V-4e, III-4e, I-4e, I-3e, I-2e and I-1e. In addition to fundus photography (Topcon TRC50IX, Topcon Corporation, Tokyo, Japan), we obtained 30˚ x 30˚ and 55˚ x 55˚ fundus autofluorescence (FAF) images (Spectralis, Heidelberg Engineering, Heidelberg, Germany). Cross-sectional images of the central and peripheral retina were obtained with a commercially available Spectral-domain optical coherence tomography (SD-OCT) instrument (Spectralis, Heidelberg Engineering, Heidelberg, Germany) using a 20°x15˚ 19-line volume scan covering the fovea as well as a 20˚ single line scan in the superior midperiphery. The patient underwent a full-field electroretinography (ERG) performed according the guidelines of the International Society for Clinical Electrophysiology of Vision (ISCEV).[22] Additionally, color vision was evaluated using Hardy-Rand-Rittler (HRR) plates.
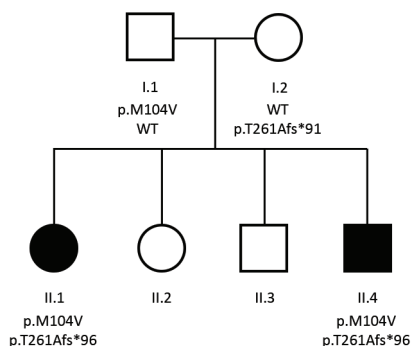

Figure 6.1. Pedigree of W08-2221. Squares indicate males, circles females. Solid symbols depict affected individuals, clear symbols mean unaffected. WT means wild type. The genotypes of individuals II.2 and II.3 are not shown because of privacy reasons.

Results

Clinical evaluation

Family W08-2221 consists of parents and four siblings of whom two are hearing impaired: a female (II.1) and a male (II.4). Hearing loss was noted since the age of four in both siblings. Physical examination did not demonstrate any dysmorphic features suggestive of syndromic disease. A CT scan of the temporal bones in individual II.1 did not show any abnormalities.

Genetic analyses and molecular modeling

Autozygosity mapping revealed 22 homozygous regions larger than one Mb including one known gene for recessive deafness, *STRC*. For 17 other known autosomal recessive deafness genes the genotypes segregated with the hearing loss upon manual inspection of the SNP genotypes. *OTOGL, PTPRQ, STRC, GJB3* and *SYNE4* were excluded by haplotype analysis of flanking VNTR markers. Mutation analysis was performed for the other genes by Sanger sequencing and three rare variants were identified. A heterozygous synonymous variant was detected in *TRIOBP* (c.4809T→C; p.= (p.Asp1603Asp), NM_001039141.2) and two variants in *USH1G* (NM_173477.2). One novel variant, c.780insGCAC, which causes a frameshift and a predicted premature stop codon (p.Tyr261Alafs*96), and a missense variant (c.310A→G; p.Met104Val). The *USH1G* variants segregated with the hearing loss in the family (Figure 6.1) and were not present in 350 Dutch control alleles. The insertion was also not present in the exome variant server (EVS), while the c.310G→A variant was identified in 4 out of 13002 European American and African American alleles.[23] The amino acid substitution p.Met104Val is predicted to be benign by Polyphen2 (score 0.066; range 0-1 with 0= benign and 1= probably damaging).[24] SIFT predicts that the substitution affects protein function (score 0.03; a score < 0.05 predicts the change to be damaging and >0.05 predicts it to be tolerated).[25] Mutation taster predicts the substitution to be disease causing with a probability of 0.99 (0-1).[26]

Molecular modeling predicts that substitution of methionine for valine in the third ankyrin domain of SANS causes a change at the surface of this domain, and therefore possible loss of hydrophobic contacts but no change in structure of the domain (Figure 6.2A). For comparison, modeling of a previously described missense mutation (p.Leu48Pro) in patients with Usher syndrome type Ig was performed.[27] This missense mutation is predicted to cause a disturbance of the protein structure (Figure 6.2B). Ankyrin domains are mainly formed by helical structures, and proline is known to disrupt helical structures. Therefore, it is expected that this missense mutation changes the helical structure of the protein and hence affects protein function (Figure 6.2B).

Audiometric evaluation

Figure 6.3A demonstrates the deterioration of air conduction thresholds of individual II.1 over time. Air conduction thresholds did not differ from bone conduction thresholds. At onset, her hearing loss was moderate, but over time it progressed to severe. The audiogram configuration was initially flat to gently downsloping, but over time the curve became steeper downsloping, demonstrating significant progression especially in the high frequencies (Table 6.1). When speech perception scores were plotted against age, scores began to deteriorate after the
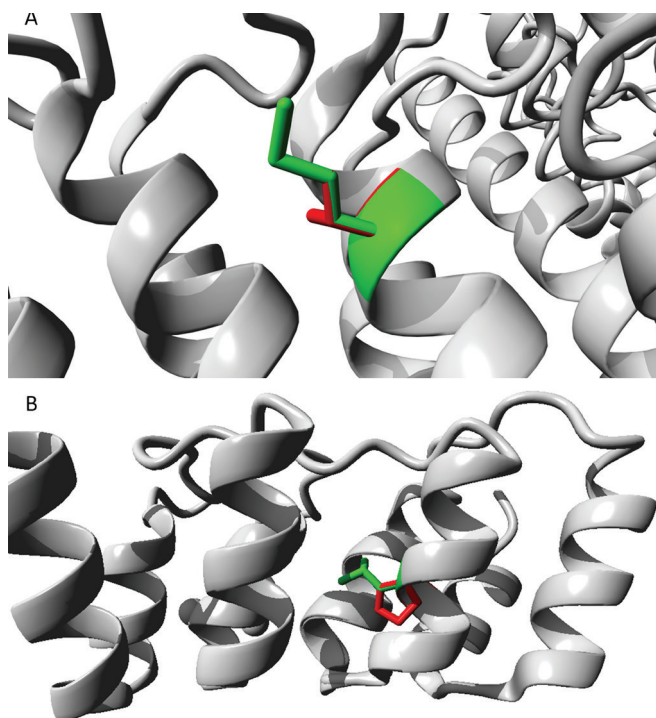
Figure 6.2. (A) Molecular modeling of missense variants in SANS. Close-up of the third ankyrin domain with wild type amino acid (methionine) in green and the variant (valine) in red. The change of methionine to a valine at position 104, leads to a change at the surface of the ankyrin domain. (B) Close-up of the first ankyrin domain with wild type (leucine) in green and the variant (proline) in red. Insertion of a proline for a leucine at position 48 causes a change in structure, due to the interference with the helix structure of the ankyrin domain.

age of 20 years. When speech perception scores were plotted against $PTA_{1, 2, 4kHz}$, individual II.1 clearly performed better than presbyacusis patients (Figure 6.4).

Patient II.4 also showed a moderate hearing loss and progression was less outspoken over time than in case II.1. Audiogram configuration remained flat to gently downsloping (Figure 6.3B) but progression was significant at 0.25, 4 and 8 kHz (Table 6.1). Speech recognition scores plotted against age were comparable to those of individual II.1 and remained stable. However, individual II.4 had just reached the age at which the scores of individual II.1 began to deteriorate. When the scores were plotted against $PTA_{1, 2, 4kHz}$, they were comparable to those of individual II.1.

Acoustic reflexes were absent in individual II.1. Loudness scaling of II.1 showed a steeper loudness growth than one would expect from normal hearing individuals for both 0.5 kHz and 2 kHz. The signal to noise ratio was worse than the average ratio of normal hearing individuals and presbyacusis patients.

Table 6.1. Annual deterioration thresholds

	0.25 (kHz)	0.5 (kHz)	1 (kHz)	2 (kHz)	4 (kHz)	8 (kHz)
II.1	-0.25	0.09	-0.25	-1.51	-1.71	-1.60
p	NS	NS	0.02	<0.0001	<0.0001	<0.0001
II.4	-0.82	-0.25	-0.09	-0.51	-1.17(0.0001)	-2.02 (0.0001)
p	0.03	NS	NS	NS		

Results of longitudinal regression analysis of individual binaural mean air conduction thresholds in dB/yr.
NS = not significant.
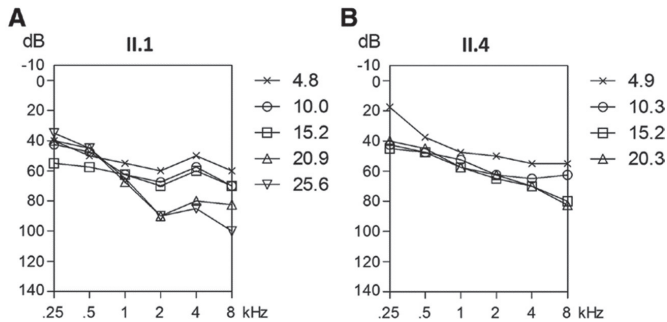
Figure 6.3. Longitudinal binaural mean air conduction threshold data of family members II.1 (A); aged 4.8-25.6 years and II.4 (B); aged 4.9-20.3 years. Age (years) is shown with a symbol key.

Vestibular evaluation
Patient II.1 complained of motion sickness. She showed a spontaneous nystagmus of 3 deg/s to the left, which was considered to be non-significant. Recording of the optokinetic nystagmus and results of all vestibule-oculomotor tests were normal. During the velocity step test, gain and start speed were slightly higher than normal; time constant and Gesamtamplitude were normal. Results of calorisation were normal as well. There was a slight asymmetry between both labyrinths, to the detriment of the right vestibulum. Based on these results, vestibular function was considered normal.

Ophthalmic evaluation
Both patients had no visual complaints, including absence of night blindness, visual field loss and decrease in central vision. Patient II.1 presented with amblyopia of the right eye, with a suboptimal visual acuity of 20/30 after occlusion therapy, whereas visual acuity reached 20/12 in the left eye. Ophthalmic examination revealed normal anterior segments and retinas. There were no signs of RP: no bone spicules, no attenuation of the retinal vasculature, no (waxy) pallor of the optic disc or degeneration of the RPE were observed (Figure 6.5A). FAF images revealed normal autofluorescence of the RPE (Figure 6.5B) and SD-OCT revealed normal retinal architecture, including intact photoreceptor layer reflectance in the macula and midperiphery (Figure 6.5D and 6.5E). Additionally, Goldmann perimetry showed normal visual field sizes and sensibility levels and HRR plates were named correctly. Rod- and cone-derived responses on full-field ERG were normal in both eyes.
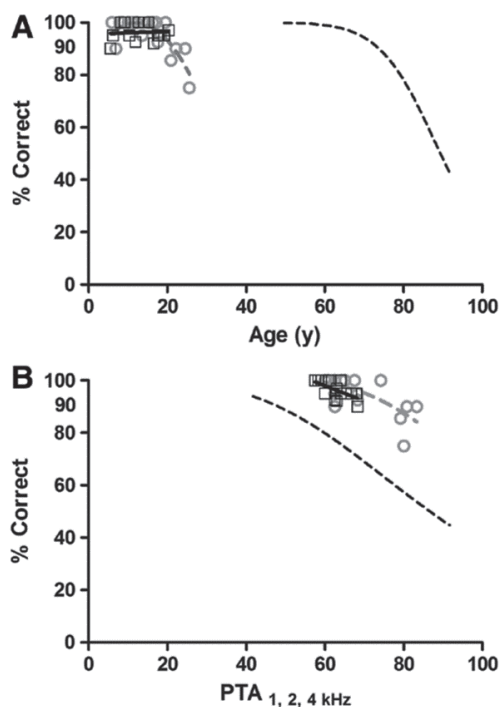
Figure 6.4. (A) Longitudinal regression analysis of mean monaural phoneme recognition score (% correct) related to age (year) of both affected family members. Scores of II.1 are indicated in grey circles, the regression line is a dashed grey curve. Scores of II.4 are indicated as black squares, the regression line is black and solid. The dashed curve indicates nonlinear regression of presbyacusis patients. (B) Longitudinal regression analysis of mean monaural phoneme recognition score (% correct) related to $PTA_{1, 2, 4 kHz}$ (dB HL). Same legend as figure 6.4A.

We concluded that subject II.1 had normal retinal appearance and function in both eyes. The amblyopia found in this patient was not considered to be a (prodromal) symptom of an Usher syndrome phenotype.
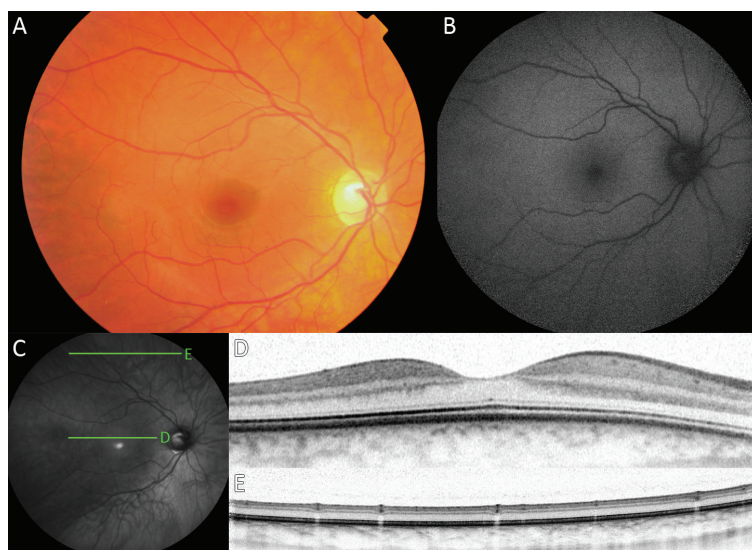
Figure 6.5. Multi-modal imaging of the right eye of patient II.1 at age 25. (A) Fundus photography of central fundus of the right eye showing no abnormalities. (B) Fundus autofluorescence imaging of the right eye with normal autofluorescence levels in the posterior pole. (C) Infra-red en face image of the posterior pole of the right eye. The green lines indicate the location of the optical coherence tomography (OCT) images depicted in panels D and E. (D) OCT image of the central retina of the right eye depicting the fovea, which reveals no retinal abnormalities and especially a normal photoreceptor layer and retinal pigment epithelium (RPE). (E) OCT image of the midperipheral retina of the right eye revealing normal retinal architecture.

Discussion

Here, we present, to our knowledge, the first cases of non-syndromic autosomal recessively inherited hearing loss caused by mutations in *USH1G*. The moderate hearing loss has an onset during early childhood. Mild progression of hearing loss, especially in the higher frequencies, was observed. Resulting in a downsloping audiogram configuration. Although it was only performed in one individual, results of psychophysical examination were in line with a cochlear, sensorineural hearing loss. No vestibular abnormalities were detected. During ophthalmic examination of patient II.1, no retinal pathology was observed, especially no signs of RP which is a clinical hallmark for Usher syndrome. This absence of ophthalmic abnormalities made us characterize the phenotype in individual II.1 as nonsyndromic. However, while absent at the age of 25 years, RP may develop at a later age, which is highly atypical for type I Usher syndrome. Atypical *USH1G*-associated Usher syndrome has been described by Kalay et al. and Bashir et al. in patients with retinal abnormalities, but without visual problems.[13,14] However, these retinal abnormalities were already observed in patients younger than individual II.1.

Of the six known Usher syndrome type I genes, five were already known to be involved in nonsyndromic autosomal recessive hearing loss, except for *USH1G*.[5,7,28-30] A number of explanations have been given for the fact that mutations in these genes either lead to syndromic or nonsyndromic hearing loss. Ouyang et al. illustrated the importance of tissue-dependent alternative splicing as a cause of phenotypic heterogeneity in Usher syndrome type 1c, since harmonin has isoforms that are only expressed in the inner ear and not in the retina.[8] However, to our knowledge, only one isoform is currently known for the *USH1G* encoded protein SANS.

The difference between Usher syndrome type 1f and DFNB23 has been correlated to the mutational effect and residual function of specific protein domains. Only missense mutations that do not affect calcium binding and rigidification of protocadherin15 (*PCDH15*) cause DFNB23 thus far.[5,28,31] Missense mutations are more likely to result in residual protein function than truncating mutations. Furthermore, Riazuddin et al. hypothesize that some residual function of myosin VIIA is retained in DFNB2 and that no residual function of the protein will be found in Usher syndrome type 1b,[7] which was also hypothesized for *CDH23* (DFNB12 and Usher syndrome type 1d).[6,30]

Families have been described with Usher syndrome type Ig carrying *USH1G* missense mutations that are expected to result in residual protein function. Therefore, we assume that the differences of the genotypic spectrum depend on the extent of residual protein function. In addition, other factors are probably also involved in the heterogeneity of the phenotypic spectrum of *USH1G*-associated disease.

When compared to other *USH1G* genotypes, the genotype described here mostly resembles the genotype of a German family described by Weil et al.[27] In this family, one allele contains a missense mutation (c.143T→C) which leads to a substitution of proline for leucine (p.Leu48Pro) in the first ankyrin domain. The second mutation (c.186-187delCA) is predicted to lead to a truncated protein (p.Ile63Leufs*71). The phenotype in the affected members of this German family deviates from that in family W08-2221 as the former demonstrates an

Usher syndrome type I phenotype. As shown by modeling, the change of methionine to valine at position 104 only alters the surface of SANS, and not the overall structure (Figure 6.2A). This may result in a reduction or loss of binding of one or more interactions partner of SANS. The p.Leu48Pro substitution is predicted to lead to a more severe structure alteration and predicted loss of hydrophobic contacts (Figure 6.2B). This may interfere more with interaction partners than the slight surface change caused by p.Met104Val. Interacting with other proteins is essential for the function of SANS, since it is a scaffold protein and is known to bind with multiple proteins of the Usher interactome.[32] Furthermore, the p.Leu48Pro mutation might affect binding of one or more proteins that are essential in both inner ear and retina whereas the p.Met104Val might affect the interaction with protein(s) that are only essential in cochlear function. To our knowledge, no interaction partners for the ankyrin domains of SANS have been identified.

Questions now rise on the prevalence of nonsyndromic hearing loss based on mutations in *USH1G.* One is probably less vigilant on *USH1G* as a causal gene for nonsyndromic hearing loss since it has not been described before to be associated with a nonsyndromic type of the disease. We assume that more patients with *USH1G*-associated isolated hearing loss will be identified in the future, especially as the c.310A→G mutation has been found in 0.03% of alleles in the EVS database. We demonstrate that several different phenotypes can trigger one to consider *USH1G* as the causative gene: when a patient presents with Usher syndrome type I or with atypical Usher syndrome, but most certainly also when a patient presents with a nonsyndromic, autosomal recessive, slightly progressive hearing loss.

Conclusion

We describe, to our knowledge, the first family with nonsyndromic sensorineural hearing loss based on mutations in *USH1G.* The hearing loss has an onset during early childhood, is progressive and has a downsloping audiogram configuration. Ophthalmic and vestibular abnormalities are absent. More knowledge on interaction partners and how they bind to SANS will probably clarify the heterogeneous spectrum of phenotypes found with mutations in *USH1G* in the near future.

References

1. Millan JM, Aller E, Jaijo T, Blanco-Kelly F, Gimenez-Pardo A, Ayuso C. An update on the genetics of usher syndrome. *Journal of ophthalmology*. 2011;2011:417217.
2. Davenport SLH, Omenn GS. The heterogeneity of Usher Syndrome Davenport, abstract. In: Littlefield JW, G EFJ, W HJ, editors. Fifth International Conference on Birth Defects; Amsterdam, Excerpta Medica1977. p. 87-8.
3. Saihan Z, Webster AR, Luxon L, Bitner-Glindzicz M. Update on Usher syndrome. *Current opinion in neurology*. 2009 Feb;22(1):19-27.
4. Van Camp G, Smith RJ. Hereditary Hearing Loss homepage. 2013 [updated June 3th, 2013]; Available from: http://hereditaryhearingloss.org/.
5. Ahmed ZM, Riazuddin S, Ahmad J, et al. PCDH15 is expressed in the neurosensory epithelium of the eye and ear and mutant alleles are responsible for both USH1F and DFNB23. *Human molecular genetics*. 2003 Dec 15;12(24):3215-23.
6. Pennings RJ, Topsakal V, Astuto L, et al. Variable clinical features in patients with CDH23 mutations (USH1D-DFNB12). *Otology & neurotology : official publication of the American Otological Society, American Neurotology Society [and] European Academy of Otology and Neurotology*. 2004 Sep;25(5):699-706.
7. Riazuddin S, Nazli S, Ahmed ZM, et al. Mutation spectrum of MYO7A and evaluation of a novel nonsyndromic deafness DFNB2 allele with residual function. *Human mutation*. 2008 Apr;29(4):502-11.
8. Ouyang XM, Xia XJ, Verpy E, et al. Mutations in the alternatively spliced exons of USH1C cause non-syndromic recessive deafness. *Human genetics*. 2002 Jul;111(1):26-30.
9. Hildebrand MS, Thorne NP, Bromhead CJ, et al. Variable hearing impairment in a DFNB2 family with a novel MYO7A missense mutation. *Clinical genetics*. 2010 Jun;77(6):563-71.
10. Weil D, Kussel P, Blanchard S, et al. The autosomal recessive isolated deafness, DFNB2, and the Usher 1B syndrome are allelic defects of the myosin-VIIA gene. *Nature genetics*. 1997 Jun;16(2):191-3.
11. Astuto LM, Bork JM, Weston MD, et al. CDH23 mutation and phenotype heterogeneity: a profile of 107 diverse families with Usher syndrome and nonsyndromic deafness. *American journal of human genetics*. 2002 Aug;71(2):262-75.
12. Wagatsuma M, Kitoh R, Suzuki H, Fukuoka H, Takumi Y, Usami S. Distribution and frequencies of CDH23 mutations in Japanese patients with non-syndromic hearing loss. *Clinical genetics*. 2007 Oct;72(4):339-44.
13. Kalay E, de Brouwer AP, Caylan R, et al. A novel D458V mutation in the SANS PDZ binding motif causes atypical Usher syndrome. *Journal of molecular medicine (Berlin, Germany)*. 2005 Dec;83(12):1025-32.
14. Bashir R, Fatima A, Naz S. A frameshift mutation in SANS results in atypical Usher syndrome. *Clinical genetics*. 2010 Dec;78(6):601-3.
15. Mustapha M, Chouery E, Torchard-Pagnez D, et al. A novel locus for Usher syndrome type I, USH1G, maps to chromosome 17q24-25. *Human genetics*. 2002 Apr;110(4):348-50.
16. Schraders M, Ruiz-Palmero L, Kalay E, et al. Mutations of the gene encoding otogelin are a cause of autosomal-recessive nonsyndromic moderate hearing impairment. *American journal of human genetics*. 2012 Nov 2;91(5):883-9.
17. Krieger E, Koraimann G, Vriend G. Increasing the precision of comparative models with YASARA NOVA--a self-parameterizing force field. *Proteins*. 2002 May 15;47(3):393-402.
18. De Leenheer EMR, McGuirt WT, Kunst HPM, Huygen PL, Smith RJ, Cremers CW. The phenotype of DFNA13/COL11A2. *Advances in oto-rhino-laryngology*. 2002;61:85-91.
19. De Leenheer EMR, Bosman AJ, Huygen PLM, Kunst HPM, Cremers CWRJ. Audiological characteristics of some affected members of a dutch DFNA13/ COL11A2 family. *Ann Otol Rhinol Laryngol*. 2004;113:922-9.
20. Plantinga RF, Cremers CWRJ, Huygen PLM, Kunst HPM, Bosman AJ. Audiological evaluation of affected members from a Ducth DFNA8/12 (TECTA) family. *JARO*. 2007;8:1-7.
21. Theunissen EJ, Huygen PL, Folgering HT. Vestibular hyperreactivity and hyperventilation. *Clinical otolaryngology and allied sciences*. 1986 Jun;11(3):161-9.
22. Marmor MF, Fulton AB, Holder GE, et al. ISCEV Standard for full-field clinical electroretinography (2008 update). *Documenta ophthalmologica Advances in ophthalmology*. 2009 Feb;118(1):69-77.

23. Server EV. NHLBI GO Exome Sequencing Project (ESP). Seattle, WA2013 [15-09-2013]; Available from: http://evs.gs.washington.edu/EVS/.
24. Adzhubei IA, Schmidt S, Peshkin L, et al. A method and server for predicting damaging missense mutations. *Nat Meth*. 2010;7(4):248-9.
25. Kumar P, Henikoff S, Ng PC. Predicting the effects of coding non-synonymous variants on protein function using the SIFT algorithm. *Nature protocols*. 2009;4(7):1073-81.
26. Schwarz JM, Rodelsperger C, Schuelke M, Seelow D. MutationTaster evaluates disease-causing potential of sequence alterations. *Nature methods*. 2010 Aug;7(8):575-6.
27. Weil D, El-Amraoui A, Masmoudi S, et al. Usher syndrome type I G (USH1G) is caused by mutations in the gene encoding SANS, a protein that associates with the USH1C protein, harmonin. *Human molecular genetics*. 2003 Mar 1;12(5):463-71.
28. Doucette L, Merner ND, Cooke S, et al. Profound, prelingual nonsyndromic deafness maps to chromosome 10q21 and is caused by a novel missense mutation in the Usher syndrome type IF gene PCDH15. *European journal of human genetics : EJHG*. 2009 May;17(5):554-64.
29. Ouyang XM, Yan D, Du LL, et al. Characterization of Usher syndrome type I gene mutations in an Usher syndrome patient population. *Human genetics*. 2005 Mar;116(4):292-9.
30. Schultz JM, Bhatti R, Madeo AC, et al. Allelic hierarchy of CDH23 mutations causing non-syndromic deafness DFNB12 or Usher syndrome USH1D in compound heterozygotes. *Journal of medical genetics*. 2011 Nov;48(11):767-75.
31. Ahmed ZM, Riazuddin S, Aye S, et al. Gene structure and mutant alleles of PCDH15: nonsyndromic deafness DFNB23 and type 1 Usher syndrome. *Human genetics*. 2008 Oct;124(3):215-23.
32. Maerker T, van Wijk E, Overlack N, et al. A novel Usher protein network at the periciliary reloading point between molecular transport machineries in vertebrate photoreceptor cells. *Human molecular genetics*. 2008 Jan 1;17(1):71-86.

6

Authors

Ramon A. C. van Huet, [1] Laurence H.M. Pierrache,[2,3] Magda A. Meester-Smoor,[2,3] Caroline C.W. Klaver,[3] L. Ingeborgh van den Born,[2] Carel B. Hoyng,[1] Ilse J de Wijs,[5] Rob W. J. Collin,[5,6] Lies H. Hoefsloot,[7] B. Jeroen Klevering[1]

Affiliations

[1]Department of Ophthalmology, Radboud University Medical Center, Nijmegen, The Netherlands
[2]The Rotterdam Eye Hospital, Rotterdam, The Netherlands
[3]Department of Ophthalmology, Erasmus Medical Center, Rotterdam, The Netherlands
[4] Department of Epidemiology, Erasmus Medical Center, Rotterdam, The Netherlands
[5]Department of Human Genetics, Radboud University Medical Center, Nijmegen, The Netherlands
[6]Radboud Institute for Molecular Life Sciences, Nijmegen, The Netherlands
[7]Department of Clinical Genetics, Erasmus Medical Center, Rotterdam, The Netherlands

The efficiency of microarray screening for autosomal recessive retinitis pigmentosa in routine clinical practice

7

Abstract

Purpose. To determine the efficacy of multiple versions of a commercially available arrayed primer extension (APEX) microarray chip for autosomal recessive retinitis pigmentosa (arRP).

Methods. We included 250 probands suspected of arRP who were genetically analyzed with the APEX microarray between January 2008 and November 2013. The mode of inheritance had to be autosomal recessive according to the pedigree (including isolated cases). If the microarray identified a heterozygous mutation, we performed Sanger sequencing of exons and exon-intron boundaries of that specific gene. The efficacy of this microarray chip with additional Sanger sequencing approach was determined by the percentage of patients that received a molecular diagnosis. We also collected the data of the genetic tests other than the APEX analysis for arRP to provide a detailed description of the molecular diagnoses in our study cohort.

Results. The APEX microarray chip for arRP identified the molecular diagnosis in 21 (8.5%) of the patients in our cohort. Additional Sanger sequencing yielded a second mutation in 17 patients (6.8%), thereby establishing the molecular diagnosis. In total, 38 patients (15.2%) received a molecular diagnosis after analysis by the microarray and additional Sanger sequencing approach. Further genetic analyses after a negative result of the arRP microarray (*n*=107) resulted in a molecular diagnosis of arRP (*n*=23), autosomal dominant RP (*n*=5), X-linked RP (*n*=2) and choroideremia (*n*=1).

Conclusions. The efficacy of the commercially available APEX microarray chips for arRP appears to be low, most likely caused by the limitations of this technique and the genetic and allelic heterogeneity of RP. Diagnostic yields up to 40% have been reported for NGS techniques that, as expected, thereby outperform targeted APEX analysis.

Introduction

Retinitis pigmentosa (RP) is a group of hereditary diseases with an incidence of approximately 1:4000.[1-4] Although the clinical variation is high, RP is generally characterized by complaints of night blindness and peripheral visual field loss caused by progressive rod photoreceptor degeneration. In later stages of the disease cones may also degenerate, which results in a decrease of central and color vision. The disease can be transmitted in all Mendelian patterns, including autosomal recessive in 50%–60% of RP patients, autosomal dominant in 30%–40% and X-linked in 5%–15%.[1] Additionally, mitochondrial inheritance has been described in <1% of RP patients,[5] and a few digenic cases have been reported.[6,7] To date, over 2,300 mutations in 45 genes have been associated with autosomal recessive RP (arRP; RetNet, https://sph.uth.edu/retnet/).[8] This allelic and genetic heterogeneity complicates mutation detection in RP patients, since the phenotype is often not specific enough to link the disease to a particular gene. In addition, only just over 50% of the arRP cases can be linked to mutations in these genes.[9,10]

Over time, multiple genotyping techniques have been developed to identify causative mutations in genes associated with RP, such as single-strand conformation analysis,[11] denaturing high-performance liquid chromatography (HPLC),[12] resequencing microarrays,[13] and arrayed primer extension (APEX) analysis.[14-16] Recently, next-generation sequencing (NGS) has shown its potential in identifying causative mutations in a selected gene set (targeted NGS)[17] and in the whole exome.[18]

Diagnostic genetic testing in nonsyndromic RP patients using the APEX microarray technology has been popular since it is a relatively low cost technique that enables screening of numerous mutations in multiple genes simultaneously. In the last decade, APEX chips have been developed for mutation analysis of the *ABCA4* gene in autosomal recessive Stargardt disease or cone-rod dystrophy,[16,19] as well as for multiple gene microarrays for Leber congenital amaurosis (LCA),[15,20] Bardet-Biedl syndrome (BBS),[21] Usher syndrome,[22] and autosomal dominant and recessive RP.[23] The efficacy with which these APEX chips lead to a molecular diagnosis is variable for the different disorders.

Identification of the genetic cause in these patients has become more important over time. It not only allows for a more accurate prognosis and appropriate genetic counseling for patients and their families, but also provides crucial information with regard to upcoming genetic therapies. The aim of this study was to evaluate the efficiency of the microarray chip for arRP in a cohort of recessive and isolated RP probands.

Methods

Patients

For this study, we selected unrelated patients from the Departments of Ophthalmology of the Radboud University Medical Center (Nijmegen, The Netherlands), Erasmus Medical Center (Rotterdam, The Netherlands) and the Rotterdam Eye Hospital (Rotterdam, The Netherlands) that were clinically suspect for RP and have been analyzed with an arRP microarray between January 2008 and November 2013. The microarray screenings were requested by the ophthalmologist who examined the patient when RP was suspected based on the simultaneous occurrence of at least two of the following criteria: (1) a history of night blindness

and/or peripheral visual field loss, (2) a positive family history for RP, (3) perimetric results compatible with RP and (4) reduced responses on electroretinography (ERG). We included the probands of families that were suspected of RP with an autosomal recessive inheritance pattern as well as isolated cases; families with presumed dominant or X-linked inheritance patterns were excluded. Only probands were included; other patients within the same family were excluded, as well as patients with insufficient clinical data. For this retrospective study the local ethics committee ruled that approval was not required and, according to the tenets of the Declaration of Helsinki, all participants gave informed consent for the use of their data.

For the selection procedure described above, we collected data from the medical records, including history and age of onset, best corrected visual acuity (BCVA), fundus appearance and full-field electroretinography (ERG) results. Full-field ERG was performed according the International Society for Clinical Electrophysiology of Vision (ISCEV) standards.[24]

Table 7.1. Overview of the genes analyzed by the latest APEX microarray chip for autosomal recessive retinitis pigmentosa (version 6.0).

Gene symbol	Full gene name	Number of mutations included in chip
ABCA4	ATP-binding cassette, sub-family A (ABC1), member 4	1
AIPL1	Aryl hydrocarbon receptor interacting protein-like 1	1
CERKL	Ceramide kinase-like	5
CNGA1	Cyclic nucleotide gated channel alpha 1	5
CNGA3	Cyclic nucleotide gated channel alpha 3	1
CNGB1	Cyclic nucleotide gated channel beta 1	3
CNGB3	Cyclic nucleotide gated channel beta 3	1
CRB1	Crumbs homolog 1	114
EYS	Eyes shut homolog	68
GRK1	G protein-coupled receptor kinase 1	1
IMPG2	Interphotoreceptor matrix proteoglycan 2	6
LRAT	Lecithin retinol acyltransferase (phosphatidyl-choline-retinol O-acyltransferase)	3
MERTK	C-mer proto-oncogene tyrosine kinase	14
PDE6A	Phosphodiesterase 6A, cGMP-specific, rod, alpha	22
PDE6B	Phosphodiesterase 6B, cGMP-specific, rod, beta	28
NR2E3	Nuclear receptor subfamily 2, group E, member 3	31
PROM1	Prominin 1	2
RBP3	Retinol binding protein 3, interstitial	1
RDH12	Retinol dehydrogenase 12 (all-trans/9-cis/11-cis)	45
RGR	Retinal G protein coupled receptor	7
RHO	Rhodopsin	2
RLBP1	Retinaldehyde binding protein 1	13
RP1	Retinitis pigmentosa 1	3
RPE65	Retinal pigment epithelium-specific protein 65kDa	100
SAG	S-antigen; retina and pineal gland (arrestin)	4
TULP1	Tubby like protein 1	25
CLRN1	Clarin 1	12
USH2A	Usher syndrome 2A	192
Total: 28		Total: 710

ATP, adenosine triphosphate; cGMP, cyclic guanosine monophosphate; kDA, kiloDalton.

Genetic microarray chip analyses

DNA was extracted from leukocytes acquired from peripheral venous blood samples according to automated nucleic acid isolation based on magnetic bead technology (Chemagic MSM I, Perkin Elmer chemagen Technologie GmbH, Baesweiler, Germany). We performed mutational screening using a commercially available genotyping microarray chip based on APEX technology (Asper Biotech, Tartu, Estonia) according to a protocol described previously.[15] An APEX reaction is based on a single base extension principle, which provides highly specific discrimination without allele-specific hybridization. In a single multiplex reaction, hundreds to thousands of variants can be analyzed simultaneously. The microarray chips used in this study included known pathogenic mutations in the coding regions and adjacent intronic sequences of genes associated with arRP.

The microarray chip initially included 501 mutations in 16 genes in 2006,[25] but was regularly updated as new mutations were being discovered. The latest version (version 6.0) included 710 mutations in 28 genes (Table 7.1). During the inclusion period of this study, five versions of this array have been used: versions 4.0 (between January and April 2008), 4.1 (between April 2008 and February 2009), 5.0 (between February 2009 and September 2010), 5.3 (between September 2010 and July 2012), and 6.0 (between July 2012 and November 2013). Sanger sequencing was performed to confirm each mutation that was identified by the microarray chip. If only a single heterozygous mutation in a certain gene was found, all exons and intron-exon boundaries of this gene were analyzed with Sanger sequencing in search for the mutation on the second allele. The pathogenicity of a mutation was determined by our in-house protocol based on the criteria described by Cotton et al,[26] which evaluates pathogenicity by evolutionary conservation of the altered nucleotide (phylogenetic profiling [PhyloP] score), the nature of the change at the amino acid level (Grantham score), and information from online *in silico* prediction tools SIFT and Polyphen-2. The effects of mutations on splice sites, if applicable, were determined by five predictor programs (SpliceSiteFinder-like, MaxEntScan, NNSPLICE, GeneSplicer, en Human Splicing Finder) as provided in Alamut Visual (various versions, Interactive Biosoftware, Rouen, France). Reference sequences as provided by Alamut Visual (Interactive Biosoftware, Rouen, France) have been used. Genes and mutations were annotated according the HGNC and HGSV nomenclature, respectively. The efficiency of each version of the microarray chip was determined by the number of patients that had a molecular diagnosis after the analysis with the microarray chip. Patients were considered to have a molecular diagnosis when it was plausible that both alleles had been identified by a variant that was predicted to be pathogenic, meaning that the variants were predicted to significantly reduce or nullify the function of the protein. Identification of two pathogenic mutations (in combination with the presence of the RP phenotype) was considered pathogenic; segregation analysis – to evaluate if the identified mutations are situated on separate alleles –was performed in some but not all families.

Further genetic analyses

To further evaluate the molecular diagnoses found in our study cohort, we also collected data of the genetic tests that have been performed after a negative result of the arRP microarray chip in these patients. The tests included targeted NGS (*n*=16), microarray analyses for autosomal dominant RP, LCA, BBS, Usher syndrome, and *ABCA4* mutation analysis (*n*=28), or Sanger

sequencing of selected genes (*n*=88). The microanalyses have been performed using the microarray chips available from Asper (Asper Biotech, Tartu, Estonia). Targeted NGS was performed by sequencing the exome with a 5500xl Genetic Analyzer (Life Technologies™, Carlsbad, CA) after DNA enrichment with the Agilent SureSelectXT Human All Exon 50Mb Kit (Agilent Technologies, Santa Clara, CA). Data was analyzed by LifeScope™ software (Life Technologies™, Carlsbad, CA). Afterwards, the variants of 160 genes known to be involved in retinal disease were selected and ordered on predicted pathogenicity. All mutations identified have been confirmed by Sanger sequencing.

Results

We included 250 probands (136 males, 54%) with the clinical diagnosis isolated or arRP. Seven patients were analyzed with the microarray version 4.0, 12 patients with version 4.1, 86 with version 5.0, 98 with version 5.3 and 47 with version 6.0. All mutations identified by the microarray chip were subsequently confirmed with Sanger sequencing.

Combining the results of all versions of the microarray chip, we identified mutations in 68 patients (27.7%). A total of 21 arRP patients (8.5%) received a confirmed molecular diagnosis by means of identification of homozygous or two heterozygous pathogenic mutations. In 47 patients (18.8%) a single heterozygous pathogenic mutation was detected. In the vast majority (182 patients, 72.8%) however, the microarray analysis did not reveal any causative mutation (Table 7.2). Additional Sanger sequencing when a heterozygous mutation was identified by the microarray chip resulted in a second pathogenic mutation in 17 patients (6.8%, Table 7.2). The microarray missed two (11.8%) of these mutations, which results in a maximum sensitivity of 95.7%. However, to determine the exact sensitivity all genes tested on the microarray chip should be sequenced. In total, the microarray screening with additional Sanger sequencing approach identified the molecular diagnosis in 38 (15.2%) of the arRP patients. Table 7.2 summarizes the numbers of patients with two, one or no mutation after microarray screening for each microarray version, as well as the numbers of solved cases after additional Sanger sequencing.

Table 7.2. Efficacy in the identification of the genetic cause of autosomal recessive retinitis pigmentosa by the Asper micro-array chip with and without additional Sanger sequencing for this disease.

Chip version	Number of patients	Number of cases after microarray analysis (%)			Number of genetically solved cases by additional Sanger sequencing (%)†
		*Genetically solved**	*Heterozygous*	*No mutations*	
4	7	0 (0)	0 (0)	7 (100)	0 (0)
4.1	12	3 (25)	2 (16.7)	7 (58.3)	0 (0)
5	86	4 (4.7)	20 (23.3)	62 (72.1)	4 (4.7)
5.3	98	11 (11.2)	16 (16.3)	71 (72.4)	11 (11.2)
6	47	3 (6.4)	9 (19.1)	35 (74.4)	2 (4.3)
Overall	250	21 (8.5)	47 (18.8)	182 (72.8)	17 (6.8)

*Patients were considered genetically 'solved' if homozygous or compound heterozygous mutations were identified. Segregation analysis was performed in some but not all families.

† Number of patients in whom the mutation on the second allele was identified by Sanger sequencing after identification of a heterozygous mutation by microarray screening.

In this study, we identified 65 different mutations in 12 genes (Table 7.3). Most mutations were identified in *USH2A* (48.5%), *PDE6A* (17.6%) and *CRB1* (10.3%). Of the 65 variants identified in this study, 39 (60%) were missense mutations, 10 (15.4%) had effects on splicing, 9 (13.8%) caused a premature stop (nonsense mutations), and 7 (10.8%) resulted in a shift of the open reading frame. Fifty-nine mutations are (likely to be) pathogenic, whereas 6 mutations appear to have no significant effects on protein function (Table 7.3). These mutations may have been included based on non-published in-house databases of collaborators. The other eight mutations were identified by Sanger sequencing.

Further genetic analyses
Additional genetic tests were performed in 107 patients (43.6%) subsequent to the microarray analysis for arRP. An overview is provided in Table 7.4. The tests were selected based on the lack of family history or the acquisition of new history and ocular examination details after running the arRP APEX. These genetic tests resulted in a molecular diagnosis in 31 patients (30%), including arRP in 23 patients (21.5%), autosomal dominant RP in five patients (4.7%), X-linked RP in two patients (1.9%) and choroideremia in one patient (0.9%). The targeted NGS approach that covered 160 genes associated with hereditary blindness resulted in a molecular diagnosis in 12 patients (75%, Table 7.4).

Table 7.3. Mutations identified by microarray chip analysis and additional Sanger sequencing in the patients included in this study.

cDNA mutation (reference sequence)	Effect (RNA/ protein)	EVS minor allele frequency in %†	Predicted pathogenicity‡	Frequency of variant in this cohort (%)	Reference
CERKL (NM_001030311.1)				*1 (0.8)*	
c.847C>T	p.Arg283*	0.048	Pathogenic	1 (0.8)	[27,28]
CLRN1 (NM_174878.2)				*1 (0.8)*	
c.149_152delins8	p.Ser50fs	0.008	Pathogenic	1 (0.8)	[29,30]
CNGA1 (NM_000087.3)				*3 (2.5)*	
c.94C>T	p.Arg32*	NA	Pathogenic	2 (1.7)	[31]
c.959C>T	p.Ser320Phe	NA	Probably pathogenic	1 (0.8)	[32]
CRB1 (NM_201253.1)				*11 (9.2)*	
c.613_619del	p.Ile205fs	NA	Pathogenic	1 (0.8)	[33,34]
c.614T>A	p.Ile205Lys	NA	Probably pathogenic	1 (0.8)	This study
c.614T>C	p.Ile205Thr	0.038	Possibly pathogenic	1 (0.8)	[35,36]
c.1602G>T	p.Lys534Asn	NA	Probably pathogenic	1 (0.8)	[17]
c.1892A>G	p.Tyr831Cys	NA	Probably pathogenic	2 (1.7)	This study
c.2234C>T	p.Thr745Met	0.008	Probably pathogenic	2 (1.7)	[37]
c.2681A>G	p.Asn894Ser	0.008	Possibly pathogenic	1 (0.8)	[25,38]
c.2842+5G>A	splicing	NA	Possibly pathogenic	1 (0.8)	[37]
c.2945C>A	p.Thr982Lys	NA	Probably pathogenic	1 (0.8)	[39]

cDNA mutation (reference sequence)	Effect (RNA/ protein)	EVS minor allele frequency in %†	Predicted pathogenicity‡	Frequency of variant in this cohort (%)	Reference
EYS (NM_001142800.1)				2 (1.7)	
c.9405T>A	p.Tyr3135*	NA	Pathogenic	2 (1.7)	40
NR2E3 (NM_014249.2)				5 (4.2)	
c.119-2A>C	splicing	NA	Possibly pathogenic	3 (2.5)	29
c.227G>A	p.Arg76Gln	0.032	Probably pathogenic	1 (0.8)	29,30
c.932G>A	p.Arg311Gln	0.024	Probably pathogenic	1 (0.8)	29
PDE6A (NM_000440.2)				21 (17.5)	
c.304C>A	p.Arg102Ser	0.015	Probably pathogenic	10 (8.3)	25,41,42
c.769C>T	p.Arg257*	0.015	Pathogenic	1 (0.8)	43
c.878C>T	p.Pro293Leu	0.361	Possibly benign	1 (0.8)	41
c.937del	p.Ile313fs	NA	Pathogenic	1 (0.8)	This study
c.1032C>T	p.Ser344Ser (splicing)	NA	Possibly pathogenic	1 (0.8)	This study
c.1171G>A	p.Val391Met	1.699	Possibly pathogenic	4 (3.3)	41
c.1705C>A	p.Gln569Lys	0.015	Probably pathogenic	1 (0.8)	41
c.1963C>T	p.His655Tyr	2.091	Possibly benign	2 (1.7)	44
PDE6B (NM_000283.3)				9 (7.5)	
c.220C>T	p.Arg74Cys	0.038	Pathogenic	1 (0.8)	45
c.655T>C	p.Tyr219His	0.538	Probably pathogenic	2 (1.7)	17
c.1107+3A>G	splicing	0.015	Probably pathogenic	1 (0.8)	17
c.1401+4_1401+48del	splicing	NA	Possibly pathogenic	1 (0.8)	This study
c.1798G>A	p.Asp600Asn	NA	Possibly pathogenic	2 (1.7)	42
c.2503+5G>C	splicing	NA	Possibly pathogenic	1 (0.8)	17
c.2503+2T>C	splicing	NA	Probably pathogenic	1 (0.8)	This study
PROM1 (NM_006017.2)				1 (0.8)	
c.1354dup	p.Tyr452fs	0.049	Pathogenic	1 (0.8)	46
RDH12 (NM_152443.2)				4 (3.3)	
c.379G>T	p.Gly127*	NA	Pathogenic	4 (3.3)	47
RPE65 (NM_000329.2)				3 (2.5)	
c.271C>T	p.Arg91Trp	0.015	Probably pathogenic	1 (0.8)	48,49
c.963T>G	p.Asn321Lys	0.077	Possibly pathogenic	1 (0.8)	50,51
c.1069dup	p.Asn356fs	NA	Pathogenic	1 (0.8)	52
USH2A (NM_206933.2)				59 (49.2)	
c.486-14G>A	Splicing	0.008	Probably pathogenic	1 (0.8)	53
c.949C>A	p. Arg317Arg (Splicing)	NA	Possibly pathogenic	1 (0.8)	54-58
c.1256G>T	p.Cys419Phe	0.008	Pathogenic	3 (2.5)	55,57,59
c.1876C>T	p.Arg626*	NA	Pathogenic	1 (0.8)	55
c.2276G>T	p.Cys759Phe	0.154	Pathogenic	16 (13.3)	35,60-64
c.2299delG	p.Glu767fs*21	0.176	Pathogenic	3 (2.5)	65
c.2522C>A	p.Ser841Tyr	0.531	Possibly pathogenic	3 (2.5)	57,66

cDNA mutation (reference sequence)	Effect (RNA/ protein)	EVS minor allele frequency in %†	Predicted pathogenicity‡	Frequency of variant in this cohort (%)	Reference
c.3368A>G	p.Tyr1123Cys	NA	Probably pathogenic	1 (0.8)	[67]
c.5728C>T	p.Gln1910*	NA	Pathogenic	1 (0.8)	This study
c.5975A>G	p.Tyr1992Cys	0.361	Possibly pathogenic	2 (1.7)	[64]
c.6049+1G>A	Splicing	NA	Pathogenic	1 (0.8)	This study
c.7054C>T	p.Pro2352Ser	NA	Probably pathogenic	1 (0.8)	This study
c.8723_ 8724del	p.Val2908fs	NA	Pathogenic	2 (1.7)	[54]
c.9262G>A	p.Glu3088Lys	0.450	Probably benign	2 (1.7)	[64]
c.9413G>A	p.Gly3138Asp	NA	Probably pathogenic	1 (0.8)	This study
c.9433C>T	p.Leu3145Phe	0.008	Probably benign	1 (0.8)	EVS (rs267598373)
c.9815C>T	p.Pro3272Leu	NA	Possibly pathogenic	1 (0.8)	[68,69]
c.10073G>A	p.Cys3358Tyr	0.054	Probably pathogenic	1 (0.8)	[25,64]
c.10525A>T	p.Lys3509*	NA	Pathogenic	1 (0.8)	[17]
c.10561T>C	p.Trp3521Arg	NA	Probably pathogenic	1 (0.8)	[58,64]
c.11677C>A	p.Pro3893Thr	1.653	Probably benign	2 (1.7)	[58,70]
c.12328T>G	p.Tyr4110Asp	NA	Probably pathogenic	1 (0.8)	This study
c.12343C>T	p.Arg4115Cys	0.077	Probably pathogenic	5 (1.7)	[54,58,70]
c.13274C>T	p.Thr4425Met	NA	Probably pathogenic	3 (2.5)	[17,54,58,70]
c.14803C>T	p.Arg4935*	0.015	Pathogenic	1 (0.8)	[53,64,71]
c.15091C>T	p.Arg5031Trp	1.284	Probably benign	1 (0.8)	[58]
c.15377T>C	p.Ile5126Thr	2.422	Probably pathogenic	1 (0.8)	[11,64,72]
c.15433G>A	p.Val5145Ile	0.408	Pathogenic	1 (0.8)	[35,62-64]

†The overall allele frequency as provided in the Exome Variant Server in both European and African Americans.

‡The pathogenicity of the mutations was determined by our in-house protocol based on the criteria described by Cotton et al[26], which evaluates pathogenicity by evolutionary conservation of the amino acid (phylogenetic profiling [PhyloP] score), the nature of the change (Grantham score), and information from online in silico prediction tools SIFT and Polyphen-2.

* indicates a premature stop.

EVS, Exome Variant Server (available at http://evs.gs.washington.edu/EVS/); NA, not available.

Discussion

Only a decade ago, microarray screening boosted diagnostic genetic analysis in genetic heterogeneous disorders such as RP by facilitating reliable fast analysis of multiple genes simultaneously with much lower costs than Sanger sequencing of the same genes. Nowadays, high-throughput NGS techniques like exome sequencing have become available and are selectively used in a diagnostic setting. The microarray technique, however, remains in a prominent position in the diagnostic genetic analysis of RP, since NGS is currently only available for a small number of patients and has long lead times (>6 months). Therefore, we evaluated the efficiency of the microarray screening in arRP and isolated RP cases to determine its place in the array of diagnostic genetic tests currently available.

The low efficacy of 15.2% solved cases after microarray screening and additional Sanger sequencing found in this study can be attributed to the method's limitations in covering the genetic and clinical characteristics of autosomal recessive and simplex RP. First, the chip only analyzes a fixed set of mutations. The latest version of the chip includes 710 mutations in 28 genes, whereas over 2,300 mutations in 45 genes are associated with arRP nowadays[8] (and RetNet, https://sph.uth.edu/retnet/). Therefore, more frequent updates and inclusion of less frequent genes and mutations are necessary to increase the chip's efficacy, although this is costly and laborious to implement. Secondly, the APEX microarray approach does not identify variants other than the set of mutations present on the array. This rigid approach lowers the chance of mutation identification for arRP patients, since the frequency of private mutations is generally relatively high because of the immense mutational heterogeneity in arRP.

In addition to the disadvantages of the test itself, the heterogeneity of genetic and clinical characteristics of autosomal recessive and simplex RP complicates genetic analysis, since the correlation between a phenotype and a specific mutations in specific gene may be weak. Moreover, isolated RP cases, which are generally considered autosomal recessive, may also have an autosomal dominant or X-linked modes of inheritance. For instance, X-linked RP caused by mutations in *RPGR* or *RP2* account for 15% of male isolated cases with retinal degenerative disease,[73] and *de novo* mutations in genes known to follow a dominant inheritance pattern account for 1-2% of isolated RP.[17,74] This is exemplified by the discovery of mutations in dominant and X-linked RP genes in seven isolated patients in the current study (Table 7.4). An approach that enables genetic analysis of autosomal recessive, dominant and X-linked cases simultaneously, such as NGS, would therefore be preferable.

The microarray chip analyses defects in the genes that are relatively frequently mutated in arRP. Yet, this contributes little to the chip's efficacy since mutations in the majority of genes account only for 1-2% or less of arRP cases.[1,8,75] Furthermore, the older versions of the chip included mutations that are considered benign (c.9262G>A in *USH2A* and c.878C>T in *PDE6A,* Table 7.3). These variants probably have been detected in arRP cases previously, and have subsequently been added to the array, without a functional assessment of their pathogenicity, especially in case of missense mutations. Recently, it has become clear that using *in silico* prediction tools and especially databases with allele frequencies in large normal cohorts, like the Exome Variant Server (EVS), provide insight in the pathogenicity of a missense mutation, and should be used if functional assessment is missing. These benign mutations lower the microarray's efficiency, and should ideally be removed from the chip. The two benign mutations identified with the microarray in this study were not on later versions of the chip.

In contrast to the microarray approach, NGS techniques such as whole exome sequencing can handle the heterogeneity of arRP and provide a thorough genetic analysis. NGS has been reported to identify the genetic cause in 19% to 40% of arRP cases (and 50% to 82% of RP cases in general), which is significantly higher than the 15.2% solved cases after microarray screening and additional Sanger sequencing found in this study.[10,17,39,76-81] In whole exome sequencing, all coding sequences (the exons) of all genes in the genome are sequenced, which enables the identification of known and novel mutations in known arRP

genes. Mutations in genes that have not yet been associated with arRP can also be identified by this approach. In whole genome sequencing all genetic material is sequenced including the exons as well as the introns, the non-coding sequences. This approach theoretically can solve even more arRP patients, for instance through the identification of intronic pathologic mutations, which have been described in retinal degeneration.[82-85] Yet, the increasing number of DNA variants that will become available when employing these techniques poses a significant challenge to data interpretation.

Future perspectives of genetic testing in RP
The genetic and allelic heterogeneity and often nonspecific clinical appearance of RP complicates diagnostic genetic testing. Although APEX microarray analysis has been the most efficient diagnostic tool for RP for years, the introduction of NGS techniques in diagnostics have shown to be superior by identifying causative mutations in up to 40% of arRP cases.[10,17,39,76-78] However, NGS comes with its own difficulties, such as data management and analysis of the large data sets, and confirming pathogenicity of identified variants.[10,17,78] The latter is crucial since the large number of genes involved in arRP increases the risk of finding a pathogenic variant that is not causative, especially when considering that each person may be carrying ~1,500 variants in their coding sequence affecting protein function,[86] and, when considering retinal degeneration genes, clear-cut heterozygous pathogenic null mutations were reported in 1 out of 4 to 5 healthy controls that were analyzed with whole genome sequencing.[87] Furthermore, costs of data management and storage may rise with the use of whole genome sequencing and the development of 'third generation' technologies, due to massive data sets.[88] The sequencing costs in NGS have been high initially, but the expenses have diminished over the years, especially since this technique became commercially available. Currently, the costs of diagnostic NGS have reduced to levels just above those of the APEX microarray analysis. Therefore, we conclude NGS is by far more cost-effective and efficient than the microarray analysis in patients with arRP and should be the diagnostic genetic analysis of preference.

Table 7.4. Results of genetic analyses other than the microarray chip for autosomal recessive RP in this study cohort

Gene name	Method	N	Results	Molecular diagnosis
Multiple	Targeted NGS on 160 blindness genes	2	Heterozygous mutation in dominant gene	
			PRPF31 c.18G>C; p.Glu6Asp	PRPF31-associated dominant RP
			BEST c.682G>C; p	BEST-associated dominant RP
		9	Homozygous or compound heterozygous mutations	
			CNGB1 c.413-1G>A; splicing	CNGB1-associated recessive RP
			CRX c.205C>T; p.Arg69Cys	CRX-associated recessive RP
			EYS c.7919G>A; p.Trp2640*	EYS-associated recessive RP
			PDE6B c.2193+1G>A; splicing c.1923_1971delinsTCTGGGTA; p.Asn643fs	PDE6B-associated recessive RP
			PDE6B c.1189G>A; p.Gly397Arg c.1859A>G; p.His620Arg	PDE6B-associated recessive RP
			IMPG2 c.513T>G; p.Tyr171* c.2716C>T; p.Arg906*	IMPG2-associated recessive RP
			TTC8 c.1363C>A; p.Gln455Lys	TTC8-associated recessive RP
			PRCD c.2T>C; p.Met1? c.64C>T; p.Arg22*	PRCD-associated recessive RP
			USH2A c.6722C>T; p.Pro2241Leu c.13316C>T; p.Thr4439Ile	USH2A-associated recessive RP
		1	Hemizygous mutation in RPGR	
			RPGR c.485_486del; p.Phe162fs	RPGR-associated X-linked RP
		1	Heterozygous mutation in recessive gene	
			USH2A c.10510C>G; p.Pro3504Ala	N/A
		3	No mutations identified	N/A
	Autosomal dominant RP microarray (APEX)	2	Heterozygous mutation in dominant gene	
			PRPF31 c.553G>T; p.Glu185*	PRPF31-associated dominant RP
			GUCY2D c.2512C>T; p.Arg838Cys	GUCY2D-associated autosomal dominant cone-rod dystrophy
		11	No mutations identified	N/A
	LCA microarray (APEX)	4	No mutations identified	N/A
	BBS microarray (APEX)	3	No mutations identified	N/A
	Usher syndrome microarray (APEX)	4	No mutations identified	N/A

Gene name	Method	N	Results	Molecular diagnosis
ABCA4	Sanger sequencing	7	Homozygous or compound heterozygous mutations	
			ABCA4 c.5882G>A; p.Gly1961Glu c.3602T>G; p.Leu1201Arg c.6320G>A; p.Arg2107His c.5461-10T>C; splicing c.615del; p.Asn2052fs c.4469G>A; p.Cys1490Tyr c.5056G>A; p.Val1686Met c.6730-19G>A; splicing c.6658C>T; p.Gln2220* c.1622T>C; p.Leu541Pro c.3113C>T; p.Ala1038Val (both homozygously present)	ABCA4-associated recessive retinal dystrophy
		6	Heterozygous mutations	
			ABCA4 c.1411G>A; p.Glu471Lys (2x) c.3899G>A; p.Arg1300Gln c.4283C>T; p.Thr1428Met c.5882G>A; p.Gly1961Glu c.5908C>T; p.Leu1970Phe	Carrier of ABCA4 mutation
	Microarray (APEX)	50	No mutations identified	N/A
	Sanger sequencing	4	No mutation identified	N/A
BBS1	Sanger sequencing	1	Homozygous mutation BBS1 c.1169T>G; p.Met390Arg	BBS1-associated recessive RP
CHM	Sanger sequencing	1	Hemizygous mutation CHM c.50-?_116+?del; deletion of exon 2	Choroideremia
		2	No mutations identified	N/A
CNGA3	Sanger sequencing	1	No mutations identified	N/A
CNGB3	Sanger sequencing	3	No mutations identified	N/A
CRB1	Sanger sequencing	3	No mutations identified	N/A

Gene name	Method	N	Results	Molecular diagnosis
EYS	Sanger sequencing	1	Homozygous mutation EYS c.6714del; p.Ile2239fs	EYS-associated recessive RP
FAM161A	Sanger sequencing	1	Compound heterozygous mutations FAM161A c.1309A>T; p.Arg437* c.1501del; p.Cys501fs	FAM161A-associated recessive RP
KCNV2	Sanger sequencing	1	No mutations identified	N/A
MERTK	Sanger sequencing	1	Homozygous mutation MERTK c.1179dup; p.Leu394fs	MERTK-associated recessive RP
NR2E3	Sanger sequencing	1	Compound heterozygous mutations NR2E3 c.119-57_166del; frameshift c.1095C>G; splicing	NR2E3-associated recessive RP
PDE6A	Sanger sequencing	2	No mutations identified	N/A
PDE6C	Sanger sequencing	1	No mutations identified	N/A
PRPH2	Sanger sequencing	1	Heterozygous mutations PRPH2 c.424C>T; p.Arg142Trp	PRPH2-associated dominant RP
RHO	Sanger sequencing	1	Homozygous mutation RHO c.759G>T; p.Met253Ile	RHO-associated recessive RP
RP1	Sanger sequencing	1	Homozygous mutation RP1 c.686del; p.Pro229fs	RP1-associated recessive RP
RPE65	Sanger sequencing	1	Heterozygous mutation RPE65 c.11+5G>A; splicing	Carrier of RPE65 mutation
RPGR	Sanger sequencing	1	Hemizygous mutation RPGR c.2993_2996del; p.Glu998fs	RPGR-associated X-linked RP
TRPM1	Sanger sequencing	1	Compound heterozygous mutations TRPM1 c.1-27C>T; UTR 5'expressing defect c.2998C>T; p.Arg1000*	Congenital stationary night blindness type 1C

* indicates a premature stop; fs = frameshift; UTR = untranslated region

References

1. Hartong DT, Berson EL, Dryja TP. Retinitis pigmentosa. *Lancet*. 2006;368(9549):1795-809.
2. Berson EL. Retinitis pigmentosa. The Friedenwald Lecture. *Invest Ophthalmol Vis Sci*. 1993;34(5):1659-76.
3. Bunker CH, Berson EL, Bromley WC, Hayes RP, Roderick TH. Prevalence of retinitis pigmentosa in Maine. *Am J Ophthalmol*. 1984;97(3):357-65.
4. Rosenberg T. Epidemiology of hereditary ocular disorders. *Dev Ophthalmol*. 2003;37:16-33.
5. Schrier SA, Falk MJ. Mitochondrial disorders and the eye. *Curr Opin Ophthalmol*. 2011 Sep;22(5):325-31.
6. Kajiwara K, Berson EL, Dryja TP. Digenic retinitis pigmentosa due to mutations at the unlinked peripherin/RDS and ROM1 loci. *Science (80-)*. 1994;264(5165):1604-8.
7. Dryja TP, Hahn LB, Kajiwara K, Berson EL. Dominant and digenic mutations in the peripherin/RDS and ROM1 genes in retinitis pigmentosa. *Invest Ophthalmol Vis Sci*. 1997;38(10):1972-82.
8. Daiger SP, Sullivan LS, Bowne SJ. Genes and mutations causing retinitis pigmentosa. *Clin Genet*. 2013 Aug;84(2):132-41.
9. Wright AF, Chakarova CF, Abd El-Aziz MM, Bhattacharya SS. Photoreceptor degeneration: genetic and mechanistic dissection of a complex trait. *Nat Rev Genet*. 2010 Apr;11(4):273-84.
10. Glockle N, Kohl S, Mohr J, et al. Panel-based next generation sequencing as a reliable and efficient technique to detect mutations in unselected patients with retinal dystrophies. *Eur J Hum Genet*. 2014 Jan;22(1):99-104.
11. Yan D, Ouyang X, Patterson DM, Du LL, Jacobson SG, Liu XZ. Mutation analysis in the long isoform of USH2A in American patients with Usher Syndrome type II. *J Hum Genet*. 2009 Dec;54(12):732-8.
12. Hjortshoj TD, Gronskov K, Philp AR, et al. Bardet-Biedl syndrome in Denmark--report of 13 novel sequence variations in six genes. *Hum Mutat*. 2010 Apr;31(4):429-36.
13. Mandal MN, Heckenlively JR, Burch T, et al. Sequencing arrays for screening multiple genes associated with early-onset human retinal degenerations on a high-throughput platform. *Invest Ophthalmol Vis Sci*. 2005 Sep;46(9):3355-62.
14. Jaijo T, Aller E, Garcia-Garcia G, et al. Microarray-based mutation analysis of 183 Spanish families with Usher syndrome. *Invest Ophthalmol Vis Sci*. 2010 Mar;51(3):1311-7.
15. Zernant J, Kulm M, Dharmaraj S, et al. Genotyping microarray (disease chip) for Leber congenital amaurosis: detection of modifier alleles. *Invest Ophthalmol Vis Sci*. 2005 Sep;46(9):3052-9.
16. Klevering BJ, Yzer S, Rohrschneider K, et al. Microarray-based mutation analysis of the ABCA4 (ABCR) gene in autosomal recessive cone-rod dystrophy and retinitis pigmentosa. *Eur J Hum Genet*. 2004 Dec;12(12):1024-32.
17. Neveling K, Collin RW, Gilissen C, et al. Next-generation genetic testing for retinitis pigmentosa. *Hum Mutat*. 2012 Jun;33(6):963-72.
18. Neveling K, Feenstra I, Gilissen C, et al. A post-hoc comparison of the utility of sanger sequencing and exome sequencing for the diagnosis of heterogeneous diseases. *Hum Mutat*. 2013 Dec;34(12):1721-6.
19. Jaakson K, Zernant J, Kulm M, et al. Genotyping microarray (gene chip) for the ABCR (ABCA4) gene. *Hum Mutat*. 2003 Nov;22(5):395-403.
20. Yzer S, Leroy BP, De Baere E, et al. Microarray-based mutation detection and phenotypic characterization of patients with Leber congenital amaurosis. *Invest Ophthalmol Vis Sci*. 2006 Mar;47(3):1167-76.
21. Pereiro I, Hoskins BE, Marshall JD, et al. Arrayed primer extension technology simplifies mutation detection in Bardet-Biedl and Alstrom syndrome. *Eur J Hum Genet*. 2011 Apr;19(4):485-8.
22. Cremers FP, Kimberling WJ, Kulm M, et al. Development of a genotyping microarray for Usher syndrome. *J Med Genet*. 2007 Feb;44(2):153-60.
23. Koenekoop RK, Lopez I, den Hollander AI, Allikmets R, Cremers FP. Genetic testing for retinal dystrophies and dysfunctions: benefits, dilemmas and solutions. *Clin Experiment Ophthalmol*. 2007 Jul;35(5):473-85.
24. Marmor MF, Fulton AB, Holder GE, Miyake Y, Brigell M, Bach M. ISCEV Standard for full-field clinical electroretinography (2008 update). *Doc Ophthalmol*. 2009;118(1):69-77.
25. Avila-Fernandez A, Cantalapiedra D, Aller E, et al. Mutation analysis of 272 Spanish families affected by autosomal recessive retinitis pigmentosa using a genotyping microarray. *Mol Vis*. 2010;16:2550-8.

26. Cotton RG, Scriver CR. Proof of "disease causing" mutation. *Hum Mutat*. 1998;12(1):1-3.

27. Tuson M, Marfany G, Gonzalez-Duarte R. Mutation of CERKL, a novel human ceramide kinase gene, causes autosomal recessive retinitis pigmentosa (RP26). *Am J Hum Genet*. 2004 Jan;74(1):128-38.

28. Nishiguchi KM, Tearle RG, Liu YP, et al. Whole genome sequencing in patients with retinitis pigmentosa reveals pathogenic DNA structural changes and NEK2 as a new disease gene. *Proc Natl Acad Sci U S A*. 2013 Oct 1;110(40):16139-44.

29. Haider NB, Jacobson SG, Cideciyan AV, et al. Mutation of a nuclear receptor gene, NR2E3, causes enhanced S cone syndrome, a disorder of retinal cell fate. *Nat Genet*. 2000 Feb;24(2):127-31.

30. Fields RR, Zhou G, Huang D, et al. Usher syndrome type III: revised genomic structure of the USH3 gene and identification of novel mutations. *Am J Hum Genet*. 2002 Sep;71(3):607-17.

31. Paloma E, Martinez-Mir A, Garcia-Sandoval B, et al. Novel homozygous mutation in the alpha subunit of the rod cGMP gated channel (CNGA1) in two Spanish sibs affected with autosomal recessive retinitis pigmentosa. *J Med Genet*. 2002 Oct;39(10):E66.

32. Dryja TP, Finn JT, Peng YW, McGee TL, Berson EL, Yau KW. Mutations in the gene encoding the alpha subunit of the rod cGMP-gated channel in autosomal recessive retinitis pigmentosa. *Proc Natl Acad Sci U S A*. 1995 Oct 24;92(22):10177-81.

33. Corton M, Tatu SD, Avila-Fernandez A, et al. High frequency of CRB1 mutations as cause of Early-Onset Retinal Dystrophies in the Spanish population. *Orphanet J Rare Dis*. 2013;8:20.

34. Lotery AJ, Malik A, Shami SA, et al. CRB1 mutations may result in retinitis pigmentosa without para-arteriolar RPE preservation. *Ophthalmic Genet*. 2001 Sep;22(3):163-9.

35. Bernal S, Ayuso C, Antinolo G, et al. Mutations in USH2A in Spanish patients with autosomal recessive retinitis pigmentosa: high prevalence and phenotypic variation. *J Med Genet*. 2003 Jan;40(1):e8.

36. den Hollander AI, Davis J, van der Velde-Visser SD, et al. CRB1 mutation spectrum in inherited retinal dystrophies. *Hum Mutat*. 2004 Nov;24(5):355-69.

37. den Hollander AI, ten Brink JB, de Kok YJ, et al. Mutations in a human homologue of Drosophila crumbs cause retinitis pigmentosa (RP12). *Nat Genet*. 1999 Oct;23(2):217-21.

38. Vallespin E, Cantalapiedra D, Riveiro-Alvarez R, et al. Mutation screening of 299 Spanish families with retinal dystrophies by Leber congenital amaurosis genotyping microarray. *Invest Ophthalmol Vis Sci*. 2007 Dec;48(12):5653-61.

39. Wang X, Wang H, Sun V, et al. Comprehensive molecular diagnosis of 179 Leber congenital amaurosis and juvenile retinitis pigmentosa patients by targeted next generation sequencing. *J Med Genet*. 2013 Oct;50(10):674-88.

40. Collin RW, Littink KW, Klevering BJ, et al. Identification of a 2 Mb human ortholog of Drosophila eyes shut/spacemaker that is mutated in patients with retinitis pigmentosa. *Am J Hum Genet*. 2008 Nov;83(5):594-603.

41. Dryja TP, Rucinski DE, Chen SH, Berson EL. Frequency of mutations in the gene encoding the alpha subunit of rod cGMP-phosphodiesterase in autosomal recessive retinitis pigmentosa. *Invest Ophthalmol Vis Sci*. 1999 Jul;40(8):1859-65.

42. Tsang SH, Tsui I, Chou CL, et al. A novel mutation and phenotypes in phosphodiesterase 6 deficiency. *Am J Ophthalmol*. 2008 Nov;146(5):780-8.

43. Bocquet B, Marzouka NA, Hebrard M, et al. Homozygosity mapping in autosomal recessive retinitis pigmentosa families detects novel mutations. *Mol Vis*. 2013;19:2487-500.

44. Simpson DA, Clark GR, Alexander S, Silvestri G, Willoughby CE. Molecular diagnosis for heterogeneous genetic diseases with targeted high-throughput DNA sequencing applied to retinitis pigmentosa. *J Med Genet*. 2011 Mar;48(3):145-51.

45. Veske A, Orth U, Rüther K, et al. Mutations in the Gene for the B-Subunit of Rod Photoreceptor Cgmp-Specific Phosphodiesterase (PDEB) in Patients with Retinal Dystrophies and Dysfunctions. In: Anderson R, LaVail M, Hollyfield J, editors. Degenerative Diseases of the Retina: Springer US; 1995. p. 313-22.

46. Pras E, Abu A, Rotenstreich Y, et al. Cone-rod dystrophy and a frameshift mutation in the PROM1 gene. *Mol Vis*. 2009;15:1709-16.

47. Perrault I, Hanein S, Gerber S, et al. Retinal dehydrogenase 12 (RDH12) mutations in leber congenital amaurosis. *Am J Hum Genet*. 2004 Oct;75(4):639-46.

48. El Matri L, Ambresin A, Schorderet DF, et al. Phenotype of three consanguineous Tunisian families with early-onset retinal degeneration caused by an R91W homozygous mutation in the RPE65 gene. *Graefes Arch Clin Exp Ophthalmol.* 2006 Sep;244(9):1104-12.

49. Samardzija M, von Lintig J, Tanimoto N, et al. R91W mutation in Rpe65 leads to milder early-onset retinal dystrophy due to the generation of low levels of 11-cis-retinal. *Hum Mol Genet.* 2008 Jan 15;17(2):281-92.

50. Lotery AJ, Namperumalsamy P, Jacobson SG, et al. Mutation analysis of 3 genes in patients with Leber congenital amaurosis. *Arch Ophthal.* 2000 Apr;118(4):538-43.

51. Simovich MJ, Miller B, Ezzeldin H, et al. Four novel mutations in the RPE65 gene in patients with Leber congenital amaurosis. *Hum Mutat.* 2001 Aug;18(2):164.

52. Singh HP, Jalali S, Narayanan R, Kannabiran C. Genetic analysis of Indian families with autosomal recessive retinitis pigmentosa by homozygosity screening. *Invest Ophthalmol Vis Sci.* 2009 Sep;50(9):4065-71.

53. Le Guedard-Mereuze S, Vache C, Baux D, et al. Ex vivo splicing assays of mutations at noncanonical positions of splice sites in USHER genes. *Hum Mutat.* 2010 Mar;31(3):347-55.

54. van Wijk E, Pennings RJ, te Brinke H, et al. Identification of 51 novel exons of the Usher syndrome type 2A (USH2A) gene that encode multiple conserved functional domains and that are mutated in patients with Usher syndrome type II. *Am J Hum Genet.* 2004 Apr;74(4):738-44.

55. Seyedahmadi BJ, Rivolta C, Keene JA, Berson EL, Dryja TP. Comprehensive screening of the USH2A gene in Usher syndrome type II and non-syndromic recessive retinitis pigmentosa. *Exp Eye Res.* 2004 Aug;79(2):167-73.

56. Pennings RJ, Huygen PL, Orten DJ, et al. Evaluation of visual impairment in Usher syndrome 1b and Usher syndrome 2a. *Acta Ophthalmol Scand.* 2004 Apr;82(2):131-9.

57. Pennings RJ, Te Brinke H, Weston MD, et al. USH2A mutation analysis in 70 Dutch families with Usher syndrome type II. *Hum Mutat.* 2004 Aug;24(2):185.

58. Dreyer B, Brox V, Tranebjaerg L, et al. Spectrum of USH2A mutations in Scandinavian patients with Usher syndrome type II. *Hum Mutat.* 2008 Mar;29(3):451.

59. Weston MD, Eudy JD, Fujita S, et al. Genomic structure and identification of novel mutations in usherin, the gene responsible for Usher syndrome type IIa. *Am J Hum Genet.* 2000 Apr;66(4):1199-210.

60. Rivolta C, Sweklo EA, Berson EL, Dryja TP. Missense mutation in the USH2A gene: association with recessive retinitis pigmentosa without hearing loss. *Am J Hum Genet.* 2000 Jun;66(6):1975-8.

61. Rivolta C, Berson EL, Dryja TP. Paternal uniparental heterodisomy with partial isodisomy of chromosome 1 in a patient with retinitis pigmentosa without hearing loss and a missense mutation in the Usher syndrome type II gene USH2A. *Arch Ophthal.* 2002 Nov;120(11):1566-71.

62. Dreyer B, Tranebjaerg L, Rosenberg T, Weston MD, Kimberling WJ, Nilssen O. Identification of novel USH2A mutations: implications for the structure of USH2A protein. *Eur J Hum Genet.* 2000 Jul;8(7):500-6.

63. Clark GR, Crowe P, Muszynska D, et al. Development of a diagnostic genetic test for simplex and autosomal recessive retinitis pigmentosa. *Ophthalmology.* 2010 Nov;117(11):2169-77 e3.

64. McGee TL, Seyedahmadi BJ, Sweeney MO, Dryja TP, Berson EL. Novel mutations in the long isoform of the USH2A gene in patients with Usher syndrome type II or non-syndromic retinitis pigmentosa. *J Med Genet.* 2010 Jul;47(7):499-506.

65. Aller E, Larrieu L, Jaijo T, et al. The USH2A c.2299delG mutation: dating its common origin in a Southern European population. *Eur J Hum Genet.* 2010 Jul;18(7):788-93.

66. Bernal S, Meda C, Solans T, et al. Clinical and genetic studies in Spanish patients with Usher syndrome type II: description of new mutations and evidence for a lack of genotype--phenotype correlation. *Clin Genet.* 2005 Sep;68(3):204-14.

67. Vozzi D, Aaspollu A, Athanasakis E, et al. Molecular epidemiology of Usher syndrome in Italy. *Mol Vis.* 2011;17:1662-8.

68. Leijendeckers JM, Pennings RJ, Snik AF, Bosman AJ, Cremers CW. Audiometric characteristics of USH2a patients. *Audiol Neurootol.* 2009;14(4):223-31.

69. Herrera W, Aleman TS, Cideciyan AV, et al. Retinal disease in Usher syndrome III caused by mutations in the clarin-1 gene. *Invest Ophthalmol Vis Sci.* 2008 Jun;49(6):2651-60.

70. Baux D, Larrieu L, Blanchet C, et al. Molecular and in silico analyses of the full-length isoform of usherin identify new pathogenic alleles in Usher type II patients. *Hum Mutat.* 2007 Aug;28(8):781-9.

71. Besnard T, Garcia-Garcia G, Baux D, et al. Experience of targeted Usher exome sequencing as a clinical test. *Molecular genetics & genomic medicine*. 2014 Jan;2(1):30-43.

72. Le Quesne Stabej P, Saihan Z, Rangesh N, et al. Comprehensive sequence analysis of nine Usher syndrome genes in the UK National Collaborative Usher Study. *J Med Genet*. 2012 Jan;49(1):27-36.

73. Branham K, Othman M, Brumm M, et al. Mutations in RPGR and RP2 account for 15% of males with simplex retinal degenerative disease. *Invest Ophthalmol Vis Sci*. 2012 Dec;53(13):8232-7.

74. Sohocki MM, Daiger SP, Bowne SJ, et al. Prevalence of mutations causing retinitis pigmentosa and other inherited retinopathies. *Hum Mutat*. 2001;17(1):42-51.

75. Berger W, Kloeckener-Gruissem B, Neidhardt J. The molecular basis of human retinal and vitreoretinal diseases. *Prog Retin Eye Res*. 2010 Sep;29(5):335-75.

76. Chen X, Zhao K, Sheng X, et al. Targeted sequencing of 179 genes associated with hereditary retinal dystrophies and 10 candidate genes identifies novel and known mutations in patients with various retinal diseases. *Invest Ophthalmol Vis Sci*. 2013 Mar;54(3):2186-97.

77. Fu Q, Wang F, Wang H, et al. Next-generation sequencing-based molecular diagnosis of a Chinese patient cohort with autosomal recessive retinitis pigmentosa. *Invest Ophthalmol Vis Sci*. 2013 Jun;54(6):4158-66.

78. Shanks ME, Downes SM, Copley RR, et al. Next-generation sequencing (NGS) as a diagnostic tool for retinal degeneration reveals a much higher detection rate in early-onset disease. *Eur J Hum Genet*. 2013 Mar;21(3):274-80.

79. Xu Y, Guan L, Shen T, et al. Mutations of 60 known causative genes in 157 families with retinitis pigmentosa based on exome sequencing. *Hum Genet*. 2014 Oct;133(10):1255-71.

80. Zhao L, Wang F, Wang H, et al. Next-generation sequencing-based molecular diagnosis of 82 retinitis pigmentosa probands from Northern Ireland. *Hum Genet*. 2015 Feb;134(2):217-30.

81. Wang J, Zhang VW, Feng Y, et al. Dependable and efficient clinical utility of target capture-based deep sequencing in molecular diagnosis of retinitis pigmentosa. *Invest Ophthalmol Vis Sci*. 2014 Oct;55(10):6213-23.

82. Steele-Stallard HB, Le Quesne Stabej P, Lenassi E, et al. Screening for duplications, deletions and a common intronic mutation detects 35% of second mutations in patients with USH2A monoallelic mutations on Sanger sequencing. *Orphanet J Rare Dis*. 2013;8:122.

83. Braun TA, Mullins RF, Wagner AH, et al. Non-exomic and synonymous variants in ABCA4 are an important cause of Stargardt disease. *Hum Mol Genet*. 2013 Dec 20;22(25):5136-45.

84. Webb TR, Parfitt DA, Gardner JC, et al. Deep intronic mutation in OFD1, identified by targeted genomic next-generation sequencing, causes a severe form of X-linked retinitis pigmentosa (RP23). *Hum Mol Genet*. 2012 Aug 15;21(16):3647-54.

85. Pomares E, Riera M, Castro-Navarro J, Andres-Gutierrez A, Gonzalez-Duarte R, Marfany G. Identification of an intronic single-point mutation in RP2 as the cause of semidominant X-linked retinitis pigmentosa. *Invest Ophthalmol Vis Sci*. 2009 Nov;50(11):5107-14.

86. Ng PC, Levy S, Huang J, et al. Genetic variation in an individual human exome. *PLoS Genet*. 2008;4(8):e1000160.

87. Nishiguchi KM, Rivolta C. Genes associated with retinitis pigmentosa and allied diseases are frequently mutated in the general population. *PLoS One*. 2012;7(7):e41902.

88. Schadt EE, Turner S, Kasarskis A. A window into third-generation sequencing. *Hum Mol Genet*. 2010 Oct 15;19(R2):R227-40.

Authors

Stanley Lambertus, M.D.[1]; Ramon A.C. van Huet, M.D.[1]; Nathalie M. Bax, M.D.[1]; Lies H. Hoefsloot, Ph.D.[2]; Frans P.M. Cremers, Ph.D.[2,3]; Camiel J.F. Boon, M.D., Ph.D.[1,4]; B. Jeroen Klevering, M.D., Ph.D.[1]; Carel B. Hoyng, M.D., Ph.D.[1]

Affiliations

[1]Department of Ophthalmology, Radboud university medical center, Nijmegen, The Netherlands
[2]Department of Human Genetics, Radboud university medical center, Nijmegen, The Netherlands
[3]Radboud Institute for Molecular Life Sciences, Radboud University Medical Center, Nijmegen, The Netherlands
[4]Department of Ophthalmology, Leiden University Medical Center, Leiden, The Netherlands

Early-onset Stargardt disease: phenotypic and genotypic characteristics

8

Abstract

Objective. To describe the phenotype and genotype of patients with early-onset Stargardt disease.

Design. Retrospective cohort study.

Participants. Fifty-one Stargardt patients with age at onset ≤10 years.

Methods. We reviewed patient medical records for age at onset, medical history, initial symptoms, best-corrected visual acuity (BCVA), ophthalmoscopy, fundus photography, fundus autofluorescence (FAF), fluorescein angiography (FA), spectral-domain optical coherence tomography (SD-OCT), and full-field electroretinography (ffERG). The *ABCA4* gene was screened for mutations.

Main outcome measures. Age at onset, BCVA, fundus appearance, FAF, FA, SD-OCT, ffERG, and presence of *ABCA4* mutations.

Results. The mean age at onset was 7.2 years (range: 1–10 years). The median times to develop BCVA of 20/32, 20/80, 20/200 and 20/500 were 3, 5, 12, and 23 years, respectively. Initial ophthalmoscopy in 41 patients revealed either no abnormalities or foveal RPE changes in 10 and 9 patients, respectively; the other 22 patients had foveal atrophy, atrophic RPE lesions, and/or irregular yellow-white fundus flecks. FA revealed a "dark choroid" in 21 out of 29 patients. In 14 out of 50 patients, foveal atrophy occurred before flecks developed. FAF showed centrifugal expansion of disseminated atrophic spots, which progressed to the eventual profound chorioretinal atrophy. SD-OCT revealed early photoreceptor damage followed by atrophy of the outer retina, RPE, and choroid. On ffERG in 26 patients, 15 had normal amplitudes, and 11 had reduced photopic and/or scotopic amplitudes at their first visit. We found no correlation between ffERG abnormalities and the rate of vision loss. Thirteen out of 25 patients had progressive ffERG abnormalities. Finally, genetic screening of 44 patients revealed ≥2 *ABCA4* mutations in 37 patients and single heterozygous mutations in 7 patients.

Conclusions. In early-onset Stargardt, ophthalmoscopy can reveal no abnormalities or minor retinal abnormalities in early disease. Yellow-white flecks can be preceded by foveal atrophy and may be visible only on FAF. Although ffERG is insufficient for predicting the rate of vision loss, abnormalities can develop. Over time, visual acuity declines rapidly in parallel with progressive retinal degeneration, resulting in profound chorioretinal atrophy. Thus, early-onset Stargardt lies at the severe end of the spectrum of *ABCA4*-associated retinal phenotypes.

Introduction

Stargardt disease (STGD1) is the most prevalent inherited juvenile-onset retinal dystrophy, with a mean age at onset of 15.2 years.[1, 2] The inheritance pattern of STGD1 is autosomal recessive, and the disease is characterized by the presence of irregular yellow-white fundus flecks in the posterior pole.[2-4] Over time, the disease progresses to include macular depigmentation and chorioretinal atrophy. Typical STGD1 patients have normal—or near-normal—panretinal cone and rod function on full-field electroretinography (ffERG); however, progressive abnormalities in photopic and scotopic amplitudes have been reported.[5-7] Blockage of choroidal fluorescence (the so-called "dark choroid" sign) on fluorescein angiography (FA) is present in 80% of STGD1 patients.[8-10] The aforementioned yellow-white fundus flecks are hyperautofluorescent on fundus autofluorescence (FAF), presumably due to an accumulation of lipofuscin fluorophores in the retinal pigment epithelium (RPE).[11, 12] Spectral-domain optical coherence tomography (SD-OCT) can reveal changes in the outer nuclear layer, as well as photoreceptor loss, RPE abnormalities, and a general thinning of the retina.[13]

Mutations in the *ABCA4* gene have been associated with a spectrum of retinal diseases ranging from mild phenotypes (for example, late-onset STGD1 with relatively preserved visual function) to severe, early-onset retinitis pigmentosa accompanied by a rapid loss of central and peripheral photoreceptors.[14-16] The *ABCA4* gene encodes the retina-specific ATP-binding cassette transporter (ABCR).[17] *ABCA4* is expressed in both cones and rods. In rod cells, the ABCR protein is localized at the rim of the outer segment discs, where ABCR transports all-*trans*-retinal from the lumen of the outer segment disc to the cytoplasm of the photoreceptor cell.[18] The accumulation of all-*trans*-retinal—and its toxic derivatives—eventually results in the death of RPE cells and photoreceptor cells.[19-21] The *ABCA4* gene has high mutation heterogeneity; more than 700 distinct mutations have been identified to date, with a wide range of effects on ABCR protein function. A model to correlate the phenotype with the functional severity of the *ABCA4* mutation has been proposed.[22, 23] According to this model, STGD1 results from mild to moderate ABCR impairment.

Among patients who are diagnosed with STGD1, the disease has remarkably wide clinical variability with respect to the general course of the disease, the retinal features, and the electrophysiological findings.[5, 8, 14, 15] STGD1 has both genetic and clinical overlap with cone-rod dystrophy, and this may cause confusion among general ophthalmologists; indeed, diagnosing STGD1 can be challenging at an early age. Therefore, obtaining an accurate description of the full spectrum of *ABCA4*-associated retinal dystrophies—including STGD1—is essential for providing appropriate patient counseling and adequate disease management, and may have important implications for selecting patients to participate in gene therapy trials. Although clinical features of STGD1 patients with a very young onset have been described in heterogeneous cohorts,[5, 7, 24, 25] there is lack of studies concerning the natural history of these patients. Here, we provide the first comprehensive description of the initial and longitudinal clinical and genetic characteristics of a large number of patients with early-onset Stargardt, which we defined as an age at onset ≤10 years.

Methods

Patients and genetic analysis

The database of the Department of Ophthalmology at Radboud university medical center (Nijmegen, the Netherlands) contains 426 patients with a clinical diagnosis of STGD1. For 258 of these patients, the *ABCA4* gene was analyzed by the Department of Human Genetics at Radboud university medical center (Nijmegen, the Netherlands). Known mutations were screened using the arrayed-primer extension (APEX) microarray (Asper Biotech, Tartu, Estonia), and exon duplications and/or deletions were detected using multiplex ligation-dependent probe amplification (MLPA, MRC-Holland P151/P152). If no mutations or only a single heterozygous mutation was identified, the exons and intron-exon boundaries were sequenced using the Sanger method to screen for mutations in the other allele. All identified mutations were confirmed using Sanger sequencing. In total, 199 patients contained ≥1 mutation in the *ABCA4* gene. Age at onset of disease was defined as the age at which symptoms were first noticed by the patient. If this information was not available, we used the patient's age at which he/she first visited an ophthalmologist.

In this study, we included 51 patients with an age at onset ≤10 years and one of the following criteria: at least two *ABCA4* mutations (n=37); one *ABCA4* mutation and the presence of yellow-white flecks (n=7); or in absence of *ABCA4* analysis, the presence of yellow-white flecks and either a dark choroid or an atrophic macular lesion (n=7).

This study was approved by the Institutional Ethics Committee and was performed in accordance with the Declaration of Helsinki. All patients provided informed consent prior to giving a blood sample and receiving additional ophthalmologic examinations.

Clinical evaluation

We defined the duration of disease as the time interval between the patient's age at onset (defined as described above) and the age at the last visit. Best-corrected visual acuity (BCVA) was measured using a Snellen chart, then transformed into the logarithm of the minimal angle of resolution (logMAR) for subsequent analysis. A logMAR value of 1.9, 2.3, or 2.7 was assigned to the patient's ability to count fingers, detect hand movements, or perceive light, respectively.[26] Fundus characteristics were documented for 41 patients using fundus photography (Topcon TRC-50IX, Topcon Corporation, Tokyo, Japan). FAF was performed in 32 patients using a confocal scanning laser ophthalmoscope (cSLO; Spectralis, Heidelberg Engineering, Heidelberg, Germany) fitted with an optically pumped solid-state laser (488-nm excitation). Atrophic chorioretinal lesions outside the fovea were stratified into the following two groups: 1) a patchy pattern consisting of mild disseminated hypoautofluorescent spots; and 2) sharply demarcated chorioretinal atrophic lesions with an absence of autofluorescence; the extent of these lesions was then classified as either 1) lesions that were limited to the posterior pole, or 2) lesions that extended beyond the vascular arcades. Cross-sectional images were obtained for 30 patients using SD-OCT (Spectralis, Heidelberg Engineering, Heidelberg, Germany). FA (Topcon TRC-50IX, Topcon Corporation, Tokyo, Japan; Spectralis, Heidelberg Engineering) was performed in 32 patients in order to determine the presence or absence of the "dark choroid" sign. FfERG was performed in 43 patients in accordance with the guidelines established by the International Society

for Clinical Electrophysiology of Vision (ISCEV)[27] using either Dawson-Trick-Litzkow (DTL) electrodes or contact lens (CL) electrodes together with the RETI-port system (Roland Consults, Stasche & Finger GmbH, Brandenburg an der Havel, Germany). DTL and CL electrodes have similarly high signal stability.[28] Based on the ffERG results, the patients were assigned to three groups as described previously[5]: group 1 consisted of patients with normal ffERG amplitudes; group 2 consisted of patients with reduced photopic amplitude (<5% of normal range: <78 µV [B-wave]) and normal scotopic amplitude; and group three consisted of patients with reduced photopic and scotopic amplitudes (<5% of normal range: <263 µV [B-wave]).

Statistical analysis
Data were analyzed using SPSS Statistics version 20.0 (IBM Corp., Armonk, NY). Kaplan-Meier "survival" curves were used to analyze the interval between the age at onset and the age at which the following endpoints were achieved: mild visual impairment (≥0.2 logMAR, Snellen ≤20/32), moderate visual impairment (≥0.6 logMAR, Snellen ≤20/80), severe visual impairment (≥1.0 logMAR, Snellen ≤20/200), and blindness (≥1.4 logMAR, Snellen ≤20/500).[29] Cox regression analysis was used to compare the ffERG groups. Differences with a P-value ≤0.05 were considered statistically significant.

Table 8.1. Summary of clinical and genetic characteristics of 51 early-onset Stargardt patients.

| Patient | Age at onset (y) | Age (y)[a] | BCVA (logMAR (Snellen))[a] | Fundus findings | | ffERG[a,b] | | Mutations | |
				Flecks	Dark choroid	Photopic	Scotopic	Allele 1	Allele 2
1	7[c]	18	0.30 (20/40)	Yes	Yes	NP	NP	c.2588G>C, c.656G>C, c.1822T>A	
2	8	14	0.89 (20/155)	Yes	NP	NP	NP	c.5461-10T>C	c.5461-10T>C
3	6	17	1.90 (CF)	Yes	Yes	N	MR	c.5461-10T>C	c.5461-10T>C
4	6	8	0.20 (20/32)	Yes	Yes	MR	N	c.2947A>G	c.5461-10T>C
5	6	57	2.30 (HM)	Yes	Yes	ND	ND	c.768G>T	c.443-?_570+?del
6	9	10	0.40 (20/50)	Yes	Yes	SR	N	c.768G>T	NI
7	6	40	1.30 (20/400)	Yes	NP	NP	NP	c.5461-10T>C	c.5714+5G>A
8	4	35	1.90 (CF)	Yes	Yes	MR	N	c.4462T>C	c.2919-?_3328+?del
9	9	25	1.90 (CF)	Yes	Yes	NP	NP	c.768G>T	NI
10	3	36	1.90 (CF)	Yes	Yes	SR	SR	c.3813G>C	NI
11	5	52	2.30 (HM)	Yes	NP	MR	MR	c.6411T>A	NI
12	7	8	1.22 (20/333)	Yes	Yes	MR	MR	c.768G>T	c.5461-10T>C
13	7	7	0.33 (20/43)	Yes	Yes	MR	MR	NP	
14	9	17	1.15 (20/286)	Yes	No	N	N	c.3874C>T	c.6543_6578del

Patient	Age at onset (y)	Age (y)[a]	BCVA (logMAR (Snellen))[a]	Fundus findings		ffERG[a,b]		Mutations	
				Flecks	*Dark choroid*	*Photopic*	*Scotopic*	*Allele 1*	*Allele 2*
15	3	14	1.00 (20/200)	Yes	NP	N	N	c.4539+1G>T	c.768G>T
16	9	11	1.10 (20/250)	Yes	No	MR	N	NP	
17	10	47	1.90 (CF)	Yes	Yes	SR	SR	NP	
18	7	48	2.30 (HM)	Yes	NP	SR	SR	c.768G>T	c.5461-10T>C
19	6	43	1.90 (CF)	Yes	NP	SR	SR	c.768G>T	c.5461-10T>C
20	8	33	1.10 (20/250)	Yes	No	N	N	c.5161-5162delAC	c.5882G>A
21	8	64	1.90 (CF)	Yes	NP	ND	ND	c.2947A>G	c.4506C>A
22	8	31	1.90 (CF)	Yes	NP	SR	SR	NP	
23	9	51	1.90 (CF)	Yes	Yes	ND	ND	c.768G>T	c.5461-10T>C
24	3	19	1.00 (20/200)	Yes	No	ND	N	c.5461-10T>C	c.6320G>A
25	9	16	1.30 (20/400)	Yes	NP	MR	N	c.214G>A	c.5461-10T>C
26	5	10	1.10 (20/250)	Yes	NP	NP	NP	c.5762_5763dup	c.2919-?_3328+?del
27	10	31	0.40 (20/50)	NP[(d)]	NP[(d)]	NP	NP	c.455G>A	c.5461-10T>C
28	9	19	0.72 (20/105)	Yes	NP	N	N	c.5461-10T>C	NI
29	1	28	1.90 (CF)	Yes	Yes	SR	N	c.5585-10T>C	NI
30	8	26	1.30 (20/400)	Yes	Yes	N	N	c.5312+1G>A	c.286A>G
31	10	22	1.90 (CF)	Yes	Yes	SR	N	c.2588G>C	c.4539+1G>T
32	9	15	0.80 (20/125)	Yes	Yes	NP	NP	c.2588G>C	c.4539+1G>T
33	7	18	1.15 (20/286)	Yes	NP	N	N	c.1957C>T, c.6320G>A, c.3449G>A	
34	10	31	1.15 (20/286)	Yes	Yes	N	N	c.5461-10T>C	c.5537T>C
35	7	11	0.80 (20/125)	Yes	NP	N	N	c.818G>A	NI
36	7	7	0.80 (20/125)	No	Yes	N	N	c.872C>T;4224G>T	c.2947A<G
37	8	22	1.15 (20/286)	Yes	NP	N	N	c.1822T>A	c.5882G>A
38	10	13	0.52 (20/67)	No	No	N	N	c.5882G>A	c.5882G>A
39	10	16	1.15 (20/286)	Yes	No	N	N	c.768G>T	c.1822T>A
40	5	24	1.30 (20/400)	Yes	Yes	MR	MR	c.768G>T	c.5461-10T>C
41	6	22	1.90 (CF)	Yes	Yes	ND	ND	c.1622T>C;3113C>T	c.1622T>C;3113C>T
42	10	22	1.30 (20/400)	Yes	Yes	MR	N	NP	
43	7	19	1.10 (20/250)	Yes	NP	N	N	NP	
44	8	19	1.00 (20/200)	Yes	NP	SR	N	NP	
45	5	15	1.00 (20/200)	Yes	Yes	MR	N	c.3335C>A	c.5461-10T>C

Patient	Age at onset (y)	Age (y)[a]	BCVA (logMAR (Snellen))[a]	Fundus findings		ffERG[a,b]		Mutations	
				Flecks	Dark choroid	Photopic	Scotopic	Allele 1	Allele 2
46	7	31	2.30 (HM)	Yes	No	ND	MR	c.1822T>A	c.5461-10T>C
47	9	20	0.85 (20/143)	Yes	NP	N	N	c.122G>A	c.286A>G
48	4	32	1.00 (20/200)	Yes	NP	NP	NP	c.5882G>A	NI
49	8	18	1.00 (20/200)	Yes	No	SR	ND	c.286A>G	c.286A>G
50	9	14	0.80 (20/125)	No	No	ND	SR	c.4773+1G>A	c.5461-10T>C
51	8	43	1.90 (CF)	Yes	No	ND	ND	c.768G>T	c.5113C>T

[a] Age, BCVA and ffERG at last examination.
[b] The abbreviations reflect the B-wave amplitude: N, normal (equal to or above the lower 5% of the range for a normal population: photopic ≥78 µV, scotopic ≥263 µV); MR, moderately reduced (1-5% or normal range: photopic ≥69 µV and <78 µV, scotopic ≥ 195 µV and <263 µV); SR, severely reduced (<1% of normal range: photopic <69 µV, scotopic <195 µV; ND, not detectable (flat amplitudes).
[c] Mean age at onset of the total cohort is used. dIn the patient's medical records fundus findings were described conform STGD1, but no detailed description or imaging was made and thus excluded from imaging analysis. Del, deletion; dup, duplication; NI, not identified; NP, not performed; y, years; CF, counting fingers; HM, hand movements.

Results

Results I: Initial clinical characteristics

A total of 51 patients (28 men and 23 women) were included in this study. The mean (±standard deviation) age at onset was 7.2 (±2.2) years (median: 8 years; range: 1-10 years).

Visual acuity. In each case, the initial symptom of the disease was a decline in visual acuity that was noticed by the patient, the patient's parents, or the school physician. Where available (n=41 patients), the mean BCVA at the first visit to an ophthalmologist was 0.51 (±0.36) logMAR (median: 0.48; range: 0-1.15), Snellen 20/65. In 13 patients, the vision loss was initially unexplained. Six of these 13 patients were diagnosed with functional vision loss, and six other patients were diagnosed initially with cone-rod dystrophy. Twenty-two of the 51 patients were diagnosed with STGD1 ≥3 years (range: 3-30 years) after the initial symptoms appeared.

Retinal features. Ophthalmoscopy performed at the first visit revealed no retinal abnormalities in 10 out of 41 patients. Nine additional patients had foveal RPE changes, and the remaining 22 patients had foveal atrophy, atrophic RPE lesions that were not limited to the fovea, and/or irregular yellow-white fundus flecks. FA in 29 patients revealed an absence of choroidal fluorescence (the so-called "dark choroid") in 21 patients. In patient 4, FAF revealed subtle hyperautofluorescence of the fovea, and SD-OCT revealed thickening of what appeared to be the external limiting membrane (Figure 8.1A$_{1,2,3}$). One year later, this patient developed several small parafoveal hyperautofluorescent flecks with no apparent abnormalities on ophthalmoscopy (Figure 8.1B$_2$).
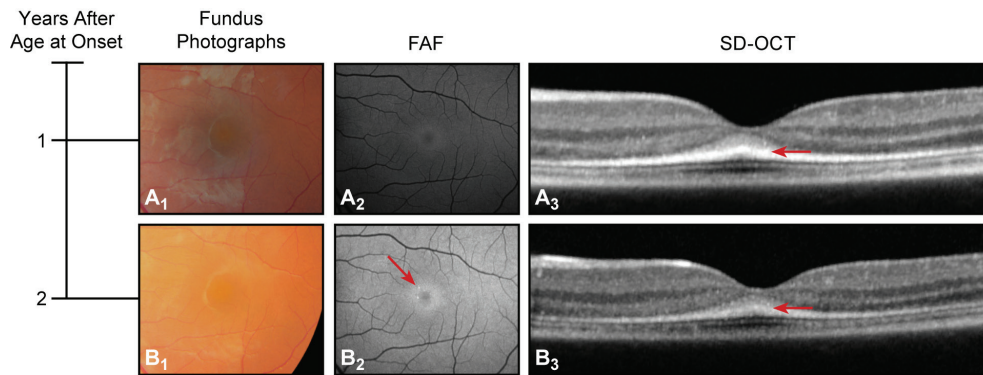
Figure 8.1. Kaplan-Meier curves showing the cumulative fraction in early-onset Stargardt with the following clinical endpoints: mild visual impairment (≥0.2 logMAR, Snellen ≤20/32, triangle), moderate visual impairment (≥0.6 logMAR, Snellen ≤20/80, square), severe visual impairment (≥1.0 logMAR, Snellen ≤20/200, circle), and blindness (≥1.4 logMAR, Snellen ≤20/500, star). Censored observations are depicted as vertical bars.

Electrophysiologic findings. At their first visit, ffERG data was collected for 26 patients, and the patients were classified based on their findings. Group 1 (patients with normal photopic and scotopic amplitudes) contained 15 patients (58%), group 2 (patients with reduced photopic amplitude and normal scotopic amplitudes) contained 4 patients (15%), and group 3 (patients with reduced photopic and scotopic amplitudes) contained 6 patients (23%). One patient could not be classified into one of these three groups because only the scotopic amplitudes were reduced moderately, although no pigmentary retinopathy was observed. We found no significant correlation between the ffERG group classification at the first visit and progression towards mild visual impairment (p=0.485), moderate visual impairment (p=0.309), severe visual impairment (p=0.203), or blindness (p=0.647).

Results II: Natural course
The mean disease duration was 17.1 (±14.5) years (median: 11 years; range: 0-56 years). The follow-up period ranged from a single examination in three patients to 47 years (mean: 12.4±12.6; median: 9 years). The clinical and genetic characteristics of the patient cohort at the last examination are summarized in Table 8.1.

Visual acuity. A survival analysis yielded a median interval and 95% confidence interval (CI) between age at onset and a decline in BCVA to mild visual impairment, moderate visual impairment, severe visual impairment, and blindness of 3 (95% CI: 1.1-4.9), 5 (95% CI: 2.2-7.8), 12 (95% CI: 9.3-14.7), and 23 (95% CI: 13.2-32.8) years, respectively (Figure 8.2). Mean patient age at the last recorded visit was 24.9 (±14.0) years (median: 20 years; range: 7-64 years), and mean BCVA was 1.29 (±0.58) logMAR (median: 1.15; range: 0.20-2.30), Snellen 20/386.
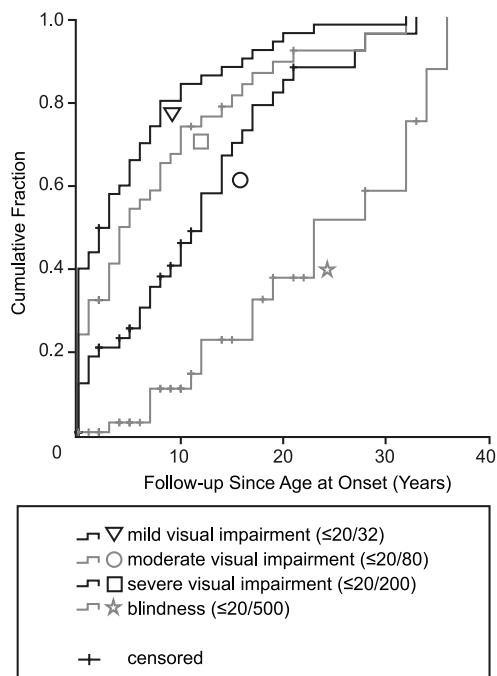
Figure 8.2. Retinal imaging of patient 4 (age at onset: 6 years; BCVA: 0.24 logMAR, Snellen 20/35; ABCA4 genotype: p.Thr983Ala and c.5461-10T>C (p.?)) at 7 (A1,2,3) and 8 (B1,2,3) years of age. Initially, only subtle foveal hyperautofluorescence was present (A2); one year later, small parafoveal hyperautofluorescent flecks were present (the arrow in B2), despite a lack of apparent abnormalities on ophthalmoscopy. SD-OCT revealed foveal thickening of the band representing the external limiting membrane (the arrows in A3-B3).

Retinal features. We observed irregular yellow-white fundus flecks in 47 out of 50 patients. These flecks were not always evident at the first examination, but they developed within an average of 2.9 (±4.1) years (median: 0 years; range: 0-17 years) of the first visit. The location of these flecks varied among the patients: in 10 patients, the flecks were present exclusively in the central macula; in 17 patients, the flecks were scattered throughout the posterior pole, but did not extend beyond the vascular arcades; finally, the remaining 20 patients presented with a fundus flavimaculatus pattern with numerous flecks in the central and mid-peripheral retina. Foveal atrophy was reported in 38 patients and occurred within 1.9 (±3.3) years (median: 0 years; range: 0-13 years) of the initial visit. Finally, 14 patients developed foveal atrophy before the appearance of fundus flecks (Figure 8.3A$_{1,2}$).

Long-term follow-up data revealed that the initial foveal atrophy progressed to more widespread chorioretinal atrophy. Over time, FAF imaging revealed centrifugal expansion of disseminated spots in 30 out of 32 patients with a mean timeframe of 9.8 (±10.5) years (median: 8 years; range: 0-40 years) (Figure 8.4B$_2$). These spots extended beyond the vascular arcades in 24 of these 30 patients with a mean of 11.2 (±11.0) years (median: 9.5 years; range: 0-40 years) following the first visit (Figure 8.4C$_2$). In 22 out of 32 patients, the spots progressed to chorioretinal atrophic lesions after a mean period of 13.5 (±12.3) years (median: 10.5 years; range: 0-40 years) (Figure 8.4C$_2$-D$_2$). In 11 of these 22 patients, the confluence of these lesions extended beyond the vascular arcades after a mean period of 23.0 (±10.3) years (median: 23 years; range: 5-40 years) (Figure 8.4E$_2$). These 11 patients who presented with the common phenotype of chorioretinal lesions beyond the vascular arcades at the final examination initially presented with flecks (n=3), foveal atrophy (n=4), or both flecks and atrophy (*n*=4) at their first examination.

Over time, SD-OCT showed thinning of the outer nuclear layer and loss of the ellipsoid zone, which preceded loss of the RPE/Bruch's membrane complex. In addition, hyperreflective abnormalities in the outer retina were present (Figure 8.4A$_3$). Progression occurred as an expanding loss of the outer nuclear layer, ellipsoid zone, RPE, and choriocapillaris
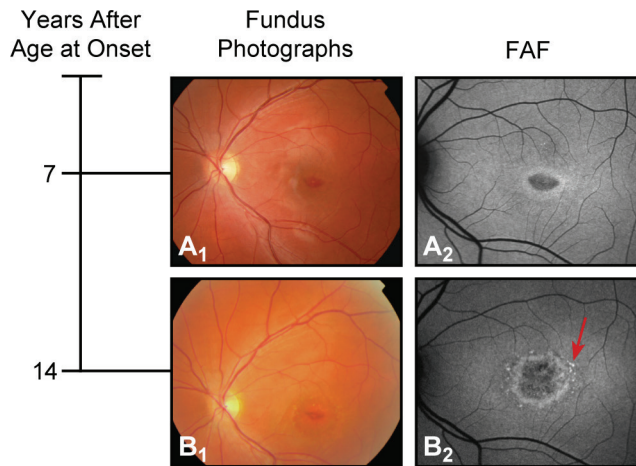
Figure 8.3. Fundus photographs and autofluorescence imaging of patient 37 (age at onset: 8 years; *ABCA4* genotype: p.Phe608Ile and p.Gly1961Glu) at 15 ($A_{1,2}$) and 22 years ($B_{1,2}$) of age, showing isolated foveal pigment alterations and a hypoautofluorescent lesion (BCVA 0.52 logMAR, Snellen 20/66). Seven years later ($B_{1,2}$), yellow-white parafoveal fundus flecks (the arrow in B_2) developed (BCVA 1.15 logMAR, Snellen 20/283).

(Figure 8.4B-E_3). Hyperreflective deposits in the inner layers of the fovea developed, corresponding to intraretinal pigmentations on fundus photography (Figure 8.4C_1-C_3).

Electrophysiologic findings. Follow-up data for 25 patients showed that four patients progressed from ffERG group 1 to group 2 within a mean of 10.5 (±4.4) years (range: 7-16 years), and nine patients progressed from group 1 to group 3 within a mean of 27.7 (±14.4) years (range: 3-47 years).

Results III: Mutation analysis

The *ABCA4* gene was screened for mutations in 44 of the 51 patients; the remaining seven patients refused genetic analysis for personal reasons. In these 44 patients, mutations in the *ABCA4* gene were identified in 81 of the 88 alleles (92%). Thirty-three of these patients had two *ABCA4* mutations, seven patients had one mutation, three patients had three mutations, and one patient had four mutations. In total, 37 distinct mutations were identified; these mutations are summarized in Table 8.2. The c.768G>T mutation was identified in 25% of the 44 patients and accounted for 13% of all identified mutations. The c.5461-10T>C mutation was identified in 36% of the patients and accounted for 22% of all identified mutations. The most prevalent *ABCA4* mutation among Dutch patients with STGD1 (c.2588G>C)[23] was identified in only 4% of the alleles. Table 8.3 summarizes the non-missense mutations that were identified in this study.

Table 8.2. *ABCA4* mutations in early-onset Stargardt patients.

Mutation	Effect	Allele		References
		Frequency	Percentage	
c.122G>A	p.Trp41*	1	1%	35
c.214G>A	p.Gly72Arg	1	1%	32
c.286A>G	p.Asn96Asp	4	5%	36
c.443-?_570+?del	p.Arg149fs	1	1%	This study
c.455G>A	p.Arg152Gln	1	1%	32, 37
c.656G>C	p.Arg219Thr	1	1%	38
c.768G>T	p.Val256Val/p.?	11	13%	16, 23, 32, 39
c.818G>A	p.Trp273*	1	1%	This study
c.872C>T	p.Pro291Leu	1	1%	34
c.1622T>C	p.Leu541Pro	2	2%	1, 16, 32, 40
c.1822T>A	p.Phe608Ile	4	5%	1, 23
c.1957C>T	p.Arg653Cys	1	1%	32, 41
c.2588G>C	p.Gly863Ala/p.DelGly863	3	4%	16, 18, 23, 32, 42
c.2919-?_3328+?del	p.Ser974_Gly1110delinsCys	2	2%	23
c.2947A>G	p.Thr983Ala	3	4%	34
c.3113C>T	p.Ala1038Val	2	2%	16, 31, 32, 40, 43
c.3335C>A	p.Thr1112Asn	1	1%	23
c.3449G>A	p.Cys1150Tyr	1	1%	This study
c.3813G>C	p.Glu1271Asp	1	1%	This study
c.3874C>T	p.Gln1292*	1	1%	34
c.4224G>T	p.Trp1408Cys	1	1%	This study
c.4462T>C	p.Cys1488Arg	1	1%	1, 8, 44, 45
c.4506C>A	p.Cys1502*	1	1%	34
c.4539+1G>T	p.?	3	4%	1, 23, 43, 44
c.4773+1G>A	p.?	1	1%	This study
c.5113C>T	p.Arg1705Trp	1	1%	34
c.5161_5162del	p.Thr1721fs	1	1%	23, 36
c.5312+1G>A	p.?	1	1%	46
c.5461-10T>C	p.?	19	22%	16, 23, 47
c.5537T>C	p.Ile1846Thr	1	1%	23, 45
c.5585-10T>C	p.?	1	1%	48
c.5714+5G>A	p.?	1	1%	1, 23, 32, 41, 43
c.5762_5763dup	p.Ala1922fs	1	1%	34
c.5882G>A	p.Gly1961Glu	5	6%	18, 31, 32, 44, 49
c.6320G>A	p.Arg2107His	2	2%	8, 31, 40, 45, 50
c.6411T>A	p.Cys2137*	1	1%	34
c.6543_6578del	p.Leu2182_Phe2193del	1	1%	1

References are shown for mutations that have been reported previously. *, stop signal; del, deletion; fs, frame shift.

8
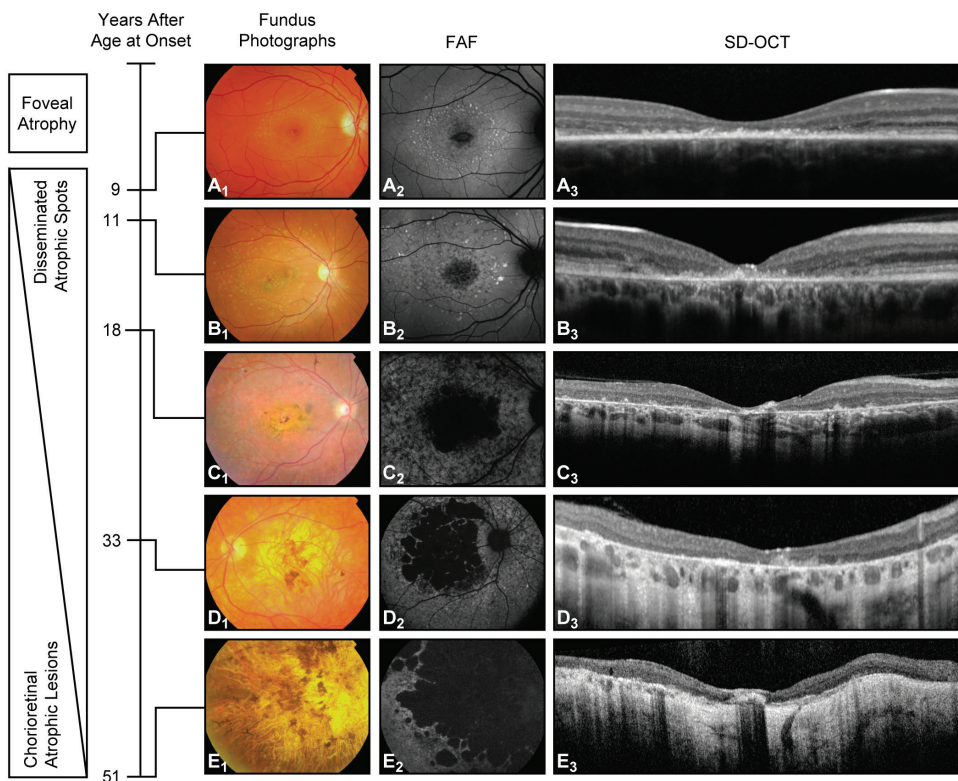
Figure 8.4. Overview of the natural course of retinal disease in early-onset Stargardt based on findings obtained from five separate patients using fundus photography, autofluorescence (FAF), and spectral-domain optical coherence tomography (SD-OCT). Early-onset Stargardt includes foveal atrophy and parafoveal hyperautofluorescent fundus flecks ($A_{1,2}$) in an early disease stage. SD-OCT reveals hyperreflective abnormalities in the outer retina, loss of the ellipsoid zone, and thinning of the outer nuclear layer (A_3). The initial foveal atrophy and parafoveal flecks then extend centrifugally ($B_{1,2}$), and disseminated hypoautofluorescent spots appear (B_2). SD-OCT reveals progression of the foveal atrophy, with thinning of the RPE/Bruch's membrane complex (B_3). Further in the course of the disease, the disseminated hypoautofluorescent spots become chorioretinal atrophic lesions, the central atrophy expands further ($C_{1,2}$), and pigmentations (C_1) are visible as hyperreflective deposits on SD-OCT (C_3). Over time, confluence of these lesions evolves centrifugally ($D_{1,2}$), extending beyond the vascular arcades ($E_{1,2}$), with further retinal thinning and atrophy of the choriocapillaris (D_3-E_3) visible on SD-OCT. $A_{1,2,3}$: patient 1 at age 17; $B_{1,2,3}$: patient 31 at age 22; $C_{1,2,3}$: patient 40 at age 24; $D_{1,2,3}$: patient 8 at age 36; $E_{1,2,3}$: patient 5 at age 57.

Table 8.3. Characteristics of the non-missense *ABCA4* mutations identified in our cohort study.

Mutation	Protein effect	SIFT	Polyphen-2	Grantham	PhyloP
c.3449G>A	p.Cys1150Tyr	Not tolerated	Benign	194	3.19
c.3813G>C	p.Glu1271Asp	Not tolerated	Possibly damaging	45	6.10
c.4224G>T	p.Trp1408Cys	Not tolerated	Probably damaging	215	5.86

The outcome of two protein prediction programs (SIFT: tolerated or not tolerated; PolyPhen: benign, possibly damaging, probably damaging), together with Grantham (>60 pathogenic) and PhyloP conservation score (>2.5 pathogenic), were used to form the final conclusion. Mutations are proposed to be pathogenic when ≥2 categories point to pathogenicity.

Discussion

In this study, we examined the clinical and genetic characteristics of patients with early-onset Stargardt, a disease that lies within the spectrum of retinal phenotypes linked to mutations in the *ABCA4* gene. Whenever a spectrum of disorders contains overlapping phenotypes as the rule rather than an exception, any cutoff point used to define a particular disease within that spectrum will be arbitrary. Therefore, we arbitrarily defined "early-onset Stargardt" as occurring with an age at onset ≤10 years of age; this definition enabled us to avoid including patients with a more typical STGD1 phenotype. Only 4% of the 51 patients in our early-onset Stargardt cohort had visual acuity ≤0.30 logMAR, Snellen <20/40 (measured at age 8 and 18 years of age in these two patients), compared to 14-37% of patients with typical STGD1 and 59% of patients with late-onset STGD1.[5, 14, 24] As patients with a relatively good visual acuity tended to return less often than those with progressive problems, these data may have overrepresented more severe cases. The majority of our patients for whom full-field ERG (ffERG) data were available developed abnormal ffERG amplitudes, consistent with a previous report by Fujinami et al.[7] However, we found no significant correlation between the ffERG group classifications (which were based on the nature of the ffERG abnormalities) at the age at onset and the speed of vision loss in this early-onset Stargardt cohort. This finding differs from STGD1 cohorts that included patients with later ages at onset.[5, 6] Our findings indicate that early-onset Stargardt can be considered a distinct severe subtype of STGD1 that is characterized by early foveal abnormalities and the rapid loss of visual function; in contrast, in late-onset STGD1, foveal sparing is common, and visual acuity is often preserved to a relatively advanced age.[14]

The diagnosis of early-onset Stargardt

The natural course of early-onset *ABCA4*-related retinal disease in our cohort reflects a broad clinical spectrum both at the time of onset and at follow-up, with varying degrees of ffERG abnormalities and yellow-white flecks and/or atrophy at a variety of locations. Thus, each combination of electrophysiological and fundoscopic findings could be considered a unique phenotype at a specific time point. Moreover, these phenotypes changed during the course of the disease, suggesting progression of the disease. Because both fundoscopic and electrophysiological criteria have been proposed for establishing a descriptive diagnosis (for instance, Stargardt disease and cone-rod dystrophy), each individual patient can potentially receive several diagnoses at one time point and at follow-up. Importantly, receiving several diagnoses can be extremely confusing to both the patient and the referring ophthalmologist.

Nevertheless, we found that the spectrum of fundus presentations in this early-onset retinal dystrophy ultimately converges to a single clinical and functional endpoint that includes profound chorioretinal atrophy and severe vision loss. Therefore, we propose that one diagnosis of "early-onset Stargardt" should be given to patients with early-onset central retinal dystrophy and *ABCA4* gene mutations. This approach will provide the patient with the benefit of receiving a single diagnosis throughout his/her entire life.

Genotype-phenotype correlation

Because early-onset Stargardt can be considered a severe phenotype, severe combinations of mutations are expected in these patients. In our cohort, the c.768G>T and c.5461-10T>C mutations were significantly more prevalent (present in 25% and 36% of our patients, respectively) than in other STGD1 cohorts (8% and 5%, respectively).[30, 31] The c.768G>T mutation is predicted to cause a splice defect that leads to nonsense-mediated decay due to absence of the corresponding mRNA; this mutation is therefore considered to be a severe pathogenic mutation. In addition, a founder effect has been suggested for this mutation due to the allele frequency of 8% among Dutch patients with STGD1.[30] On the other hand, the c.5461-10T>C mutation does not appear to be pathogenic, as heterologous expression of this mutation failed to reveal a splicing defect.[32] However, this mutation is rare among control patients but is present in 5% of patients with general STGD1. Therefore, the c.5461-10T>C mutation may be in linkage disequilibrium with another, currently unidentified severe pathogenic mutation.[31] Equally important, the most prevalent *ABCA4* mutation among Dutch patients with STGD1—c.2588G>C, which was reported in approximately one-third of typical STGD1 cases[33]—was present in only 4% of the *ABCA4* alleles in our cohort of patients with early-onset Stargardt. To date, no homozygous carriers of this mutation have been identified,[23] supporting the hypothesis that this is a relatively mild mutation. The low prevalence of this presumably mild mutation in our cohort is consistent with a previously proposed genotype-phenotype model that correlates the degree of residual ABCR activity with the severity of the phenotype.[17, 23]

We identified *ABCA4* mutations in all of our patients who received genetic screening; in contrast, the detection rate in routine clinical practice is 73%.[34] This difference can be explained—at least in part—by the inclusion criteria; patients who lacked a detected *ABCA4* mutation, only would have been included if yellow-white flecks and either a dark choroid or an atrophic macular lesion were present. However, our database did not contain such patients who received genetic screening and had an early-onset disease. This finding supports the notion that early onset is highly predictive for identifying *ABCA4* mutations,[34] possibly because of the relatively higher percentage of severe mutations, which are more readily identified and/or recognized.

It remains unclear why the fovea is affected early in the course of STGD1 in some patients, whereas it can be spared—even for many decades—in other patients carrying compound heterozygous mutations, including one severe *ABCA4* mutation.[14, 15] Other factors must therefore play a role in the development of foveal atrophy in early-onset Stargardt; possible factors can include pathogenic mutations or single-nucleotide polymorphisms in genes other than *ABCA4,* as well as aberrant cellular processes. For example, the accumulation of all-*trans*-retinal in photoreceptor cells can directly increase cellular stress, thereby triggering apoptotic signaling pathways.[35] Next-generation sequencing of all retina-specific genes may help identify the genetic factors that determine whether or not the fovea is involved early in the course of STGD1.

Clinical significance of early-onset Stargardt

Although diagnosing STGD1 at an early age is challenging, delaying diagnosis can have serious consequences. For example, 22 of the patients in our study did not receive the correct diagnosis for at least three years, and vision loss was initially unexplained in 13 patients. Recognizing early-onset Stargardt early in the disease course enables the timely start of potential measures—such as sunlight protection and low-vision counseling—and can prevent the inappropriate prescription of vitamin A supplements. Therefore, patients who are suspected of having early-onset Stargardt should be examined thoroughly using FAF and SD-OCT, particularly when no abnormalities (or mild foveal abnormalities) are present in a child with central vision loss that is otherwise unexplained. This diagnosis should also be confirmed by screening for the presence of *ABCA4* mutations. Finally, in light of future therapeutic options such as gene therapy for treating *ABCA4*-related retinal disorders, obtaining a thorough understanding of the phenotypic spectrum and clinical course of STGD1 is essential for identifying the patients who will benefit most from these treatments.

8

References

1. Lewis RA, Shroyer NF, Singh N, et al. Genotype/Phenotype analysis of a photoreceptor-specific ATP-binding cassette transporter gene, ABCR, in Stargardt disease. Am J Hum Genet 1999;64(2):422-34.
2. Stargardt K. Über familliäre, progressive Degeneration in der Maculagegend des Auges. Graefes Arch Clin Exp Ophthalmol 1909(71):534-50.
3. Franceschetti A. A special form of tapetoretinal degeneration: fundus flavimaculatus. Trans Am Acad Ophthalmol Otolaryngol 1965;69(6):1048-53.
4. Klevering BJ, Blankenagel A, Maugeri A, et al. Phenotypic spectrum of autosomal recessive cone-rod dystrophies caused by mutations in the ABCA4 (ABCR) gene. Investigative Ophthalmology & Visual Science 2002;43(6):1980-5.
5. Lois N, Holder GE, Bunce C, et al. Phenotypic subtypes of Stargardt macular dystrophy-fundus flavimaculatus. Arch Ophthalmol 2001;119(3):359-69.
6. Zahid S, Jayasundera T, Rhoades W, et al. Clinical phenotypes and prognostic full-field electroretinographic findings in Stargardt disease. American Journal of Ophthalmology 2013;155(3):465-73 e3.
7. Fujinami K, Lois N, Davidson AE, et al. A longitudinal study of stargardt disease: clinical and electrophysiologic assessment, progression, and genotype correlations. American Journal of Ophthalmology 2013;155(6):1075-88 e13.
8. Fishman GA, Stone EM, Grover S, et al. Variation of clinical expression in patients with Stargardt dystrophy and sequence variations in the ABCR gene. Arch Ophthalmol 1999;117(4):504-10.
9. Armstrong JD, Meyer D, Xu S, Elfervig JL. Long-term follow-up of Stargardt's disease and fundus flavimaculatus. Ophthalmology 1998;105(3):448-57; discussion 57-8.
10. Querques G, Leveziel N, Benhamou N, et al. Analysis of retinal flecks in fundus flavimaculatus using optical coherence tomography. British Journal of Ophthalmology 2006;90(9):1157-62.
11. Sparrow JR, Gregory-Roberts E, Yamamoto K, et al. The bisretinoids of retinal pigment epithelium. Progress in Retinal and Eye Research 2012;31(2):121-35.
12. Charbel Issa P, Barnard AR, Singh MS, et al. Fundus autofluorescence in the Abca4(-/-) mouse model of Stargardt disease--correlation with accumulation of A2E, retinal function, and histology. Investigative Ophthalmology & Visual Science 2013;54(8):5602-12.
13. Ergun E, Hermann B, Wirtitsch M, et al. Assessment of central visual function in Stargardt's disease/fundus flavimaculatus with ultrahigh-resolution optical coherence tomography. Invest Ophthalmol Vis Sci 2005;46(1):310-6.
14. Westeneng-van Haaften SC, Boon CJ, Cremers FP, et al. Clinical and Genetic Characteristics of Late-onset Stargardt's Disease. Ophthalmology 2012;119(6):1199-210.
15. Fujinami K, Sergouniotis PI, Davidson AE, et al. Clinical and molecular analysis of stargardt disease with preserved foveal structure and function. Am J Ophthalmol 2013;156(3):487-501 e1.
16. Maugeri A, Klevering BJ, Rohrschneider K, et al. Mutations in the ABCA4 (ABCR) gene are the major cause of autosomal recessive cone-rod dystrophy. Am J Hum Genet 2000;67(4):960-6.
17. Klevering BJ, Deutman AF, Maugeri A, et al. The spectrum of retinal phenotypes caused by mutations in the ABCA4 gene. Graefes Arch Clin Exp Ophthalmol 2005;243(2):90-100.
18. Allikmets R, Singh N, Sun H, et al. A photoreceptor cell-specific ATP-binding transporter gene (ABCR) is mutated in recessive Stargardt macular dystrophy. Nat Genet 1997;15(3):236-46.
19. Molday LL, Rabin AR, Molday RS. ABCR expression in foveal cone photoreceptors and its role in Stargardt macular dystrophy. Nat Genet 2000;25(3):257-8.
20. Sun H, Smallwood PM, Nathans J. Biochemical defects in ABCR protein variants associated with human retinopathies. Nat Genet 2000;26(2):242-6.
21. Sparrow JR, Wu Y, Kim CY, Zhou J. Phospholipid meets all-trans-retinal: the making of RPE bisretinoids. J Lipid Res 2010;51(2):247-61.
22. van Driel MA, Maugeri A, Klevering BJ, et al. ABCR unites what ophthalmologists divide(s). Ophthalmic Genet 1998;19(3):117-22.
23. Maugeri A, van Driel MA, van de Pol DJ, et al. The 2588G-->C mutation in the ABCR gene is a mild frequent founder mutation in the Western European population and allows the classification of ABCR mutations in patients with Stargardt disease. Am J Hum Genet 1999;64(4):1024-35.
24. Rotenstreich Y, Fishman GA, Anderson RJ. Visual acuity loss and clinical observations in a large series of patients with Stargardt disease. Ophthalmology 2003;110(6):1151-8.

25. Burke TR, Yzer S, Zernant J, et al. Abnormality in the external limiting membrane in early Stargardt Disease. Ophthalmic Genet 2012.

26. Schulze-Bonsel K, Feltgen N, Burau H, et al. Visual acuities "hand motion" and "counting fingers" can be quantified with the freiburg visual acuity test. Investigative Ophthalmology & Visual Science 2006;47(3):1236-40.

27. Marmor MF, Fulton AB, Holder GE, et al. ISCEV Standard for full-field clinical electroretinography (2008 update). Doc Ophthalmol 2009;118(1):69-77.

28. Kuze M, Uji Y. Comparison between Dawson, Trick, and Litzkow electrode and contact lens electrodes used in clinical electroretinography. Japanese Journal of Ophthalmology 2000;44(4):374-80.

29. Colenbrander A. Visual standards: aspects and ranges of vision loss with emphasis on population surveys. Report prepared for the International Council of Ophthalmology (ICO) at the 29th International Congress of Ophthalmology, Sydney, 2002. San Francisco: Pacific Vision Foundation; 2002.

30. Cremers FP, Maugeri A, den Hollander AI, Hoyng CB. The expanding roles of ABCA4 and CRB1 in inherited blindness. Novartis Found Symp 2004;255:68-79; discussion -84, 177-8.

31. Webster AR, Heon E, Lotery AJ, et al. An analysis of allelic variation in the ABCA4 gene. Invest Ophthalmol Vis Sci 2001;42(6):1179-89.

32. Rivera A, White K, Stohr H, et al. A comprehensive survey of sequence variation in the ABCA4 (ABCR) gene in Stargardt disease and age-related macular degeneration. Am J Hum Genet 2000;67(4):800-13.

33. Maugeri A, Flothmann K, Hemmrich N, et al. The ABCA4 2588G>C Stargardt mutation: single origin and increasing frequency from South-West to North-East Europe. Eur J Hum Genet 2002;10(3):197-203.

34. Ernest PJ, Boon CJ, Klevering BJ, et al. Outcome of ABCA4 microarray screening in routine clinical practice. Molecular Vision 2009;15:2841-7.

35. Cideciyan AV, Swider M, Aleman TS, et al. ABCA4 disease progression and a proposed strategy for gene therapy. Hum Mol Genet 2009;18(5):931-41.

36. Papaioannou M, Ocaka L, Bessant D, et al. An analysis of ABCR mutations in British patients with recessive retinal dystrophies. Invest Ophthalmol Vis Sci 2000;41(1):16-9.

37. September AV, Vorster AA, Ramesar RS, Greenberg LJ. Mutation spectrum and founder chromosomes for the ABCA4 gene in South African patients with Stargardt disease. Investigative Ophthalmology & Visual Science 2004;45(6):1705-11.

38. Jaakson K, Zernant J, Kulm M, et al. Genotyping microarray (gene chip) for the ABCR (ABCA4) gene. Hum Mutat 2003;22(5):395-403.

39. Yatsenko AN, Shroyer NF, Lewis RA, Lupski JR. Late-onset Stargardt disease is associated with missense mutations that map outside known functional regions of ABCR (ABCA4). Hum Genet 2001;108(4):346-55.

40. Rozet JM, Gerber S, Souied E, et al. Spectrum of ABCR gene mutations in autosomal recessive macular dystrophies. European Journal of Human Genetics 1998;6(3):291-5.

41. Fumagalli A, Ferrari M, Soriani N, et al. Mutational scanning of the ABCR gene with double-gradient denaturing-gradient gel electrophoresis (DG-DGGE) in Italian Stargardt disease patients. Human Genetics 2001;109(3):326-38.

42. Allikmets R, Shroyer NF, Singh N, et al. Mutation of the Stargardt disease gene (ABCR) in age-related macular degeneration. Science 1997;277(5333):1805-7.

43. Cremers FP, van de Pol DJ, van Driel M, et al. Autosomal recessive retinitis pigmentosa and cone-rod dystrophy caused by splice site mutations in the Stargardt's disease gene ABCR. Hum Mol Genet 1998;7(3):355-62.

44. Stone EM, Webster AR, Vandenburgh K, et al. Allelic variation in ABCR associated with Stargardt disease but not age-related macular degeneration. Nature Genetics 1998;20(4):328-9.

45. Briggs CE, Rucinski D, Rosenfeld PJ, et al. Mutations in ABCR (ABCA4) in patients with Stargardt macular degeneration or cone-rod degeneration. Invest Ophthalmol Vis Sci 2001;42(10):2229-36.

46. Zernant J, Schubert C, Im KM, et al. Analysis of the ABCA4 gene by next-generation sequencing. Invest Ophthalmol Vis Sci 2011;52(11):8479-87.

47. Roberts LJ, Nossek CA, Greenberg LJ, Ramesar RS. Stargardt macular dystrophy: common ABCA4 mutations in South Africa--establishment of a rapid genetic test and relating risk to patients. Mol Vis 2012;18:280-9.

48. Lenassi E, Jarc-Vidmar M, Glavac D, Hawlina M. Pattern electroretinography of larger stimulus field size and spectral-domain optical coherence tomography in patients with Stargardt disease. British Journal of Ophthalmology 2009;93(12):1600-5.
49. Simonelli F, Testa F, de Crecchio G, et al. New ABCR mutations and clinical phenotype in Italian patients with Stargardt disease. Investigative Ophthalmology & Visual Science 2000;41(3):892-7.
50. Paloma E, Martinez-Mir A, Vilageliu L, et al. Spectrum of ABCA4 (ABCR) gene mutations in Spanish patients with autosomal recessive macular dystrophies. Human Mutation 2001;17(6):504-10.

Authors

Ramon A.C. van Huet, MD;[1] Nathalie M. Bax, MD;[1] Sarah C. Westeneng-Van Haaften, MD;[1] Muhamad Muhamad, BSc;[1] Marijke N. Zonneveld-Vrieling,[2] Lies H. Hoefsloot, PhD;[2] Frans P.M. Cremers, PhD;[2,3] Camiel J.F. Boon, MD, PhD;[1,4] B. Jeroen Klevering, MD, PhD;[1] Carel B. Hoyng, MD, PhD[1]

Affiliations

[1]Department of Ophthalmology, Radboud University Medical Center, Nijmegen, The Netherlands
[2]Department of Human Genetics, Radboud University Medical Center, Nijmegen, The Netherlands
[3]Nijmegen Center of Molecular Life Sciences, Radboud University Medical Center, Nijmegen, The Netherlands
[4]Department of Ophthalmology, Leiden University Medical Center, Leiden, The Netherlands

Foveal sparing in
Stargardt disease

9

Abstract

Purpose. To provide a clinical and genetic description of a patient cohort with Stargardt disease (STGD1) with identifiable foveal sparing.

Methods. Patients with retinal atrophy (defined as an absence of autofluorescence) that surrounds the fovea by at least 180° and does not include the fovea were defined as having foveal sparing; eyes with visual acuity (VA) worse than 20/200 were excluded. We reviewed the medical files and extracted data regarding medical history, VA, ophthalmoscopy, static perimetry, fundus photography, spectral-domain optical coherence tomography (SD-OCT), fluorescein angiography (FA), fundus autofluorescence (FAF), and electroretinography (ERG). We screened each patient's *ABCA4* gene for mutations.

Results. Seventeen eyes with foveal sparing were identified in 13 unrelated patients. In 4 eyes, the fovea gradually became atrophic after the initial foveal sparing. The mean age at onset was 51 years (range: 32-67 years). VA was 20/40 or better in all foveal sparing eyes, and 20/25 or better in 41%. FAF imaging revealed hyperautofluorescent flecks and parafoveal retinal atrophy, SD-OCT revealed sharply delineated atrophy, and perimetry revealed parafoveal scotomas with intact foveal sensitivity. Finally, genetic screening identified mutations in 19 of the 26 *ABCA4* gene alleles.

Conclusions. Foveal sparing occurs mainly in patients with late-onset STGD1 and represents the milder end of the clinical spectrum in STGD1. The anatomy, metabolism, and biochemistry of the retina, as well as genetic variations in genes other than *ABCA4*, can influence the etiology of foveal sparing. Identifying these fovea-protecting factors will facilitate the future development of strategies designed to treat STGD1.

Introduction

Within the retina, the macula provides the highest visual acuity and contains the highest density of cones.[1, 2] Therefore, a loss of central vision is a hallmark feature of macular dystrophies. There are, however, exceptions to this rule. Foveal sparing is an intriguing phenomenon in which retinal atrophy surrounds a relatively preserved fovea, leaving central visual acuity largely unaffected. Although foveal sparing has been reported in a variety of conditions, including Stargardt disease (STGD1),[3-5] mitochondrial retinal dystrophy associated with the m.3243A>G mutation,[6] and geographic atrophy in age-related macular degeneration (AMD),[7-11] its etiology remains poorly understood.

STGD1 is an autosomal recessive retinal dystrophy that typically presents within the first two decades of life.[12] Although the clinical presentation of STGD1 varies widely, it is usually characterized by a progressive loss of central vision, irregular yellow-white fundus flecks, and the so-called "beaten bronze" atrophic macular lesions.[13-15] STGD1 has been linked to mutations in the *ABCA4* gene, which encodes an adenosine triphosphate (ATP)-binding cassette transporter (ABCR) expressed specifically in the cones and rods of the retina.[16, 17] Defects in ABCR function cause the accumulation of all-*trans*-retinal and its cytotoxic derivatives (e.g., diretinoid-pyridinium-ethanolamine) in photoreceptors and retinal pigment epithelial (RPE) cells, ultimately causing RPE cell death and the subsequent loss of photoreceptors.[18]

Mutations in *ABCA4* have been linked to a spectrum of phenotypes ranging from mild macular dystrophy to severe early-onset panretinal dystrophy.[3, 19-22] We previously postulated that disease severity may be correlated to the functional severity of the particular mutation in the resulting ABCR protein.[19, 23-25] The substantial clinical variability among patients with STGD1—including an age at onset of the symptoms that can range from 5-72 years of age, diverse fundoscopic features, diverse electrophysiological findings, and a variable time course of vision loss—suggests the presence of several strong modifying factors.[3,13, 14]

Recently, Fujinami et al. reported the clinical and molecular genetic findings of a cohort of STGD1 patients with relatively preserved foveal structure and function (based on seemingly normal autofluorescence at the fovea). Their study revealed the presence of two basic— yet distinct—STGD1 phenotypes, namely STGD1 patients with foveal sparing and STGD1 patients with early-onset foveal atrophy.[26] However, the onset of foveal involvement in STGD1 can vary substantially and can occur in later disease stages, for example in late-onset STGD1.[3] This heterogeneity complicates the selection of homogeneous cohorts for clinical studies to investigate the subtype of STGD1 patients with foveal sparing.

Here, we report the clinical characteristics and the natural course of foveal sparing in a cohort of STGD1 patients with foveal sparing, and we explore the mechanisms that may underlie this phenomenon.

Methods

Patients and genetic analysis

The patient selection process is depicted in Figure 9.1. The database of the Department of Ophthalmology at Radboud University Medical Center (Nijmegen, the Netherlands) contains 425 clinically suspected cases of STGD1. For 257 of these patients, an *ABCA4* genetic screen

9

for known mutations was performed in the Department of Human Genetics at Radboud University Medical Center (Nijmegen, the Netherlands) using arrayed primer extension analysis (APEX) microarrays (Asper Biotech, Tartu, Estonia). Because STGD1 is autosomal recessive, if the Asper microarray screen revealed only one mutation in a given patient, we sequenced the exons and intron-exon boundaries in *ABCA4* to identify the mutation in the second allele. All mutations were confirmed using Sanger sequencing. The presence of one or two mutations in the *ABCA4* gene confirmed the diagnosis of STGD1 in 198 patients. For our study, we selected cases in which foveal sparing was documented using fundus photography and/or fundus autofluorescence (FAF) imaging. Patients with RPE atrophy (defined as an absence of autofluorescence surrounding the fovea by least 180°) that did not include the fovea were defined as having foveal sparing. Eyes with visual acuity of 20/200 or worse were presumed to have little or no foveal function and were therefore excluded. Twelve unrelated STGD1 patients with foveal sparing in at least one eye were included in this study. We also included one additional patient who initially presented with foveal sparing; in this patient, the fovea became atrophic as the disease progressed. To exclude pseudo-Stargardt pattern dystrophy,[27] the *PRPH2* gene was sequenced in all 13 patients.

This study was performed in accordance with the tenets of the Declaration of Helsinki, and all participating patients gave their informed consent prior to providing a blood sample and receiving additional ophthalmologic examinations.

Clinical examination

Clinical data were collected from the medical records of the 13 eligible patients. The data collected included the patient's age at onset, medical history, initial symptoms, and the overall course of the retinal disorder. Age at onset was defined as the age at which the initial symptoms were noted by the patient. We defined the duration of symptomatic disease as the time from the age at onset to the patient's current age. In the patients who were initially asymptomatic, the age at their first visit to the ophthalmologist was used to define disease duration.

The standard ophthalmic examination included a measurement of best-corrected visual acuity (BCVA) using Snellen visual acuity charts and ophthalmoscopy. The central visual field was assessed using a Humphrey perimeter (Carl Zeiss Meditec, Jena, Germany) using central 10-2, 24-2, or 30-2 threshold tests in two, two, and four patients, respectively. Fundus photography (Topcon TRC50IX, Topcon Corporation, Tokyo, Japan) was performed in ten patients. Fluorescein angiography (FA) was performed in ten patients to screen for the presence of the dark choroid sign. Full-field electroretinography (ffERG; 8 patients) and multifocal ERG (mfERG; 7 patients) were performed using Dawson-Trick-Litzkow (DTL) electrodes and the RETI-port system (Roland Consults, Stasche & Finger GmbH, Brandenburg an der Havel, Germany). Both the ffERG and mfERG recordings were performed in accordance with the guidelines of the International Society for Clinical Electrophysiology of Vision (ISCEV).[28]

Cross-sectional images were obtained using spectral-domain optical coherence tomography (SD-OCT; Heidelberg Engineering, Heidelberg, Germany) in 12 patients; a 20°x15° 19-line scan covering the fovea was used. Total retinal thickness, outer nuclear layer (ONL) thickness, and photoreceptor-RPE (PR+RPE) complex thickness were measured at the foveal dip and at 0.25, 0.5, 1, 1.5, 2, and 2.5 mm eccentric distances using Heidelberg

Eye Explorer software (Version 1.6.4.0, Heidelberg Engineering, Heidelberg, Germany). ONL thickness was measured from the outer plexiform layer to the external limiting membrane (ELM), PR+RPE thickness was measured from the ELM to Bruch membrane, and total retinal thickness was measured from the vitreous-retinal interface to RPE-Bruch membrane complex. Clinically normal values for total retinal thickness, ONL thickness, and PR+RPE thickness were obtained from 25 age-matched individuals (mean age: 46 years; range: 27-62 years) with no retinal or vitreoretinal disease; we performed a post-acquisition interpolation of the normal data using custom programs (MatLab R2011a, The MathWorks Inc., Natick, MA).

We acquired FAF images using a confocal scanning laser ophthalmoscope (cSLO, Spectralis, Heidelberg Engineering, Heidelberg, Germany). After the pupil was dilated, 30° and/or 55° field-of-view FAF images were obtained from all patients (except case 11) using an optically pumped solid-state laser with 488-nm excitation. Two independent observers (authors R.A.C.v.H. and N.M.B.) measured the size of the atrophic lesions (determined using the absence of autofluorescence) as described previously.[29]
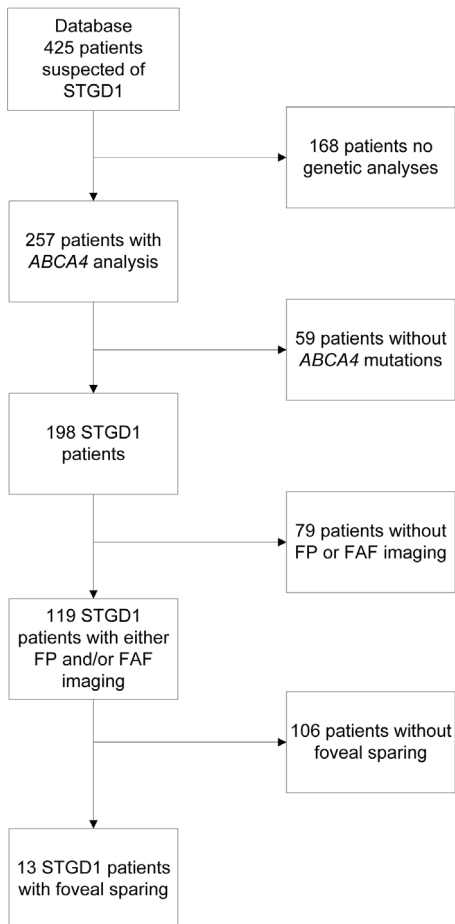
Figure 9.1. Flow-chart depicting the selection process of Stargardt patients with foveal sparing for inclusion in the study. FAF, fundus autofluorescence; FP, fundus photography; STGD1, Stargardt disease.
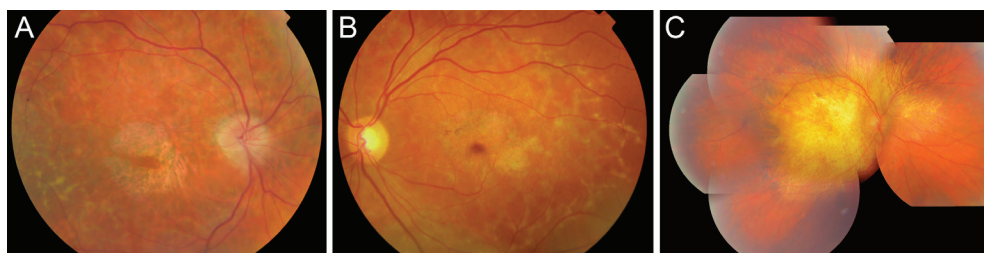
Figure 9.2. Fundus photographs of three patients with STGD1. A, Fundus photograph of the right eye of patient 4 (at age 60), showing fundus flavimaculatus flecks and parafoveal atrophy of the retinal pigment epithelium (RPE). B, Fundus photograph of the left eye of case 5 (at age 45), showing fundus flavimaculatus flecks and parafoveal atrophy of the RPE. C, Mosaic of fundus photographs of the right eye of case 12 (at age 73), showing profound central atrophy of the RPE; this patient previously had foveal sparing.

Results

Clinical characteristics

Of the 198 patients with a confirmed diagnosis of STGD1, 13 unrelated patients (7%) had foveal sparing. The clinical characteristics of these 13 patients (including all 26 eyes) are summarized in Table 9.1. This cohort included five women and eight men; all 13 patients were of Caucasian descent, with a mean age at onset of 52 years (range: 32-67 years). The mean disease duration was 9 years (range: 1-34 years). These patients were diagnosed between the age of 39 and 82 years (mean: 57 years). None of the patients were using hydroxychloroquine at the time of the study, nor had they used this drug in the past.

Foveal sparing was present in 17 of the 26 eyes (65%), and five of the 13 patients (38%) had bilateral foveal sparing. In seven of the patients with unilateral foveal sparing, five of the contralateral eyes had no signs of RPE atrophy or parafoveal atrophic RPE lesions that surrounded the fovea by less than 180°. In the remaining two eyes, and in both eyes in patient 12, the fovea degenerated after initial foveal sparing (Table 9.1).

Nine of the 13 patients (69%) initially experienced a decline in visual acuity. Other initial symptoms included paracentral scotoma in four patients (31%), metamorphopsia in two patients (15%), and nyctalopia in one patient (8%). Two patients (patients 2 and 13; 15%) initially experienced no visual complaints, but were referred to our department because of fundus abnormalities found during ophthalmologic screening for glaucoma or thyroid eye disease; after nine and six years, respectively, these two patients experienced a perceived decrease in visual acuity (Table 9.1). BCVA was 20/40 or better in all 17 eyes with foveal sparing; 7 of these 17 eyes (41%) had a BCVA of 20/25 or better. In the four eyes in which atrophy ultimately affected the fovea, BCVA had decreased to ≤20/200 from an initial acuity of 20/25 to 20/40 when the fovea was spared.

In 12 patients, a fundus examination revealed irregular flavimaculatus flecks scattered throughout the posterior pole and occasionally extending anterior to the vascular arcades (Figures 9.2A-B and 9.3A). One patient had small perifoveal yellow-white dots. Patient 12, who had bilateral foveal degeneration, developed extensive chorioretinal atrophy of the posterior pole and the midperiphery during the patient's 26 years of follow-up (Figure 9.2C).

Masking of the choroidal background fluorescence (i.e., a so-called "dark choroid") was evident on FA imaging in seven patients, four of whom carried a single heterozygous *ABCA4* mutation (Tables 9.1 and 2). The flavimaculatus flecks were visible as an irregular pattern of hyperfluorescence and hypofluorescence on FA imaging (Figure 9.3B), and they appeared as hyperautofluorescent flecks on FAF imaging (Figures 9.3C and 9.4). The chorioretinal atrophy corresponded with sharply delineated areas that included both an absence of autofluorescence and structural thinning of the outer retinal layers on OCT (Figure 9.3D). Static perimetry revealed sharply delineated absolute parafoveal scotomas (Figure 9.4) with subnormal foveal sensitivity (median: 35 dB; range: 20-39 dB). Foveal sensitivity was not measurable (<0 dB) in patient 12, which is consistent with the anatomical findings and other functional results obtained from this patient.
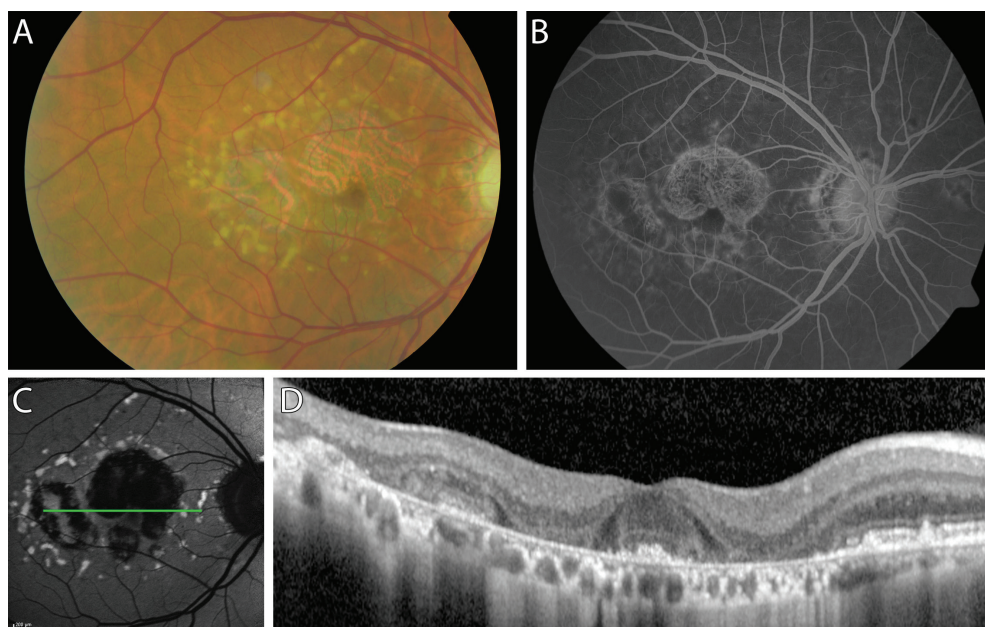
Figure 9.3. Multimodal imaging of the right fundus of patient 3 at age 62. A, Fundus photograph showing irregular flavimaculatus flecks and atrophy of the central retinal pigment epithelium (RPE); note that the fovea is spared. B, Fluorescein angiograph showing the "dark choroid" sign, hyperfluorescence, visible choroidal vessels due to window defects, and a normal-appearing fovea. C, Fundus autofluorescence image showing hyperautofluorescent flecks and RPE atrophy with foveal sparing. The green horizontal line indicates the scanning level of the optical coherence tomography (OCT) scan in panel D. D, An OCT scan through the fovea clearly shows the preserved cone photoreceptors in the fovea surrounded by atrophy of the outer retina and RPE.

The results of the ffERG recordings in ten eyes with foveal sparing are summarized in Table 9.1. In these ten eyes, photopic amplitude was normal in seven eyes (70%) and moderately reduced in three eyes (30%), and scotopic amplitude was normal in eight eyes (80%) and moderately reduced in two eyes (20%). In the four eyes that developed an atrophic fovea after initial foveal sparing, the photopic and scotopic amplitudes were either normal or severely reduced (Table 9.1).
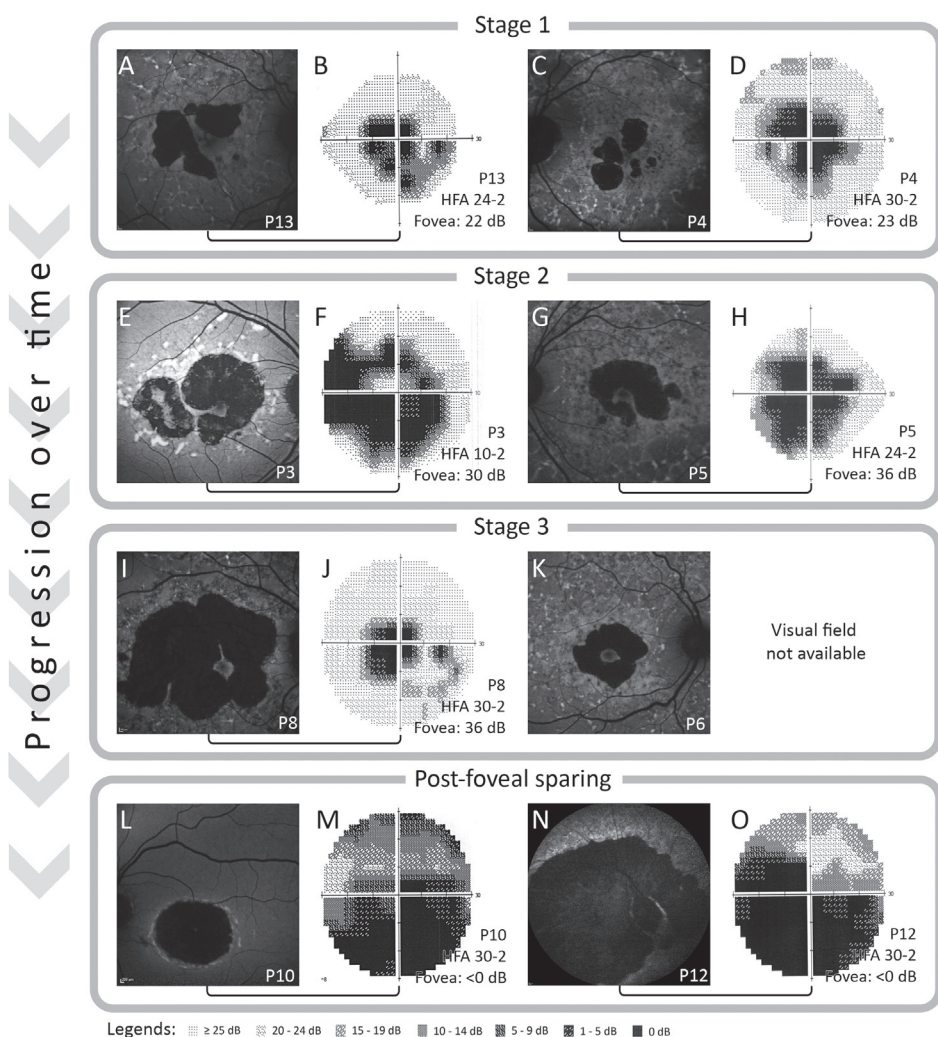
Figure 9.4. Natural course of fundus and perimetric changes in STGD1 with foveal sparing. FAF imaging can be used to identify the three stages that occur in foveal sparing. In stage 1, confluent parafoveal RPE lesions surround the macula, leaving several connections of intact RPE with the surrounding vital RPE (stage 1; A, C). Over time, the RPE atrophy progresses, and the lesions interconnect, leaving only one isthmus of RPE (stage 2; E, G). Further disease progression leads to an isolated fovea that is surrounded completely by RPE atrophy (stage 3; I, K). Eventually, RPE atrophy overcomes foveal resistance, leading to foveal degeneration (post-foveal sparing; L, N). Static perimetry examination reveals absolute perifoveal scotomas with intact foveal sensitivity in all eyes with foveal sparing (B, D, F, H, J). Large absolute scotomas with diminished foveal sensitivity were observed in the post-foveal sparing eyes (M, O). A/B, FAF (A) and 24-2 perimetry (B) in patient 13 at age 63. C/D FAF (C) and 30-2 perimetry (D) in patient 4 at age 60 and 61, respectively. E/F FAF (E) and 10-2 perimetry (F) in patient 3 at age 64 and 65, respectively. G/H, FAF (G) and 24-2 perimetry (H) in patient 5 at age 45. I/J, FAF (I) and 30-2 perimetry (J) in patient 8 at age 66 and 65, respectively. K, FAF in patient 6 at age 58. L/M, FAF (L) and 30-2 perimetry (M) in patient 10 at age 53. N/O, FAF (N) and 30-2 perimetry (O) in patient 12 at age 73.

Table 9.1 Clinical characteristics of the patients included in this study at most recent visit.

ID/Sex/AO (y)/Age (y)	Foveal sparing	Initial symptoms	Visual acuity		Ophthalmoscopy	Perimetry	ffERG*		Dark choroid on FA
			RE	LE			Scotopic RE/LE	Photopic RE/LE	
P1/F/53/57	RE	Paracentral scotoma, metamorphopsia	20/40	20/25	RE: macular RPE atrophy surrounding the fovea, yellow-white fundus flecks in posterior pole LE: hypopigmentation and yellow-white flecks in posterior pole	Humphrey24-2: (56y) BE: Pericentral scotoma of ~10°, FS: 36-34dB	N/N (56y)	N/N (56y)	Yes
P2/M/58/61	BE	Initially no symptoms, 9 years later VA↓	20/40	20/30	RPE atrophy with small foveal peninsula, yellow-white fundus flecks reaching up to the midperiphery	Humphrey 10-2: (59y) BE: Absolute pericentral scotoma (superior>inferior), FS: 24-28 dB	N/N (49y)	MR/MR (49y)	Yes
P3/M/60/63	BE	VA↓, nyctalopia	20/25	20/25	RPE atrophy surrounding the small foveal residue, yellow-white irregular flecks reaching as far as the vascular arcades	Humphrey 10-2: (65y) BE: Absolute pericentral scotoma, FS: 30-34 dB	NP	NP	Yes
P4/M/57/60	BE	VA↓	20/30	20/30	RPE atrophy spots (confluent in RE) around the fovea, yellow-white irregular flecks reaching up to the midperiphery	Humphrey 30-2: BE: Absolute pericentral scotoma of ~20°, FS 20-23 dB	N/N	N/N	No
P5/F/43/45	BE	VA↓	20/30	20/30	RPE atrophy surrounding the fovea, fundus flavimaculatus flecks reaching up to vascular arcades	Humphrey 24-2: RE: mixed relative and absolute pericentral scotoma of ~20° with inferior-temporal absolute defect, FS: 39 dB. LE: absolute pericentral scotoma of ~20°, FS: 36 dB	MR/MR	N/MR	NP

9

ID/Sex/AO (y)/Age (y)	Foveal sparing	Initial symptoms	Visual acuity RE	Visual acuity LE	Ophthalmoscopy	Perimetry	ffERG* Scotopic RE/LE	ffERG* Photopic RE/LE	Dark choroid on FA
P6/M/57/59	BE	VA↓	20/25	20/25	RPE atrophy surrounding the fovea completely in RE and incompletely (~270°) in LE, yellow-white irregular flecks in posterior pole as well as diffusely spread hypopigmented spots	NP	NP	NP	No
P7/F/NA/81	LE	Metamorphopsia	20/25	20/25	Yellow-white irregular flecks within the posterior pole. Parafoveal RPE atrophy lesions in LE.	NP	NP	NP	NP
P8/F/32/66	RE	VA↓	20/30	20/20	RE: Macular RPE atrophy with small foveal residue, small macular intraretinal pigmentations, hypopigmented RPE in posterior pole LE: RPE atrophy lesions in posterior pole, hypopigmented RPE in posterior pole.	Humphrey 30-2: (65y) RE: Pericentral absolute scotoma of ~15°, FS: 36 dB LE: Three paracentral spots of absolute visual field loss, FS: 34 dB	N/MR (65y)	N/N (65y)	Yes
P9/M/NA/63	RE	VA↓	20/40	20/15	Macular RPE atrophy lesions in the RE confluent surrounding the fovea, yellow-white flecks in posterior pole	NP	NP	NP	Yes
P10/F/39/53	RE (LE: post-foveal sparing)	Paracentral scotoma	20/25	20/200	Perifoveal RPE atrophy lesions in RE, macular RPE atrophy in LE, small yellow-white spots in perifoveal region in BE.	NP	N/N (47y)	N/N (47y)	No

Table 9.1 Clinical characteristics of the patients included in this study at most recent visit (continued)

ID/Sex/AO (y)/Age (y)	Foveal sparing	Initial symptoms	Visual acuity RE	Visual acuity LE	Ophthalmoscopy	Perimetry	ffERG* Scotopic RE/LE	ffERG* Photopic RE/LE	Dark choroid on FA
P11/M/67/68	LE (RE post-foveal sparing)	VA↓	20/200	20/30	Confluent RPE spots in the posterior pole surrounding the fovea in LE, fovea already degenerated in RE, irregular yellow-white flecks surrounding the atrophic lesions	NP	NP	NP	Yes
P12/M/50/74	BE: post-foveal sparing	Paracentral scotoma	CF	CF	Profound chorioretinal atrophy in posterior pole, small border of yellow-white surrounds atrophy	Humphrey 30-2: (low test reliability) BE mixed relative and absolute central scotoma, inferior worse than superior quadrants, FS: <0 dB	SR/SR	SR/SR	NP
P13/M/52/63	RE	Initially no symptoms, 6 years later VA↓, para-central scotoma	20/25	20/25	Confluent RPE spots in perifoveal region, yellow-white flecks reaching up to the midperiphery	Humphrey 30-2: (63y) BE: Pericentral absolute scotoma. FS: 35-37dB	N/SR (60y)	N/N (60y)	Yes

*The abbreviations reflect the amplitude: N, normal (equal to or above the lower 5% of the range for a normal population: photopic ≥78 μV, scotopic ≥263 μV); MR, moderately reduced (1-5% of normal range: photopic ≥69 μV and <78 μV, scotopic ≥ 195 μV and <263 μV); SR, severely reduced (<1% of normal range: photopic <69 μV, scotopic <195 μV).

AO, Age at onset; BE, both eyes; CF, counting fingers; F, female; FA, fluorescein angiography; ffERG, full-field electroretinography; FS, foveal sensitivity; LE, left eye; M, male; NP, not performed; RE, right eye; RPE, retinal pigment epithelium; VA↓, decrease in visual acuity.

9

In three patients (patient 5, right eye; patient 8, left eye; and patient 13, left eye), the scotopic amplitude was reduced more markedly than the amplitude of photopic flash responses, although none of these patients had peripheral pigmentary retinopathy. No clear correlation was found between ffERG response and disease duration, visual acuity, or fundoscopic characteristics. We also measured mfERG in eight eyes with foveal sparing and found that the P1-response amplitudes in the central two rings (representing the foveal retina) were relatively intact compared to the outer three rings, which showed severely reduced responses.
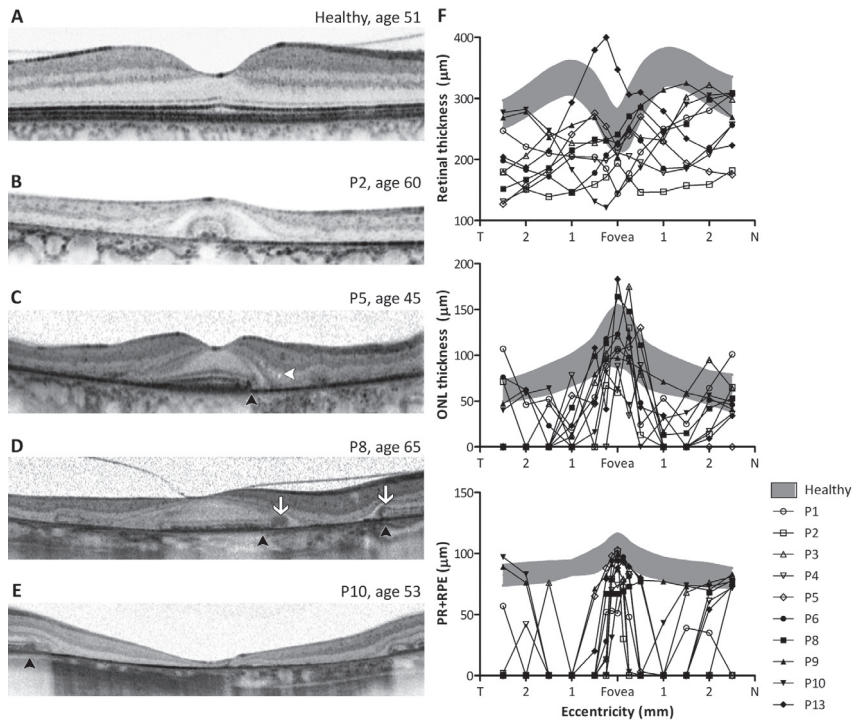
Figure 9.5. OCT analysis of Stargardt patients with foveal sparing. Panels A through E show the structural aspects of the macula in a healthy individual (A; age 51), case 2 (B; age 60), case 3 (C; age 45), case 8 (D; age 65), and case 10 (E; age 53). The white arrows in panel D indicate the locations of signs resembling outer retinal tubulation. The black arrowheads in panels C, D, and E indicate the locations of abrupt photoreceptor layer disturbances without gradual outer and/or inner segment loss. The white arrowhead in panel C indicates the presence of microcysts in the inner nuclear layer. F, Summary of thickness measurements of the total retina (top panel), ONL (middle panel), and PR+RPE (lower panel). The gray shaded areas show the distribution (mean ± 2SD) of the total retinal, ONL, and PR+RPE thickness in 25 age-matched healthy individuals (mean age: 46 years). ONL, outer nuclear layer; PR+RPE, photoreceptor-retinal pigment epithelium complex.

Retinal structure

SD-OCT imaging was performed in 12 patients and revealed highly localized damage to the lamellar architecture of the macula. We observed parafoveal atrophy of photoreceptors and RPE cells with sharp borders, represented by a loss of the bands associated with the ELM, the ellipsoid inner segments, and the RPE (Figure 9.5B-E).[30] These bands were

present in the fovea, however, although many of the bands that corresponded to the ELM and ellipsoid inner segments were irregular. In addition, the longer outer segments—which are characteristic of cone photoreceptors in the foveal dip—were not observed in any of these 12 eyes (Figure 9.5A-D). In three eyes, we observed signs reminiscent of outer retinal tubulation at the border of the atrophic lesions (Figure 9.5D), although no rosette-like structures (as described by Zweifel and colleagues) were observed.[31] Microcystoid macular edema was present in three eyes (Figure 9.5C), and epiretinal gliosis with retinal wrinkling extending over the fovea was observed in one eye.

An analysis of the retinal lamellar architecture revealed that the overall retinal thickness in the foveal and parafoveal regions was generally decreased (Figure 9.5F). The thickness of both the ONL and PR+RPE layers was normal at the foveal center in most patients. However, in the parafoveal region, the PR+RPE was usually nearly absent, whereas the ONL was progressively thinner in this region (Figure 9.5F).

Natural course of foveal sparing
An analysis of the longitudinal FAF data, which were available for six patients, enabled us to investigate the natural course of foveal sparing. In general, fundus flavimaculatus flecks were observed in the early stages, in some cases even before symptoms developed. Within one to two decades of diagnosis (range: 10-18 years), one or more sharply delineated parafoveal RPE atrophic areas appeared (Figure 9.4A). Over time, these lesions expanded and reached confluence around the fovea, thus producing the foveal sparing phenotype. We observed three distinct stages in the development of foveal sparing; these stages characterize the natural course of the phenomenon. In stage 1, parafoveal atrophic lesions emerge, with several intact RPE connections between the fovea and the surrounding vital RPE (Figure 9.4A and 9.4C). In stage 2, the atrophic RPE lesions interconnect, leaving only a single isthmus of RPE, thus resulting in a "peninsula-like" appearance (Figure 9.4E and 9.4G). Stage 3 is characterized by an isolated fovea that is surrounded completely by RPE atrophy (Figure 9.4I and 9.4K). We measured the expansion rate of the atrophic lesions in four patients using the FAF follow-up data (Table 9.2). The rate of expansion ranged from 0.832 to 2.363 mm^2/year in these patients, and the rate was positively correlated to the size of the atrophic lesions. Given this wide range of expansion rates, it is unclear how long foveal sparing is present before the foveal structure and function become significantly affected by the profound atrophy; however, we observed that the foveal structure and function were relatively preserved for up to six years in patients 8 and 12. Eventually, the remaining foveal tissue became progressively smaller, and atrophy of the central fovea was observed in four eyes (in patients 10, 11 and 12, Figures 9.4L, 9.4N and 9.5E); this was accompanied by a decline in central vision to 20/200 or worse.

9

Table 9.2. Results of progression analysis on fundus autofluorescence (FAF) imaging during follow-up in STGD1 patients with foveal sparing.

ID	Age at initial visit (years)	Duration follow-up		Eye	Atrophy at initial visit (mm²)*	Atrophy at follow-up (mm²)*	Expansion during follow-up (mm²)*	Progression rate (mm²/ year)*
		Days	*Years*					
P1	57	597	1.6	Right	3.517	4.877	1.36	0.832
P2	59	842	2.3	Right	11.792	15.770	3.978	1.726
				Left	11.202	16.43	5.228	2.268
P8	63	1657	4.5	Right	16.308	27.027	10.719	2.363
P9	62	420	1.1	Right	3.570	4.601	1.031	0.897

*Measurements were performed by two authors (RACvH and NMB), and the average of the two measurements are shown. Mean interobserver variance was 2.7% (range: 0.4%-9.8%).

Genetic analysis and mutation screening

An examination of the pedigrees of the 13 unrelated patients with foveal sparing revealed a recessive inheritance pattern in five patients; the other eight patients appeared to be isolated cases. Mutations in the *ABCA4* gene were identified in 19 of the 26 alleles (73%, Table 9.3). We identified compound heterozygous mutations in six patients (46%) and single heterozygous mutations in the other seven patients (54%). In total, 13 different *ABCA4* variants were identified, including nine missense mutations, two splice site mutations, one nonsense mutation, and one synonymous variant that affects splicing.[23] Each of these variants has been described previously (Table 9.3).

The mutational effects of five of the identified mutations have been reported previously (Table 9.4). Although functional data regarding the effects of the other eight mutations is not available, we can speculate on the functional effect of the nonsense mutation (p.Gln1292*). Assuming that the resulting mRNA is not subject to nonsense-mediated decay, the resulting truncated protein will lack the second extracytoplasmic domain and the nucleotide-binding domain, which are involved in substrate and ATP binding, respectively.[32] Table 9.5 summarizes the identified missense mutations in *ABCA4*, including allele frequencies in the exome variant server (EVS) and scores obtained from selected predictive tools. No differences in phenotype were observed between patients carrying severe mutations and patients carrying mild mutations. Finally, no pathogenic mutations in the *PRPH2* gene were identified in this cohort, thereby excluding the possibility of pseudo-Stargardt pattern dystrophy.[27]

Table 9.3. ABCA4 mutations in STGD1 patients with foveal sparing

ID	Allele 1		Allele 2		References
	DNA variant	Effect	DNA variant	Effect	
P1	c.5461-10T→C	Unknown	NI	NA	35, 36
P2	c.3113C→T	p.Ala1038Val	c.3874C→T	p.Gln1292*	16, 37, 38, 58
P3	c.5461-10T→C	Unknown	c.5537T→C	p.Ile1846Thr	23, 35, 39, 58
P4	c.4363T→C	p.Cys1455Arg	NI	NA	40
P5	c.1822T→A	p.Phe608Ile	c.4685T→C	p.Ile1562Thr	23, 40, 41
P6	c.768G→T	Splice defect	c.3113C→T	p.Ala1038Val	16, 23, 37
P7	c.5196+1G→T	Splice defect	NI	NA	45, 58
P8	c.3874C→T	p.Gln1292*	NI	NA	38
P9	c.5461-10T→C	Unknown	NI	NA	35, 58
P10	c.1822T→A	p.Phe608Ile	NI	NA	23, 41
P11	c.286A→G	p.Asn96Asp	NI	NA	43
P12	c.1805G→A	p.Arg602Gln	c.4462T→C	p.Cys1488Arg	37, 39, 42-44
P13	c.3874C→T	p.Gln1292*	c.1928T→G	p.Val643Gly	38, 45

NI, not identified. * = nonsense mutation. NA, not applicable

Discussion

Here, we present the clinical characteristics of 13 STGD1 patients with foveal sparing in one or both eyes. The majority of these patients were diagnosed with late-onset STGD1; only three patients developed symptoms prior to the age of 45 (Table 9.1). In eyes with foveal sparing, visual acuity was relatively preserved; nevertheless, most of the patients experienced some loss of vision, which caused them to seek ophthalmologic care. In these instances, ophthalmoscopy readily revealed advanced retinal disease, with yellow-white irregular pisciform flecks and profound RPE atrophy adjacent to the fovea. Automated perimetry revealed perifoveal scotomas of various sizes with intact foveal sensibility. This combination of mild vision loss together with profound retinal abnormalities is typical among STGD1 patients with foveal sparing.

Recently, Fujinami et al. reported the clinical and molecular findings of a cohort of Stargardt patients with a foveal sparing phenotype.[26] In their study, the authors included STGD1 patients with a functional fovea, irrespective of the presence of parafoveal RPE atrophy; thus, they studied a heterogeneous cohort of 40 patients. In contrast, in our cohort we defined foveal sparing as profound RPE atrophy that surrounded the fovea by at least 180 degrees and spared the fovea's structure and function. This clinical presentation is an rare finding among STGD1 patients, and our strict selection criterion resulted in a small but homogeneous cohort with a consistent phenotype and excluded STGD1 patients with late-onset disease that initiated with foveal atrophy. Moreover, our definition of foveal sparing is consistent with previously reported cases of foveal sparing in patients with other degenerative diseases.[6, 8, 33, 34] Despite the differences between our cohort and that the cohort described by Fujinami et

al., the visual acuity and electrophysiology findings in their paper are similar to the findings in our study; nevertheless, none of our patients were carriers of the *ABCA4* p.Arg2030Gln missense mutation, which was suggested previously to be prevalent among STGD1 patients with foveal sparing.[26]

Table 9.4. Functional implications of ABCA4 mutations

DNA variant (Effect)	Type of mutation	No. of Alleles	Predicted Effect on ABCR function	Classification of Mutations
c.768G→T (splice defect)	Splice site	1	No protein produced[23]	Severe
c.1805G→A (p.Arg602Gln)	Missense	1	No protein function due to mislocalization of the protein to the inner segment of the photoreceptor[42]	Severe
c.3113C→T (p.Ala1038Val)	Missense	2	Decreased ATP binding and ATPase activity[37]	Mild/Moderate
c.4462T→C (p.Cys1488Arg)	Missense	1	Decreased ATPase activity, reduced all-*trans*-retinal binding[37, 44]	Mild/Moderate
c.5461-10T→C (Unknown)	Splice site	3	Splice site intact, but presumed to be linked with an unidentified pathologic *ABCA4* mutation (linkage disequilibrium)[59]	Unknown

ATP, adenosine triphosphate; ATPase, adenosine triphosphatase.

The etiology of foveal sparing

In our study, screening the *ABCA4* gene identified 19 pathogenic mutations that were described previously in STGD1 and/or other *ABCA4*-associated retinopathies (Table 9.3);[16, 23, 35-45] interesting, however, foveal sparing was not described in any of the patients who were previously reported to carry these mutations. In a previously proposed model that links phenotype severity to the degree of residual ABCR function,[23, 24] late-onset STGD1 with foveal sparing was placed at the mild end of the spectrum of *ABCA4*-associated retinopathies.[3] Indeed, none of our STGD1 patients with foveal sparing had two *ABCA4* variants that are associated with a severe loss of ABCR function. However, our knowledge regarding the functional consequences of *ABCA4* mutations identified to date is limited (Table 9.4). It can be extremely difficult to assess the effect of most missense variants using *in silico* predictions and allele frequencies in healthy individuals, for whom this information is often incomplete (Table 9.5); in addition, assessing the combined effect of carrying two *ABCA4* variants is particularly difficult. Functional assays are needed in order to form definitive conclusions regarding the effects of these mutations.

Because foveal sparing can be present in phenotypes that are independent of *ABCA4* mutations, including AMD and mitochondrial retinal dystrophy,[6, 8-12, 17, 20, 25, 44, 45] genetic factors other than *ABCA4* mutations are likely involved. These factors could include single-nucleotide polymorphisms (SNPs) and even mutations in retina-specific genes other than

ABCA4, which suggests that a digenic or triallellic trait—in combination with the identified *ABCA4* mutations—may underlie the degenerative pattern observed in our patients. Moreover, anatomical, metabolic, and/or biochemical factors may underlie foveal sparing. For example, the average peak density of cones in the fovea is 199,000 cones/mm^2, but can range from 98,200 to 324,100 cones/mm^2.[2] The initial number of cones in the fovea cones may play a role in the development of foveal sparing; however, adaptive optics imaging techniques—which can provide the resolution needed to determine photoreceptor density *in vivo*—are not generally available in most ophthalmology practices. Another factor to consider is that S ("blue") cone photoreceptors, which are absent in the foveal center, seem to be more vulnerable to retinal disease than M and L cones, although this selective vulnerability has not been reported in STGD1.[46, 47] Moreover, parafoveal rods appear to be more vulnerable than cones to the effects of aging and all-*trans*-retinal – mediated damage.[48-50] This difference may arise from the sole dependence of rods on the RPE for replenishing 11-*cis*-retinal; in contrast, cones are also supplied by Müller cells.[51] Furthermore, cone cells have a slower turnover rate of outer segments compared to rods,[52] although this does not necessarily result in higher all-*trans*-retinal levels in RPE cells, as regeneration is faster in cones than in rods.[51] Macular pigments, which can filter out high-energy light, may also serve a protective role, given that light exposure is crucial in the pathogenesis of STGD1.[53, 54] In addition, rod-derived cone viability factor (RdCVF), which is believed to prevent cone degeneration,[55] may also play a role. Importantly, the absolute levels of macular pigments and RdCVF may differ between STGD1 patients with foveal sparing and STGD1 patients without foveal sparing.

Differential diagnosis and clinical significance of foveal sparing
When forming a diagnosis, foveal sparing – associated clinical entities other than late-onset STGD should be considered, including geographic atrophy in AMD, mitochondrial retinal dystrophy associated with the m.3243A→G mutation, central areolar choroidal dystrophy, and pseudo-Stargardt pattern dystrophy.[6, 9, 10, 27, 29] Importantly, misdiagnosing this condition can lead to inappropriate genetic counseling (these diseases display unique inheritance patterns) and/or an inaccurate estimate of the prognosis. Furthermore, in the event of an incorrect diagnosis of AMD, prescribing vitamin A – rich nutritional supplements can accelerate the accumulation of all-*trans*-retinal – derived toxins and increase the rate of disease progression, as shown in the retinas of homozygous *Abca4*-knockout mice.[56] STGD1 with foveal sparing can be diagnosed based on the presence of characteristic pisciform flecks together with RPE atrophy surrounding the fovea, a "dark choroid" sign on FA, and genetic analysis of the *ABCA4* gene. FAF imaging can clearly highlight the fundus flecks, which appear as hyperautofluorescent flecks, and RPE atrophy, which appears as an absence of autofluorescence. Retinal dystrophies that closely resemble STGD1 can follow other patterns of inheritance—for example, due to mutations in mitochondrial DNA—or can be autosomal dominant, with variable penetrance and expression. The fact that the "dark choroid" sign is present in approximately 85% of patients with STGD1[57] suggests a pivotal role for genetic analysis in the diagnosis of retinal dystrophies.

In conclusion, foveal sparing is a clinical phenomenon that occurs primarily in patients with late-onset STGD1 and is associated with the relative preservation of visual acuity, although visual acuity ultimately deteriorates by the end-stage of the disease. STGD1 patients with foveal sparing may be promising candidates for future therapeutic trials, as delayed degeneration of the fovea increases the time window for applying therapeutic interventions such as gene therapy. Although the mechanisms that underlie foveal sparing are currently unclear, expanding our knowledge of the metabolic and biochemical processes that lead to foveal sparing can facilitate the development of therapeutic strategies aimed at preserving foveal function.

Table 9.5. Characteristics of the missense mutations identified in *ABCA4* in this study.

Variants with unknown pathogenicity

DNA Variant	Effect	PhyloP[1]	Gran-tham[2]	Allele frequency in EVS[3]	SIFT (Class: score)[4]	Polyphen-2 (Class: score)[5]	Align GVGD[6]	Hypothetic effect
c.286A>G	p.Asn96Asp	3.27	23	1 in 8600	Deleterious (score: 0.00)	Possibly damaging: 0.852	Class C15	Unclear
c.1822T>A	p.Phe608Ile	3.27	21	1 in 8600	Deleterious (score: 0.00)	Possibly damaging: 0.937	Class C15	Unclear
c.1928T>G	p.Val643Gly	4.81	109	24 in 8600	Deleterious (score: 0.00)	Benign: 0.213	Class C65	Mild
c.4363T>C	p.Cys1455Arg	4.64	180	N/A	Deleterious (score: 0.00)	Probably damaging: 0.999	Class C65	Moderate/severe
c.4685T>C	p.Ile1562Thr	3.19	89	17 in 8600	Deleterious (score: 0.02)	Benign:0.060	Class C25	Mild
c.5537T>C	p.Ile1846Thr	4.81	89	N/A	Deleterious (score: 0.00)	Probably damaging: 0.997	Class C65	Moderate/severe

Variants with known pathogenicity

DNA Variant	Effect	PhyloP	Gran-tham	Allele frequency in EVS	SIFT (Class: score)	Polyphen-2 (Class: score)	Align GVGD	Effect
c.1805G>A	p.Arg602Gln	4.24	43	1 in 8600	Deleterious (score: 0.00)	Possibly damaging: 0.896	Class C35	Severe[7]
c.3113C>T	p.Ala1038Val	6.34	64	19 in 8600	Deleterious (score: 0.00)	Benign: 0.009	Class C65	Mild/moderate[8]
c.4462T>C	p.Cys1488Arg	4.89	180	N/A	Deleterious (score: 0.00)	Possibly damaging: 0.874	Class C65	Mild/moderate[8,9]

EVS, exome variant server; N/A, not available; PhyloP, phylogenetic profiling.

1. Siepel A, Pollard KS, Haussler D. Proceedings of the 10th International Conference on Research in Computational Molecular Biology (RECOMB 2006: April 2–5, 2006, Venice Lido, Italy) 2006. New methods for detecting lineage-specific selection; pp. 190–205.
2. Grantham R. Amino acid difference formula to help explain protein evolution. *Science.* 1974 Sep 6;185(4154):862-4.
3. Available at http://evs.gs.washington.edu/EVS/.
4. Available at http://sift.jcvi.org.
5. Available at http://genetics.bwh.harvard.edu/pph2/.
6. Tavtigian SV, Byrnes GB, Goldgar DE, Thomas A. Classification of rare missense substitutions, using risk surfaces, with genetic- and molecular-epidemiology applications. *Hum Mutat.* 2008 Nov;29(11):1342-54.
7. Wiszniewski W, Zaremba CM, Yatsenko AN, et al. ABCA4 mutations causing mislocalization are found frequently in patients with severe retinal dystrophies. Hum Mol Genet 2005;14:2769-2778.
8. Sun H, Smallwood PM, Nathans J. Biochemical defects in ABCR protein variants associated with human retinopathies. Nat Genet 2000;26:242-246.
9. Biswas-Fiss EE, Kurpad DS, Joshi K, Biswas SB. Interaction of extracellular domain 2 of the human retina-specific ATP-binding cassette transporter (ABCA4) with all-trans-retinal. J Biol Chem 2010;285:19372-19383.

9

References

1. Curcio CA, Sloan KR, Jr., Packer O, Hendrickson AE, Kalina RE. Distribution of cones in human and monkey retina: individual variability and radial asymmetry. *Science (80-)* 1987;236:579-582.
2. Curcio CA, Sloan KR, Kalina RE, Hendrickson AE. Human photoreceptor topography. *J Comp Neurol* 1990;292:497-523.
3. Westeneng-van Haaften SC, Boon CJ, Cremers FP, Hoefsloot LH, den Hollander AI, Hoyng CB. Clinical and Genetic Characteristics of Late-onset Stargardt's Disease. *Ophthalmology* 2012;119:1199-1210.
4. Rotenstreich Y, Fishman GA, Anderson RJ. Visual acuity loss and clinical observations in a large series of patients with Stargardt disease. *Ophthalmology* 2003;110:1151-1158.
5. Nakao T, Tsujikawa M, Sawa M, Gomi F, Nishida K. Foveal sparing in patients with Japanese Stargardt's disease and good visual acuity. *Jpn J Ophthalmol* 2012;56:584-588.
6. de Laat P, Smeitink JA, Janssen MC, Keunen JE, Boon CJ. Mitochondrial Retinal Dystrophy Associated with the m.3243A>G Mutation. *Ophthalmology* 2013;120:2684-2696.
7. Baker CI, Dilks DD, Peli E, Kanwisher N. Reorganization of visual processing in macular degeneration: replication and clues about the role of foveal loss. *Vision Res* 2008;48:1910-1919.
8. Forte R, Querques G, Querques L, Leveziel N, Benhamou N, Souied EH. Multimodal evaluation of foveal sparing in patients with geographicatrophy due to age-related macular degeneration. *Retina* 2013;33:482-489.
9. Mones J, Biarnes M, Trindade F, Arias L, Alonso J. Optical coherence tomography assessment of apparent foveal swelling in patients with foveal sparing secondary to geographic atrophy. *Ophthalmology* 2013;120:829-836.
10. Schmitz-Valckenberg S, Fleckenstein M, Helb HM, Charbel Issa P, Scholl HP, Holz FG. In vivo imaging of foveal sparing in geographic atrophy secondary to age-related macular degeneration. *Invest Ophthalmol Vis Sci* 2009;50:3915-3921.
11. Sunness JS, Rubin GS, Zuckerbrod A, Applegate CA. Foveal-Sparing Scotomas in Advanced Dry Age-Related Macular Degeneration. *J Vis Impair Blind* 2008;102:600-610.
12. Stargardt K. Über familliäre, progressive Degeneration in der Maculagegend des Auges. *Graefes Arch Clin Exp Ophthalmol* 1909;534-550.
13. Fishman GA, Stone EM, Grover S, Derlacki DJ, Haines HL, Hockey RR. Variation of clinical expression in patients with Stargardt dystrophy and sequence variations in the ABCR gene. *Arch Ophthalmol* 1999;117:504-510.
14. Lois N, Holder GE, Bunce C, Fitzke FW, Bird AC. Phenotypic subtypes of Stargardt macular dystrophy-fundus flavimaculatus. *Arch Ophthalmol* 2001;119:359-369.
15. Lois N, Holder GE, Fitzke FW, Plant C, Bird AC. Intrafamilial variation of phenotype in Stargardt macular dystrophy-Fundus flavimaculatus. *Invest Ophthalmol Vis Sci* 1999;40:2668-2675.
16. Allikmets R, Singh N, Sun H, et al. A photoreceptor cell-specific ATP-binding transporter gene (ABCR) is mutated in recessive Stargardt macular dystrophy. *Nat Genet* 1997;15:236-246.
17. Molday LL, Rabin AR, Molday RS. ABCR expression in foveal cone photoreceptors and its role in Stargardt macular dystrophy. *Nat Genet* 2000;25:257-258.
18. Sparrow JR, Wu Y, Kim CY, Zhou J. Phospholipid meets all-trans-retinal: the making of RPE bisretinoids. *J Lipid Res* 2010;51:247-261.
19. Cremers FP, van de Pol DJ, van Driel M, et al. Autosomal recessive retinitis pigmentosa and cone-rod dystrophy caused by splice site mutations in the Stargardt's disease gene ABCR. *Hum Mol Genet* 1998;7:355-362.
20. Birch DG, Peters AY, Locke KL, Spencer R, Megarity CF, Travis GH. Visual function in patients with cone-rod dystrophy (CRD) associated with mutations in the ABCA4(ABCR) gene. *Exp Eye Res* 2001;73:877-886.
21. Klevering BJ, Yzer S, Rohrschneider K, et al. Microarray-based mutation analysis of the ABCA4 (ABCR) gene in autosomal recessive cone-rod dystrophy and retinitis pigmentosa. *Eur J Hum Genet* 2004;12:1024-1032.
22. Klevering BJ, Maugeri A, Wagner A, et al. Three families displaying the combination of Stargardt's disease with cone-rod dystrophy or retinitis pigmentosa. *Ophthalmology* 2004;111:546-553.
23. Maugeri A, van Driel MA, van de Pol DJ, et al. The 2588G-->C mutation in the ABCR gene is a mild frequent founder mutation in the Western European population and allows the classification of ABCR mutations in patients with Stargardt disease. *Am J Hum Genet* 1999;64:1024-1035.

24. van Driel MA, Maugeri A, Klevering BJ, Hoyng CB, Cremers FP. ABCR unites what ophthalmologists divide(s). *Ophthalmic Genet* 1998;19:117-122.
25. Klevering BJ, Deutman AF, Maugeri A, Cremers FP, Hoyng CB. The spectrum of retinal phenotypes caused by mutations in the ABCA4 gene. *Graefes Arch Clin Exp Ophthalmol* 2005;243:90-100.
26. Fujinami K, Sergouniotis PI, Davidson AE, et al. Clinical and molecular analysis of stargardt disease with preserved foveal structure and function. *Am J Ophthalmol* 2013;156:487-501 e481.
27. Boon CJ, van Schooneveld MJ, den Hollander AI, et al. Mutations in the peripherin/RDS gene are an important cause of multifocal pattern dystrophy simulating STGD1/fundus flavimaculatus. *Br J Ophthalmol* 2007;91:1504-1511.
28. Marmor MF, Fulton AB, Holder GE, et al. ISCEV Standard for full-field clinical electroretinography (2008 update). *Doc Ophthalmol* 2009;118:69-77.
29. Boon CJ, Klevering BJ, Cremers FP, et al. Central areolar choroidal dystrophy. *Ophthalmology* 2009;116:771-782, 782 e771.
30. Spaide RF, Curcio CA. Anatomical correlates to the bands seen in the outer retina by optical coherence tomography: literature review and model. *Retina* 2011;31:1609-1619.
31. Zweifel SA, Engelbert M, Laud K, Margolis R, Spaide RF, Freund KB. Outer retinal tubulation: a novel optical coherence tomography finding. *Arch Ophthal* 2009;127:1596-1602.
32. Tsybovsky Y, Molday RS, Palczewski K. The ATP-binding cassette transporter ABCA4: structural and functional properties and role in retinal disease. *Adv Exp Med Biol* 2010;703:105-125.
33. Sunness JS, Bressler NM, Maguire MG. Scanning laser ophthalmoscopic analysis of the pattern of visual loss in age-related geographic atrophy of the macula. *Am J Ophthalmol* 1995;119:143-151.
34. Rath PP, Jenkins S, Michaelides M, et al. Characterisation of the macular dystrophy in patients with the A3243G mitochondrial DNA point mutation with fundus autofluorescence. *Br J Ophthalmol* 2008;92:623-629.
35. Maugeri A, Klevering BJ, Rohrschneider K, et al. Mutations in the ABCA4 (ABCR) gene are the major cause of autosomal recessive cone-rod dystrophy. *Am J Hum Genet* 2000;67:960-966.
36. Roberts LJ, Nossek CA, Greenberg LJ, Ramesar RS. Stargardt macular dystrophy: common ABCA4 mutations in South Africa--establishment of a rapid genetic test and relating risk to patients. *Mol Vis* 2012;18:280-289.
37. Sun H, Smallwood PM, Nathans J. Biochemical defects in ABCR protein variants associated with human retinopathies. *Nat Genet* 2000;26:242-246.
38. Ernest PJ, Boon CJ, Klevering BJ, Hoefsloot LH, Hoyng CB. Outcome of ABCA4 microarray screening in routine clinical practice. *Mol Vis* 2009;15:2841-2847.
39. Webster AR, Heon E, Lotery AJ, et al. An analysis of allelic variation in the ABCA4 gene. *Invest Ophthalmol Vis Sci* 2001;42:1179-1189.
40. Rosenberg T, Klie F, Garred P, Schwartz M. N965S is a common ABCA4 variant in Stargardt-related retinopathies in the Danish population. *Mol Vis* 2007;13:1962-1969.
41. Lewis RA, Shroyer NF, Singh N, et al. Genotype/Phenotype analysis of a photoreceptor-specific ATP-binding cassette transporter gene, ABCR, in Stargardt disease. *Am J Hum Genet* 1999;64:422-434.
42. Wiszniewski W, Zaremba CM, Yatsenko AN, et al. ABCA4 mutations causing mislocalization are found frequently in patients with severe retinal dystrophies. *Hum Mol Genet* 2005;14:2769-2778.
43. Papaioannou M, Ocaka L, Bessant D, et al. An analysis of ABCR mutations in British patients with recessive retinal dystrophies. *Invest Ophthalmol Vis Sci* 2000;41:16-19.
44. Biswas-Fiss EE, Kurpad DS, Joshi K, Biswas SB. Interaction of extracellular domain 2 of the human retina-specific ATP-binding cassette transporter (ABCA4) with all-trans-retinal. *J Biol Chem* 2010;285:19372-19383.
45. Allikmets R, Shroyer NF, Singh N, et al. Mutation of the Stargardt disease gene (ABCR) in age-related macular degeneration. *Science (80-)* 1997;277:1805-1807.
46. Pokorny J SV, Verriest G, Pinckers A. *Congenital and Acquired Color Vision Defects*. New York: Grune & Stratton; 1979.
47. Greenstein VC, Hood DC, Ritch R, Steinberger D, Carr RE. S (blue) cone pathway vulnerability in retinitis pigmentosa, diabetes and glaucoma. *Invest Ophthalmol Vis Sci* 1989;30:1732-1737.
48. Curcio CA. Photoreceptor topography in ageing and age-related maculopathy. *Eye (Lond)* 2001;15:376-383.
49. Curcio CA, Millican CL, Allen KA, Kalina RE. Aging of the human photoreceptor mosaic: evidence for selective vulnerability of rods in central retina. *Invest Ophthalmol Vis Sci* 1993;34:3278-3296.

9

50. Okano K, Maeda A, Chen Y, et al. Retinal cone and rod photoreceptor cells exhibit differential susceptibility to light-induced damage. *J Neurochem* 2012;121:146-156.
51. Wang JS, Kefalov VJ. The cone-specific visual cycle. *Prog Retin Eye Res* 2011;30:115-128.
52. Anderson DH, Fisher SK, Erickson PA, Tabor GA. Rod and cone disc shedding in the rhesus monkey retina: a quantitative study. *Exp Eye Res* 1980;30:559-574.
53. Weiter JJ, Delori F, Dorey CK. Central sparing in annular macular degeneration. *Am J Ophthalmol* 1988;106:286-292.
54. Aleman TS, Cideciyan AV, Windsor EA, et al. Macular pigment and lutein supplementation in ABCA4-associated retinal degenerations. *Invest Ophthalmol Vis Sci* 2007;48:1319-1329.
55. Leveillard T, Mohand-Said S, Lorentz O, et al. Identification and characterization of rod-derived cone viability factor. *Nat Genet* 2004;36:755-759.
56. Radu RA, Yuan Q, Hu J, et al. Accelerated accumulation of lipofuscin pigments in the RPE of a mouse model for ABCA4-mediated retinal dystrophies following Vitamin A supplementation. *Invest Ophthalmol Vis Sci* 2008;49:3821-3829.
57. Fishman GA, Farber M, Patel BS, Derlacki DJ. Visual acuity loss in patients with Stargardt's macular dystrophy. *Ophthalmology* 1987;94:809-814.
58. Kitiratschky VB, Grau T, Bernd A, et al. ABCA4 gene analysis in patients with autosomal recessive cone and cone rod dystrophies. *Eur J Hum Genet* 2008;16:812-819.
59. Rivera A, White K, Stohr H, et al. A comprehensive survey of sequence variation in the ABCA4 (ABCR) gene in Stargardt disease and age-related macular degeneration. *Am J Hum Genet* 2000;67:800-813.

Authors

Nicole T.M. Saksens[1], Ramon A.C. van Huet[1], Janneke J.C. van Lith-Verhoeven[1,2], Anneke I. den Hollander[1,3], Carel B. Hoyng[1], Camiel J.F. Boon[1,4]

Affiliations

[1]*Department of Ophthalmology, Radboud University Medical Center, Nijmegen, the Netherlands*
[2]*Department of Ophthalmology, St. Elisabeth Hospital, Tilburg, the Netherlands*
[3]*Department of Human Genetics, Radboud University Medical Center, Nijmegen, the Netherlands*
[4]*Department of Ophthalmology, Leiden University Medical Center, Leiden, the Netherlands*

Dominant Cystoid Macular Dystrophy

10

Abstract

Objective. To describe the clinical characteristics and long-term follow-up in patients with autosomal dominant cystoid macular dystrophy (DCMD).

Design. Retrospective case series study.

Participants. Ninety-seven patients with DCMD.

Methods. Extensive ophthalmic examination, including visual acuity (VA), fundus photography, fluorescein angiography (FA), fundus autofluorescence (FAF) imaging, optical coherence tomography (OCT), color vision testing, dark adaptation testing, full-field electroretinography (ERG), and electro-oculography (EOG). Blood samples were obtained for DNA extraction and subsequent haplotype analysis.

Main Outcome Measures. Age at onset; VA; fundus appearance; characteristics on FA, FAF, OCT, ERG, and EOG.

Results. Cystoid fluid collections (CFCs) were the first retinal abnormalities detectable in DCMD, developing during childhood. At long-term follow-up, the CFCs decreased in size and number, and eventually disappeared with concurrent development of progressive chorioretinal atrophy and hyperpigmented deposits in the posterior pole. DCMD could be classified into 3 stages, based on characteristics on ophthalmoscopy, FAF, FA and OCT, as well as on results of electrophysiology. The staging system correlated with age and VA. In stage 1 DCMD (20 patients, 22%), patients were generally under the age of 20 and presented with CFCs with fine folding of the internal limiting membrane and mild pigment changes. In stage 2 DCMD (48 patients, 52%), the CFCs tended to decrease in size, and moderate macular chorioretinal atrophy developed. Patients with stage 3 DCMD (24 patients, 26%) were generally over the age of 50 and showed profound chorioretinal atrophy, as well as coarse hyperpigmented deposits in the posterior pole. Most patients were (highly) hyperopic (72 patients, 92%). All DCMD patients shared the disease haplotype at the DCMD locus at 7p15.3.

Conclusions. DCMD is a progressive retinal dystrophy, characterized primarily by early-onset cystoid fluid collections in the neuroretina, which distinguishes this disorder from other retinal dystrophies. The phenotypic range of DCMD can be classified into three stages. The genetic locus for this retinal dystrophy has been mapped to 7p15.3, but the involved gene is currently unknown.

Introduction

Dominant cystoid macular dystrophy (DCMD) is an autosomal-dominantly inherited retinal disorder that primarily affects the macula.[1, 2] A hallmark feature and presenting symptom of DCMD is the appearance of cystoid intraretinal fluid collections (CFCs) in the macula that resemble cystoid macular edema before any other visible retinal abnormalities appear. The onset of these CFCs is generally in the first or second decade of life. Most patients with DCMD have moderate to high axial hyperopia.[3-5] As the disease progresses, the CFCs diminish, and progressive central vision loss develops between 20-50 years of age due to progressive chorioretinal atrophy.[1, 5]

DCMD has been linked to a genetic interval on chromosome 7p15-p21,[6] but the causative gene has not been identified to date. DCMD has also been abbreviated as CYMD (OMIM 153880). In the Netherlands, one large family with DCMD is known and extensive genealogical studies revealed a common Dutch ancestor, who supposedly lived in the early 18th century.[4] In addition to this large Dutch family, one unrelated American family from Greek ancestry,[7] and an American and a Spanish patient,[8] have been described with presumed DCMD.[7, 9]

Little is known about the spectrum and variability of fundus abnormalities in DCMD, as well as the visual outcome. We report the clinical characteristics and follow-up data of the large Dutch DCMD family with 97 affected family members. Based on multimodal imaging and electrophysiological studies, we propose a clinical classification system for DCMD in 3 stages. In addition, we evaluate the therapeutic options and discuss a possible pathophysiologic disease sequence.
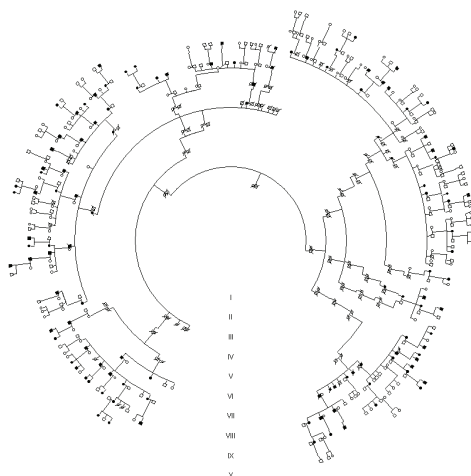
Figure 10.1. Diagram showing that all dominant cystoid macular dystrophy patients in The Netherlands belong to 1 large pedigree with a common ancestor.

Methods

Clinical Assessment

This study included 97 patients with DCMD, who were all examined at the Institute of Ophthalmology of the Radboud University Medical Center (Nijmegen, the Netherlands) between October 1958 and August 2013. All patients belong to one large pedigree, descending from one common Dutch ancestor (Figure 10.1).[4] Most patients originated from the southeast region of the Netherlands. Patients received the diagnosis of DCMD based on the aspect of the lesions on ophthalmoscopy, fluorescein angiography (FA) and optical coherence tomography (OCT).[4] In addition, genealogical research and haplotype analysis confirmed the diagnosis DCMD.

The medical history, age at onset, (best-corrected) Snellen visual acuity (VA), fundus appearance, including slit-lamp examination, fundus examination by indirect ophthalmoscopy, and fundus photography, as well as results of electrophysiological testing were retrieved from medical records. To analyze the course of the visual acuity over time, we recorded the age at which the decrease in VA exceeded 20/40, 20/60, and ≤ 20/200 for survival analyses. Fundus autofluorescence (FAF) imaging was performed with a confocal scanning laser ophthalmoscope (Spectralis; Heidelberg Engineering, Heidelberg, Germany; excitation light 488 nm). FAF follow-up images were available in 9 patients. Based on ophthalmoscopy and/or autofluorescence, mild atrophy of the retinal pigment epithelium (RPE) was defined as indistinct granular hypopigmented RPE changes, and profound atrophy was defined as sharply demarcated areas of chorioretinal atrophy in the macula, corresponding with a decrease and absence of autofluorescence. Spectral-domain OCT (Spectralis™, Heidelberg Engineering, Heidelberg, Germany) was performed using the "Macular Thickness Map" protocol provided by the manufacturer (Heidelberg Eye Explorer Software, version 1.6.4.0; Heidelberg Engineering, Heidelberg, Germany). Follow-up OCT scans were available in 14 patients to detect progression of retinal changes. Follow-up FA data were available in 29 of them. In addition electro-oculography (EOG), full-field electroretinography (ERG), visual field analysis by means of Goldmann perimetry (stimuli V4e-III4e-I4e-I3e-I2e-I1e), dark adaptation, and color vision testing were performed in selected patients as described previously (Table 10.1).[10] Altogether, follow-up data were available in 71 DCMD patients. Furthermore, 10 DCMD patients were invited for an additional, extensive clinical examination to complete the follow-up data resulting in a better appreciation of the disease course and characteristics. EOG and full-field ERG recordings were performed according to the standards of the International Society for Clinical Electrophysiology of Vision (ISCEV).[11-13] EOG Arden ratios were registered and stratified as normal (≥1.8), mildly reduced (<1.8, but ≥1.5), or severely reduced (<1.5). Full-field ERG was defined as normal (equal to or above the lower 5% of the range for a normal population: photopic ≥78 µV, scotopic ≥263 µV), subnormal in case of moderately reduced amplitudes of the B-wave (1-5% of normal range: photopic ≥69 µV and <78 µV, scotopic ≥195 µV and <263 µV) or as abnormal in case of severely reduced amplitudes (<1% of normal range: photopic <69 µV, scotopic <195 µV). The study adhered to the tenets of the Declaration of Helsinki, and Ethics Committee approval was obtained. Informed consent was received from all examined subjects.

Peripheral venous blood samples were obtained from 69 patients for analysis of the haplotypes at the previously described DCMD locus.[6] The haplotypes at the DCMD locus were also determined in 52 unaffected family members. The genomic DNA was isolated as described elsewhere.[14] Haplotype analysis was performed with microsatellite markers (D7S493 and D7S673) surrounding the genetic locus located at 7q15-p21.

Results

Clinical Findings

General characteristics. The study cohort included 97 patients, of which 55 were female (57%) and 42 male (43%), as well as 52 unaffected family members. The age at the first visit of the DCMD patients to our department ranged from 1 month to 72 years (median: 27 years). The mean age at onset of visual symptoms was 12.9 years (range: 2–45 years), and showed a remarkable trend of a lower age at onset in younger generations (p=0.02). At first presentation, the fundus aspect ranged from no abnormalities or only an absence of the foveal reflex and mild pigment changes in the fovea (Figure 10.2A) to profound chorioretinal atrophy with extensive hyperpigmentation in the posterior pole (Figure 10.2M).

All patients experienced a certain degree of central vision loss, with a progressive decline, but the course of the VA loss was highly variable among patients as shown in Figure 10.3. The age at which patients reached the level of legal blindness (VA ≤20/200) in the better eye, despite optimal refractive correction, varied widely from 10 to 65 years (median: 43.5 years). Two patients (2%) became totally blind (no light perception) in 1 eye, at the age of 58 and 73, respectively, due to serous retinal detachment that resulted in phthisis bulbi despite several vitreoretinal procedures. In addition to vision loss, 7 patients (7%) reported difficulties with night vision, and 5 patients (5%) with advanced disease experienced (para)central scotoma. Four female patients (7%) noticed a more rapid and irreversible visual decline during hormonal events, like first menarche, pregnancy, and menopause.

Hyperopia was a frequent finding in DCMD patients. Information about the refractive error of the eye was available in 78 patients, of which 72 presented with hyperopia, with a mean hyperopic refraction of +5.78 diopters (D, range of spherical equivalents (SE): +1.00 to +13.00 D), of which 30 patients (38%) were highly hyperopic (SE ≥+6.00 D). The axial length measurements were available in 24 eyes of 12 patients, performed with A-scan ultrasound measurement. In all cases, the axial length was significantly below normal (mean: 19.6 mm; range: 18.6–21.0 mm).

Acute angle-closure glaucoma occurred in 6 patients (6%), at a mean age of 48 years (range: 42-58 years). Although normal intraocular pressure could be accomplished by either topical treatment, laser intervention, surgical treatment or a combination, all 6 patients experienced irreversible vision loss. In 1 patient with acute angle-closure glaucoma, laser iridotomy and iridectomy treatment had insufficient effect. Finally, this patient received a Baerveldt tube implant which resulted in hypotonia, causing a serous retinal detachment. This was treated with pars plana vitrectomy with oil tamponade and laser treatment. The retina eventually redetached, resulting in complete blindness with phtisis bulbi leading to evisceration of this eye. The other eye was treated preventively with laser iridotomy resulting

10
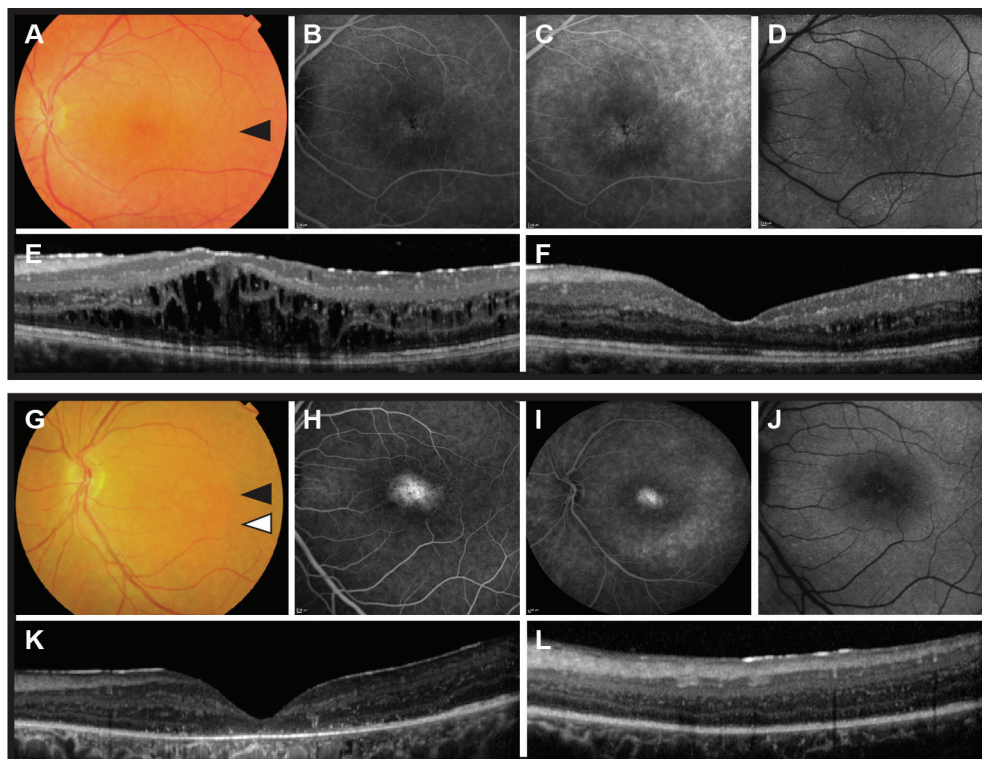
Figure 10.2. Clinical classification of dominant cystoid macular dystrophy (DCMD) into 3 stages: (A-F) stage 1 DCMD, (G-L) stage 2 DCMD, and (M-R) stage 3 DCMD. A, Color fundus photograph of a 15-year-old patient with stage 1 DCMD (visual acuity, 20/63; spherical equivalent [SE], +4.00 diopters [D]; subjectively fluctuating vision for 4 years) showing cystoid fluid collections (CFCs) and fine pigment changes in the macula. B, Fluorescein angiogram (FA; early phase) showing mild hyperfluorescence of the foveal fluid collections. C, Fluorescein angiography (late phase) image showing hyperfluorescent CFCs located in the fovea and more diffuse hyperfluorescence in the macula. D, Fundus autofluorescence image showing areas of mildly increased autofluorescence at the cystoid areas and diffuse hyperautofluorescence within the vascular arcades. E, Horizontal optical coherence tomography (OCT) scan through the fovea (scanning plane indicated by black arrowhead in A) showing CFCs in the inner and outer nuclear layer. F, Six months before, only some small CFCs were visible on OCT at the same level as in (E), demonstrating the fluctuating course of the CFCs without any treatment intervention. G, Color fundus photograph of a 32-year-old patient with stage 2 DCMD (visual acuity, 20/100; SE, +1.50 D) showing pigment changes in the macula and mild residual CFCs. H, I, Fluorescein angiogram showing a central hyperfluorescent lesion caused by a retinal pigment epithelium (RPE) window defect and residual edema in the early (H) and late (I) phase, surrounded by mild, indistinct hyperfluorescence. J, Fundus autofluorescence image showing moderately decreased autofluorescence in the central macula, corresponding with atrophy of the RPE in the fovea on OCT (K) at the level of the black arrowhead in (G). L, horizontal OCT scan through the scanning plane indicated by the white arrowhead in (G) showing possible mild thickening of the outer nuclear layer, but an RPE layer that seemed largely intact.

in a prolonged normal intra-ocular pressure. One patient with a narrow anterior chamber angle was treated preventively with phaco-emulsification, but nevertheless acute glaucoma developed in 1 eye.

Disease Spectrum and Clinical Classification. The spectrum of retinal abnormalities in this DCMD cohort could be subdivided generally into 3 stages by an experienced retina specialist (C.J.F.B.) based on ophthalmoscopy and supported by the findings obtained from multimodal imaging (Table 10.1). These 3 stages were delineated by analyzing ophthalmoscopic findings in combination with FA, FAF, and SD-OCT, which were available in 92 DCMD patients.

Stage 1 DCMD (20 patients, 22%; Table 10.1) was characterized by wrinkling of the internal limiting membrane, CFCs and mild granular pigment changes in the macula (Figure 10.2A). The CFCs were visible as mildly hyperautofluorescent areas in the fovea and perimacular area on fundus autofluorescence (Figure 10.2D); on OCT the CFCs were located in the inner and outer nuclear layer of the retina (Figure 10.2E). FA clearly showed an aspect of hyperfluorescent cystoid macular edema, and in 60% evidence of mild perifoveal capillary dilation was seen (Figure 10.2B and 10.2C). In 14 patients (70%) the CFCs gradually increased in size, number, and extent during follow-up, affecting the entire posterior pole. However, during this progression the degree of CFCs was highly variable, corresponding with intra-individual variability of the VA (Figure 10.2E-F and Figure 10.4A-E). In addition to the CFCs, in two patients with stage 1 DCMD the OCT also showed a serous detachment of the neuroretina with a fluctuating course.

The mean VA was 20/37 and decreased to less than 20/125 in only 4 patients (20%). In one patient with stage 1 DCMD and large CFCs who had a VA of 20/200, the VA recovered to 20/50 after remission of the cysts by treatment with acetazolamide.
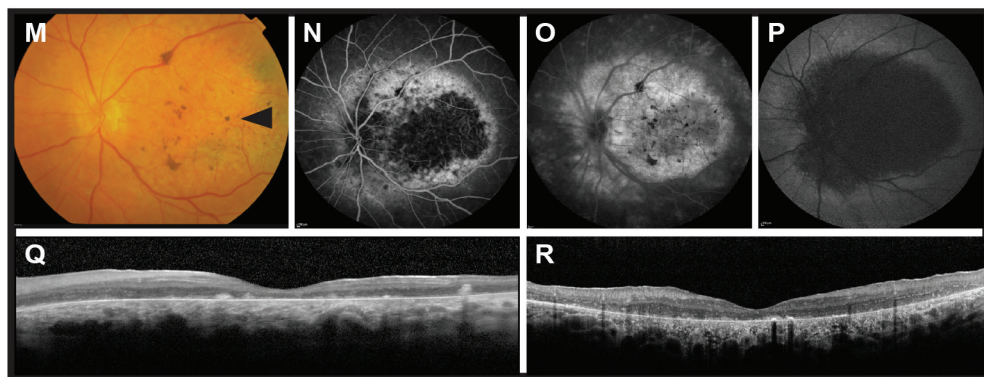
(**Figure 10.2. continued**) M, Color fundus photograph of a 67-year-old patient with stage 3 DCMD (visual acuity, 20/800; SE, +7.00 D) showing profound chorioretinal atrophy in the macula with attenuated arterioles and coarse hyperpigmentations. N, O, Early- (N) and late- (O) phase FA showing early hypofluorescence and some late staining in the deeply atrophic central macula encircled by hyperfluorescence that seems to be diffuse edema, extending beyond the vascular arcade and optic nerve. P, Fundus autofluorescence image showing a large area of markedly decreased autofluorescence as a result of RPE atrophy in and beyond the macula. Q, Horizontal OCT scan (scanned through plane indicated by black arrowhead in (M)) showing chorioretinal atrophy in the macula, with hyperreflective lesions consistent with the hyperpigmentations on color fundus photograph (M). R, Vertical OCT scan through the fovea of the fellow (right) eye showing marked attenuation of the outer photoreceptor and RPE layers, although there appears to be a certain degree of persistent thickening of the inner and outer nuclear layer centrally in the macula.
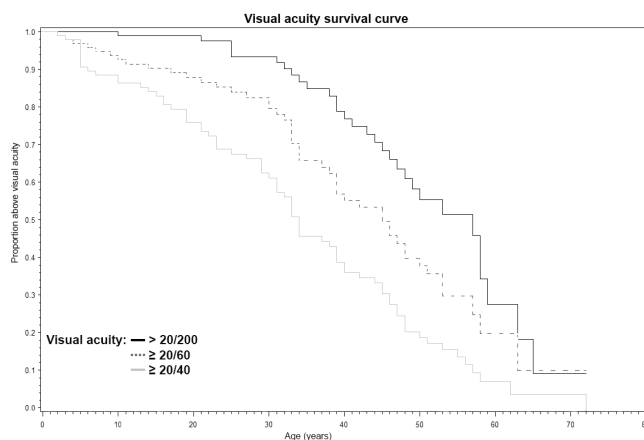
Figure 10.3. Kaplan-Meier survival curves of visual acuity (VA) of worse than 20/40 (a threshold of visual disability, according to the United States definition reflecting the legal inability to drive a car); VA of worse than 20/60 (a cutoff point for low vision defined by the World Health Organization criteria associated with increasing difficulties in reading without visual aids); VA of 20/200 or worse (a threshold of legal blindness according to World Health Organization criteria) related to age. The median ages at which the VA in our cohort exceeded 20/40, exceeded 20/60, and decreased to 20/200 or less were, 34, 45, and 57 years, respectively.

In *stage 2* DCMD (48 patients, 52%; Table 10.1), the CFCs tended to become progressively smaller over time (Figure 10.2K). Unlike stage 1 DCMD, only 5 cases showed evidence of perifoveal capillary dilatation on FA. Mildly atrophic lesions appeared in the macula, with a corresponding decrease in VA (Figure 10.2G, 10.2J and 10.2K).

In *stage 3* DCMD (24 patients, 26%; Table 10.1), the macula was affected by profound chorioretinal atrophy (Figure 10.2M-R). In the macula and mid-peripheral retina, multiple coarse hyperpigmentations were present in all patients, who also showed attenuated arterioles in varying degrees (Figure 10.2N). In this advanced disease stage, CFCs were no longer present on OCT (Figure 10.2Q and 10.2R). A variable degree of small whitish punctate deposits in the vitreous were seen in stage 2 and 3 DCMD.

The VA decreased to the level of legal blindness in 18 patients (75%) with stage 3 DCMD. Most patients (88%) were above the age of 50 years. The majority (77%) of the full-field ERG results were abnormal without selective cone or rod impairment in stage 3 DCMD (Figure 10.5). The EOG and full-field ERG results in all stages are depicted in Table 10.1. An atypical phenotype was seen in 4 patients with stage 3 DCMD (17%). In 2 patients (8%) a phenotype reminiscent of Coats' disease developed at the age of 56 and 61, respectively, consisting of an exudative serous retinal detachment with RPE atrophy and coarse hyperpigmentations (Figure 10.6A-B). Furthermore, two patients (44 and 57 years) originating from two different branches of the pedigree, showed a retinal phenotype similar to end-stage retinitis pigmentosa, with attenuated arterioles, peripheral pigment changes resembling bone spicules, a waxy-pale optic disc, in addition to advanced chorioretinal atrophy in the posterior pole (Figure 10.6C-D).

Table 10.1. Three Stages of Dominant Cystoid Macular Dystrophy

Stage	Mean Age [range] (n=92)	Mean VA [range] (n=92)	Fundoscopy (n=92)	Optical coherence tomography (n=30)	Fundus autofluorescence (n=20)	Fluorescein Angiography (n=54)	Electro-oculography† (n=65)	Electro-retinography‡ (n=61)	Goldmann perimetry (n=29)	Dark adaptation§ (n=34)	Color vision testing (n=50)
I	12.8 [0-32] (n=20)	20/37 [20/15 – 20/200] (n=20)	- Fine folding of ILM - CFCs - Mild granular pigment changes in the macula (n=20)	- CFCs (n=10)	- Mildly increased FAF in the macula (n=6)	- Hyperfluorescent CFCs - Perifoveal capillary dilation (n=15)	55% Normal 45% Mildly reduced (n=20)	100% Normal (n=13)	100% Normal (n=5)	38% Abnormal (n=8)	35% Diminished red-sensitivity (n=20)
II	37.7 [21-50] (n=48)	20/54 [20/20 – CF] (n=48)	- Mild but visible chorioretinal macular atrophy - CFCs (n=48)	- Mild retinal atrophy - Small CFCs (n=12)	- Moderately decreased FAF in the macula (n=9)	- Hyperfluorescent CFCs (n=26)	32% Normal 68% Mildly-severely reduced (n=34)	86% Normal 14% Subnormal (cone and rod) (n=35)	25% Peripheral visual field constriction (n=16)	33% Abnormal (n=18)	76% Blue-yellow Defect (n=17)
III	59.9 [44-72] (n=24)	20/212 [20/40-HM] (n=24)	- Profound, chorioretinal atrophy in the macula - Coarse hyper-pigmentations - Attenuated arterioles (n=24)	- Profound chorioretinal atrophy - No CFCs (n=8)	- Large area of decreased FAF corresponding to profound RPE atrophy (n=5)	- Early hypofluorescence with late staining of atrophic area, surrounded by hyperfluorescence (n=13)	73% Severely reduced (n=11)	23% Subnormal 77% Abnormal (cone and rod) (n=13)	63% Peripheral visual field constriction (n=8)	75% Abnormal (n=8)	100 % Blue-yellow defect 77% Additional red-green defect (n=13)

CF = counting fingers; CFCs = cystoid fluid collections; FA = fluorescein angiography; FAF = fundus autofluorescence; HM = hand movements; ILM = internal limiting membrane; RPE = retinal pigment epithelium; VA = visual acuity. †At examination. ‡Expressed in International Society for Clinical Electrophysiology of Vision Arden ratios: normal (>1.8), mildly reduced (<1.8, but >1.5), severely reduced (<1.5). ‡Full-field ERG results are defined as normal (photopic, >78 mV; scotopic, >263 mV), subnormal (photopic, >69 mV and <78 mV; scotopic, >195 mV and <263 mV) or abnormal (photopic: <69 mV, scotopic: <195 mV). §Abnormal dark adaptation responses are defined by an absolute threshold at 30 minutes raised at least 1.0 log U above reference values.

10

Natural course | Course with treatment
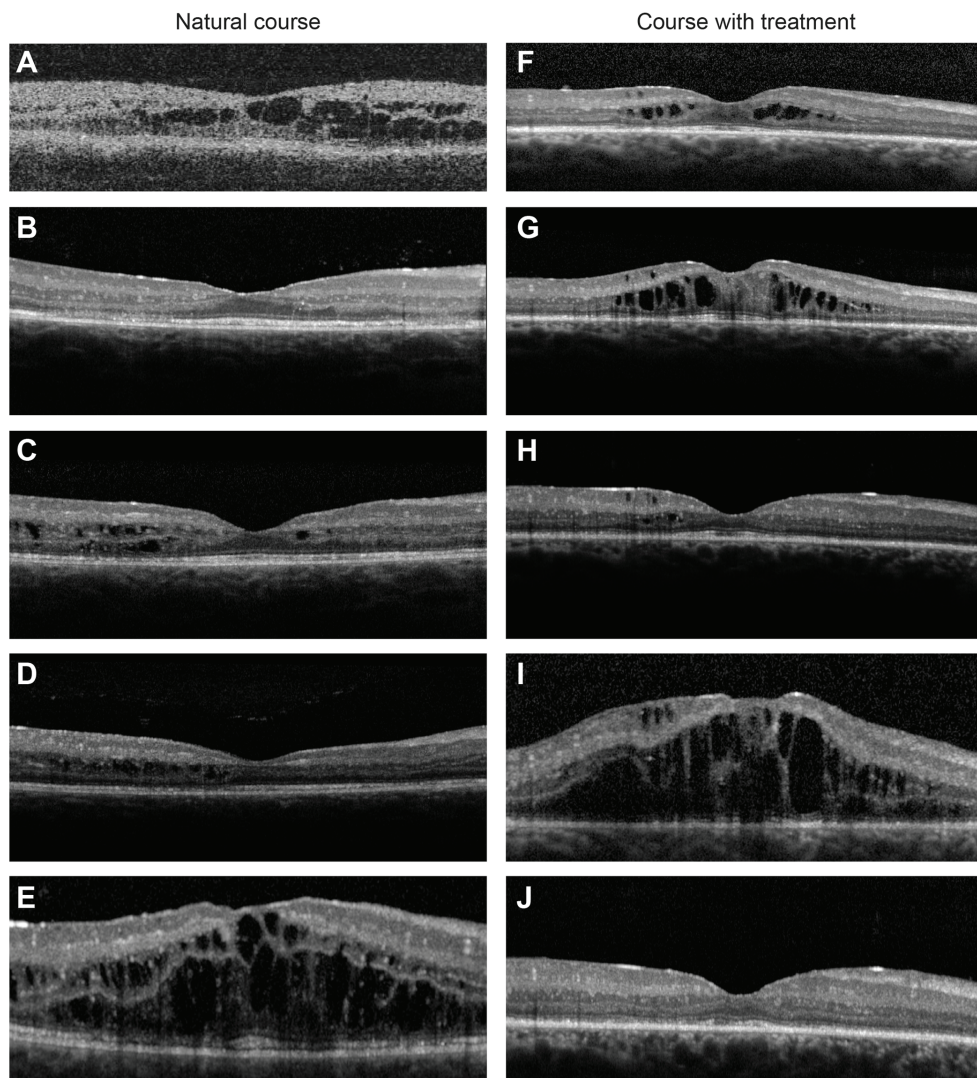
Figure 10.4. Follow-up of 2 dominant cystoid macular dystrophy (DCMD) patients with cystoid fluid collections (CFCs) on (A) time-domain or (B-J), spectral-domain optical coherence tomography (OCT). A-E, Patient with stage 1 DCMD and fluctuation of CFCs without treatment over 7 years. The OCT follow-up data of the left eye shows the fluctuating natural course of CFCs. **A**, At 8 years of age, OCT clearly showing moderate CFCs in the inner and outer nuclear layers without visual symptoms (visual acuity [VA], 20/20; spherical equivalent [SE], +4.00 diopters [D]). During the ensuing years, she experienced vision loss with fluctuating vision. **B**, At 11 years of age, no fluid collections were present on OCT, but funduscopy showed fine pigment changes in the fovea with some wrinkling of the internal limiting membrane. The patient experienced fluctuating vision for 1 year (VA in this eye, 20/40). **C**, Two months after the image in (B) was obtained, mild CFCs recurred and her visual symptoms increased (VA decreased to 20/63). **D**, Three years after the image in (C) was obtained, the CFCs and vision symptoms decreased, whereas the VA increased to 20/50. **E**, Five months after the image in (D) was obtained, extensive and large CFCs recurred, associated with vision loss (VA, 20/63). F-J, Stage 1 DCMD patient treated with octreotide-acetate (20 mg intramuscular monthly) and oral acetazolamide (250 mg 1-4 times daily), reducing the CFCs and showing a possible dose-dependent effect of acetazolamide on OCT follow-up of 1 year.

Figure 10.4. (continued) **F**, Nineteen-year-old patient with late stage 1 DCMD with mild CFCs causing visual symptoms before starting treatment (VA, 20/ 25; SE, +3.25 D). **G**, One year later, despite treatment with monthly intramuscular octreotide-acetate injections (20 mg) and oral acetazolamide 125 mg twice daily either separately or combined, CFCs increased with loss of vision (VA, 20/50). **H**, Increasing the dose of acetazolamide to 250 mg 3 times daily, in addition to octreotide-acetate treatment, resulted in a significant decrease of CFCs within 2 weeks, with an increase in VA to 20/32. **I**, The CFCs increased markedly within 2 weeks after lowering the dose of acetazolamide to 250 mg twice daily, with a corresponding vision loss (VA, 20/80). **J**, Raising the dose of acetazolamide to 250 mg 4 times daily resulted in a significant resolution of the CFCs within the next 2 weeks, with in an increase in VA to 20/50.
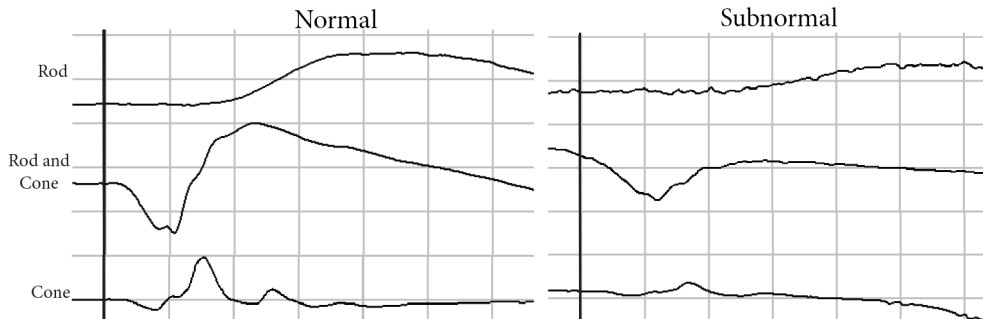
Figure 10.5. Representative full-field electroretinograms (ERGs) of 3 patients with dominant cystoid macular dystrophy (DCMD) showing normal, subnormal, and abnormal results of the rod, rod and cone, cone, and 30-hertz flicker ERG. Left, Normal full-field ERG results in a 15-year-old patient with stage 1 DCMD (visual acuity [VA], 20/50; spherical equivalent [SE], +4.25 diopters [D]). Middle, Subnormal cone- and rod-driven responses on full-field ERG in a 67-year-old patient with stage 3 DCMD (VA, 20/800; SE, +7.25 D). Right, Abnormal photopic and scotopic full-field ERG results in a 58-year-old patient with stage 3 DCMD (VA, 1/200; SE, +4.00 D).

Both patients showed fundoscopic signs of CFCs in their childhood. These two patients had difficulties with night vision, with markedly abnormal dark adaptation and marked constriction of the peripheral visual field on Goldmann perimetry. Full-field ERG showed no scotopic response and a decreased photopic response corresponding to a rod-cone dystrophy dysfunction pattern. Both patients had a subnormal EOG with mildly reduced Arden ratios. Both patients shared the genetic DCMD locus, and their affected parents showed a typical DCMD phenotype without these retinitis pigmentosa-like features.

The different stages of DCMD correlated significantly with age (r=0.871; p<0.001), VA (r=-0.562; p<0.001), EOG test results (r=-0.404; p<0.001) and ERG findings (r=-0.590; p<0.001) (Table 10.1). During progression of the disease, electrophysiological testing became more abnormal and constriction of the peripheral visual field developed in stage 2 and stage 3 DCMD. Of the 16 patients with stage 2 DCMD, 1 patient (6%) showed no abnormalities, 11 patients (69%)
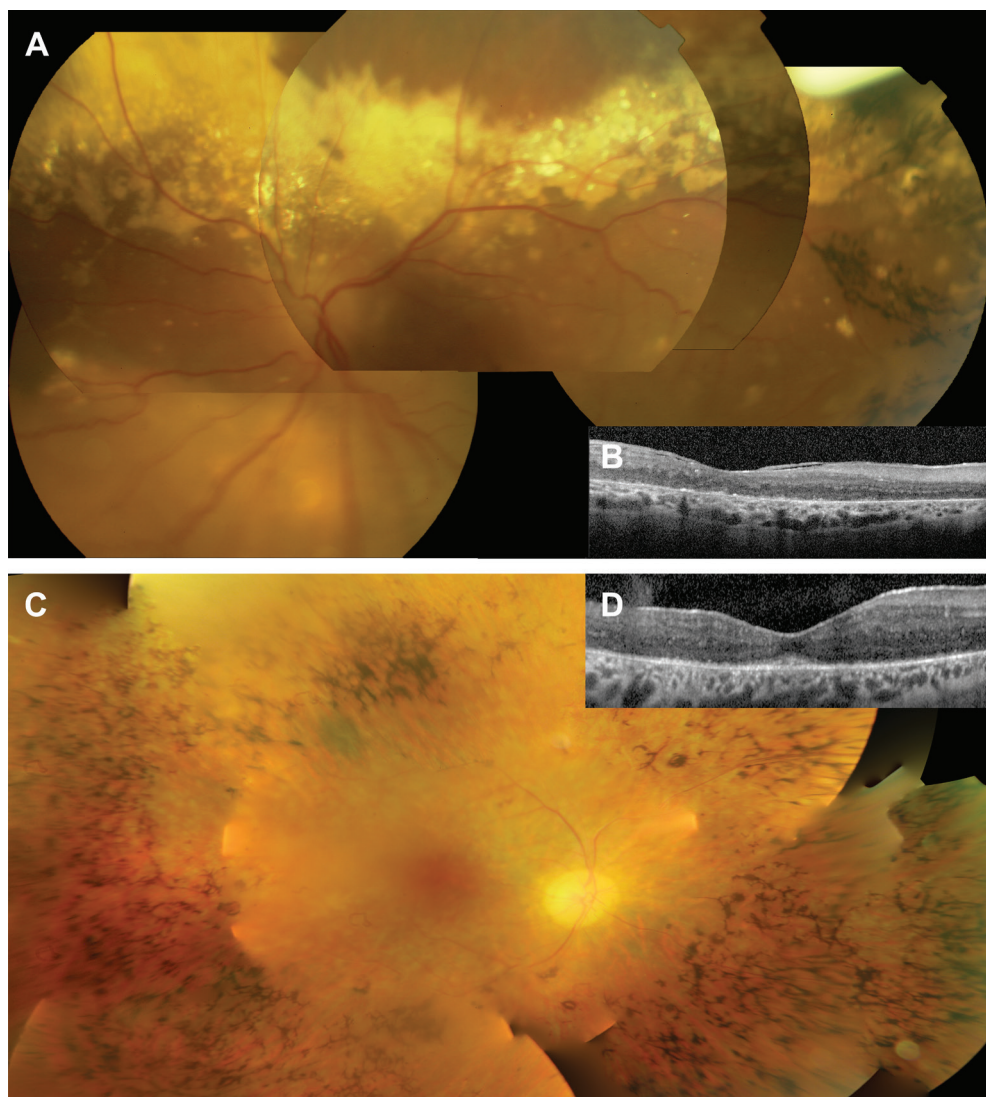
Figure 10.6. Atypical cases of dominant cystoid macular dystrophy (DCMD). A-B, Coats-like exudative abnormalities in a 62-year-old DCMD patient (visual acuity [VA], light perception; spherical equivalent [SE], +4.25 diopters [D]). **A**, Composite color fundus photograph showing a serous retinal detachment with exudates superior to the upper vascular arcade and temporal pigment accumulations mimicking bone spicules. This patient experienced vision loss at the age of 30 years, with cystoid fluid collections (CFCs) in the macula. **B**, Horizontal optical coherence tomography scan through the scanning plane indicated by the black arrowhead in (A) showing retinal atrophy and a mild epiretinal membrane. C-D, Retinitis pigmentosa-like phenotype in a 44-year-old patient with stage 3 DCMD (VA, 20/63; SE, +7.00 D) who also experienced night blindness and constriction of the peripheral visual fields. **C**, Composite color fundus photograph showing peripheral bone-spicule-like pigment changes, a waxypale optic disc, attenuated arterioles, and chorioretinal atrophy. Vision loss started at the age of 7 years with funduscopic foveal pigment changes and wrinkling of the internal limiting membrane. Because of loss of follow-up, no findings of CFCs are available, but in that period he experienced fluctuating vision loss. **D**, Optical coherence tomography scan through the fovea (black arrowhead in [C]) showing retinal pigment epithelium atrophy in the macula with some structural sparing of the fovea.

demonstrated small central absolute scotomata / sensitivity loss, and 4 (25%) patients showed sensitivity loss of the central retina with mild constriction of the peripheral visual field (40-50° nasal and 60-80° temporal for the II4e isopter). All stage 3 DCMD patients showed central absolute scotomata (15° for the V4e isopter) of which 5 patients (63%) additionally showed a moderate constricted peripheral visual field in Goldmann perimetry (25-45° nasal and 45-65° temporal for the III4e isopter and 0-25° nasal and 30-35° temporal for the I4e isopter) and 2 (25%) presented with nyctalopia. These were the 2 patients with the retinitis pigmentosa-like phenotype (Figure 10.4C).

In all DCMD stages, dark adaptation testing could be normal as well as abnormal, but abnormal test results were most often present in DCMD stage 3 (6/8; 75%). In stage 1 and 2 only 38% (3/8) and 33% (6/18), respectively, has an abnormal dark adaptation. From the 15 patients with abnormal dark adaptation, 8 underwent Goldmann perimetry, which revealed a constricted peripheral visual field in 3 patients (38%), who also had pigment lesions in their peripheral retina. Abnormalities of color vision testing were seen in all DCMD stages, ranging from anomaloscopic diminished red-sensitivity in stage 1 (35%), to an acquired blue-yellow defect in stage 2 (76%) and 3 (100%), with an additional red-green defect when fixation became eccentric in 10/13 stage 3 DCMD patients (77%).

Follow-up. Follow-up data were available for 71 patients, with a mean follow-up time of 17 years (range: 0.5-44 years). Fifteen patients (21%) progressed from stage 1 to stage 2 after a mean follow-up time of 17 years (range: 4-28 years) and 9 patients (13%) progressed from stage 2 to stage 3 after a mean time of 23 years (range: 10-35 years) (Figure 10.7). Additionally, a progression from stage 1, via stage 2, to stage 3 was observed in 3 patients (4%) after a mean time of 32 years (range: 29-34 years).

The degree of CFCs was observed to decrease progressively with advancing disease stages, while chorioretinal atrophy and pigmentary abnormalities concurrently became more pronounced. Visual acuity, EOG and full-field ERG data of patients who progressed from one stage of DCMD to the next stage are summarized in Table 10.2.

Treatment. During the natural course of DCMD stage 1 and 2, the degree of CFCs varied largely over time in 26 patients (mean follow-up: 18 years; range 4-43 years) (Figure 10.4A-E), but the fluid collections could also be influenced by treatment (Figure 10.4F-J). In an attempt to reduce the CFCs, 16 patients with stage 1 or 2 DCMD used acetazolamide, a carbonic anhydrase inhibitor, generally for several years (mean 40 months; range 2-221 months). In 10 of these patients (63%), oral administration of acetazolamide for several years (mean 56 months; range 2-221 months) seemed to result in a reduction of CFCs on OCT, with an improvement of the VA (mean VA from 20/46 to 20/35). In 2 patients (13%), the treatment resulted in reduction of CFCs without VA improvement. The daily dose in which a significant reduction of CFCs was seen on OCT ranged from 125 mg twice a day to 250 mg four times daily.

Octreotide-acetate, a somatostatin analogue assumed to promote the removal of intraretinal edema across the RPE,[15] was used in 16 patients with stage 1 or 2 DCMD for several years (mean 68 months; range 6-151 months).

10
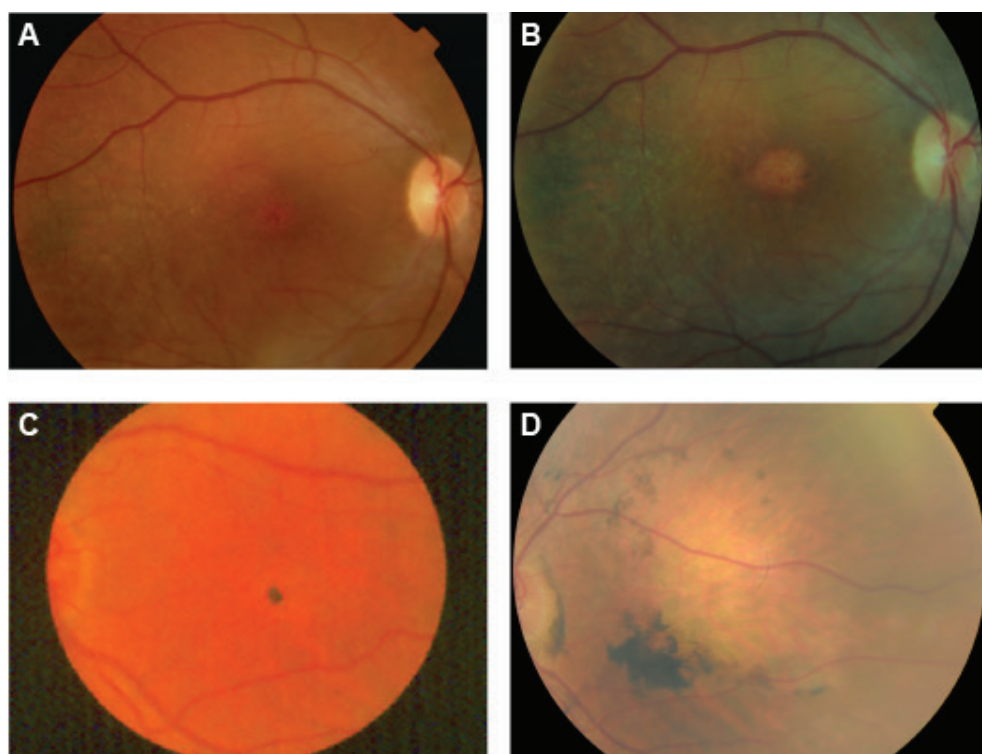
Figure 10.7. Long-term follow-up of dominant cystoid macular dystrophy (DCMD). A-D, Follow-up images showing (A, B) progression during stage 2 DCMD and (C, D) progression to stage 3 DCMD. A, Color fundus photograph of a 35-year-old patient with early stage 2 DCMD (visual acuity [VA], 20/160; spherical equivalent [SE], +7.00 diopters [D]) showing pigmentary changes of the retinal pigment epithelium and some small cystoid fluid collections (CFCs). At the age of 7 years, vision loss started and pigmentary changes and CFCs were seen. B, Ten years later, a central atrophic lesion developed with absence of CFCs. C,D, Follow-up color fundus photographs showing progression from stage 2 to stage 3 DCMD. C, Color fundus photograph of a 38-year-old patient with stage 2 DCMD (VA, 20/100; SE, +5.50 D) showing mild atrophic hypopigmentation and a central spot of hyperpigmentation.D, Thirty-five years later, a progression to profound chorioretinal atrophy with marked hyperpigmentations and some arteriolar attenuation was seen. The VA at this stage was 20/400.

Table 10.2. Follow-up results of patients who progressed to another stage of Dominant Cystoid Macular Dystrophy

Stage progres-sion	Stage	VA Mean	EOG* Normal	Mildly reduced	Severely reduced	Full-field ERG † Normal	Subnor-mal	Abnormal
1 → 2	1	20/25	6/8	2/8	0/8	2/2	0/2	0/2
	2	20/63	2/8	5/8	1/8	2/2	0/2	0/2
2 → 3	2	20/63	0/9	6/9	3/9	2/5	2/5	1/5
	3	20/300	0/9	3/9	6/9	0/5	0/5	5/5

*Electro-oculography Arden ratios were stratified as normal (>1.8), mildly reduced (<1.8 but _1.5), or severely reduced (<1.5). †Full-field electroretinography results were defined as normal in cases of normal amplitudes of the B-wave (photopic, >78 mV; scotopic, >263 mV), subnormal in cases of moderately reduced amplitudes (photopic, >69 mV and <78 mV; scotopic, >195 mV and <263 mV), or as abnormal in cases of severely reduced amplitudes (photopic, <69 mV; scotopic, <195 mV).

In 12 patients (75%), octreotide-acetate administered 20 mg intramuscular monthly for several years (mean 84 months; range 14-151 months) seemed effective in reducing CFCs and improving the VA with a mean increase in VA of 20/125, but in two patients (13%) side effects like nausea, diarrhea, fatigue and cholelithiasis were present, resulting in cessation of this treatment in 1 patient. Four patients (25%) treated with octreotide-acetate stopped the treatment because of the lack of effect on VA. In 3 of them, no effect on CFCs was detectable on OCT.

During six years of follow-up, in three patients with stage 1 DCMD who were treated, the mean VA increased from 20/34 to 20/25, whereas in four patients with stage 1 DCMD who were not treated, the mean VA decreased from 20/29 to 20/35. In stage 2 DCMD patients, the mean VA decreased from 20/51 to 20/67 in 12 treated patients with a follow-up of 17 years and in 12 untreated patients, the mean VA decreased from 20/54 to 20/87 during 15 years of follow-up.

Haplotype Analysis
Linkage analysis previously showed that DCMD is linked to the interval D7S493 – D7S526 at 7p15-p21,[6] but the disease-associated gene and mutation have not yet been identified. In 69 of the 97 clinically affected DCMD patients (71%), the haplotypes at the DCMD locus were analyzed, and all carried the disease-associated haplotype. The genetic DCMD locus seemed to be completely penetrant. Haplotype analysis in the 52 clinically unaffected family members revealed the absence of the DCMD haplotype in all. One DCMD patient with the genetic DCMD locus was also tested for the *BEST1* gene, but he showed no mutations in this gene.

Discussion

Clinical characteristics and staging of Dominant Cystoid macular dystrophy
Dominant cystoid macular dystrophy is a unique retinal dystrophy, because the appearance of CFCs in the macula is the first and most prominent abnormality at the onset of the disease, resembling cystoid macular edema.[16] The spectrum of severity of DCMD ranges from an absence of the foveal reflex with mild CFCs and some pigment changes in the macula early in the course of the disease, to profound chorioretinal atrophy in the posterior pole in the late stage of DCMD. In this study, we propose a clinical classification system for DCMD into three stages. This classification system is based on ophthalmoscopy and multimodal imaging, and correlates well with age, VA and results on EOG and full-field ERG (Table 10.1). We observed an evolution of DCMD through the proposed stages, supporting that DCMD is a progressive disease.

The age at onset of visual symptoms in DCMD is generally in childhood, but seems to vary depending on the generation. The apparently earlier age at onset in more recent generations may be due to an increased awareness and earlier screening of younger family members as a result of their affected father or mother.

All patients show a gradual decrease in VA, and most progress to visual disability at a relatively early age. In advanced DCMD, the VA generally evolves to finger counting (20/800), or even worse when relatively rare complications such as serous retinal detachment or acute angle-closure glaucoma occur. Due to the short axial length of the eye, glaucoma

can accompany the retinal abnormalities, and (high) hyperopia is present in most DCMD patients, similar to other retinal dystrophies such as the bestrophinopathies which are caused by mutations in the *BEST1* gene.[17, 18]

The finding that EOG abnormalities generally preceded photopic and scotopic dysfunction on full-field ERG indicates that impaired RPE function occurs earlier in the course of DCMD, whereas the panretinal photoreceptor function is affected later in the disease.[1] Since half of the stage 1 DCMD patients with macular CFCs had normal EOG results, primary panretinal RPE dysfunction with dysfunctional ionic homeostasis, as observed in *BEST1*-related dystrophies such as Best vitelliform macular dystrophy and autosomal recessive bestrophinopathy,[17] is presumably not present in DCMD. Presence of primary CFCs without reduced EOG might be explained by primary dysfunction of a cell population other than the RPE and photoreceptors, such as the Müller cells.

In addition to the large DCMD family described in the present study, two cases and one small family with features of DMCD have been described.[7-9] The clinical findings of a Spanish patient with presumed DCMD are consistent with DCMD stage 2.[9] In an American DCMD family from Greek ancestry,[7] the EOG results in affected patients were normal, and none of the examined children of affected family members, 10 to 18 years of age, showed any abnormalities. This does not support an autosomal dominant mode of inheritance, and rather suggests a different disease than the typical DCMD phenotype observed in our large Dutch family.

Differential diagnosis
Several other retinal diseases with early-onset CFCs should be considered in the differential diagnosis of DCMD, such as X-linked juvenile retinoschisis, retinitis pigmentosa, phenotypes associated with mutations in the *BEST1* gene, and uveitis. In the absence of a genetic association with the DCMD locus in a patient with presumed DCMD, one should review the clinical evidence for DCMD carefully, and consider the possibility of one of the following clinical entities associated with early-onset CFCs.

X-linked juvenile retinoschisis, which is inherited in an X-linked pattern in contrast to DCMD, gives rise to vision loss in boys at a young age and progresses to atrophy and alterations of the RPE,[19] like in DCMD. The "cystoid" schisis cavities are mainly situated in the inner and outer nuclear layer,[20] like the CFCs in DCMD, but the schisis cavities in X-linked juvenile retinoschisis often become confluent, with only small strands of tissue bordering these spaces on OCT, and without apparent fluorescein leakage into the schisis spaces on FA, in contrast to the CFCs in DCMD.[21] Also, a typical radial pattern is visible in the fovea on FAF and red-free images in X-linked juvenile retinoschisis cases, which is not observed in DCMD. The full-field ERG in X-linked juvenile retinoschisis characteristically shows an "electronegative" aspect,[19] in contrast to DCMD.

Like stage 3 DCMD, retinitis pigmentosa can present with hyperpigmentation in the (mid) peripheral fundus, and cystoid macular edema.[22] However, compared to DCMD, patients with retinitis pigmentosa experience night blindness early in the course of the disease, and retinitis pigmentosa patients characteristically show early arteriolar attenuation and bone-spicule pigmentary changes, with a rod-cone dysfunction on full-field ERG that outweighs

EOG abnormalities. In contrast to bone-spicule hyperpigmentation in retinitis pigmentosa, the hyperpigmented abnormalities in DCMD are typically more coarse and mainly located in the posterior pole.

Phenotypes associated with *BEST1* gene mutations – inherited either autosomal dominantly or recessively - can have somewhat similar retinal lesions and abnormalities, like an abnormal EOG that outweighs full-field ERG abnormalities, hyperopia and CFCs in the macula.[16-18] In contrast to DCMD, all patients with *BEST1*-related dystrophies have a severely abnormal EOG at onset, and *BEST1*-related fundus abnormalities usually include highly autofluorescent yellowish deposits in the macula.[17]

Posterior uveitis should also be considered, since DCMD can be accompanied by a variable degree of whitish punctate deposits (although these are not cells) in the vitreous body in stage 2 and 3 disease. Finally, the clinical characteristics of vascular causes of cystoid macular edema such as diabetic retinopathy, retinal venous occlusions, as well as age-related macular degeneration,[23] allow an easy distinction from DCMD.

Genetic Background

Dominant cystoid macular dystrophy is inherited autosomal dominantly, but the associated gene and mutation have not yet been identified.[6] We show that the genetic defect in DCMD appears to be completely penetrant in the large family in this study. The *KLHL7* gene, causing autosomal dominant retinitis pigmentosa,[24] is located within the critical interval of the DCMD locus, which might explain why two DCMD patients in our study exhibited abnormalities and phenotypic characteristics of retinitis pigmentosa (Figure 10.6C-D). However, no coding variant in the coding region of the *KLHL7* gene was detected in our DCMD family. This, however, does not exclude the presence of a deep intronic mutation or a mutation affecting a regulatory element of the *KLHL7* gene. Alternatively, due to the distinct disease characteristics between the families described by Friedman et al and our DCMD family, it is plausible that another gene at the DCMD locus can be involved in the disease rather than *KLHL7*. Further analysis of all genes located within the DCMD locus at the genomic and at a transcriptional level using next-generation sequencing technologies may identify the causative mutation of DCMD in the near future. Identification of the associated gene can provide insight into the pathogenesis of the disease, and may improve our understanding on the development of hyperopia and cystoid fluid collections in other rare and common retinal diseases.

Pathophysiology and treatment

Cystoid fluid accumulation in the macula is the first clinically visible abnormality in DCMD. This indicates that the CFCs in DCMD are the direct result of the primary genetic defect and its immediate pathophysiological consequences. Interestingly, a histopathological study on 2 donor eyes of a 78-year-old American patient with presumed DCMD has been published.[25] Large intraretinal cystoid spaces were observed in the macula, with mildly attenuated retinal vessels, atrophy and marked disorganization of the inner nuclear layer. The large cyst-like spaces within the inner nuclear layer were surrounded by Müller cell fibers and pigment-laden cells with remnants of photoreceptor segments, and degeneration of Müller cells was seen. Based on these findings, the authors suggested a primary pathologic process

10

affecting Müller cells in DCMD.[25] These histopathological findings correlate well with the clinical findings in our DCMD cohort, which could support primary Müller cell dysfunction in DCMD.[8] If this is the case, DCMD would be a rare example of retinal dystrophy that results from a genetic defect that primarily affects Müller cell function. The gene defect in DCMD might interfere with capillary permeability, resulting in a disturbance of the inner blood-retinal barrier and early CFCs.

It is also possible that CFCs in DCMD are the result of primary dysfunction of the RPE, as the EOG becomes abnormal early in the course of the disease. It is unlikely that the photoreceptors are primarily affected, at least on the panretinal level, as the full-field ERG remains normal for a long time. Cystoid macular edema in the outer neuroretinal layers, such as in the course of retinitis pigmentosa, is presumed to be caused by a dysfunction of the outer blood-retina barrier.[26-28] In DCMD, CFCs located in the outer nuclear layer are possibly induced by dysfunction of the RPE layer, comparable to cystoid macular edema that occurs in retinitis pigmentosa.[29]

Cystoid macular edema in the inner neuroretinal layers, such as in pseudophakic macular edema and diabetic retinopathy, is predominantly caused by a failure of the inner blood-retinal barrier.[27, 30] The CFCs located in the inner nuclear layer in DCMD could also be caused by a dysfunctional macular inner blood-retinal-barrier, which depends on Müller cells, astrocytes, and pericytes.[27] This could be supported by the fundoscopic and fluorescein angiographic finding of perifoveal capillary dilation early in the course of the disease.

We suggest that the Müller cells, the RPE, or both, may be the primarily affected cells in DCMD, resulting in CFCs early in the course of the disease.

Previous studies in patients with retinal dystrophies showed that treatment with acetazolamide reduced intraretinal fluid collections,[18, 22, 31-34] although the effect can be dose-dependent,[18] but the exact mechanism is unclear. Boon et al. suggested that acetazolamide may interact with carbonic anhydrase subtypes XIV and II in the RPE and Müller cells, resulting in intracellular acidification with consequently Cl^- transport in the RPE, with water following passively.[18] Treatment with acetazolamide has previously been shown to be ineffective in treating CFCs in most DCMD patients at a daily dose of 250 mg,[35] but we now demonstrate that the effect can be dose dependent in DCMD, as treatment with higher doses can indeed be effective in DCMD patients. A possible rebound effect that has been postulated in half of the retinitis pigmentosa patients with cystoid macular edema treated with acetazolamide for 8 to 12 weeks,[31] was present in only 2 of the 16 DCMD patients after 1.5 and 6 years of treatment with acetazolamide. Treatment seems be most effective in DCMD patients with stage 1 and has a less strong influence on the long term VA in stage 2 DCMD patients.

In conclusion, we describe the clinical spectrum, which can be subdivided into three clinical stages, in the largest DCMD cohort to date. CFCs are a hallmark feature in earlier disease, but during progression the CFCs diminish and chorioretinal atrophy develops. Haplotype analysis using microsatellite markers at the DCMD locus at 7p15.3 confirmed the diagnosis, and the disease was fully penetrant in our DCMD cohort. Future studies will be directed towards determining the causative gene by next-generation sequencing at a genomic and transcriptional level. The elucidation of the causative gene and pathogenesis in DCMD will

not only give important insight into this intriguing and peculiar retinal dystrophy, but the findings can also shed a light on the pathogenesis of hyperopia and cystoid macular edema in other retinal dystrophies, uveitis, diabetic macular edema or following ophthalmic surgery, and provide a new target for treatment.

10

References

1. Deutman AF, Pinckers AJ, Aan de Kerk AL. Dominantly inherited cystoid macular edema. Am J Ophthalmol 1976;82(4):540-8.
2. Notting JG, Pinckers JL. Dominant cystoid macular dystrophy. Am J Ophthalmol 1977;83(2):234-41.
3. Pinckers A, Notting JG, Lion F. [Dominant cystoid macular dystrophy (author's transl)]. J Fr Ophtalmol 1978;1(2):107-10.
4. Pinckers A, Deutman AF, Lion F, Aan de Kerk AL. Dominant cystoid macular dystrophy (DCMD). Ophthalmic Paediatr Genetics 1983;3(3):11.
5. Pinckers A, Deutman AF, Notting JG. Retinal functions in dominant cystoid macular dystrophy (DCMD). Acta Ophthalmol (Copenh) 1976;54(5):579-90.
6. Kremer H, Pinckers A, van den Helm B, et al. Localization of the gene for dominant cystoid macular dystrophy on chromosome 7p. Hum Mol Genet 1994;3(2):299-302.
7. Fishman GA, Goldberg MF, Trautmann JC. Dominantly inherited cystoid macular edema. Ann Ophthalmol 1979;11(1):21-7.
8. Schadlu R, Shah GK, Prasad AG. Optical coherence tomography findings in autosomal dominant macular dystrophy. Ophthalmic Surg Lasers Imaging 2008;39(1):69-72.
9. Mendivil A. Bilateral cystoid macular edema in a 21-year-old woman. Surv Ophthalmol 1996;40(5):407-12.
10. Boon CJ, Klevering BJ, Cremers FP, et al. Central areolar choroidal dystrophy. Ophthalmology 2009;116(4):771-82, 82 e1.
11. Brown M, Marmor M, Vaegan, et al. ISCEV Standard for Clinical Electro-oculography (EOG) 2006. Doc Ophthalmol 2006;113(3):205-12.
12. Marmor MF, Holder GE, Seeliger MW, et al. Standard for clinical electroretinography (2004 update). Doc Ophthalmol 2004;108(2):107-14.
13. Marmor MF, Fulton AB, Holder GE, et al. ISCEV Standard for full-field clinical electroretinography (2008 update). Doc Ophthalmol 2009;118(1):69-77.
14. Miller SA, Dykes DD, Polesky HF. A simple salting out procedure for extracting DNA from human nucleated cells. Nucleic Acids Res 1988;16(3):1215.
15. Hogewind BF, Pieters G, Hoyng CB. Octreotide acetate in dominant cystoid macular dystrophy. Eur J Ophthalmol 2008;18(1):99-103.
16. Saksens NT, Fleckenstein M, Schmitz-Valckenberg S, et al. Macular dystrophies mimicking age-related macular degeneration. Prog Retin Eye Res 2014;39:23-57.
17. Boon CJ, Klevering BJ, Leroy BP, et al. The spectrum of ocular phenotypes caused by mutations in the *BEST1* gene. Prog Retin Eye Res 2009;28(3):187-205.
18. Boon CJ, van den Born LI, Visser L, et al. Autosomal recessive bestrophinopathy: differential diagnosis and treatment options. Ophthalmology 2013;120(4):809-20.
19. Sieving PA, Bingham EL, Kemp J, et al. Juvenile X-linked retinoschisis from XLRS1 Arg213Trp mutation with preservation of the electroretinogram scotopic b-wave. Am J Ophthalmol 1999;128(2):179-84.
20. Gregori NZ, Lam BL, Gregori G, et al. Wide-field spectral-domain optical coherence tomography in patients and carriers of X-linked retinoschisis. Ophthalmology 2013;120(1):169-74.
21. Ganesh A, Stroh E, Manayath GJ, et al. Macular cysts in retinal dystrophy. Curr Opin Ophthalmol 2011;22(5):332-9.
22. Thobani A, Fishman GA. The use of carbonic anhydrase inhibitors in the retreatment of cystic macular lesions in retinitis pigmentosa and X-linked retinoschisis. Retina 2011;31(2):312-5.
23. Jittpoonkuson T, Garcia PM, Rosen RB. Correlation between fluorescein angiography and spectral-domain optical coherence tomography in the diagnosis of cystoid macular edema. Br J Ophthalmol 2010;94(9):1197-200.
24. Friedman JS, Ray JW, Waseem N, et al. Mutations in a BTB-Kelch protein, *KLHL7*, cause autosomal-dominant retinitis pigmentosa. Am J Hum Genet 2009;84(6):792-800.
25. Loeffler KU, Li ZL, Fishman GA, Tso MO. Dominantly inherited cystoid macular edema. A histopathologic study. Ophthalmology 1992;99(9):1385-92.
26. Bringmann A, Reichenbach A, Wiedemann P. Pathomechanisms of cystoid macular edema. Ophthalmic Res 2004;36(5):241-9.

27. Kaur C, Foulds WS, Ling EA. Blood-retinal barrier in hypoxic ischaemic conditions: basic concepts, clinical features and management. Prog Retin Eye Res 2008;27(6):622-47.
28. Newsome DA. Retinal fluorescein leakage in retinitis pigmentosa. Am J Ophthalmol 1986;101(3):354-60.
29. Scorolli L, Morara M, Meduri A, et al. Treatment of cystoid macular edema in retinitis pigmentosa with intravitreal triamcinolone. Arch Ophthalmol 2007;125(6):759-64.
30. Yannuzzi LA. A perspective on the treatment of aphakic cystoid macular edema. Surv Ophthalmol 1984;28 Suppl:540-53.
31. Grover S, Apushkin MA, Fishman GA. Topical dorzolamide for the treatment of cystoid macular edema in patients with retinitis pigmentosa. Am J Ophthalmol 2006;141(5):850-8.
32. Genead MA, McAnany JJ, Fishman GA. Topical dorzolamide for treatment of cystoid macular edema in patients with choroideremia. Retina 2012;32(4):826-33.
33. Ghajarnia M, Gorin MB. Acetazolamide in the treatment of X-linked retinoschisis maculopathy. Arch Ophthalmol 2007;125(4):571-3.
34. Hori K, Ishida S, Inoue M, et al. Treatment of cystoid macular edema with oral acetazolamide in a patient with best vitelliform macular dystrophy. Retina 2004;24(3):481-2.
35. Pinckers A, Cruysberg JR, Kremer H, Aandekerk AL. Acetazolamide in dominant cystoid macular dystrophy. A pilot study. Ophthalmic Paediatr Genet 1993;14(2):95-9.

10

Authors

Ramon A.C. van Huet[1], MD; Clasien J. Oomen[1,2], PhD; Astrid S. Plomp[3], MD, PhD; Maria M. van Genderen[4], MD, PhD; B. Jeroen Klevering[1], MD, PhD; Reinier O. Schlingemann[5], MD, PhD; Caroline C.W. Klaver[6,7], MD, PhD; L. Ingeborgh van den Born[8], MD, PhD; Frans P.M. Cremers[2,9], PhD and the RD5000 study group

Affiliations

[1]Department of Ophthalmology, Radboud University Medical Center, Nijmegen, the Netherlands
[2]Department of Human Genetics, Radboud University Medical Center, Nijmegen, the Netherlands
[3]Department of Clinical Genetics, Academic Medical Center, Amsterdam, the Netherlands
[4]Bartiméus, Institute for the Visually Impaired, Zeist, the Netherlands
[5]Department of Ophthalmology, Academic Medical Center, Amsterdam, the Netherlands
[6]Department of Ophthalmology, Erasmus Medical Center, Rotterdam, the Netherlands
[7]Department of Epidemiology, Erasmus Medical Center, Rotterdam, the Netherlands
[8]The Rotterdam Eye Hospital, Rotterdam, the Netherlands
[9]Radboud Institute for Molecular Life Sciences, Radboud University Medical Center, Nijmegen, The Netherlands

RD5000 study group:

Nathalie M. Bax1, Carel B. Hoyng1, Stanley Lambertus1, Wendy A. van Zelst-Stams2, Arthur A.B. Bergen3, José Schuil4, Mary J. van Schooneveld5, MD, PhD, Laurence Pierrache6, Magda A. Meester-Smoor6;

Camiel J.F. Boon, Department of Ophthalmology, Leiden University Medical Center, the Netherlands

Jan Willem R. Pott, Department of Ophthalmology, University Medical Centre Groningen, University of Groningen, the Netherlands

Redmer van Leeuwen, Department of Ophthalmology, University Medical Center Utrecht, the Netherlands

Hester Y. Kroes, Department of Medical Genetics, University Medical Center Utrecht, the Netherlands

Yvonne de Jong-Hesse, Department of Ophthalmolgy, Free University Medical Center, the Netherlands

F. Nienke Boonstra4, and Donders Institute for Brain, Cognition and Behaviour, Department Cognitive Neuroscience, Radboud University Medical Centre, Nijmegen, the Netherlands

The RD5000 database: facilitating clinical, genetic and therapeutic studies on inherited retinal diseases

11

Abstract

Inherited retinal diseases (IRDs) represent a clinical and genetic heterogeneous group of chorioretinal disorders. The frequency of persons affected by an IRD due to mutations in the same gene varies from 1 in 10,000 to less than 1 in a million. In order to perform meaningful genotype-phenotype analyses for rare genetic conditions, it is necessary to collect data from sizable populations. Although several standardized functional tests are widely used, ophthalmologic data are usually stored in local databases and not in multi-center databases that are linked with other centers. In order to be able to register ophthalmologic data of all Dutch patients with IRDs into one database, we developed the RD5000 database (RD5000db) that can harbor all ophthalmological and selected genetic data. Authorization rights for the management, data entry and data sharing have been set-up, rendering this database into a user-friendly, secure and widely used repository that will facilitate future studies into molecular genetics and therapies for IRDs. RD5000db has the potential to grow into a European standard for the registration of data from IRDs.

Introduction

Inherited retinal diseases (IRDs) constitute a clinically heterogeneous group of disorders that involve degeneration of the photoreceptors, retinal pigment epithelium (RPE) and/or choroid.[1-4] The incidence rates vary from 1 in 10,000 (for Stargardt disease) to less than 1 in a million for rare clinical subtypes.[5-9] The diseases affect both sexes, and include major causes of blindness in children and young adults worldwide, although some patients remain asymptomatic until middle-age. The phenotypic variability is caused by genetic defects in a large number of genes. In the last 25 years, over 200 genes associated with both syndromic and nonsyndromic IRDs (RetNet, available at https://sph.uth.edu/retnet/) were identified.[4, 10, 11]

The internet offers several public and license-protected databases that contain genetic data on IRDs, such as the Leiden Open (source) Variation Databases (LOVDs, available at http://www.lovd.nl/3.0/home), the Human Gene Mutation Database (HGMD, available at http://www.hgmd.org/), and the retina international mutation database available at http://www.retina-international.org/sci-news/databases/mutation-database/). Still, databases containing clinical data are, to our knowledge, not publically available. Instead, most specialized medical centers use a database exclusively accessible by that specific center. This lack of publically available clinical data is most likely due to privacy legislation and medical ethics. On the other hand, there are websites that provide an overview of genetic and clinical features of IRDs published in literature, such as the Retinal Network (RetNet, available at https://sph.uth.edu/retnet/) and the Online Mendelian Inheritance in Man (OMIM, available at http://www.omim.org/).

Since incidence rates are low in IRDs, national collaborations are the first step to get an overview of cohort sizes, the distribution of certain genetic defects and the matching clinical features. This will also be important to identify persons for (gene) specific therapeutic trials. In this light, 11 Dutch ophthalmic centers collaborated in a project named RD5000[§] to set up a database with anonymized clinical and genetic data: the RD5000 database (RD5000db, available for members at http://www.RD5000db.nl). To obtain larger cohort sizes for studies on specific genotypes, phenotypes or genotype-phenotype correlations, international expansion of the database is possible and desirable.

Objectives of the RD5000 database

To our knowledge, the RD5000db is the first multi-centered, web-based database available in the field of inherited retinal diseases. Main objectives are (1) standardization of clinical and genetic data registration, (2) pseudo-anonymized ('pseudomized') storage of data, and (3) web-based, controlled data sharing among participating medical centers. The pseudomized character of the data storage lies in the absence of personal characteristics that could lead to the identification of a specific patient, and the presence of a center specific internal patient identification number. This results in anonymized data for the centers that have access to the database, and personalized data for the patient's medical center that also owns the source data files. Data access by other centers is controlled: only a few general features

---

[§]   The name 'RD5000' was based on the estimated prevalence of 5000 patients with inherited retinal diseases in the Netherlands.

are commonly available in a 'catalogue'; access to all other details can be granted either for clinical reasons (e.g. when the patient attends an ophthalmologist or geneticist in another center participating in RD5000db) or research reasons (e.g. for a specific research question; see Data access below). This controlled access allows the professionals to be in charge of the data to be shared.

Database design
We reviewed literature on existing databases in the field of ophthalmic retinal disease. The Ophthabase database (used in Tuebingen, Germany) was used for database structure and lay-out.[12] Additionally, the biobank of the string-of-pearls initiative (The Netherlands, Dutch: Parelsnoer initiatief) was used for their way of structuring multicenter data entry and access to patient data (see Data access).[13] Additionally, jurisdiction and expert opinion on national privacy legislation and patient data were obtained.

Source code. The source code of Ophthabase® (developed by Institute for Ophthalmic Research, Tübingen, Germany, as part of EVI-GENORET Project) was generously provided for further development. HTML design and data model of Ophthabase ® were used as a starting point for RD5000db and were altered to the specifications of RD5000db by the company First8 (www.first8.com). RD5000db is built in Java 1.7 (Oracle Corporation, Redwood Shores, CA, USA) and runs on an Apache Tomcat 7.0 (The Apache Software Foundation, Forest Hill, MD, USA) application server and uses PostgreSQL 8.4 (EnterpriseDB Corporation, Bedfort, MA, USA) as a relational database. The web interface is built using Apache Wicket 6 (The Apache Software Foundation, Forest Hill, MD, USA) and uses Spring Core (Pivotal Software, Palo Alto, CA, USA) framework to interact with services, which contain the business logic. Hibernate (Red Hat Inc., Raleigh, NC, USA), which implements the Java Persistence application programming interface 2 standard, is used to query the database. Spring Security (Pivotal Software, Palo Alto, CA, USA) is used for authorization and authentication and is used to implement the roles and rights system. Access from the web is always redirected from http to https which uses SSL (Secure Socket Layer) to ensure encrypted transportation of the data over the internet.

Data entry. The RD5000db is set up as a research database that contains pseudomized patient data. The internal IDs are used to relate the data stored in RD5000db to information in the medical files of the centers in which the patient is treated (pseudomisation). Although no personal data that could identify a patient is stored in the database, initials, date of birth and gender are entered to construct a hash code that is used to identify double entries. Since only the hash code is stored, the initials and date of birth are not accessible, but the year of birth and gender remain visible to users.

The data forms are organized around the pseudomized *Basic Patient Data* (Appendix Figure A11.1.2). The structure of RD5000db was based on the case report form (CRF) and standard operative procedures (SOPs) that were formulated by the RD5000 consortium, as well as on the data structure of Ophthabase.
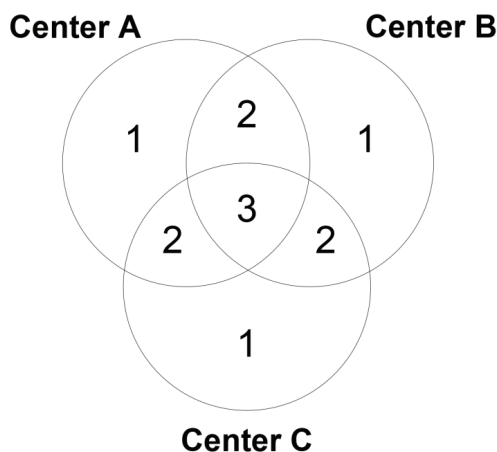
Figure 11.1. Visualization of data access in case patient data are entered from one, two or three centers. The numbers indicate the number of centers that have access to the patient's data. If more than three centers are involved, the principle is followed analogously.

We designed five different data forms: patient history, genetics/DNA sample, clinical examinations, technical examinations and diagnoses forms. More details on the different data entry forms are provided in the Appendix 11.1 and Figures A11.1.1-A11.1.7 (available at the end of this chapter). Numerous clinical and technical examinations can be entered when follow-up data (longitudinal data) are available. Furthermore, image files of imaging techniques or examination reports can be uploaded to support the clinical data. The database allows patients to be registered in multiple centers that can all contribute to the data volume of a single the patient (Figure 11.1), which is not uncommon in The Netherlands. Family data are initially entered in the family history section of the history form (see Appendix 11.1). This data only include the number of affected individuals within the family, their relation to the patient and (if available) internal registration numbers of the parents. However, RD5000db provides the ability to assign family members that are entered in the database to a family ID in the *Family* tab (Appendix Figure A11.2.1).

Informed consent. We endeavored to enroll patients in the RD5000db with their approval to adhere to the tenets of the Declaration of Helsinki, although the data entered in the database is pseudomized and patient's personal details are only available to the center the patient attends to (via the internal ID), which makes informed consent not obligatory. Nevertheless, we created an informed consent to obtain patient approval for data entry in the database.

Privacy. Due to the sensitive nature of the collected data we carefully considered how to handle privacy correctly according to the Dutch privacy regulations. At first the idea was to encrypt all the data using a public key infrastructure (PKI). In this set-up, only the super administrator of RD5000db would have access to the private key. However, in this approach maintenance by our hosting provider or ICT implementation party would be complicated.

The data were therefore anonymized in such a way that it is not possible to directly identify a patient. However, the center that a patient attends to can identify the patient by means of a separate registration system that is not connected in any physical or electronic way to the RD5000db application. In the RD5000db, this is possible by the internal ID that is linked to a patient in that specific center, hence, only members of that center can acquire the patient's privacy sensitive details from their own center's registration systems. Only a very limited amount of information is available to members of the other centers with access to the RD5000db. They can, however, obtain additional anonymous patient data upon permission from the review committee (see Data access).

Identifying double entries. We introduced a hash code based on date of birth, initials and gender to prevent double entry of a patient. However, this procedure has its limitations: initials are not always completely registered in the hospital's registration systems and in some cases, names may be noted incorrectly on the medical files. For some individuals the distinction between first and family names is not clear, resulting in a different order of the initials that constructs a different hash code. Preventing double entry is however important, especially in these small groups of patients. When a double entry is suspected, the system administrator executes an audit trail based on year of birth, gender and diagnosis, and verifies personal details of the presumed double entries with the responsible physicians (who are generally from two different centers), before merging the entries.

Search engines. The RD5000db includes two search engines to explore patient data: the search engine of the database located on the *Catalogue* tab that searches all entries, and the search engine on the *Patients* tab that searches only patients accessible to the user (Figures A11.2.2 and A11.2.3). Both search engines are identical in composition, but differ in function. The *Catalogue* tab presents a limited set of data for all patients in the database, allowing the users to have an indication of the population that has been entered in RD5000db. This information can be used for formulating a research question and obtaining data access to other patients, the procedure of which is elaborated below (see Data access). The search function in the *Patients* tab provides the full data of the patients entered by the user's centre, or of the patients the user has obtained access to.

Authorization roles. The hierarchy in authorization roles in RD5000db involves one *system administrator*, who has access to all data and roles of all users database-wide, and multiple *center administrators*, who have access to all data and roles of users in their center. Each center has two additional roles available: (1) *writers*, who can read, edit and add data to patients of their center, as well as add patients to the database and (2) *readers*, who have read-only access to data from patients of their center. Both the reader and writer roles can be assigned to multiple users.

The system administrator has the main supervising role in the system which includes organizational tasks, including add/delete roles of center administrators, handle requests to delete patients from the database, merge patient's data in case of multiple entries of a single patient, change access rights per patient per form and search all patients (see Data

access). The center administrator has the supervising role within a center and takes care of communication to the system administrator, provides help to the users in his center, adds and removes users and changes user roles of his center, and provides passwords to users within the center.

Data access. The database is available at https://www.RD5000db.nl. To sign up to the database, the registration form has to be completed, including a specific center key (provided by the center administrator). After registration, a password will be sent to the user, to log into RD5000db and access patient data. By default, the user has access to all the patients linked to its own center. Which actions the user can perform, depends on the role assigned to him (see Authorization roles).

Patients linked to two or more centers can be accessed by each of these centers (Figure 11.1). Regulations on data management state that one center does not alter data entered by another center. Since technical and clinical examinations are stored as separate files for different time points, additional data can easily be added. Violations are tracked in the audit trails (see Audit Logging). When a patient with initials, date of birth and gender identical to an existing entry is entered into the database, users receive the double entry notification. After verification of the patient details, the system administrator can assign the patient to both centers.

For specific research questions, an RD5000db-user can receive access to the data of patients of other centers by formulating a research question application for the RD5000db review committee (Figure 11.2). The RD5000db review committee consists of RD5000-members, one of each participating center. A positive decision from this committee enables the system administrator to grant the researcher access to the requested data (Figure 11.2). The access granted can be specified up to the level of specific forms (without access to the data on other forms of this patient). This same procedure is applicable in case an external researcher would wish to have data from the RD5000db. The only difference is that in case the requestis granted, data are sent in an export file to the external researcher instead of granting access to the database.

Data export. Patient data can be exported in two forms. Firstly, each single form can be exported in PDF format and can be stored in patient's medical files if desired. Secondly, in the *Reporting* tab patient data can be exported to a Windows Excel® 2007 Worksheet format (.xslx), which enables further data analyses by various statistical programs. The Excel export file includes the data of all patients the user has access to. Any filtering of the data should be done after data export. The variables are organized in separate tabs of the worksheet based on the forms of the database. In each tab, the data are arranged based on RD5000 ID. Longitudinal data, such as clinical and technical examination data of multiple visits, are presented in a single row per examination, each identified with the RD5000 ID and the examination date. Where value lists are used in the database, numeric values are present in the export worksheet, which can be identified using the codebook with the corresponding labels that is available in the last tab of the worksheet.

A SPSS syntax document was written to simplify data import and management in SPSS (available for RD5000 members at http://www.RD5000.nl). By running the syntax, the data of all Excel worksheet tabs is imported into SPSS synthesizing one entry with correct labeling and subheadings. The syntax files is structured with subheadings, which enables selective use of parts of the syntax code.

Audit logging

All actions (inserts, updates and deletes) towards the database are stored in an audit log (also in the database). With this audit log, a registration is made that includes the details of the specific user, the time of the action, as well as the details of the actions. These details can be retrieved upon request.

Figure 11.2. Flowchart on the process to request access to data. Each center in principle only has access to the data entered by their own center. Colleagues from other centers obtain access to the data from other centers only after approval by a review committee which contains representatives of all data-contributing centers. External researchers can only obtain data through this review committee. Upon authorization, the system administrator will give internal researchers access to the data, and provide the requested data to the external researchers in a report file.

Current status and usability of the RD5000 database

The RD5000db was launched online at September 1st, 2012. In the meantime, 1,923 patients with retinal dystrophies have been registered in the database (reference date June 1st, 2014), with a mean age of 41 years (range: 1-102 years). In this cohort, 62 different diagnoses were made based on clinical phenotype and inheritance pattern. Clinical and/or technical examinations were registered for 469 patients (24.3%) with an average number of visits of 4.5 (range: 1-17 for technical examinations and 1-22 for clinical examinations. Follow-up periods varied between 0-51 years. DNA samples were available for 1,235 patients (64.2%). Of these, 684 patients (35.6% of all entries) were genetically solved, and 188 additional patients (9.8% of all entries) carried putatively causative mutations, but have not yet been solved completely. Causative or putatively causative mutations were found in 77 different genes.

Time needed for entry of one patient is mainly dependent on the source data and the amount of details to be entered. Initially, comprehensive data entry takes up to 40 minutes per patient on average. However, for a trained person this time may be reduced to a maximum of 25 minutes for a full data record.

Future plans

Data quality surveillance. In the near future, we will cope with some of the problems we encountered in the past two years. One issue of high priority is the double entry check that is intended to prevent the repeated entry of a patient. The current hash code that combines the patient's initials, date of birth and gender has proven to be insufficiently solid, since we found 11 double entries up to now in 1,923 records. The entry of the initials has shown to be the most variable and inconsistent factor, since registrations in hospitals often are incomplete or incorrect. A solution may be the entry of a citizen identification number (Dutch: Burger Service Nummer, BSN) using Trusted Third Party (TTP) procedures, which warrants pseudomisation that complies with the strictest privacy legislations. Furthermore, standard procedures for checking data quality will be written, thereby preventing errors in the data entry, such as misspelled gene names and other free text fields. Finally, there is currently no compulsory minimal clinical dataset, which may be very useful for several research questions that rely on detailed clinical data. However, the data requirements will be different for each research question, complicating the definition of the minimal dataset.

Funding. Up to now, the costs for the development of RD5000db have been covered by Dutch blindness foundations. However, once the database is routinely used, it stands to reason that each participating center contributes an annual fee to host, maintain and update the database. Information about the set-up and maintenance costs for the database can be found in Appendix 11.3.

International expansion of the database. Currently, the RD5000db is available for 11 Dutch ophthalmologic centers. In the near future, we want to include data of a few international centers. RD5000db thereby has the potential to develop into a pan-European database for the detailed registration of clinical data. By increasing the number of patient records, its potential will grow significantly and facilitate many different studies in the fields of genetics, genotype-phenotype comparisons, and the application of novel therapies.

11

References

1. Berson EL. Retinitis pigmentosa. The Friedenwald Lecture. Invest Ophthalmol Vis Sci 1993;34:1659-1676.
2. Hartong DT, Berson EL, Dryja TP. Retinitis pigmentosa. Lancet 2006;368:1795-1809.
3. Michaelides M, Hardcastle AJ, Hunt DM, Moore AT. Progressive cone and cone-rod dystrophies: phenotypes and underlying molecular genetic basis. Surv Ophthalmol 2006;51:232-258.
4. den Hollander AI, Black A, Bennett J, Cremers FP. Lighting a candle in the dark: advances in genetics and gene therapy of recessive retinal dystrophies. J Clin Invest 2010;120:3042-3053.
5. Bunker CH, Berson EL, Bromley WC, Hayes RP, Roderick TH. Prevalence of retinitis pigmentosa in Maine. Am J Ophthalmol 1984;97:357-365.
6. Hamel C. Retinitis pigmentosa. Orphanet J Rare Dis 2006;1:40.
7. Hamel CP. Cone rod dystrophies. Orphanet J Rare Dis 2007;2:7.
8. Mockel A, Perdomo Y, Stutzmann F, Letsch J, Marion V, Dollfus H. Retinal dystrophy in Bardet-Biedl syndrome and related syndromic ciliopathies. Prog Retin Eye Res 2011;30:258-274.
9. Kalatzis V, Hamel CP, Macdonald IM, First International Choroideremia Research S. Choroideremia: towards a therapy. Am J Ophthalmol 2013;156:433-437 e433.
10. Berger W, Kloeckener-Gruissem B, Neidhardt J. The molecular basis of human retinal and vitreoretinal diseases. Prog Retin Eye Res 2010;29:335-375.
11. Roosing S, Thiadens AA, Hoyng CB, Klaver CC, den Hollander AI, Cremers FP. Causes and consequences of inherited cone disorders. Prog Retin Eye Res 2014.
12. Tröger E, Wilke R, Prokofyeva E, Zrenner E. Ophthabase: a generic extensible patient registry system. Acta Ophthalmol 2008;86:0.
13. Talmon JL, Ros MG, Legemate DA. PSI: The Dutch Academic Infrastructure for shared biobanks for translational research. Summit on Translat Bioinforma 2008;2008:110-114.

Appendix 11.1: Data entry forms

The database structure is depicted in Figure A11.1.1 (available at: http://www.iovs.org/content/suppl/2014/11/17/55.11.7355.DC1/IOVS-14-15317-s01.pdf). Patients are entered into the RD5000db database by the *basic patient data* form (Figure A11.1.2). Personal data including date of birth, initials and gender are registered at patient enrollment in RD5000db for the use of a check on double entries of a single patient. After registration of the patient, only the year of birth remains visible, whereas initials are not visible to users after the basic patient data form has been saved. Other details that are entered in this form are the centers the patient visited, including the patient's internal registration number and responsible physician, with a maximum of three centers.

The *patient history* form (Figure A11.1.3) contains modules on the initial diagnosis, visual and general symptoms, ophthalmic history, medication and family history. Seven visual complaints most prevalent in IRDs and 16 syndromic features present in syndromic IRDs are documented, with the possibility to specify each complaint further with e.g. age at onset of this specific complaint or its location (if applicable). The module on family history registers data on the patient's siblings, as well as the generations of the patient's parents and children.

The *genetics/DNA sample* form (Figure A11.1.4) primarily states the presence of a DNA sample of this specific patient. Additionally, both causative and non-causative variants can be registered. If the effects of a mutation are not known, these variants are registered in the 'mutations of uncertain pathogenicity' module. The correct module appears based on the conclusion of genetic analysis that was selected. The method used for genetic analysis can be specified further as well as version numbers of used gene sets, kits etc can be registered. Gene names are registered in HGNC nomenclature, whereas both complementary DNA changes and protein changes are noted for the variants/mutations.

In the *clinical examination* form (Figure A11.1.5), data of ophthalmic examinations are registered, including visual acuity (including subjective refractive error), fixation, eye motility, intra-ocular pressure and slit-lamp biomicroscopy of the anterior segment and posterior segments. Except for fixation and eye motility data, all data are entered for each eye separately. Each module contains a button to copy data of the right eye to the fields of the left eye, since IRDs are generally symmetrical. Data of the anterior and posterior segments are entered by a drop-down menu stating the options 'normal', 'abnormal' and 'not applicable'. Additional fields to specify observations appear if the option 'abnormal' is selected. If the data entry fields do not cover the observed details, a free text field enables registration of these additional data.

The *technical examination* form (Figure A11.1.6) enables registration of data acquired from perimetry, color vision tests, full-field or multifocal electroretinography (ERG), electro-oculography (EOG), dark adaptation, and commonly used imaging techniques, including fundus photography, optical coherence tomography (OCT), fundus autofluorescence (FAF) and fluorescein angiography (FA). Like the clinical examination form, all data are entered for

each eye separately and buttons to copy data from the right to the left eye fields are present. Furthermore, each module contains the option to upload a file, e.g. a scan of the perimetric results, the ERG graphs or digital files of imaging examinations.

The *diagnoses* form (Figure A11.1.7) enables registration of the diagnoses made in the patient. The final ophthalmic diagnosis is selected from an extended list of retinal diagnoses and syndromes. Other ophthalmic diagnoses or general relevant diagnoses can be entered from the 10th revision of the International Classification of Diseases (ICD-10).

Four different field types are used in the database: value lists, check boxes, radio buttons and iterate values/dates. The default value for most value lists is "Please select…". All value lists contain a "not applicable" value, which means these data are not available, in contrast to "not known", which should be used if the patient cannot provide the data. Radio buttons are only used in the technical examination form, mainly to specify if the examination referred to has been performed.

To enhance usability, we minimized the amount of mandatory fields. Mandatory fields include the examination date in both clinical and technical examination forms, because the saved forms are arranged by these dates. The technical examination form has multiple mandatory fields, which specify whether an examination has been performed or not.
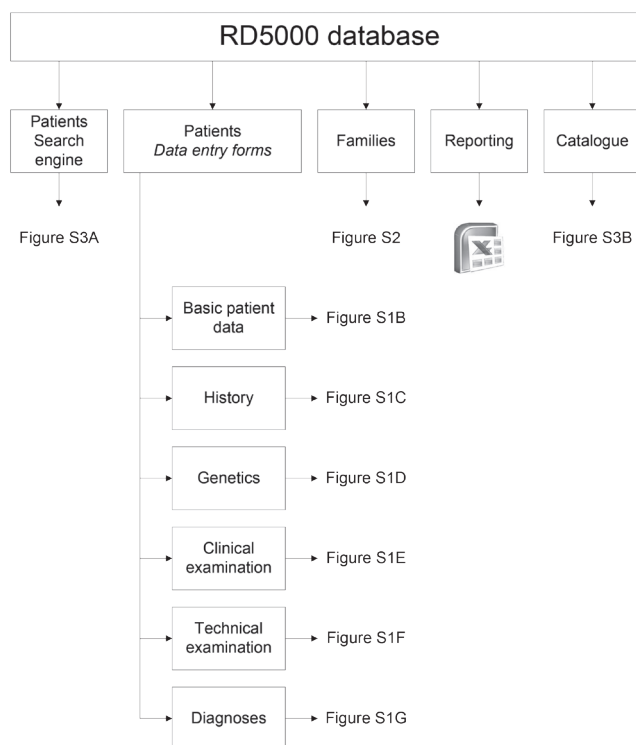
Figure A11.1. http://www.iovs.org/content/suppl/2014/11/17/55.11.7355.DC1/IOVS-14-15317-s01.pdf

RD5000 Database (Logged in as Ramon van Huet Edit profile Logout)

Patients   Families   Reporting   Catalogue
Currently loaded patient: 1200011, Internal ID at Center A: id_10, Family: F1200001

Basic patient data

General Information

Year of birth	1981	Informed consent RP5000 obtained	☐
Gender *	Female	Upload informed consent	
		RP5000 ID	1200011

Center A

Center Name *	Radboud University Nijmegen Medical Center
Internal ID at Center A *	id_10
Responsible physician	Perry, Harriet

Center B

Center Name	Please select...
Internal ID at Center B	
Responsible physician	

Center C

Center Name	Please select...
Internal ID at Center C	
Responsible physician	

Back

Figure A11.1.2: http://www.iovs.org/content/suppl/2014/11/17/55.11.7355.DC1/IOVS-14-15317-s02.pdf

Patients	Families	Reporting	Catalogue

Currently loaded patient: 1300590, Internal ID at Center A: Huet, Family: None

History

[Save] [Back]

Initial diagnosis

Diagnosis

	👁 ✕

Established at age	
Established in year	

Visual symptoms

Decrease in visual acuity	Please select... ▾
Age of onset	
Night vision impairment	Please select... ▾
Age of onset	
Visual field defects	Please select... ▾
Age of onset	
Location	Please select... ▾
Reading ability	Please select... ▾
Age of onset	
Color vision impairment	Please select... ▾
Age of onset	
Susceptibility to glare/photophobia	Please select... ▾
Age of onset	
Amblyopia known	Please select... ▾
Location	Please select... ▾

Subjective course of disease

Course	Please select... ▾

Ophthalmic history

Previous ophthalmic history, including surgery

Location	Please select... ▾
Year	
Description	☐ Cataract extraction

[Remove]
[Add]

Pharmalogical history

Is a regular medication taken	Please select... ▾
Specify medication (dosage/day, example 3dd 250mg)	
Vitamin A taken regularly	Please select... ▾
Specify dosage (µg/day)	

Risk factors

Alcohol	Please select... ▾
Quantity (IE/wk)	
Drug abuse	Please select... ▾

Figure A11.1.3: http://www.iovs.org/content/suppl/2014/11/17/55.11.7355.DC1/IOVS-14-15317-s03.pdf

11

Specify	
Nicotine	Please select... ▼
Cigarettes per day	Please select... ▼

General history

Congenital malformations	Please select... ▼
Specify	
Deafness	Please select... ▼
Age of diagnosis	
Specify	
Obesity	Please select... ▼
Age of diagnosis	
Diabetes	Please select... ▼
Balance problems	Please select... ▼
Mental retardation	Please select... ▼
Kidney malformation	Please select... ▼
Heart failure	Please select... ▼
Hypertension	Please select... ▼
Respiratory disorder	Please select... ▼
Fertility disorder	Please select... ▼
Specify	
Hypogonadism	Please select... ▼
Other endocrinological disorders	Please select... ▼
Specify	
Polydactyly	Please select... ▼
Specify	
Abnormalities in dental assembly	Please select... ▼
Specify	
Neuromuscular disorders	Please select... ▼
Specify	
Comment	
Complications during pregnancy/birth	Please select... ▼
Specify	

Family data

Number of affected family members	
Parents of this individual affected	Please select... ▼
Brothers/sisters of this individual affected	Please select... ▼
Number of affected	
Number of unknown status	
Number of nonaffected	
Children of this individual affected	Please select... ▼
Number of affected	

Figure A11.1.3: (Continued)

Number of nonaffected		
Twins	Please select...	▼
Number of affected		
Number of unknown status		
Number of nonaffected		
Consanguinity in this family	Please select...	▼
Degree of consanguinity	Please select...	▼
Specify		
(Grand)parents originate from same village	Please select...	▼
Putative inheritance pattern in this family	Please select...	▼
Internal ID mother		
Internal ID father		
Origin maternal grandmother	Please select...	▼
Origin maternal grandfather	Please select...	▼
Origin paternal grandmother	Please select...	▼
Origin paternal grandfather	Please select...	▼
Upload pedigree	Bladeren...	
Comment		

Save Back

Figure A11.1.3: (Continued)

Patients   **Families**   **Reporting**   **Catalogue**
Currently loaded patient: 1300590, Internal ID at Center A: Huet, Family: None

Genetics

Save   Back

Genetics

Is a DNA sample available *	Please select... ▾
Patient genetically solved?	Please select... ▾
Inheritance pattern based on the genetic findings	Please select... ▾

Causative mutations

For nomenclature, click here: **http://www.hgvs.org/mutnomen/**

Locus 1 (causative mutation)

Gene (HGMD name) *	
Mutation 1 (cDNA)	
Mutation 1 (protein)	
Mutation 2 (cDNA)	
Mutation 2 (protein)	

Remove
Add

Mutations of uncertain pathogenicity

For nomenclature, click here: **http://www.hgvs.org/mutnomen/**

Locus 1 (causative mutation)

Gene (HGMD name) *	
Mutation 1 (cDNA)	
Mutation 1 (protein)	
Mutation 2 (cDNA)	
Mutation 2 (protein)	

Remove
Add

Screened genes

For nomenclature, click here: **http://www.hgvs.org/mutnomen/**

Screened gene 1

Gene (HGMD name)	
Accession no. cDNA	
Molecular method	☐ Genotype microarray (APEX) ☐ Sanger sequencing ☐ Targeted NGS: Chromosomal area ☐ Targeted NGS: Gene set ☐ Exome NGS: All human genes ☐ PCR ☐ Other
Specify other molecular method	

Figure A11.1.4: http://www.iovs.org/content/suppl/2014/11/17/55.11.7355.DC1/IOVS-14-15317-s04.pdf

APEX microarray; specify array and year; see Asper Ophthalmics.

☐ AMD
☐ ADOA
☐ AD RP
☐ AR RP
☐ Syndrome
☐ CSNB
☐ Corneal dystrophy
☐ LCA
☐ LHON
☐ ABCA4
☐ USHER
☐ VMD
☐ XL-RP

Targeted NGS-chromosomal area: Specify hg build and area (e.g. hg19 chr21:33,031,597-33,041,570; see Human (Homo sapiens) Genome Browser Gateway) or flanking RS numbers.

Targeted NGS-Gene set: Specify gene set

Used filter: IRD-genes — Please select...

Used filter version

Used enrichment probes — Please select...

Specify used enrichment probes

Mapping information

Additional information

Remove
Add

Save Back

Figure A11.1.4: (Continued)

Patients   Families   Reporting   Catalogue
Currently loaded patient: 1300590, Internal ID at Center A: Huet, Family: None

Clinical examination

Save   Back

Examination date

| Examination date * | | 17 |
| Age on examination date | | |

Refraction/visual acuity

Right eye			Left eye		
Optimal subjective refraction			Optimal subjective refraction		
Spherical			Spherical		
Cylindrical			Cylindrical		
° axis			° axis		
Best corrected visual acuity			Best corrected visual acuity		
Decimal			Decimal		
Snellen			Snellen		
logMAR			logMAR		
Lower than ETDRS	Please select...	▼	Lower than ETDRS	Please select...	▼

Copy fields from Right eye to Left eye

Fixation

| Fixation | Please select... | ▼ |

IOP

Right eye			Left eye		
IOP (mm Hg)			IOP (mm Hg)		

Copy fields from Right eye to Left eye

Motility

| Nystagmus | Please select... | ▼ |

Anterior segment

Right eye			Left eye		
Cornea	Please select...	▼	Cornea	Please select...	▼
Specify			Specify		
Anterior chamber	Please select...	▼	Anterior chamber	Please select...	▼
Specify			Specify		
Iris	Please select...	▼	Iris	Please select...	▼
Specify			Specify		
Lens	Please select...	▼	Lens	Please select...	▼
Cataract specifications	Please select...	▼	Cataract specifications	Please select...	▼
Cataract visual significance	Please select...	▼	Cataract visual significance	Please select...	▼

Copy fields from Right eye to Left eye

Figure A11.1.5: http://www.iovs.org/content/suppl/2014/11/17/55.11.7355.DC1/IOVS-14-15317-s05.pdf

Vitreous

Right eye	Left eye
Vitreous	Vitreous

Copy fields from Right eye to Left eye

Fundus

Right eye		Left eye	
Optic disc		*Optic disc*	
Optic disc	Please select... ▾	Optic disc	Please select... ▾
Atrophy (pallor)	Please select... ▾	Atrophy (pallor)	Please select... ▾
Waxy aspect of optic disc	☐	Waxy aspect of optic disc	☐
Peripapillar atrophy	☐	Peripapillar atrophy	☐
Glaucomatous excavation	☐	Glaucomatous excavation	☐
Glaucomatous excavation - C/D-ratio		Glaucomatous excavation - C/D-ratio	
Prominent	☐	Prominent	☐
Drusen	☐	Drusen	☐
Other		Other	
Retinal vessels		*Retinal vessels*	
Retinal vessels	Please select... ▾	Retinal vessels	Please select... ▾
Attenuation	Please select... ▾	Attenuation	Please select... ▾
Sheating	☐	Sheating	☐
Other		Other	
Macula		*Macula*	
Macula	Please select... ▾	Macula	Please select... ▾
Pigmentation	☐	Pigmentation	☐
Pigmentation - specification	☐ Bull's eye ☐ Hyperpigmentation ☐ Hypopigmentation ☐ RPE atrophy ☐ Other	Pigmentation - specification	☐ Bull's eye ☐ Hyperpigmentation ☐ Hypopigmentation ☐ RPE atrophy ☐ Other
Specify		Specify	
Edema	☐	Edema	☐
Schisis	☐	Schisis	☐
Tapetal reflex	☐	Tapetal reflex	☐
Epiretinal gliosis	☐	Epiretinal gliosis	☐
Choroidal alterations	☐	Choroidal alterations	☐
Yellowish flecks	☐	Yellowish flecks	☐
Periphery		*Periphery*	
Periphery	Please select... ▾	Periphery	Please select... ▾
Pigmentations	☐	Pigmentations	☐
Quantity	Please select... ▾	Quantity	Please select... ▾
Shape	☐ Bone spicule-like ☐ Round	Shape	☐ Bone spicule-like ☐ Round
Predominant localization	☐ Mid periphery ☐ Posterior pole ☐ Paravascular ☐ Sectorial	Predominant localization	☐ Mid periphery ☐ Posterior pole ☐ Paravascular ☐ Sectorial
Specify sectorial		Specify sectorial	
Yellowish flecks	☐	Yellowish flecks	☐
RPE alterations	Please select... ▾	RPE alterations	Please select... ▾
RPE atrophy	☐	RPE atrophy	☐
Other RPE alterations		Other RPE alterations	

Figure A11.1.5: (Continued)

Figure A11.1.5: (Continued)

RD5000 Database (Logged in as Ramon van Huet Edit profile Logout)

Patients   Families   Reporting   Catalogue
Currently loaded patient: 1300590, Internal ID at Center A: Huet, Family: None

Technical examination

Save   Back

Examination date

Examination date *		17
Age on examination date		

Visual field

Right eye			Left eye		
Visual field test performed *	○ No ⦿ Yes		Visual field test performed *	○ No ⦿ Yes	
Type	Please select...	▾	Type	Please select...	▾
Findings	Please select...	▾	Findings	Please select...	▾
Specify abnormalities			Specify abnormalities		
Upload	Bladeren...		Upload	Bladeren...	

Copy fields from Right eye to Left eye

Color vision test

Right eye		Left eye	
Color test performed *	○ No ⦿ Yes	Color test performed *	○ No ⦿ Yes
Type of test	☐ HRR ☐ Panel D15 ☐ Ishihara ☐ 100 Hue ☐ Other	Type of test	☐ HRR ☐ Panel D15 ☐ Ishihara ☐ 100 Hue ☐ Other
Specify		Specify	
Conclusion HRR	☐ Normal ☐ Protan defect ☐ Deutan defect ☐ Tritan defect ☐ Not applicable	Conclusion HRR	☐ Normal ☐ Protan defect ☐ Deutan defect ☐ Tritan defect ☐ Not applicable
Conclusion HRR Severity	Please select... ▾	Conclusion HRR Severity	Please select... ▾
Conclusion Panel D15	☐ Normal ☐ Protan defect ☐ Deutan defect ☐ Tritan defect ☐ Not applicable	Conclusion Panel D15	☐ Normal ☐ Protan defect ☐ Deutan defect ☐ Tritan defect ☐ Not applicable
Conclusion Ishihara	☐ Normal ☐ Protan defect ☐ Deutan defect ☐ Tritan defect ☐ Not applicable	Conclusion Ishihara	☐ Normal ☐ Protan defect ☐ Deutan defect ☐ Tritan defect ☐ Not applicable
Conclusion 100 Hue	☐ Normal ☐ Protan defect ☐ Deutan defect ☐ Tritan defect ☐ Not applicable	Conclusion 100 Hue	☐ Normal ☐ Protan defect ☐ Deutan defect ☐ Tritan defect ☐ Not applicable
Conclusion other vision tests	☐ Normal ☐ Protan defect ☐ Deutan defect ☐ Tritan defect ☐ Not applicable	Conclusion other vision tests	☐ Normal ☐ Protan defect ☐ Deutan defect ☐ Tritan defect ☐ Not applicable

Copy fields from Right eye to Left eye

Figure A11.1.6: http://www.iovs.org/content/suppl/2014/11/17/55.11.7355.DC1/IOVS-14-15317-s06.pdf

Ganzfeld ERG

Right eye	
ffERG performed [*]	○ No ◉ Yes
b/a quotient	[_____]

Scotopic amplitudes

Dim single flash b-wave	Please select... ▾
Standard flash a-wave	Please select... ▾
Standard flash b-wave	Please select... ▾
Oscillatory potentials	Please select... ▾

Scotopic implicit times

Dim single flash b-wave	Please select... ▾
Standard flash a-wave	Please select... ▾
Standard flash b-wave	Please select... ▾
Oscillatory potentials	Please select... ▾

Photopic: amplitudes

30 Hz flicker	Please select... ▾
Single flash a-wave	Please select... ▾
Single flash b-wave	Please select... ▾

Photopic: implicit times

30 Hz flicker	Please select... ▾
Single flash a-wave	Please select... ▾
Single flash b-wave	Please select... ▾

Upload
Upload [_____] [Bladeren...]

[Copy fields from Right eye to Left eye]

Left eye	
ffERG performed [*]	○ No ◉ Yes
b/a quotient	[_____]

Scotopic amplitudes

Dim single flash b-wave	Please select... ▾
Standard flash a-wave	Please select... ▾
Standard flash b-wave	Please select... ▾
Oscillatory potentials	Please select... ▾

Scotopic implicit times

Dim single flash b-wave	Please select... ▾
Standard flash a-wave	Please select... ▾
Standard flash b-wave	Please select... ▾
Oscillatory potentials	Please select... ▾

Photopic: amplitudes

30 Hz flicker	Please select... ▾
Single flash a-wave	Please select... ▾
Single flash b-wave	Please select... ▾

Photopic: implicit times

30 Hz flicker	Please select... ▾
Single flash a-wave	Please select... ▾
Single flash b-wave	Please select... ▾

Upload
Upload [_____] [Bladeren...]

Multifocal ERG

Right eye	
Multifocal ERG performed [*]	○ No ◉ Yes

Amplitudes	Ring	1	2	3	4	5
Not applicable		◉	○	◉	○	◉
Within normal range		◉	○	◉	○	◉
Moderately reduced		◉	○	◉	○	◉
Severely reduced		◉	○	◉	○	◉
Not detectable		◉	○	◉	○	◉

Implicit times	Ring	1	2	3	4	5
Not applicable		◉	○	◉	○	◉
Within normal range		◉	○	◉	○	◉
Moderately reduced		◉	○	◉	○	◉
Severely reduced		◉	○	◉	○	◉
Not detectable		◉	○	◉	○	◉

Upload
Upload [_____] [Bladeren...]

[Copy fields from Right eye to Left eye]

Left eye	
Multifocal ERG performed [*]	○ No ◉ Yes

Amplitudes	Ring	1	2	3	4	5
Not applicable		◉	○	◉	○	◉
Within normal range		◉	○	◉	○	◉
Moderately reduced		◉	○	◉	○	◉
Severely reduced		◉	○	◉	○	◉
Not detectable		◉	○	◉	○	◉

Implicit times	Ring	1	2	3	4	5
Not applicable		◉	○	◉	○	◉
Within normal range		◉	○	◉	○	◉
Moderately reduced		◉	○	◉	○	◉
Severely reduced		◉	○	◉	○	◉
Not detectable		◉	○	◉	○	◉

Upload
Upload [_____] [Bladeren...]

Figure A11.1.6: (Continued)

ERG interpretation

Right eye	
Interpretation *	Please select... ▾
Options	○ Rod dystrophy pattern
	○ Cone dystrophy pattern
	○ Rod-cone dystrophy pattern
	○ Cone-rod dystrophy pattern
	○ Negative ERG
	○ Enhanced s-cone
	○ Maculadystrophy pattern
	○ Other
Other	
Comment	

Left eye	
Interpretation	Please select... ▾
Options	○ Rod dystrophy pattern
	○ Cone dystrophy pattern
	○ Rod-cone dystrophy pattern
	○ Cone-rod dystrophy pattern
	○ Negative ERG
	○ Enhanced s-cone
	○ Maculadystrophy pattern
	○ Other
Other	
Comment	

Copy fields from Right eye to Left eye

EOG

Right eye	
EOG was performed *	○ No ● Yes
Raw data	Please select... ▾
Arden ratio	
Delay of light peak > 2 min	☐
Conclusion EOG	▾
Comment	
Upload	Bladeren...

Left eye	
EOG was performed *	○ No ● Yes
Raw data	Please select... ▾
Arden ratio	
Delay of light peak > 2 min	☐
Conclusion EOG	▾
Comment	
Upload	Bladeren...

Copy fields from Right eye to Left eye

Dark adaptation

Right eye	
Dark adaptation was performed *	○ No ● Yes
Dark adaptation *	Please select... ▾
Elevation (Log)	

Left eye	
Dark adaptation was performed *	○ No ● Yes
Dark adaptation	Please select... ▾
Elevation (Log)	

Copy fields from Right eye to Left eye

Photography

Right eye	
Photography was performed *	○ No ● Yes
Upload	Bladeren...

Left eye	
Photography was performed *	○ No ● Yes
Upload	Bladeren...

Copy fields from Right eye to Left eye

Figure A11.1.6: (Continued)

Optical coherence tomography

Right eye		Left eye	
OCT was performed *	Please select... ▾	OCT was performed *	Please select... ▾
Foveal thickness (μ)		Foveal thickness (μ)	
Not measurable	☐	Not measurable	☐
Central photoreceptor degeneration	○ Not applicable ○ Not determinable ○ No ○ Yes	Central photoreceptor degeneration	○ Not applicable ○ Not determinable ○ No ○ Yes
Peripheral photoreceptor degeneration	○ Not applicable ○ Not determinable ○ No ○ Yes	Peripheral photoreceptor degeneration	○ Not applicable ○ Not determinable ○ No ○ Yes
Central RPE atrophy	○ Not applicable ○ Not determinable ○ No ○ Yes	Central RPE atrophy	○ Not applicable ○ Not determinable ○ No ○ Yes
Peripheral RPE atrophy	○ Not applicable ○ Not determinable ○ No ○ Yes	Peripheral RPE atrophy	○ Not applicable ○ Not determinable ○ No ○ Yes
Central atrophy of choriocapillary	○ Not applicable ○ Not determinable ○ No ○ Yes	Central atrophy of choriocapillary	○ Not applicable ○ Not determinable ○ No ○ Yes
Peripheral atrophy of the choriocapillaris	○ Not applicable ○ Not determinable ○ No ○ Yes	Peripheral atrophy of the choriocapillaris	○ Not applicable ○ Not determinable ○ No ○ Yes
Peripheral intraretinal pigmentations	○ Not applicable ○ Not determinable ○ No ○ Yes	Peripheral intraretinal pigmentations	○ Not applicable ○ Not determinable ○ No ○ Yes
Cystoid macular edema	○ Not applicable ○ Not determinable ○ No ○ Yes	Cystoid macular edema	○ Not applicable ○ Not determinable ○ No ○ Yes
Epiretinal membrane	○ Not applicable ○ Not determinable ○ No ○ Yes	Epiretinal membrane	○ Not applicable ○ Not determinable ○ No ○ Yes
Retinal schisis	○ Not applicable ○ Not determinable ○ No ○ Yes	Retinal schisis	○ Not applicable ○ Not determinable ○ No ○ Yes
Vitreoretinal traction	○ Not applicable ○ Not determinable ○ No ○ Yes	Vitreoretinal traction	○ Not applicable ○ Not determinable ○ No ○ Yes
Foveal hypoplasia	○ Not applicable ○ Not determinable ○ No ○ Yes	Foveal hypoplasia	○ Not applicable ○ Not determinable ○ No ○ Yes
Other		Other	
Upload	Bladeren...	Upload	Bladeren...

Copy fields from Right eye to Left eye

Figure A11.1.6: (Continued)

Autofluorescence

Right eye	
Autofluorescence was performed *	Please select... ▾
Macula	Please select... ▾
Periphery	Please select... ▾
Ring present	Please select... ▾
Comment	
Upload	Bladeren...

[Copy fields from Right eye to Left eye]

Left eye	
Autofluorescence was performed *	Please select... ▾
Macula	Please select... ▾
Periphery	Please select... ▾
Ring present	Please select... ▾
Comment	
Upload	Bladeren...

Fluorescence Angiography (FA)

Right eye	
FA was performed *	○ No ◉ Yes
Cystoid macular edema	○ Not applicable ○ Not determinable ○ No ○ Yes
Window defect	○ Not applicable ○ Not determinable ○ No ○ Yes
Vasculitis	○ Not applicable ○ Not determinable ○ No ○ Yes
Dark choroid	○ Not applicable ○ Not determinable ○ No ○ Yes
Non-perfusion	○ Not applicable ○ Not determinable ○ No ○ Yes
Scar staining	○ Not applicable ○ Not determinable ○ No ○ Yes
Details	

Left eye	
FA was performed *	○ No ◉ Yes
Cystoid macular edema	○ Not applicable ○ Not determinable ○ No ○ Yes
Window defect	○ Not applicable ○ Not determinable ○ No ○ Yes
Vasculitis	○ Not applicable ○ Not determinable ○ No ○ Yes
Dark choroid	○ Not applicable ○ Not determinable ○ No ○ Yes
Non-perfusion	○ Not applicable ○ Not determinable ○ No ○ Yes
Scar staining	○ Not applicable ○ Not determinable ○ No ○ Yes
Details	

[Copy fields from Right eye to Left eye]

[Save] [Back]

Figure A11.1.6: (Continued)

Figure A11.1.7: http://www.iovs.org/content/suppl/2014/11/17/55.11.7355.DC1/IOVS-14-15317-s07.pdf

```
          Benign concentric annular macular dystrophy
          Bietti crystalline retinopathy
          Doyne's honeycombed dystrophy/Malattia leventinese
          North Carolina macular dystrophy
          Occult macular dystrophy
          Syndromic retinal dystrophies - see 'Syndromes'
          Sorsby macular dystrophy
        X-linked retinoschisis
          X-linked retinoschisis
          X-linked retinoschisis female carrier
        Other (please specify)
    Stationary retinal dystrophies
      Color vision defects
          Achromatopsia (Rod monochromatism)
          Blue-cone monochromatism
          Incomplete achromatopsia
          Other (please specify)
      Congenital stationary night blindness (CSNB)
          adCSNB
          arCSNB
        xlCSNB
            xlCSNB
            xlCSNB female carrier
        CSNB with specific retinal abnomalities
            Fundus albipunctatus
            Fleck retina of Kandori
            Oguchi disease
          Other (please specify)
        Other (please specify)
    Hereditary vitreoretinal degenerations
        Stickler and other syndromic vitreoretinal degenerations - see 'Syndromes'
        Autosomal dominant vitreoretinochoroidopathy
        Erosive vitreoretinopathy
        Familial exudative vitreoretinopathy
        Jansen syndrome
        Wagner syndrome
        Other (please specify)
  Syndromes
    Cockayne syndrome
        Cockayne syndrome type 1
        Cockayne syndrome type 2
        Cockayne syndrome type 3
    Mitochondrial syndromes including retinopathy
        Kearns-Sayre syndrome
        Maternally inherited diabetes and deafness (MIDD)
        Mitochondrial encephalomyopathy, lactic acidosis, and stroke-like episodes (MELAS)
        Myoclonic Epilepsy with Ragged Red Fibers (MERRF)
        Neuropathy, ataxia and RP (NARP) syndrome
    Neuronal ceroid lipofuscinosis (Batten disease)
        Classic infantile Batten disease (Haltia-Santavuori disease/Hagberg-Santavuori disease)
        Classic late-infantile Batten disease (Jansky-Bielschowsky disease)
        Classic late-infantile Batten disease (Jansky-Bielschowsky disease)
        Adult Batten disease (Kufs disease)
    Refsum disease
        Infantile Refsum disease
        Adult-onset Refsum disease
    Usher syndrome
        Usher syndrome type 1
        Usher syndrome type 2
        Usher syndrome type 3
    Vitreoretinal syndromes
      Stickler syndrome
          Stickler syndrome type 1
          Stickler syndrome type 2
          Stickler syndrome type 3
        Knobloch syndrome
        Marshall syndrome
      Alstrom syndrome
      Bassen-Kornzweig syndrome (abetalipoproteinemia)
      Bardet-Biedl syndrome
      Block-Sulzberger syndrome (incontinentia pigmenti)
      Boucher-Neuhauser syndrome
      Charcot-Marie-Tooth disease
    Joubert syndrome
        Joubert syndrome
        Joubert syndrome female carrier (X-Linked)
      Kearns-Sayre syndrome
      Laurence-Moon syndrome
      Mucopolysaccharidosis 1 (Hurler-Scheie syndrome)
    Mucopolysaccharidosis 2 (Hunter syndrome, X-linked)
        Mucopolysaccharidosis 2 (Hunter syndrome, X-linked)
        Mucopolysaccharidosis 2 (Hunter syndrome, X-linked) female carrier
    Norrie disease
        Norrie disease
        Norrie disease carrier
```

Figure A11.1.7: (Continued)

Figure A11.1.7: (Continued)

Appendix 11.2: Supplemental figures
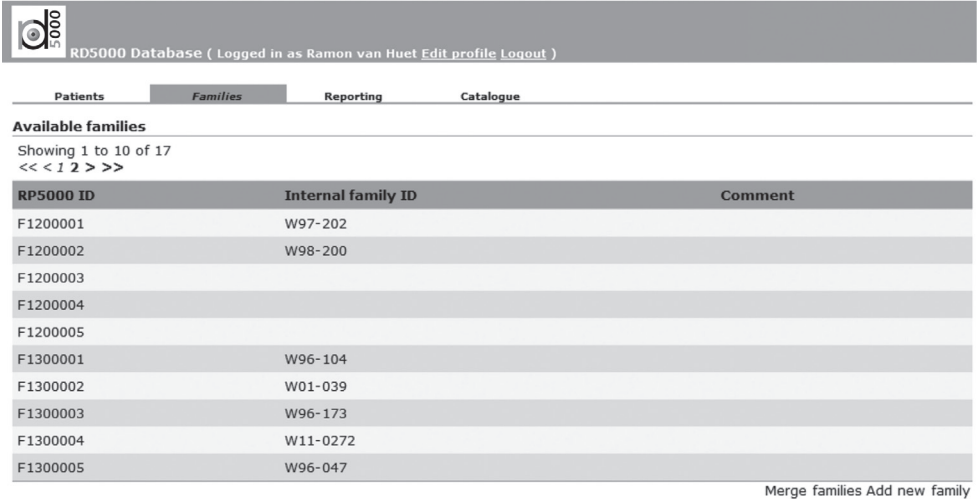
Figure A11.2.1: http://www.iovs.org/content/suppl/2014/11/17/55.11.7355.DC1/IOVS-14-15317-s08.pdf
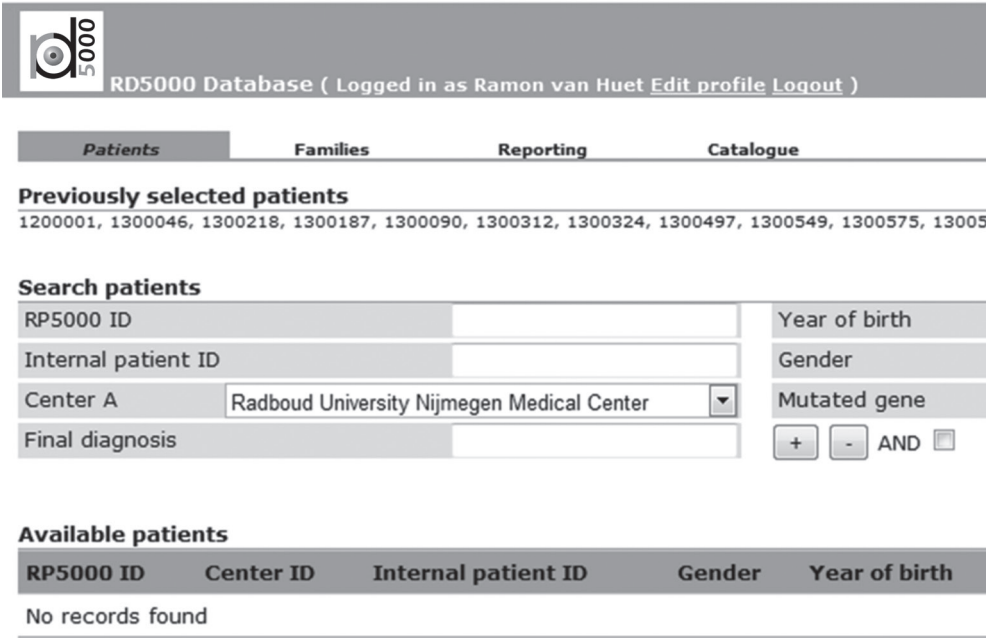
Figure A11.2.2: http://www.iovs.org/content/suppl/2014/11/17/55.11.7355.DC1/IOVS-14-15317-s09.pdf

Figure A11.2.3: http://www.iovs.org/content/suppl/2014/11/17/55.11.7355.DC1/IOVS-14-15317-s10.pdf

Appendix 11.3: Costs

The basic technical set-up costs of the database, with Ophthabase as a basic structure, were approximately € 85,000. Based on the current use that includes 11 centers, the running costs are about € 1,000 per month, which warrants maintenance, system stability, regular back-up of the database and of the source code, security updates and support. On top of that, the consortium manager spends 6 hours per week on both organizational tasks of the consortium and system administration. Currently, the costs can be covered by the funding from Dutch blindness foundations.

11

General discussion

12

This thesis contains studies on phenotypic and molecular characteristics of a group of selected inherited retinal dystrophies (IRDs) and discusses the genotype-phenotype correlations. This chapter considers IRDs in a broader perspective, and discusses current and future perspectives on phenotypic evaluation, genotype-phenotype correlations and therapeutic possibilities. These items are subsequently integrated in the future management of patients with IRDs, which perfectly fits the personalized-medicine approach.

Clinical aspects of inherited retinal dystrophies

Clinical heterogeneity

One characteristic that applies to virtually all IRDs is *heterogeneity*. This is reflected in the tremendous number of genes and mutations involved, as well as the wide variation in phenotypes, even when one considers a single clinical entity like for example *MAK*-associated retinitis pigmentosa (RP). This clinical heterogeneity has expanded over time due to an increase in clinical parameters. New multimodal applications have appeared such as fundus perimetry (microperimetry), which combines retinal en face imaging with perimetry to provide topographic retinal sensitivity levels, as well as the preferred point of fixation.[1] In addition, new approaches for clinical examination have been developed and found their way into routine ophthalmic practice in the past few decades, like for example high-resolution (spectral domain) optical coherence tomography (OCT) and fundus autofluorescence (FAF) imaging.[2-4] The OCT technique is currently refined by adaptive optics to increase the spatial resolution, up to cellular levels,[5,6] and are applied in new examinations, like for example in OCT-based microangiography and OCT changes in retinal responses to light stimulation (functional OCT).[5,7] These new techniques provide very detailed structural and functional information, which increases our understanding of the retinal physiology and the effects of certain genetic defects.

One desired test still missing in the pallet of retinal parameters is an objective measurement of topographic retinal function. Functional OCT aims at this, but focuses on (1) optical changes induced by light, an indirect parameter of photoreceptor function, and (2) retinal structure, which also does not always correlate with visual function. For example, RP patients with a central island of photoreceptors of 5-10˚ on OCT imaging often reveal a visual field extending to 40-50˚ degrees eccentricity. Multifocal electroretinography (mfERG) provides the macular neuronal action potential, which may be a more direct parameter of the functionality of photoreceptor, bipolar and ganglion cells, but it is easily disturbed by fixation losses and does not appreciate retinal structure. Performing mfERG with simultaneous retinal image tracking could provide a stable repeatable localization of the responses measured. Ideally, en face imaging, (functional) OCT and mfERG should be integrated to provide objective data on topographic retinal functionality. This data can be useful in follow-up of patients, and be of great value in the selection of patients and evaluation of treatment effects in therapeutic trials.

Genetic causes of clinical heterogeneity

IRDs are generally considered to be monogenic diseases: the disease is caused by defects in a single gene. However, we often cannot determine evident genotype-phenotype

correlations among IRD patients, and observe clinical variance between families and even within families. This may indicated the involvement of other (genetic) factors. Changes in so-called *modifier genes* have often been attributed to cause clinical variance in IRD patients.[8-11] In this concept, all retinal genes could influence the retinal phenotype, since they harbor for instance heterozygous mutations (in genes that lead to disease with recessive inheritance patterns) or single nucleotide polymorphisms (SNPs) that may change the resilience of a specific pathway or the general retinal condition, and make the retina more or less susceptible to degeneration.

In light of this, it is debatable if retinal dystrophies, or any genetic disease, can be considered truly monogenic, since the genetic context is always of influence up to some degree. Of course, IRDs are considered monogenic because the causative genetic defects are identified in one specific gene that fits a Mendelian inheritance pattern and without these defects the retina would function as in normal-sighted individuals. However, the retina is a very complex tissue that survives and functions because of numerous proteins expressed from approximately 19,500 genes.[12] SNPs occur in all individuals and clear-cut pathologic mutations occur in 1 out of 4-5 individuals in the general population,[13] so this large number of genes involved in the retinal tissue implicates that modifier effects probably are of influence in *each* IRD patient. Yet, these modifier effects may be of different magnitude since one pathway may be imbalanced more easily compared to the other.

Genetic analysis by whole exome sequencing provides data on variants found in all retinal genes, and therefore on the 'retinal genotype' of a patient. However, knowledge on the functional consequences of these variants is often lacking. It is difficult and laborious to determine these effects, which may – especially in case of SNPs - be small or even nearly indifferent from normal protein function. Moreover, other factors such as differences in gene expression levels, epigenetics and nutritional status may have their share in determining the retinal phenotype apart from modifier effects. Much knowledge has to be gained on the factors influencing the retinal phenotype and mutual interactions between these factors. We are far from getting a complete genetic profile of each IRD patient, yet new techniques for genetic analysis like next-generation sequencing (NGS) enable analysis of whole pathways or all retinal genes known up to now. This may provide insight in the probable 'multigenic' character of these diseases, and lead to clear associations between the genetic findings and the phenotype. The large amount of data generated by NGS however complicates variant prioritization, but the main difficulty will be the low number of patients with comparable genetic and clinical features to verify findings, as in this approach the specific genetic combinations may be found in only a single patient. This may increase the need of international collaborations and international databases on genotypes and phenotypes. Additionally, bioinformatics may get a prominent role in verification of research findings by means of theoretic models, prediction tools and other bioinformatic approaches.

Another fascinating observation is that mutations in some genes can cause retinal disease in both rod-cone or cone-rod patterns, like we observed in *C8orf37*-associated retinal disease (see **chapter 4**), and also has been described among patients with mutations in *CERKL, MERTK, CRX* or *PROM1*.[14-24] How can mutations in one gene result in almost opposite

degeneration patterns? To cause preliminary degeneration in rods (rod-cone pattern) or cones (cone-rod pattern), the gene needs to be expressed in both types of photoreceptors. If a gene is expressed in only one type of photoreceptor, for example rods, the rod degeneration is expected to preceed cone degeneration, since the cones degenerate secondarily due to the loss of rods in this scenario, resulting in a rod-cone dystrophy. This, however, still does not explain the difference in degeneration pattern among patients. Mutational differences would not directly result in opposite degeneration patterns, unless there are domains in the protein that are more important in either rods or cones. The same may occur if rods and cones have specific isoforms of the protein. Another explanation may be that the degeneration pattern is determined by variants in other genes involved in the same pathway. These pathways may differ in detail among rods and cones, which can result in a more pronounced degeneration in one of the photoreceptor cell types. However, we often lack data on protein function, isoforms expressed in the retina, or simultaneous defects in pathway-related genes. Further analysis of genetic changes in specific pathways, as well as analysis of corresponding features of such genes may provide insight in the origin of the differences in degeneration pattern.

Systemic features of inherited retinal dystrophies
Many syndromic forms of IRDs, especially RP and CRD, have been described in literature. These syndromes can be caused by mitochondrial and metabolic defects, but also may rise from defects in *ciliary* genes, which are genes involved in the structure and functioning of the hair-like cellular organelle called the cilium that is present in virtually each cell in the human body. First considered rudimentary, the cilium is recognized as essential in numerous tissues, such as the retina, the inner ear, the olfactory system, the kidneys, respiratory tract epithelium and the liver.[25,26] In the retina, the connecting cilium and outer segment in the photoreceptors are highly modified primary cilia (see also **chapter 1**).

In patients with IRDs, extra-ocular features are often underappreciated, and evaluation of the presence of these symptoms almost seems to be academic. However, history taking with a focus on the most prevalent syndromic features related to IRDs can provide an impression if the IRD is syndromic. Mockel and colleagues provided a detailed overview of the extra-ocular tissues that can be affected in syndromic forms of retinal degeneration.[26] Most frequent symptoms include hearing and balance abnormalities, renal failure and nephronophthisis, cardiac and respiratory anomalies, olfactory deficiencies, polydactyly, obesity, cognitive impairment, fertility disorders, hypogonadism and dental anomalies. Presence of extra-ocular symptoms can guide genetic analysis, although this may be of less importance with the introduction of NGS techniques. More importantly, syndromic disease may be applicable for symptomatic treatment, and patients should be referred to the right specialist if necessary.

The mere presence of an extra-ocular symptom, however, does not necessarily confirm the diagnosis of a syndromic disease, since extra-ocular symptoms also occur in the general population and patients may suffer from other pathology simultaneously to but independent from their retinal dystrophy. On the other hand, the absence of extra-ocular symptoms during history taking does not exclude syndromic disease either, since these extra-ocular symptoms may develop in a later disease stage than the ocular symptoms, or may be present subclinically. However, little is known of the prevalence of subclinical syndromic features

in IRD patients or the general population. Our studies on *ABHD12*-associated disease (**chapter 5**) and *USH1G*-associated disease (**chapter 6**) highlight that such disease often present as a phenotypic spectrum in which tissues can be affected to different degrees, which has also been observed in other ciliary genes such as *USH2A*, *BBS1* and *RPGR*.[27-33] If syndromic features are present but the diagnostic criteria of none of the known syndromes is met, descriptive diagnoses are often used. If patients do meet the diagnostic criteria of a known syndrome, new genotype-phenotype associations may occur, such as Usher syndrome in patients with *RPGR* mutations. The use of NGS techniques and a focus on extra-ocular symptoms may reveal such new associations.

Nomenclature of inherited retinal dystrophies
The nomenclature of IRDs is complicated and confusing, and is insufficient for the heterogenic nature of IRDs. The currently used nomenclature historically grew from clinical observations in an era in which the genetic causes were not known, and was already complicated by overlap in clinical appearance (e.g. RP with macular involvement and CRD) and misnomers (e.g. retinitis pigmentosa is not caused by inflammation or infection). The identification of many genes involved in IRDs illustrated the overlap in pathology (e.g. Stargardt disease (STGD1) and fundus flavimaculatus). This led to a 'subtype classification' of RP and CRD, where each gene causes a specific type of RP or CRD. Moreover, the lack of therapeutic consequences did not aid IRD nomenclature, although receiving the right diagnosis becomes vital now highly personalized gene-specific therapies are coming into perspective.

Diseases are generally classified by the combination of specific clinical features and a specific pathologic process. However, reported clinical observations did not always lead to classifications applicable in practice, as can be observed in the phenotypic and electrophysiological classifications that have been described in STGD1.[34,35] Yet, these classifications do not seem to be able to provide a suitable classification for STGD1, since the pathologic process underlying the heterogeneous character is not understood completely. The clinical classification based on the age at onset that we optioned in our studies on STGD1 (see **chapter 8 and 9** of this thesis) is applicable in each patient, and seems to provide a general indication on severity of the disease. However, since no genetic associations with the clinical differences were found, this classification also lacks a pathologic background, and therefore probably can be improved.

An important, yet underappreciated, factor in nomenclature of IRDs is *time*. Clinical phenotypes of progressive IRD change during the patient's life, which may complicate the correct diagnosing. If, for example, an electroretinogram (ERG) reveals a cone-rod pattern the differentiation between RP and CRD seems obvious, while in advanced disease, when the scotopic and photopic ERG responses often are equally reduced or nonrecordable and the fundus becomes more atrophic, differentiation between RP and CRD becomes more difficult. Additionally, an IRD may progress from one phenotype into a phenotype that does not fit the initial diagnosis, and, because of this, patients not incidentally receive multiple diagnoses during their lifetime. However, the pathologic process did not change, and therefore the diagnosis should not be changed, especially when genetically confirmed. For example, a 70-years-old patient with STGD1 with an atrophic posterior pole, pigmentary

12

changes and severely affected photopic ERG still has STGD1, although the phenotype would currently be classified as CRD.

Receiving the wrong diagnosis or multiple diagnoses can be very confusing for the patient, especially now patients have easy access to a huge amount of information on the Internet. Detailed history taking, perimetry, (previous) ophthalmic examinations, genetic testing, and advertency to the disease stage can help in providing the right diagnosis. In some IRD cases however, diagnosing is unclear despite of a thorough history taking and clinical evaluation, such as some of the patients with *C8orf37*-associated retinal dystrophies described in **chapter 4**. The diagnosis of RP with early macular involvement is mainly descriptive, while differentiation with early-onset CRD and Leber congenital amaurosis (LCA) is debatable.

The facts discussed above make it difficult to propose a more consistent method of nomenclature for the heterogeneous progressive IRDs. The overlap in clinical appearance tempts the use of universal terms like 'photoreceptor dystrophy', which, on the other hand, lacks any descriptive value of the clinical features of the disease. Slightly more specific terms such as 'rod-cone dystrophy' or 'cone-rod dystrophy' can be useful, although these electrophysiological classifications are not always obvious. The age of onset provides an indication of the progression rate of the IRD as well as the disease stage a patient is in when the age is known. This can be reflected in terms such as 'early-onset' or 'late-onset', although 'childhood-onset', 'adolescence-onset' and 'adult-onset' are more specific and preferable. In light of the upcoming gene augmentation therapies, it seems vital to include the causative gene in the diagnosis, although this seems ambiguous since the retinal phenotype probably is the result of the variants in multiple retinal genes (see above). These factors – general diagnosis, onset and causative gene – can be used as a more systematic approach that is applicable in most patients. In this approach the nomenclature provides more information on the clinical and genetic features of the disease than the currently used subtype classification used in RP and CRD. However, new insights in the genetic background and their relation to the phenotype may provide a better classification of IRDs, i.e. based on the defective gene or pathway.

Management of IRD patients

Up to now, the management of patients with IRDs mainly involved a follow-up of the progression of visual field and visual acuity loss, (prenatal) genetic counseling, recommending the use of sunglasses and low-vision aids if necessary, and/or providing information on therapy trials and participation in these studies. Some studies suggested that treatment with vitamin A, fish oils (docosahexaenoic, DHA) or both resulted in a slower decline of ERG amplitudes and visual field in patients with RP.[36-40] In 2013, however, a Cochrane systematic review by Rayapudi et al concluded that there is no clear evidence for benefit of treatment with vitamin A and/or DHA for RP patients.[41] An important issue here is that these studies treated RP as if it was one disease. We know now that numerous genes are involved in the pathogenesis of RP, and that vitamin A suppletion could well be beneficial in one form of RP while being harmful in another. For example, vitamin A suppletion is harmful in patients carrying *ABCA4* mutations, due to the increased accumulation of toxic vitamin A derivates (especially A2E). Nevertheless, the studies on vitamin A suppletion mentioned above found a beneficial

effect despite the heterogeneous cohort, which implies that in some forms of RP vitamin A is beneficial. To what extend cannot be said, since the distribution of genetic causes in these cohorts is not known. Recently, studies involving administration of a specific vitamin A derivate in RP cases with defects in genes involved in the retinoid cycle (*RPE65*, *LRAT*) reported beneficial effects (see Upcoming treatments below).[42-44]

Several trials evaluated the effects of valproic acid (VPA) in RP patients. VPA is generally used as an anticonvulsant, migraine prophylaxis or in the treatment of bipolar disease. It inhibits histone deacetylase, downregulates complement proteins, and increases the levels of neurotrophic factors.[45-50] Clemson et al initially reported beneficial effects of VPA administration in RP patients, although the scientific rationale and conclusions of this study were questioned.[51-53] Several studies have been published since: some reporting beneficial effects, some reporting harmful effects.[54-57] A study on the effects of VPA on Rd1 and Rd10 mice found no beneficial effects on photoreceptor survival, while they observed harmful effects when administered in an early disease stage.[58] Although the mechanisms in which VPA has its effect on the retina need to be elucidated, a randomized double-blinded trial with VPA in RP patients is currently ongoing (www.clinicaltrials.gov).

The management of IRDs further involves measures that help patients cope with their visual handicap. IRD patients should be encouraged to visit vision-rehabilitation clinics in which visual aids can be offered to improve (night) vision.[59-61] For some patients and their family members it can be helpful to join a support group to discuss problems and solutions involved in living with a visual handicap. Other measures focus on other forms of ocular pathology that may accompany IRDs, whether or not associated with the retinal dystrophy, but that *can* be treated. Subcapsular posterior cataract, for instance, occurs in about 50% of RP patients.[62-65] Patients with lens opacities that substantially affect distance or near vision can benefit of cataract extraction. Another example would be epiretinal membrane peeling in IRD patients when this condition causes loss of vision and/or metamorphopsia.[66] Patients with cystoid macular edema (CME) may benefit from treatment with carbonic anhydrase inhibitors (CAIs).[67-76] Treatment of CME with intravitreal steroids may as well be beneficial, but its efficiency seems to be limited over time.[77-81] Intravitreal treatment with vascular endothelial growth factor (VEGF) antibodies has been reported to decrease CME in one study,[82] but generally had no beneficial effect on the oedema.[83-85] Moreover, intravitreal anti-VEGFs may theoretically be harmful in IRD patients, since VEGF levels are reportedly decreased in RP patients.[86]

Upcoming treatments

The insights in the genetic background of IRDs have led to a better understanding of the molecular defects causing the various diseases. This sourced a new era of research into therapeutic options for retinal disease that focus on repairing or passing by the specific genetic deficit, renew retinal photosensitivity or replace lost tissue. Each therapeutic approach has specific characteristics and focuses on specific patient populations. The therapeutic approaches that currently are under evaluation are briefly reviewed in the paragraphs below. Table 12.1 provides an overview of the clinical trials currently open to patients.

Genetic therapy includes various approaches used to overcome or by-pass the genetic defect by gene augmentation, gene suppression or modulation of the splicing process, or delay retinal degeneration by introduction of genes expressing neuroprotective factors. An important factor in determining the approach necessary is the effect the mutations have on protein function, e.g loss-of-function effects, gain-of-function effects, or dominant-negative effects (the mutated protein has negative effects on the functional protein product of the other allele).[87] *Gene augmentation therapy* (GAT) can be used in case of loss-of-function defects. GAT involves introduction of a wildtype cDNA copy of the mutated gene, which produces a functional protein and potentially restores the related pathways.[88-90] In dominant-negative effects GAT can be attributed to reach sufficient levels of the functional protein. Challenges that appeared in this approach are the limited cargo size of some of the viral vectors used, the level of transduction of viral vectors for photoreceptor and retinal pigment epithelium (RPE) cells, the route of drug delivery, immune responses against the viral vector, and duration of the therapeutic effect after a single administration.[87] This strategy focuses on stopping disease progression (although improvement of visual function has been observed as well[88]), and therefore will be mainly applicable for patients with relatively intact retinal structure and/or good visual function.

Clinical studies on GAT for *RPE65*-associated retinal disease have shown remarkable effects,[89] and probably receive FDA approval shortly. This really boosted the research on GAT for other diseases (Table 12.1), as well as genetic therapy in general.

GAT can also be used to elevate the expression of genes for neuroprotective factors in the retina, and thereby prolong the survival of photoreceptors regardless of their genetic defect. Factors that have been involved in this approach are ciliary neurotrophic factor (CNTF), brain-derived neurotrophic factor (BDNF), glial-cell derived neurotrophic factor (GDNF), X-linked inhibitor of apoptosis (XIAP), and rod-derived cone viability factor (RdCVF).[91-100] Advantages of this approach are that these factors are highly diffusible, and the therapeutic gene can be administered to any tissue close by the retina resulting in a paracrine effect.[87] The main downside of this approach is that this therapy does not prevent retinal degeneration, which eventually occurs albeit at a later point in the disease course. This approach focuses on the patients with a fairly intact retina, although it may be beneficial in advanced disease as well, as CNTF has shown to be beneficial in geographic atrophy in age-related macular degeneration.[101]

In some dominantly inherited diseases with gain-of-function or dominant-negative effects, the mutated protein has negative effects on protein or cellular function. Introduction of a wild-type cDNA copy of the mutated gene does not reduce this negative effect, and *gene* or *allele silencing* is essential. Suppression of the mutated gene or allele can be reached by the use ribozymes, or RNA interference.[102-105] If haploinsufficiency occurs after suppression, introduction of a wildtype copy of the gene with GAT may be necessary, a strategy known as 'suppression and replacement'.[87] Challenges in this approach include route of drug delivery, specificity for the gene that should be suppressed and reaching sufficient suppression. This approach also focuses on patients with relatively intact retinal tissue and function.

Table 12.1 Overview of the currently open clinical trials as noted at www.clinicaltrials.gov.

Therapeutic approach	Trial Identifier	Condition	Age criteria	Intervention	Phase	Estimated enrollment	Estimated study completion date
Gene augmentation therapy	NCT01505062	Usher syndrome type 1B	≥ 18 years	UshStat	I/II	18	January 2017
	NCT00821340	RPE65-associated retinal dystrophy	≥ 8 years	rAAV2-hRPE65	I	10	January 2017
	NCT01482195	MERTK-associated retinal dystrophy	14-70 years	rAAV2-VMD2-hMERTK	I	6	August 2023
	NCT01461213	Choroideremia	≥ 18 years	rAAV2.REP1	I/II	12	June 2016
	NCT02077361	Choroideremia	≥ 18 years	rAAV2.REP1	I	12	December 2018
	NCT01367444	Stargardt macular degeneration due to ABCA4 mutations	≥ 18 years	StarGen	I/IIa	28	October 2015
	NCT02317887	X-linked juvenile retinoschisis	≥ 18 years	AAV8-scRS/IRBPhRS	I/II	100	June 2016
Stem cell-based therapy	NCT02280135	RP patients	18-70 years	Intravitreal injection of Autologous bone marrow Stem Cell	I	10	August 2016
	NCT01914913	RP patients	18-65 years	Autologous bone marrow derived mono nuclear stem cell transplantation	I/II	15	November 2016
	NCT01736059	Among others: patients with RP or inherited macular degeneration	≥ 18 years	CD34+ bone marrow stem cells intravitreal	I	15	December 2015
	NCT02320812	RP patients	≥ 18 years	Human retinal progenitor cells	I/II	16	December 2016
	NCT01469832	Patients with STGD1, FF or JMD	≥ 18 years	Sub-retinal Transplantation of Human Embryonic Stem Cell Derived Retinal Pigmented Epithelial (hESC-RPE) Cells	I/II	16	December 2014
	NCT01920867	Among others patients with inherited retinal dystrophies	≥ 18 years	Retrobulbar, subtenon, intravenous, intravitreal, or intraocular injection of autologous bone marrow derived stem cells	N/A	300	August 2017

12

Therapeutic approach	Trial identifier	Condition	Age criteria	Intervention	Phase	Estimated enrollment	Estimated study completion date
	NCT01345006	STGD1 patients	≥ 18 years	Sub-retinal Transplantation of Human Embryonic Stem Cell Derived Retinal Pigmented Epithelial (MA09-hRPE) Cells	I/II	16	December 2014
	NCT01625559	STGD1 patients	≥ 20 years	Sub-retinal Transplantation of Human Embryonic Stem Cell Derived Retinal Pigmented Epithelial(MA09-hRPE) Cells	I	3	October 2014
	NCT01518127	STGD1 and AMD patients	18-80 years	Intravitreal injection of autologous bone marrow stem cells	I/II	10	December 2013
Retinal implants	NCT01024803	Patients with retinal degeneration	18-78 years	Device: Retina Implant model Alpha. Surgical implantation of medical device into eye	N/A	45	December 2016
	NCT01864486	RP, CRD and CHM patients	≥ 25 years	Device: Intelligent Retinal Implant System	N/A	20	N/A
	NCT01999049	RP patients	≥ 25 years	Observational study of the Argus® II Retinal Prosthesis System	N/A	10	January 2017
	NCT02303288	RP patients	≥ 25 years	Device: Argus® II Retinal Prosthesis System	N/A	18	November 2018
	NCT01490827	Patients with outer retinal degeneration	≥ 25 years	Argus® II Retinal Prosthesis System Post-Market Surveillance Study	N/A	45	May 2016
	NCT01860092	RP patients	≥ 25 years	Post-Approval Study of the Argus® II Retinal Prosthesis System	N/A	53	N/A
Vitamin A suppletion	NCT02018692	RP patients	12-18 years	9-*cis*-beta carotene rich Alga *Dunaliella Bardawil* powder	I/II	30	N/A
	NCT01680510	RP patients	≥ 18 years	9-*cis*-beta carotene rich Alga *Dunaliella Bardawil* powder	II/III	100	January 2015

AMD, age-related macular degeneration; CNTF, ciliary neurotrophic factor; CHM, choroideremia; CRD, cone-rod dystrophy; FF, fundus flavimaculatus; JMD, juvenile macular dystrophy; rhNGF, recombinant human nerve growth factor; RP, retinitis pigmentosa; RPE, retinal pigment epithelium; STGD1, Stargardt disease.

Approximately 11% of the mutations involved in IRDs affect splicing processes.[106,107] These mutations result in the inclusion of intronic sequences or the exclusion of exonic sequences in the messenger RNA (mRNA). *Splicing correction* for a small subset of splicing defects can be reached by the use of antisense oligonucleotides (AONs), which are synthetic molecules of generally around 20 nucleotides that mimic RNA structure. AONs can be directed towards specific mutated pre-mRNA sequences, where they bind and mask the pre-mRNA code containing the mutation to prevent recognition by the spliceosome, resulting in e.g. skipping of pseudo-exon that is inserted by an intronic mutation.[107,108] Other strategies in splicing correction have been proposed, including the introduction of an adapted U1 component of the splice complex that is able to bind the mutated splice donor site.[109-111]

Optogenetics is a therapeutic approach in which light-gated ion channels are introduced in the remaining neurons of degenerated retinas that have lost photosensitivity because of a high degree of photoreceptor cell death. These ion channels, e.g. halorhodopsin, channelrhodopsin or archaerhodopsin, modulate membrane potentials (induce depolarization or hyperpolarization) when stimulated by photons, and thereby restore photosensitivity albeit in different cells than it originally was located in.[112] The major challenges in this approach lie in choosing the right optogenetic tool and targeting the correct retinal cells.[113-115] Other difficulties are the high levels of light needed to get light responses, and the high number of optogenetic protein expression, since these optogenetic tools do not benefit from amplification of the G-coupled cascade as normal opsins do.[87,116] In contrast to the gene therapy approaches mentioned above, this approach focuses on patients with photoreceptor loss but intact bipolar and ganglion cells, which generally remain intact even in end-stage disease.

Oral (suppletion) therapy with a vitamin A derivate has been performed in patients suffering from Leber congenital amaurosis (LCA) due to *RPE65* or *LRAT* mutations, two genes that are involved in the retinoid cycle (see **chapter 1**). These patients received oral administration of synthetic 9-*cis*-retinyl acetate for 7 days, which resulted in a rapid improvement of visual field and visual acuity.[42] As observed in mice, 9-*cis*-retinyl acetate is thought to decrease the content of unbound chromophore, reducing the constitutive activation of the phototransduction cascade which is the cause of the retinal degeneration in *RPE65* mutants, and thus slowing down photoreceptor degeneration.[43,44,117] Although tested in a small cohort, the retinoid substrate was well tolerated and did not cause serious adverse events.[42] Like gene therapy, this therapeutic approach focuses on patients with relatively intact retinal structure, although it is applicable in more advanced disease. Long-term side effects as well as duration of the beneficial effects have to be evaluated yet.

Stem cell therapy involves the administration of stem cell-derived retinal cells into the subretinal space, and have been optioned to repair retinal tissue defects in several retinal degenerative diseases, such as STGD1, RP and age-related macular degeneration.[118,119] The eye's immunoprivileged nature makes it attractive for regenerative therapies involving stem cells. Different approaches are used, including transplantation of stem cell-derived RPE, photoreceptors or both.[119] Currently, phase I/II trials are performed to assess safety, graft survival tolerance and activity of pluripotent stem cell progeny.[118,120] In contrast to gene therapy, stem cell-based therapies focus on patients with damaged (outer) retinas, which

generally are observed in patients with advanced disease. Although clinical applications are still in their infancy, stem cell therapy approaches show a high potential, and could well become the therapy of choice in advanced retinal degeneration in the future.[120,121]

Implantation of retinal chips is another therapeutic approach that focuses on patients in even more advanced stage disease. Roughly, there are three kinds of retinal chips: the epiretinal, subretinal and suprachoroidal implants.[122,123] Epiretinal implants stimulate the remaining retinal ganglion cells directly, whereas subretinal implants replace the lost outer retina and stimulate the interneurons and ganglion cells. Epiretinal implants are generally more easily implanted compared to subretinal chips.[122] Two systems are currently commercially available: the Argus II epiretinal implant by Second Sight Medical Products Inc. (Sylmar, CA, USA), and the Alpha-IMS subretinal implant made by Retina Implant AG (Reutlingen, Germany).[123] Currently, retinal implants are used in patients with end-stage disease that even cannot perceive hand movements (light perception level or worse) because the low spatial resolution that can be reached: the best recorded visual acuity in patients with the Argus II implant was 20/1260, and 20/546 in patients with the Alpha-IMS implant. Other challenges involve device survival, contrast sensitivity, color vision, temporal resolution, and binocular vision (so far implants have only been implanted unilaterally).[123,124]

Tongue stimulators have been developed in the past decade, and enable patients to provide information on the patient's surroundings by electrostimulation of the tongue provided from a matrix of electrodes worn inside the mouth. The system (BrainPort Technology, WIBCAB Inc., Middleton, WI) catches the scenery with a camera, whose capture is translated into an impulse by a computer.[125] This approach enables better orientation and navigation in (congenitally) blind individuals, and patients with this device even reached a 'tactile'-acuity of 20/430 measured with the Snellen's tumbling E test after a 9 hour training.[126-128] This relatively simple and noninvasive approach can also be used if the optic nerve has degenerated. Main downside is that the tongue stimulator hinders speech; yet the stimuli feel like a tickle or vibration and are not painful. A clinical trial with 75 patients has been performed, but awaits publication of the results (www.clinicaltrials.gov).

In general, therapies that aim at curing the cause of the disease are considered preferable, and hence much hope is directed towards the genetic therapy approaches. When available and effective, the these therapies probably will be superior compared to the other approaches, at least for patients in the early stage of their disease. On the other hand, one study on gene augmentation therapy in LCA2 (*RPE65*-associated LCA) revealed ongoing degeneration after treatment.[129] This degeneration was assigned to photoreceptors that already were too damaged to prevent apoptosis in, as well as to photoreceptors that were not reached by the virus vectors and left untreated.[130] This is difficult in patients in early disease phases, but even more problematic in patients in advanced disease, in whom stem cell transplantation may be a more appropriate approach. Determining the optimal treatment window for each approach will be tough and time-consuming, especially in the 'transition phase' where genetic therapies become gradually less beneficial and stem-cell transplantation is not amenable because loss of retinal tissue has not occurred yet. Combinational therapy, for example GAT to correct the genetic defect and simultaneously introduce neuroprotective factors, can be beneficial

in these patients. Moreover, it will still take many years, probably decades, before gene-specific therapeutic approaches have been developed for most forms of IRD, and in the meantime many patients will progress into a disease phase where gene therapy alone is not sufficient anymore. The other approaches, which also show great potential, should not be considered rudimentary since their treatment may be necessary in addition to gene therapy.

The stem cell-based therapies are expected to progress enormously in the coming years. Its gene-independent nature and applicability in a broad spectrum of retinal diseases gives this approach great potential. However, the main downside – the degeneration processes continue in the non-treated areas of the retina– may make that this therapy may not be the solution on its own. Yet, it could extend the use of gene therapy if it would be possible to restore the retinal tissue with stem cell-derived photoreceptors and/or RPE cells, and treat the molecular defect with a gene therapy approach. When these therapies become available, further research has to show if this strategy is beneficial compared to one therapy alone, and determine which order is preferable. Induced pluripotent stem cells (iPSC) have shown potential in stem cell-based therapy, but since iPSCs are derived from the patient itself they harbor the genetic defect as well. Performing gene correction on the iPSCs prior to transplantation may solve this matter.

The retinal implant approach focuses on patients in end-stage disease. However, if genetic and stem cell therapies are applicable, this patient group tends to disappear. Yet, research on retinal implants is necessary, since the implants may also be beneficial in patients with any disease that leads to severe macular atrophy and an intact peripheral retina. The resolution of the image generated by the chip needs to be improved to the level of visual acuity that can be reached by the peripheral retina (generally about finger counting to 20/200). Then, these chips may become therapeutic options for STGD1 or age-related macular degeneration in a moderate disease stage. However, we do not know yet what the effect will be if patient get a chip implanted while the peripheral retina is still functional. Is the vision generated by the chip compatible with the vision from the peripheral retina? Will the photoreceptors neighboring the chip also be stimulated by pulses from the electrode array and lead to additional light sensations? How does the surviving retina respond to chip implantation in such cases? Will implantation of a chip damage the remaining functional areas of the retina and cause further degeneration? Anyway, the long-term results have to be determined yet. Not only on implant survival and function, but also on the endurance of the materials used, for example the waterproof, biocompatible encapsulation of the electronic circuits (is there a risk of siderosis bulbi or chalcosis bulbi?). For now, the retinal implants seem to be the last resort in the treatment of retinal dystrophies.

The development of new therapy strategies comes with ethical challenges. The development of a therapy from the proof-of-principle studies to the clinical trials necessary for government approval is very expensive. If the targeted disease is (extremely) rare, as is the case for many subtypes of IRD, the high costs of developing such treatment make it an unappealing prospect for pharmaceutical companies, since the limited number of patients are not sufficient to recover the big expenses from. Who will then develop these therapies if drug companies will not? Investigator-driven research may have problems of gaining sufficient

12

amounts of funding to perform these studies, since the expenses of investigator-driven research come from subsidies provided by the government or patient organizations, and yet, the therapy trials for more frequent forms of IRD will also gain more attention of these organizations since more patients benefit from such a therapy. International collaborations may collect sufficient funding to pay for trials on therapies for IRDs, but may counteract in raising costs and slowing down research proceedings. The concerns on research budget are less problematic for non-gene-specific therapies like stem cell transplantation and retinal implants, because they have a far broader patient population and therefore receive more interest of the pharmaceutical industry.

To make research on drugs for orphan diseases more attractive for investors, governmental agencies have been created in the European Union, United States and other countries. These orphan drug legislations offer tax benefits, fast drug approval by health authorities, and longer patents that guarantee extended exclusivity in the market.[131] By these actions, several drugs for orphan diseases have been developed in the last decade. However, drug costs are generally high since the company's intent to earn back the costs of research, development, regulatory and government drug coverage approval, and patients with serious medical conditions are willing to pay high prices to receive treatment. The limited number of patients and the lack of competition within the market further increase prices. Yet, the high prices of genetic therapy may only be manageable by the wealthy if the costs have to be covered by the patients themselves, which is morally unacceptable. All patients have an expectation of treatment whether their condition is common or rare. Fortunately, orphan drugs are usually covered in health insurances, but in this way the general population is burdened with the high expenses of few individuals. Ideally, the pharmaceutical industry is part of the solution allowing access to orphan drugs. Some companies do not pass the developmental costs in the drug's price since they consider these costs as their research effort and contribution to a greater good.

The high expenses of these drugs increase the importance of detailed selection of patients amenable for treatment. A diverse population may qualify for a specific therapy, even in gene-specific therapies. Gene therapy, for example, can be beneficial in patients in early disease stages as well as patients in advanced disease stages with some spared visual function, like in some forms of RP that have profound constriction of the visual field but intact visual acuity in advanced disease. Individual assessment of the expected long-term clinical benefits will be necessary. An agency representing ophthalmologists, geneticists and ethicists may be necessary for the development of guidelines on the use of these expensive treatments for IRDs, although the (inter) national ophthalmic bodies, such as the European Society of Ophthalmology and the American Academy of Ophthalmology, will likely play a role in this as well.

Since genetic therapies (neuroprotective enhancement and optogenetics excluded) aim at treating the specific genetic defect, these approaches may – apart from therapeutic treatment – also be used as preventive measures when patients are treated before retinal degeneration occurs. Early detection of genetic mutations is in this case vital. Individuals from families with IRD patients can be genetically screened to detect patients that may develop retinal disease,

which than could be treated preventively. However, many IRD cases are isolated, like 46% of RP cases.[132] To identify the isolated cases, genetic testing could be added to the neonatal heel prick screening (Guthrie test) or performed during prenatal screening (in case of LCA). Yet, genetic tests are not included in the Guthrie test up to now because of ethical concerns,[133] and require a huge sequencing capacity and are expensive. Moreover, if the genetic test identifies causative mutations for retinal disease, what treatment window should be used? Obviously, the onset of the disease is the main indication for the moment of treatment, and if disease starts at the age of 30, treatment may be postponed until early adulthood although the onset often is variable and difficult to predict. However, if disease initiates during infancy treatment should be administered within months after birth. Yet, safety and effectiveness of treatment at such age have to be determined, as well as the effects it may have on retinal/vision development. And in patients that are born with severe dystrophic retinas, like some LCA patients, administration of gene therapy in the first months of life will even be too late, and intrauterine treatment would be necessary. Yet, both ethical and practical dilemmas on intrauterine gene therapy are numerous, and probably not easy to overcome. Altogether, preventive measures using gene therapy approaches may be possible in families with IRD patients, but probably will take long before prevention will be possible on population basis.

Conclusion

We experience an era of changing perspectives within the field of IRDs. In the coming years, the molecular diagnostics for IRDs will be expanded and we will be able to identify the genetic defect in the majority of IRD patients. However, much knowledge has to be gained on the other factors (genotype, epigenetics, nutritional status) involved in the retinal phenotype, which may lead to strong genotype-phenotype correlations. In the field of therapeutics developments generally go slower, although they proceed steadily. The first gene augmentation therapy for *RPE65* defects is in the final phase of governmental approval and probably will become commercially available in the coming years. This stimulates research on gene therapies for IRDs due to defects in other genes. Some aspects of clinical research, such as ethical review board approval, may proceed faster, but it will still take long before more therapies will be available since each form of retinal dystrophy requires its own approach. Further research on the various therapeutic approaches is essential, since none of the therapies has shown to be capable of stopping disease or reclaim full visual function yet, and combinational therapies may be the 'next-generation' therapeutic approach for retinal dystrophies.

12

References

1. Rohrschneider K, Bultmann S, Springer C. Use of fundus perimetry (microperimetry) to quantify macular sensitivity. *Prog Retin Eye Res.* 2008 Sep;27(5):536-48.
2. Delori FC, Dorey CK, Staurenghi G, Arend O, Goger DG, Weiter JJ. In vivo fluorescence of the ocular fundus exhibits retinal pigment epithelium lipofuscin characteristics. *Invest Ophthalmol Vis Sci.* 1995 Mar;36(3):718-29.
3. Kiernan DF, Mieler WF, Hariprasad SM. Spectral-domain optical coherence tomography: a comparison of modern high-resolution retinal imaging systems. *Am J Ophthalmol.* 2010 Jan;149(1):18-31.
4. Triolo G, Pierro L, Parodi MB, et al. Spectral domain optical coherence tomography findings in patients with retinitis pigmentosa. *Ophthalmic Res.* 2013;50(3):160-4.
5. Drexler W, Fujimoto JG. State-of-the-art retinal optical coherence tomography. *Prog Retin Eye Res.* 2008 Jan;27(1):45-88.
6. Jacob J, Paques M, Krivosic V, et al. Meaning of visualizing retinal cone mosaic on adaptive optics images. *Am J Ophthalmol.* 2015 Jan;159(1):118-23 e1.
7. Drexler W. Cellular and functional optical coherence tomography of the human retina: the Cogan lecture. *Invest Ophthalmol Vis Sci.* 2007 Dec;48(12):5339-51.
8. Khanna H, Davis EE, Murga-Zamalloa CA, et al. A common allele in RPGRIP1L is a modifier of retinal degeneration in ciliopathies. *Nat Genet.* 2009 Jun;41(6):739-45.
9. Ebermann I, Phillips JB, Liebau MC, et al. PDZD7 is a modifier of retinal disease and a contributor to digenic Usher syndrome. *J Clin Invest.* 2010 Jun;120(6):1812-23.
10. Sanchez-Alcudia R, Corton M, Avila-Fernandez A, et al. Contribution of mutation load to the intrafamilial genetic heterogeneity in a large cohort of spanish retinal dystrophies families. *Invest Ophthalmol Vis Sci.* 2014;55(11):7562-71.
11. Venturini G, Rose AM, Shah AZ, Bhattacharya SS, Rivolta C. CNOT3 is a modifier of PRPF31 mutations in retinitis pigmentosa with incomplete penetrance. *PLoS Genet.* 2012;8(11):e1003040.
12. Li M, Jia C, Kazmierkiewicz KL, et al. Comprehensive analysis of gene expression in human retina and supporting tissues. *Hum Mol Genet.* 2014 Aug 1;23(15):4001-14.
13. Nishiguchi KM, Rivolta C. Genes associated with retinitis pigmentosa and allied diseases are frequently mutated in the general population. *PLoS One.* 2012;7(7):e41902.
14. Aleman TS, Soumittra N, Cideciyan AV, et al. CERKL mutations cause an autosomal recessive cone-rod dystrophy with inner retinopathy. *Invest Ophthalmol Vis Sci.* 2009 Dec;50(12):5944-54.
15. Avila-Fernandez A, Riveiro-Alvarez R, Vallespin E, et al. CERKL mutations and associated phenotypes in seven Spanish families with autosomal recessive retinitis pigmentosa. *Invest Ophthalmol Vis Sci.* 2008 Jun;49(6):2709-13.
16. Tuson M, Marfany G, Gonzalez-Duarte R. Mutation of CERKL, a novel human ceramide kinase gene, causes autosomal recessive retinitis pigmentosa (RP26). *Am J Hum Genet.* 2004 Jan;74(1):128-38.
17. Mackay DS, Henderson RH, Sergouniotis PI, et al. Novel mutations in MERTK associated with childhood onset rod-cone dystrophy. *Mol Vis.* 2010;16:369-77.
18. Shahzadi A, Riazuddin SA, Ali S, et al. Nonsense mutation in MERTK causes autosomal recessive retinitis pigmentosa in a consanguineous Pakistani family. *Br J Ophthalmol.* 2010 Aug;94(8):1094-9.
19. Ostergaard E, Duno M, Batbayli M, Vilhelmsen K, Rosenberg T. A novel MERTK deletion is a common founder mutation in the Faroe Islands and is responsible for a high proportion of retinitis pigmentosa cases. *Mol Vis.* 2011;17:1485-92.
20. Ksantini M, Lafont E, Bocquet B, Meunier I, Hamel CP. Homozygous mutation in MERTK causes severe autosomal recessive retinitis pigmentosa. *Eur J Ophthalmol.* 2012 Jul-Aug;22(4):647-53.
21. Sohocki MM, Sullivan LS, Mintz-Hittner HA, et al. A range of clinical phenotypes associated with mutations in CRX, a photoreceptor transcription-factor gene. *Am J Hum Genet.* 1998 Nov;63(5):1307-15.
22. Michaelides M, Gaillard MC, Escher P, et al. The PROM1 mutation p.R373C causes an autosomal dominant bull's eye maculopathy associated with rod, rod-cone, and macular dystrophy. *Invest Ophthalmol Vis Sci.* 2010 Sep;51(9):4771-80.
23. Pras E, Abu A, Rotenstreich Y, et al. Cone-rod dystrophy and a frameshift mutation in the PROM1 gene. *Mol Vis.* 2009;15:1709-16.

24. Zhang Q, Zulfiqar F, Xiao X, et al. Severe retinitis pigmentosa mapped to 4p15 and associated with a novel mutation in the PROM1 gene. *Hum Genet*. 2007 Nov;122(3-4):293-9.

25. Hildebrandt F, Benzing T, Katsanis N. Ciliopathies. *N Engl J Med*. 2011 Apr 21;364(16):1533-43.

26. Mockel A, Perdomo Y, Stutzmann F, Letsch J, Marion V, Dollfus H. Retinal dystrophy in Bardet-Biedl syndrome and related syndromic ciliopathies. *Prog Retin Eye Res*. 2011 Jul;30(4):258-74.

27. Estrada-Cuzcano A, Koenekoop RK, Senechal A, et al. BBS1 mutations in a wide spectrum of phenotypes ranging from nonsyndromic retinitis pigmentosa to Bardet-Biedl syndrome. *Arch Ophthalmol*. 2012 Nov;130(11):1425-32.

28. Bernal S, Ayuso C, Antinolo G, et al. Mutations in USH2A in Spanish patients with autosomal recessive retinitis pigmentosa: high prevalence and phenotypic variation. *J Med Genet*. 2003 Jan;40(1):e8.

29. McGee TL, Seyedahmadi BJ, Sweeney MO, Dryja TP, Berson EL. Novel mutations in the long isoform of the USH2A gene in patients with Usher syndrome type II or non-syndromic retinitis pigmentosa. *J Med Genet*. 2010 Jul;47(7):499-506.

30. Rivolta C, Sweklo EA, Berson EL, Dryja TP. Missense mutation in the USH2A gene: association with recessive retinitis pigmentosa without hearing loss. *Am J Hum Genet*. 2000 Jun;66(6):1975-8.

31. Seyedahmadi BJ, Rivolta C, Keene JA, Berson EL, Dryja TP. Comprehensive screening of the USH2A gene in Usher syndrome type II and non-syndromic recessive retinitis pigmentosa. *Exp Eye Res*. 2004 Aug;79(2):167-73.

32. Moore A, Escudier E, Roger G, et al. RPGR is mutated in patients with a complex X linked phenotype combining primary ciliary dyskinesia and retinitis pigmentosa. *J Med Genet*. 2006 Apr;43(4):326-33.

33. Zito I, Downes SM, Patel RJ, et al. RPGR mutation associated with retinitis pigmentosa, impaired hearing, and sinorespiratory infections. *J Med Genet*. 2003 Aug;40(8):609-15.

34. Fishman GA, Stone EM, Grover S, Derlacki DJ, Haines HL, Hockey RR. Variation of clinical expression in patients with Stargardt dystrophy and sequence variations in the ABCR gene. *Arch Ophthal*. 1999 Apr;117(4):504-10.

35. Lois N, Holder GE, Bunce C, Fitzke FW, Bird AC. Phenotypic subtypes of Stargardt macular dystrophy-fundus flavimaculatus. *Arch Ophthal*. 2001 Mar;119(3):359-69.

36. Berson EL, Rosner B, Sandberg MA, et al. A randomized trial of vitamin A and vitamin E supplementation for retinitis pigmentosa. *Arch Ophthal*. 1993 Jun;111(6):761-72.

37. Berson EL. Treatment of retinitis pigmentosa with vitamin A. *Digit J Ophthalmology*. 1998;4(7):1-4.

38. Berson EL, Rosner B, Sandberg MA, et al. Vitamin A supplementation for retinitis pigmentosa. *Arch Ophthal*. 1993 Nov;111(11):1456-9.

39. Berson EL, Rosner B, Sandberg MA, Weigel-DiFranco C, Willett WC. omega-3 intake and visual acuity in patients with retinitis pigmentosa receiving vitamin A. *Arch Ophthal*. 2012 Jun;130(6):707-11.

40. Rotenstreich Y, Belkin M, Sadetzki S, et al. Treatment with 9-cis beta-carotene-rich powder in patients with retinitis pigmentosa: a randomized crossover trial. *JAMA ophthalmology*. 2013 Aug;131(8):985-92.

41. Rayapudi S, Schwartz SG, Wang X, Chavis P. Vitamin A and fish oils for retinitis pigmentosa. *Cochrane Database Syst Rev*. 2013;12:CD008428.

42. Koenekoop RK, Sui R, Sallum J, et al. Oral 9-cis retinoid for childhood blindness due to Leber congenital amaurosis caused by RPE65 or LRAT mutations: an open-label phase 1b trial. *Lancet*. 2014 Oct 25;384(9953):1513-20.

43. Van Hooser JP, Aleman TS, He YG, et al. Rapid restoration of visual pigment and function with oral retinoid in a mouse model of childhood blindness. *Proc Natl Acad Sci U S A*. 2000 Jul 18;97(15):8623-8.

44. Van Hooser JP, Liang Y, Maeda T, et al. Recovery of visual functions in a mouse model of Leber congenital amaurosis. *J Biol Chem*. 2002 May 24;277(21):19173-82.

45. Yasuda S, Liang MH, Marinova Z, Yahyavi A, Chuang DM. The mood stabilizers lithium and valproate selectively activate the promoter IV of brain-derived neurotrophic factor in neurons. *Mol Psychiatry*. 2009 Jan;14(1):51-9.

46. Suuronen T, Nuutinen T, Ryhanen T, Kaarniranta K, Salminen A. Epigenetic regulation of clusterin/apolipoprotein J expression in retinal pigment epithelial cells. *Biochem Biophys Res Commun*. 2007 Jun 1;357(2):397-401.

12

47. Kim HJ, Rowe M, Ren M, Hong JS, Chen PS, Chuang DM. Histone deacetylase inhibitors exhibit anti-inflammatory and neuroprotective effects in a rat permanent ischemic model of stroke: multiple mechanisms of action. *J Pharmacol Exp Ther*. 2007 Jun;321(3):892-901.
48. Chen PS, Wang CC, Bortner CD, et al. Valproic acid and other histone deacetylase inhibitors induce microglial apoptosis and attenuate lipopolysaccharide-induced dopaminergic neurotoxicity. *Neuroscience*. 2007 Oct 12;149(1):203-12.
49. Dragunow M, Greenwood JM, Cameron RE, et al. Valproic acid induces caspase 3-mediated apoptosis in microglial cells. *Neuroscience*. 2006 Jul 21;140(4):1149-56.
50. Gottlicher M, Minucci S, Zhu P, et al. Valproic acid defines a novel class of HDAC inhibitors inducing differentiation of transformed cells. *EMBO J*. 2001 Dec 17;20(24):6969-78.
51. Clemson CM, Tzekov R, Krebs M, Checchi JM, Bigelow C, Kaushal S. Therapeutic potential of valproic acid for retinitis pigmentosa. *Br J Ophthalmol*. 2011 Jan;95(1):89-93.
52. Sandberg MA, Rosner B, Weigel-DiFranco C, Berson EL. Lack of scientific rationale for use of valproic acid for retinitis pigmentosa. *Br J Ophthalmol*. 2011 May;95(5):744.
53. van Schooneveld MJ, van den Born LI, van Genderen M, Bollemeijer JG. The conclusions of Clemson et al concerning valproic acid are premature. *Br J Ophthalmol*. 2011 Jan;95(1):153; author reply -4.
54. Kumar A, Midha N, Gogia V, Gupta S, Sehra S, Chohan A. Efficacy of oral valproic acid in patients with retinitis pigmentosa. *J Ocul Pharmacol Ther*. 2014 Sep;30(7):580-6.
55. Shanmugam PM, Minija CK, Ramanjulu R, Tekwani P, Saxena M. Effect of short-term oral valproic Acid on vision and visual field in retinitis pigmentosa. *Ophthalmology and therapy*. 2012 Dec;1(1):6.
56. Sisk RA. Valproic acid treatment may be harmful in non-dominant forms of retinitis pigmentosa. *Br J Ophthalmol*. 2012 Aug;96(8):1154-5.
57. Bhalla S, Joshi D, Bhullar S, Kasuga D, Park Y, Kay CN. Long-term follow-up for efficacy and safety of treatment of retinitis pigmentosa with valproic acid. *Br J Ophthalmol*. 2013 Jul;97(7):895-9.
58. Mitton KP, Guzman AE, Deshpande M, et al. Different effects of valproic acid on photoreceptor loss in Rd1 and Rd10 retinal degeneration mice. *Mol Vis*. 2014;20:1527-44.
59. Mancil RM, Mancil GL, King E, et al. Improving nighttime mobility in persons with night blindness caused by retinitis pigmentosa: A comparison of two low-vision mobility devices. *J Rehabil Res Dev*. 2005 Jul-Aug;42(4):471-86.
60. Hartong DT, Jorritsma FF, Neve JJ, Melis-Dankers BJ, Kooijman AC. Improved mobility and independence of night-blind people using night-vision goggles. *Invest Ophthalmol Vis Sci*. 2004 Jun;45(6):1725-31.
61. Berson EL, Rabin AR, Mehaffey L, 3rd. Advances in night vision technology. A pocketscope for patients with retinitis pigmentosa. *Arch Ophthal*. 1973 Dec;90(6):427-31.
62. Pruett RC. Retinitis pigmentosa: clinical observations and correlations. *Trans Am Ophthalmol Soc*. 1983;81:693-735.
63. Fishman GA, Anderson RJ, Lourenco P. Prevalence of posterior subcapsular lens opacities in patients with retinitis pigmentosa. *Br J Ophthalmol*. 1985 Apr;69(4):263-6.
64. Heckenlively J. The frequency of posterior subcapsular cataract in the hereditary retinal degenerations. *Am J Ophthalmol*. 1982 Jun;93(6):733-8.
65. Berson EL, Rosner B, Simonoff E. Risk factors for genetic typing and detection in retinitis pigmentosa. *Am J Ophthalmol*. 1980 Jun;89(6):763-75.
66. Hagiwara A, Yamamoto S, Ogata K, et al. Macular abnormalities in patients with retinitis pigmentosa: prevalence on OCT examination and outcomes of vitreoretinal surgery. *Acta Ophthalmol*. 2011 Mar;89(2):e122-5.
67. Takezawa M, Tetsuka S, Kakehashi A. Tangential vitreous traction: a possible mechanism of development of cystoid macular edema in retinitis pigmentosa. *Clin Ophthalmol*. 2011;5:245-8.
68. Molday RS. Focus on molecules: retinoschisin (RS1). *Exp Eye Res*. 2007 Feb;84(2):227-8.
69. Luna G, Kjellstrom S, Verardo MR, et al. The effects of transient retinal detachment on cavity size and glial and neural remodeling in a mouse model of X-linked retinoschisis. *Invest Ophthalmol Vis Sci*. 2009 Aug;50(8):3977-84.
70. Larsen M, Engler CB, Haim M, Lund-Andersen H. Blood-retina barrier permeability is independent of trace substance lipid solubility in retinitis pigmentosa and in the healthy eye. *Int Ophthalmol*. 1997;21(4):229-34.

71. Gass JDM. Stereoscopic atlas of macular diseases : diagnosis and treatment. 4th ed. St. Louis ;: Mosby; 1997.

72. Fishman GA, Cunha-Vaz J, Salzano T. Vitreous fluorophotometry in patients with retinitis pigmentosa. *Arch Ophthal*. 1981 Jul;99(7):1202-7.

73. Mallick KS, Zeimer RC, Fishman GA, Blair NP, Anderson RJ. Transport of fluorescein in the ocular posterior segment in retinitis pigmentosa. *Arch Ophthal*. 1984 May;102(5):691-6.

74. Salvatore S, Fishman GA, Genead MA. Treatment of cystic macular lesions in hereditary retinal dystrophies. *Surv Ophthalmol*. 2013 Nov-Dec;58(6):560-84.

75. Apushkin MA, Fishman GA, Janowicz MJ. Monitoring cystoid macular edema by optical coherence tomography in patients with retinitis pigmentosa. *Ophthalmology*. 2004 Oct;111(10):1899-904.

76. Cox SN, Hay E, Bird AC. Treatment of chronic macular edema with acetazolamide. *Arch Ophthal*. 1988 Sep;106(9):1190-5.

77. Ozdemir H, Karacorlu M, Karacorlu S. Intravitreal triamcinolone acetonide for treatment of cystoid macular oedema in patients with retinitis pigmentosa. *Acta Ophthalmol Scand*. 2005 Apr;83(2):248-51.

78. Scorolli L, Morara M, Meduri A, et al. Treatment of cystoid macular edema in retinitis pigmentosa with intravitreal triamcinolone. *Arch Ophthal*. 2007 Jun;125(6):759-64.

79. Sallum JM, Farah ME, Saraiva VS. Treatment of cystoid macular edema related to retinitis pigmentosa with intravitreal triamcinolone acetonide: case report. *Adv Exp Med Biol*. 2003;533:79-81.

80. Saraiva VS, Sallum JM, Farah ME. Treatment of cystoid macular edema related to retinitis pigmentosa with intravitreal triamcinolone acetonide. *Ophthalmic Surg Lasers Imaging*. 2003 Sep-Oct;34(5):398-400.

81. Minnella AM, Falsini B, Bamonte G, et al. Optical coherence tomography and focal electroretinogram evaluation of cystoid macular edema secondary to retinitis pigmentosa treated with intravitreal triamcinolone: case report. *Eur J Ophthalmol*. 2006 Nov-Dec;16(6):883-6.

82. Yuzbasioglu E, Artunay O, Rasier R, Sengul A, Bahcecioglu H. Intravitreal bevacizumab (Avastin) injection in retinitis pigmentosa. *Curr Eye Res*. 2009 Mar;34(3):231-7.

83. Querques G, Prascina F, Iaculli C, Noci ND. Intravitreal pegaptanib sodium (Macugen) for refractory cystoid macular edema in pericentral retinitis pigmentosa. *Int Ophthalmol*. 2009 Apr;29(2):103-7.

84. Artunay O, Yuzbasioglu E, Rasier R, Sengul A, Bahcecioglu H. Intravitreal ranibizumab in the treatment of cystoid macular edema associated with retinitis pigmentosa. *J Ocul Pharmacol Ther*. 2009 Dec;25(6):545-50.

85. Melo GB, Farah ME, Aggio FB. Intravitreal injection of bevacizumab for cystoid macular edema in retinitis pigmentosa. *Acta Ophthalmol Scand*. 2007 Jun;85(4):461-3.

86. Salom D, Diaz-Llopis M, Garcia-Delpech S, et al. Intravitreal ranibizumab in the treatment of cystoid macular edema associated with retinitis pigmentosa. *J Ocul Pharmacol Ther*. 2010 Oct;26(5):531-2.

87. Dalkara D, Sahel JA. Gene therapy for inherited retinal degenerations. *Comptes rendus biologies*. 2014 Mar;337(3):185-92.

88. Maguire AM, High KA, Auricchio A, et al. Age-dependent effects of RPE65 gene therapy for Leber's congenital amaurosis: a phase 1 dose-escalation trial. *Lancet*. 2009 Nov 7;374(9701):1597-605.

89. Maguire AM, Simonelli F, Pierce EA, et al. Safety and efficacy of gene transfer for Leber's congenital amaurosis. *N Engl J Med*. 2008 May 22;358(21):2240-8.

90. Jacobson SG, Cideciyan AV, Ratnakaram R, et al. Gene therapy for leber congenital amaurosis caused by RPE65 mutations: safety and efficacy in 15 children and adults followed up to 3 years. *Arch Ophthal*. 2012 Jan;130(1):9-24.

91. Liang FQ, Aleman TS, Dejneka NS, et al. Long-term protection of retinal structure but not function using RAAV.CNTF in animal models of retinitis pigmentosa. *Mol Ther*. 2001 Nov;4(5):461-72.

92. Okoye G, Zimmer J, Sung J, et al. Increased expression of brain-derived neurotrophic factor preserves retinal function and slows cell death from rhodopsin mutation or oxidative damage. *J Neurosci*. 2003 May 15;23(10):4164-72.

93. Buch PK, MacLaren RE, Duran Y, et al. In contrast to AAV-mediated Cntf expression, AAV-mediated Gdnf expression enhances gene replacement therapy in rodent models of retinal degeneration. *Mol Ther*. 2006 Nov;14(5):700-9.

12

94. Dalkara D, Kolstad KD, Guerin KI, et al. AAV mediated GDNF secretion from retinal glia slows down retinal degeneration in a rat model of retinitis pigmentosa. *Mol Ther*. 2011 Sep;19(9):1602-8.

95. McGee Sanftner LH, Abel H, Hauswirth WW, Flannery JG. Glial cell line derived neurotrophic factor delays photoreceptor degeneration in a transgenic rat model of retinitis pigmentosa. *Mol Ther*. 2001 Dec;4(6):622-9.

96. Chen J, Flannery JG, LaVail MM, Steinberg RH, Xu J, Simon MI. bcl-2 overexpression reduces apoptotic photoreceptor cell death in three different retinal degenerations. *Proc Natl Acad Sci U S A*. 1996 Jul 9;93(14):7042-7.

97. Leonard KC, Petrin D, Coupland SG, et al. XIAP protection of photoreceptors in animal models of retinitis pigmentosa. *PLoS One*. 2007;2(3):e314.

98. Shan H, Ji D, Barnard AR, et al. AAV-mediated gene transfer of human X-linked inhibitor of apoptosis protects against oxidative cell death in human RPE cells. *Invest Ophthalmol Vis Sci*. 2011;52(13):9591-7.

99. Zadro-Lamoureux LA, Zacks DN, Baker AN, Zheng QD, Hauswirth WW, Tsilfidis C. XIAP effects on retinal detachment-induced photoreceptor apoptosis [corrected]. *Invest Ophthalmol Vis Sci*. 2009 Mar;50(3):1448-53.

100. Leveillard T, Sahel JA. Rod-derived cone viability factor for treating blinding diseases: from clinic to redox signaling. *Sci Transl Med*. 2010 Apr 7;2(26):26ps16.

101. Zhang K, Hopkins JJ, Heier JS, et al. Ciliary neurotrophic factor delivered by encapsulated cell intraocular implants for treatment of geographic atrophy in age-related macular degeneration. *Proc Natl Acad Sci U S A*. 2011 Apr 12;108(15):6241-5.

102. Wilson RC, Doudna JA. Molecular mechanisms of RNA interference. *Annu Rev Biophys*. 2013;42:217-39.

103. Kurreck J. Antisense and RNA interference approaches to target validation in pain research. *Curr Opin Drug Discov Devel*. 2004 Mar;7(2):179-87.

104. Dias N, Stein CA. Antisense oligonucleotides: basic concepts and mechanisms. *Mol Cancer Ther*. 2002 Mar;1(5):347-55.

105. Doherty EA, Doudna JA. Ribozyme structures and mechanisms. *Annu Rev Biophys Biomol Struct*. 2001;30:457-75.

106. Stenson PD, Mort M, Ball EV, et al. The Human Gene Mutation Database: 2008 update. *Genome Med*. 2009;1(1):13.

107. Bacchi N, Casarosa S, Denti MA. Splicing-correcting therapeutic approaches for retinal dystrophies: where endogenous gene regulation and specificity matter. *Invest Ophthalmol Vis Sci*. 2014 May;55(5):3285-94.

108. Collin RW, den Hollander AI, van der Velde-Visser SD, Bennicelli J, Bennett J, Cremers FP. Antisense Oligonucleotide (AON)-based Therapy for Leber Congenital Amaurosis Caused by a Frequent Mutation in CEP290. *Molecular therapy Nucleic acids*. 2012;1:e14.

109. Schmid F, Hiller T, Korner G, Glaus E, Berger W, Neidhardt J. A gene therapeutic approach to correct splice defects with modified U1 and U6 snRNPs. *Hum Gene Ther*. 2013 Jan;24(1):97-104.

110. Schmid F, Glaus E, Barthelmes D, et al. U1 snRNA-mediated gene therapeutic correction of splice defects caused by an exceptionally mild BBS mutation. *Hum Mutat*. 2011 Jul;32(7):815-24.

111. Glaus E, Schmid F, Da Costa R, Berger W, Neidhardt J. Gene therapeutic approach using mutation-adapted U1 snRNA to correct a RPGR splice defect in patient-derived cells. *Mol Ther*. 2011 May;19(5):936-41.

112. Busskamp V, Picaud S, Sahel JA, Roska B. Optogenetic therapy for retinitis pigmentosa. *Gene Ther*. 2012 Feb;19(2):169-75.

113. Bi A, Cui J, Ma YP, et al. Ectopic expression of a microbial-type rhodopsin restores visual responses in mice with photoreceptor degeneration. *Neuron*. 2006 Apr 6;50(1):23-33.

114. Lagali PS, Balya D, Awatramani GB, et al. Light-activated channels targeted to ON bipolar cells restore visual function in retinal degeneration. *Nat Neurosci*. 2008 Jun;11(6):667-75.

115. Busskamp V, Duebel J, Balya D, et al. Genetic reactivation of cone photoreceptors restores visual responses in retinitis pigmentosa. *Science (80-)*. 2010 Jul 23;329(5990):413-7.

116. Cepko CL. Emerging gene therapies for retinal degenerations. *J Neurosci*. 2012 May 9;32(19):6415-20.

117. Woodruff ML, Wang Z, Chung HY, Redmond TM, Fain GL, Lem J. Spontaneous activity of opsin apoprotein is a cause of Leber congenital amaurosis. *Nat Genet*. 2003 Oct;35(2):158-64.

118. Ramsden CM, Powner MB, Carr AJ, Smart MJ, da Cruz L, Coffey PJ. Stem cells in retinal regeneration: past, present and future. *Development*. 2013 Jun;140(12):2576-85.

119. Seiler MJ, Aramant RB. Cell replacement and visual restoration by retinal sheet transplants. *Prog Retin Eye Res*. 2012 Nov;31(6):661-87.

120. Schwartz SD, Regillo CD, Lam BL, et al. Human embryonic stem cell-derived retinal pigment epithelium in patients with age-related macular degeneration and Stargardt's macular dystrophy: follow-up of two open-label phase 1/2 studies. *Lancet*. 2014 Oct 15.

121. Schwartz SD, Hubschman JP, Heilwell G, et al. Embryonic stem cell trials for macular degeneration: a preliminary report. *Lancet*. 2012 Feb 25;379(9817):713-20.

122. Arango-Gonzalez B, Leitritz MA, Fischer D, Gerberding M, Paquet-Durand F, Ueffing M. [Current therapeutic approaches in inherited retinal degeneration: from genes to chip]. *Klin Monbl Augenheilkd*. 2014 Mar;231(3):222-31.

123. Zrenner E. Fighting blindness with microelectronics. *Sci Transl Med*. 2013 Nov 6;5(210):210ps16.

124. Zrenner E, Bartz-Schmidt KU, Benav H, et al. Subretinal electronic chips allow blind patients to read letters and combine them to words. *Proc Biol Sci*. 2011 May 22;278(1711):1489-97.

125. Danilov Y, Tyler M. Brainport: an alternative input to the brain. *J Integr Neurosci*. 2005 Dec;4(4):537-50.

126. Chebat DR, Schneider FC, Kupers R, Ptito M. Navigation with a sensory substitution device in congenitally blind individuals. *Neuroreport*. 2011 May 11;22(7):342-7.

127. Chebat DR, Rainville C, Kupers R, Ptito M. Tactile-'visual' acuity of the tongue in early blind individuals. *Neuroreport*. 2007 Dec 3;18(18):1901-4.

128. Sampaio E, Maris S, Bach-y-Rita P. Brain plasticity: 'visual' acuity of blind persons via the tongue. *Brain Res*. 2001 Jul 27;908(2):204-7.

129. Hauswirth WW, Aleman TS, Kaushal S, et al. Treatment of leber congenital amaurosis due to RPE65 mutations by ocular subretinal injection of adeno-associated virus gene vector: short-term results of a phase I trial. *Hum Gene Ther*. 2008 Oct;19(10):979-90.

130. Lok C. Curing blindness: Vision quest. *Nat New Biol*. 2014 Sep 11;513(7517):160-2.

131. Llinares J. A regulatory overview about rare diseases. *Adv Exp Med Biol*. 2010;686:193-207.

132. Bunker CH, Berson EL, Bromley WC, Hayes RP, Roderick TH. Prevalence of retinitis pigmentosa in Maine. *Am J Ophthalmol*. 1984;97(3):357-65.

133. Thomas C. The use and control of heel prick blood samples. *Med Law*. 2005 Jun;24(2):259-77.

12

Summary

Samenvatting

Summary

Inherited retinal dystrophies (IRDs) are a group of rare generally monogenetic diseases that are genetically and clinically highly heterogeneous. Specific phenotypes within the IRD group can be caused by mutations in many genes, sometimes even more than 60 genes as is the case for retinitis pigmentosa (RP). On the other hand, many genes involved in inherited retinal disease can give rise to multiple phenotypes. In the last decade, the pathological pathways underlying these diseases started to unravel as numerous genotype-phenotype correlations have been described. However, because of the heterogeneity of IRDs there remain many unsolved questions. The aim of this thesis is to provide detailed clinical descriptions of some forms of IRDs, as well as describe correlations between the molecular genetic background and the phenotype. This may enable better counseling of patients and their families, and is vital in the follow-up of the therapeutic effect in clinical trials on IRD treatments.

Chapter 1 serves as a general introduction on retinal anatomy, the processes that lead to vision, assessment of the retinal function, and the basic principles of molecular genetics. Additionally, the general clinical and genetic principles of retinal dystrophies are addressed.

In **chapter 2**, we provided the first detailed clinical description in patients with RP caused by recessive mutations in *IMPG2*. In this international collaborative study, we included 17 RP patients with *IMPG2* mutations that were clinically examined in detail, using extensive medical history taking, slit-lamp biomicroscopy, ophthalmoscopy, perimetry, electroretinography (ERG), optical coherence tomography (OCT), fundus autofluorescence (FAF) imaging, fundus photography, and color vision tests. These patients revealed the classic RP features including night blindness and visual field loss, as well as optic disc pallor, attenuated retinal vessels, bone spicules and generalized atrophy of the retina and choriocapillaris. Additionally, we observed macular abnormalities in all patients, ranging from subtle mottling of the macular pigment epithelium to macular chorioretinal atrophy. This macular involvement was accompanied by severe decrease in central vision. This, in combination with the concentric loss of visual field, leads to relatively early, yet severe, visual impairment in patients with *IMPG2*-associated RP.

Chapter 3 describes the clinical observations in RP patients with mutations in the *MAK* gene. In this evaluation, we also focused on the presence of extra-ocular symptoms, since *MAK* encodes a ciliary protein and therefore may give rise to syndromic disease. In this study, we included 11 patients from 5 international ophthalmic centers. The patients were examined in detail, and in addition a questionnaire to evaluate the presence of clinical syndromic features was used. We performed the University of Pennsylvania Smell Identification Test (UPSIT) in several patients to rule out subclinical olfactory disability, since MAK is expressed in murine olfactory neurons, and smell disabilities often go unnoticed. The analyses resulted that

nonsense and missense mutations in *MAK* cause a fairly classic RP in which visual acuity may be normal up to high age, although profound concentric visual field loss. No extra-ocular symptoms were noted, and the UPSIT results were within the age-corrected normal limits. In addition, we provided an overview of the ciliary genes that cause nonsyndromic retinal disease, which elaborates on the retinal and extra-ocular symptoms observed in disease caused by these genes.

Chapter 4 provides the clinical aspects of retinal disease caused by mutations in *C8orf37*. Eight patients – 4 diagnosed with RP and 4 with cone-rod dystrophy (CRD) – were examined with routine ophthalmic examination, kinetic perimetry, ERG, as well as multimodal imaging (OCT, FAF and fundus photography) and evaluation of extra-ocular symptoms. The RP patients showed the classic RP symptoms of night blindness and concentric visual field loss, as well as severe loss of visual acuity up to levels of light perception in an early disease stage. The CRD patients revealed a classic CRD that initiated with a decrease in visual acuity. Two of the CRD patients had a history of postaxial polydactyly, which indicates that mutations in *C8orf37* may give rise to syndromic disease. The occurrence of extra-ocular features may imply that C8orf37 has a ciliary function. However, the exact function of C8orf37 is not known, which makes genotype-phenotype correlations impossible.

In **chapter 5**, we evaluated the genetic findings and phenotypic characteristics of patients from three families with *ABHD12* gene mutations. The *ABHD12* mutations were located with whole exome sequencing (WES). The patients were clinically evaluated by ophthalmologists, neurologists and otologist, since mutations in *ABHD12* have been associated with the polyneuropathy-hearing loss-ataxia-RP-early-onset cataract (PHARC) syndrome. We identified five new mutations, including the first missense mutations described in this gene. The patients of two families had symptoms that fit the PHARC syndrome, whereas one family did not have any neurologic disabilities or hearing loss. In this study, we could widen the clinical spectrum associated to *ABHD12* mutations, which ranges from nonsyndromic RP to complete PHARC syndrome. However, a clear genotype-phenotype correlation could not be established.

Chapter 6 describes the molecular findings in a Dutch family with autosomal recessively inherited hearing loss due to pathologic mutations in *USH1G*, a gene known to be involved in Usher syndrome type I and atypical Usher syndrome. The members of this Dutch family revealed early-onset progressive hearing loss with a downsloping audiogram configuration. Extensive ophthalmic and vestibular examinations demonstrated no abnormalities that are usually associated with Usher syndrome type I. With these findings we expanded the phenotypic spectrum of mutations in *USH1G*.

In **chapter 7**, we evaluated the efficiency of commercially available arrayed primer extension (APEX) microarray chip for autosomal recessive RP. We included 250 probands suspected of autosomal recessive RP who were genetically analyzed with the APEX microarray. The mode of inheritance had to be autosomal recessive (including isolated cases) according

to the pedigree. The efficiency of this microarray chip with additional Sanger sequencing approach was determined by the percentage of patients that received a molecular diagnosis. The APEX microarray chip for autosomal recessive RP identified the molecular diagnosis in 8.5% of the patients in our cohort; 15.2% after additional Sanger sequencing in patients in whom the microarray analysis identified heterozygous mutation. Hence, next generation sequencing (NGS) techniques – reported to reach diagnostic yields up to 40% - outperform the APEX microarray approach by far.

Chapter 8 provides the genetic and clinical findings in patients with early-onset Stargardt disease. In this retrospective study, we included 51 Stargardt patients with an age at onset of 10 years or lower. We observed a decline in visual acuity to levels of counting fingers in a median of 23 years. Initial fundus examination revealed no abnormalities in 10 patients, foveal RPE alterations in 9 patients, and foveal atrophy whether or not accompanied by yellow-white fundus flecks in 22 patients. In 14 out of 50 patients, foveal atrophy occurred before the typical yellow-white fundus flecks appeared, which complicates early correct diagnosing. We identified *ABCA4* mutations in all patients, but did not find clear mutational associations with the early onset and severe retinal degeneration observed in this cohort. Yet, early-onset Stargardt lies at the severe end of the spectrum of *ABCA4*-associated retinal phenotypes.

Chapter 9 describes the genetic and clinical characteristics of patients with Stargardt disease that reveal foveal sparing. We defined foveal sparing as retinal atrophy that surrounds the fovea by at least 180° and does not include the fovea. From our database, we identified 13 unrelated patients that revealed foveal sparing in one or both eye (17 eyes in total). Foveal sparing eyes revealed a visual acuity of 20/40 or better, and 41% reached visual acuity levels of 20/25 or higher. However, eventually the fovea degenerates as the parafoveal atrophy expands, which results in a decline in visual acuity to 20/200 to counting fingers. Genetic analysis revealed at least one *ABCA4* mutations in each patient, although no correlation with a specific mutation could be identified. The anatomy, metabolism, and biochemistry of the retina, as well as genetic variations in genes other than *ABCA4*, can influence the etiology of foveal sparing. Identifying these fovea-protecting factors will facilitate the future development of strategies designed to treat Stargardt disease. Foveal sparing occurs mainly in patients with late-onset Stargardt disease and represents the milder end of the clinical spectrum caused by *ABCA4* mutations.

In **chapter 10**, we evaluated the clinical characteristics of autosomal dominant cystoids macular dystrophy (DCMD). We collected the long-term clinical data of 97 patients with DCMD, including multimodal imaging techniques (fluorescein angiography, FAF and OCT) and electrophysiologic examinations (ERG as well as electrooculography). We obtained blood samples from all patients for haplotype analysis. DCMD patients initially reveal macular cystoids fluid collections (CFCs) that eventually lead to chorioretinal atrophy and hyperpigmented deposits in the posterior pole. Most patients (92%) were (highly) hyperopic. We recognized 3 grades of DCMD, based on the fundoscopic, imaging and electrophysiological characteristics. In grade 1, patients were under the age of 20 and presented with CFCs with

fine folding of the internal limiting membrane and mild pigment changes. In grade 2, the CFCs tended to decrease in size, and moderate macular chorioretinal atrophy developed. In grade 3, patients were generally over the age of 50 and showed profound chorioretinal atrophy, as well as coarse hyperpigmented deposits in the posterior pole. All DCMD patients shared the disease haplotype at the DCMD locus at 7p15.3, but the involved gene is currently unknown.

Chapter 11 describes the RD5000 database that we developed to register all ophthalmological and selected genetic data of patients with inherited retinal dystrophies in the Netherlands. In order to perform meaningful genotype-phenotype analyses for rare genetic conditions, it is necessary to collect data from sizable populations. Although standardized functional tests are widely used, ophthalmologic data are usually stored in local databases and not in multi-center databases that are linked with other centers. Eleven Dutch ophthalmogenetic centers are connected to the RD5000 database. Authorization rights for the management, data entry and data sharing have been set-up, rendering this database into a user-friendly, secure and widely used repository that will facilitate future studies into molecular genetics and therapies for IRDs. RD5000db has the potential to grow into a European standard for the registration of data from IRDs.

Chapter 12 discusses the studies described in this thesis and their implications for researchers, physicians and patients. The general discussion attempts to shed a light on the clinical heterogeneity observed in inherited retinal dystrophies by discussing possible genetic modifying factors. This chapter additionally provides an overview of the therapeutic approaches that are currently evaluated, as well as the expected potential of these treatments and ethical complications.

Samenvatting

Erfelijke retinadystrofieën omvat een groep van zeldzame, veelal monogenetische ziektebeelden die een grote genetische en klinische heterogeniteit laten zien. Specifieke fenotypes, zoals bijvoorbeeld retinitis pigmentosa (RP), kunnen veroorzaakt worden door mutaties in meer dan 60 genen. Daarentegen kan het overgrote deel van de genen betrokken in retinadystrofieën verschillende klinische ziektebeelden veroorzaken. In de laatste decennia zijn verscheidene genotype-fenotype correlaties beschreven, die inzicht in de pathologische processen onderliggend aan deze ziekten geven. Echter de grote heterogeniteit laat veel vragen onbeantwoord. Dit proefschrift heeft als doel om een gedetailleerde klinische beschrijving van een aantal specifieke vormen van retinadystrofieën te geven, en daarbij de correlaties tussen de genetische achtergrond en de klinische kenmerken te beschrijven. Dit kan tot een betere (genetische) voorlichting aan patiënten en hun families leiden, en is essentieel voor het beoordelen van het effect van interventies in klinische studies.

Hoofdstuk 1 geeft een algemene introductie in de retinale anatomie, de processen die tot zicht leiden, beoordeling van de retinale functie, evenals de basisprincipes van de genetica. Tevens worden de klinische en genetische achtergrond van de retinadystrofieën beschreven in dit proefschrift besproken.

In **hoofdstuk 2** geven wij een gedetailleerde klinische beschrijving van patiënten met RP op basis van mutaties in het *IMPG2* gen. In deze internationale studie hebben wij 17 patiënten met *IMPG2*-geassocieerde RP geïncludeerd die klinisch onderzocht zijn met uitgebreide anamnese, spleetlamp onderzoek, fundoscopie, perimetrie, elektroretinografie (ERG), optische coherentie tomografie (OCT), fundus autofluorescentie (FAF), fundus fotografie, en kleurenzien testen. De patiënten vertoonde de klassieke RP kenmerken van nachtblindheid, perifeer gezichtsveldverlies, een wasachtige bleke papil, vernauwde retinale bloedvaten, intraretinale beenbalkpigmentatie en gegeneraliseerde atrofie van de retina en choriocapillaris. Daarnaast vertoonde alle patiënten maculaire afwijkingen, welke varieerde van subtiele pigmentalteraties tot chorioretinale atrofie. Deze betrokkenheid van de achterpool ging gepaard met ernstig visusverlies, wat in combinatie met de perifere gezichtsvelduitval tot een ernstige, relatief vroeg optredende visuele beperking veroorzaakt in patiënten met RP door mutaties in *IMPG2*.

Hoofdstuk 3 beschrijft de klinische observaties in RP patiënten met mutaties in het *MAK* gen. Hierbij hebben wij ons tevens gericht op de aanwezigheid van extra-oculaire symptomen, aangezien *MAK* een ciliair proteïne codeert en daardoor tot een syndroom zou kunnen leiden. In deze studie konden wij 11 patiënten uit 5 internationale centra includeren. De patiënten werden klinisch gedetailleerd onderzocht, waarbij eveneens een vragenlijst werd afgenomen die de aanwezigheid van syndromale kenmerken evalueerde. Aanvullend hierop

werd in enkele patiënten een University of Pennsylvania Smell Identification Test (UPSIT) afgenomen ter uitsluiting van subklinische beperkingen van de reukzin, aangezien MAK tot uiting komt in de olfactoire neuronen in de muis, en beperkingen van de reukzin vaak niet opgemerkt worden. De analyses toonde dat nonsense en missense mutaties in *MAK* tot een relatief klassieke vorm van RP leiden met visusbehoud tot op hoge leeftijd, hoewel het gezichtsveld een forse concentrische beperking laat zien. Er waren geen syndromale symptomen aanwezig, en de UPSIT resultaten vielen binnen de leeftijdsgecorrigeerde normaalwaarden. Daarnaast geeft dit hoofdstuk een overzicht van de ciliaire genen die niet-syndromale retinadystrofieën veroorzaken, waarbij de nadruk ligt op de retinale en extra-oculaire symptomen in deze specifieke retinadystrofieën.

Hoofdstuk 4 biedt de klinische aspecten van *C8orf37*-geassocieerde retinadystrofie. Acht patiënten – vier met RP en vier met kegel-staaf dystrofie (CRD) – werden onderzocht met routine oogonderzoek, gezichtsveldonderzoek, ERG, OCT, FAF, fundus fotografie en evaluatie van extra-oculaire kenmerken. De RP patiënten lieten een klassiek RP beeld zien met nachtblindheid en concentrische gezichtsveldbeperking, met daarbij een ernstige visusdaling tot lichtperceptie niveau relatief vroeg in het ziekteproces. De CRD patiënten toonde een klassieke CRD die begon met een visusdaling en vervolgens progressie tot in een centraal scotoom vertoonde. Twee van de CRD patiënten hadden een voorgeschiedenis met postaxiale polydactylie. Dit zou kunnen wijzen op syndromale ziekte veroorzaakt door mutaties in het *C8orf37* gen en dat C8orf37 een ciliaire functie heeft. De exacte functie van C8orf37 is daarentegen nog onbekend en dit maakt genotype-fenotype correlaties onmogelijk.

In **hoofdstuk 5** evalueren we de genetische en klinische bevindingen van patiënten uit drie families met *ABHD12* mutaties. De mutaties zijn met ' whole exome sequencing' (WES) aangetoond. Mutaties in *ABHD12* zijn geassocieerd met het polyneuropathie-gehoorverlies-ataxie-RP-cataract (PHARC) syndroom en daarom werden de patiënten onderzocht door een oogarts, neuroloog en keel-neus-oorarts. Wij vonden vijf nieuwe mutaties waaronder de eerste missense mutatie beschreven in *ABHD12.* In twee families lieten de patiënten symptomen zien passend bij het PHARC syndroom, terwijl in de andere familie geen neurologische afwijkingen en gehoorverlies voorkwam. In deze studie konden we het klinische spectrum dat geassocieerd is met *ABHD12* mutaties verbreden. Dit spectrum reikt van niet-syndromale RP tot aan een volledig PHARC syndroom. Desondanks kon er geen duidelijk genotype-fenotype correlatie gevonden worden.

Hoofdstuk 6 beschrijft de moleculaire bevindingen in een Nederlandse familie met autosomaal recessieve gehoorverlies door pathologische mutaties in het *USH1G* gen. Dit gen is eerder geassocieerd met type 1 Usher syndroom en een atypische vorm van het Usher syndroom. De patiënten uit deze familie lieten een progressief gehoorverlies zien met een zogenaamd aflopend verloop op het audiogram. Uitgebreid oogheelkundig en vestibulair onderzoeken lieten geen afwijkingen zien, welke bij het type 1 Usher syndroom

aanwezig zouden zijn. Met deze bevindingen is het klinische spectrum geassocieerd met mutaties in *USH1G* uitgebreid.

In **hoofdstuk 7** onderzochten wij de efficiëntie van de 'arrayed primer extension' (APEX) microarray chip voor autosomaal recessieve RP. In deze studie werden 250 probanden geïncludeerd waarin op klinische gronden de diagnose autosomaal recessieve RP was gesteld en genetische analyse met behulp van de APEX microarray was verricht. Alleen probanden met een autosomaal recessief overervingspatroon in de stamboom (inclusief geïsoleerde casus) werden geïncludeerd. De efficiëntie van deze microarray chip met aanvullende Sanger sequencing werd bepaald door het percentage patiënten waarin een genetisch bevestiging van de klinische diagnose gevonden werd. De APEX microarray chip voor autosomaal recessieve RP kon een genetische bevestiging geven in 8.5% van de patiënten; dit percentage lag op 15.2% wanneer aanvullend Sanger sequencing werd gebruikt in de gevallen dat de microarray een heterozygote mutatie had gevonden. Geconcludeerd dient te worden dat de APEX microarray analyse voor autosomaal recessieve RP slechter presteren dan de huidige 'next generation sequencing' (NGS) technieken – waarvan efficiënties tot 40% zijn gerapporteerd.

Hoofdstuk 8 beschrijft de klinische en genetische bevindingen in patiënten met de ziekte van Stargardt waarin de ziekte zich uiterlijk op een leeftijd van 10 jaar openbaart. In deze retrospectieve studie konden wij 51 Stargardt patiënten includeren. De visus in deze patiënten daalde in een tijdsbestek van 23 jaar tot het niveau van vingers tellen. Bij het eerste oogheelkundige onderzoek werden in 10 patiënten geen fundus afwijkingen gevonden. Negen patiënten toonde retinaal pigment epitheel (RPE) alteraties en 22 patiënten foveale atrofie al dan niet gecombineerd met de typische geel-witte fundus vlekjes. In 14 patiënten was de foveale atrofie eerder aanwezig dan de geel-witte fundus vlekjes, wat vroege diagnostisering bemoeilijkt. Alle patiënten droegen mutaties in het *ABCA4* gen, maar er konden geen duidelijke associaties tussen specifieke mutaties en het klinische beeld gevonden worden. De 'early-onset' ziekte van Stargardt behoort tot de ernstigere ziekten veroorzaakt door *ABCA4* mutaties.

In **hoofdstuk 9** beschrijft de genetische en klinische kenmerken van Stargardt patiënten met 'foveal sparing'. Wij definiëren foveal sparing als retinale atrofie die minimaal 180° rondom de fovea ligt en niet de fovea betrekt. Vanuit onze database met Stargardt patiënten konden wij 13 ongerelateerde patiënten vinden die foveal sparing in één of beide ogen (17 ogen in totaal). De visus in deze ogen bedroeg 20/40 of beter, en minimaal 20/25 in 41% van de patiënten. Uiteindelijk degenereert de fovea als de parafoveale atrofie uitbreidt, wat resulteert in een visusdaling naar 20/200 tot vingers tellen. Genetische analyse liet minimaal één *ABCA4* mutatie gevonden in elke patiënt, maar er werd geen correlatie gevonden tussen een specifieke mutatie en het klinische beeld. De retinale anatomie, metabolisme, biochemie en variaties in andere genen dan *ABCA4* kunnen betrokken zijn bij het ontstaan van het foveal sparing fenomeen. Het ontrafelen van deze fovea-beschermende factoren kan openingen bieden voor therapeutische strategieën voor de ziekte van Stargardt. Foveal sparing komt

met name voor in de 'late-onset' vorm van de ziekte van Stargardt, en representeert daarmee de mildere kant van het klinische spectrum veroorzaakt door *ABCA4* mutaties.

In **hoofdstuk 10** evalueren wij de klinische kenmerken van autosomaal dominante cystoide macula dystrofie (DCMD). We hebben de klinische data – verzamelt over vele jaren – van 97 patiënten met DCMD verzameld, inclusief data uit verschillende beeldvormende technieken (fluorescentie angiografie, FAF en OCT) en elektrofysiologisch onderzoek (ERG en elektrooculografie). We verzamelde bloedmonsters van alle patiënten voor haplotype analyse. In de vroege ziektefase laten DCMD patiënten maculaire vocht collecties zien, die uiteindelijk tot chorioretinale atrofie en pigment deposities in de achterpool zullen leiden. De meeste patiënten (92%) zijn (hoog) hypermetroop. Wij herkenden 3 fasen van DCMD gebaseerd op de fundoscopische, beeldvormende en elektrofysiologische kenmerken. In de eerste fase zijn patiënten jonger dan 20 jaar en presenteren zich met retinale vochtcollecties, fijne vouwing van de membrana limitans interna en milde pigment alteraties. In de tweede fase verminderen de vochtcollecties qua omvang en geleidelijk ontstaat chorioretinale atrofie. De derde fase – de patiënten zijn doorgaans de 50 jaar gepasseerd – laat duidelijke chorioretinale atrofie en harde pigment deposities in de achterpool zien. Haplotype analyse toonde dat alle DCMD patiënten het DCMD locus op 7p15.3 hadden; het oorzakelijke gen is tot op heden niet bekend.

Hoofdstuk 11 omschrijft de RD5000 database, die wij hebben ontwikkeld om alle oogheelkundige en specifieke genetische data van Nederlandse patiënten met een retinadystrofie vast te leggen. Om genotype-fenotype analyse voor zeldzame genetische aandoeningen te kunnen verrichten is het belangrijk om data te verzamelen van grote populaties. Oogheelkundige data wordt doorgaans alleen genoteerd in lokale databases en niet in databases waar meerdere centra aan verbonden zijn. Er zijn momenteel elf Nederlandse oftalmogenetische centra aan de RD5000 database verbonden. Er werden protocollen opgezet omtrent de autorisatierechten van databeheer, -invoer en het delen van data, waardoor de RD5000 database een gebruiksvriendelijke, veilige en veel gebruikte database kan worden, die kan bijdragen aan toekomstige genetische, klinische en therapeutische studies naar retinadystrofieën. De RD5000 database heeft de potentie om uit te groeien naar een Europese database.

Hoofdstuk 12 bediscussieert de studies opgenomen in dit proefschrift en bespreekt de implicaties die deze studies hebben voor onderzoekers, (oog)artsen en patiënten. Het hoofdstuk probeert licht te schijnen op de klinische heterogeniteit van retinadystrofieën door de overige genetische factoren die mogelijk van invloed zijn op de fenotypes te bespreken. Daarnaast biedt dit hoofdstuk een overzicht van de therapeutische strategieën die momenteel worden onderzocht, en bespreekt de verwachtingen en potentie van deze behandelingen evenals de ethische bezwaren.

Curriculum Vitae

Ramon Alexander Christian van Huet was born on the first of March 1986 in Arnhem, the Netherlands. He completed secondary school at the "Arentheem College" in Arnhem where he became interested in biology and genetics. In 2004, he started his medical studies at the Radboud University Nijmegen, where he graduated in December 2010. During his medical studies, he got interested in Ophthalmology, which was further amplified by his (senior) internships in Ophthalmology. During his scientific internship in Ophthalmology, he got the opportunity to combine Ophthalmology with Genetics in a research project on the correlations between the genotype and phenotype in patients with retinitis pigmentosa.

After finishing his medical studies, he continued this research in a Ph.D. project on the clinical and genetic aspects of inherited retinal dystrophies at the Department of Ophthalmology of the Radboud university medical center in Nijmegen, which resulted in this thesis and the RD5000 database.

In January 2014, he started a residency in Ophthalmology in the same institute.

List of publications

Publications related to this thesis

van Huet RA, Pierrache LH, Meester-Smoor MA, Klaver CC, van den Born LI, Hoyng CB, de Wijs IJ, Collin RW, Hoefsloot LH, Klevering BJ. The efficiency of microarray screening for autosomal recessive retinitis pigmentosa in routine clinical practice is low. *Mol Vis.* 2015 Apr; 28(21):461-76.

Oonk AM, **van Huet RA**, Leijendeckers JM, Oostrik J, Venselaar H, van Wijk E, Beynon A, Kunst HP, Hoyng CB, Kremer H, Schraders M, Pennings RJ. Nonsyndromic Hearing Loss Caused by *USH1G* Mutations: Widening the *USH1G* Disease Spectrum. *Ear Hear.* 2015 Mar-Apr;36(2):205-11.

Lambertus S, **van Huet RA**, Bax NM, Hoefsloot LH, Cremers FP, Boon CJ, Klevering BJ, Hoyng CB. Early-onset stargardt disease: phenotypic and genotypic characteristics. *Ophthalmology.* 2015 Feb;122(2):335-44.

Saksens NT, **van Huet RA**, van Lith-Verhoeven JJ, den Hollander AI, Hoyng CB, Boon CJ. Dominant cystoid macular dystrophy. *Ophthalmology.* 2015 Jan;122(1):180-91.

van Huet RA, Siemiatkowska AM, Özgül RK, Yücel D, Hoyng CB, Banin E, Blumenfeld A, Rotenstreich Y, Riemslag FC, den Hollander AI, Theelen T, Collin RW, van den Born LI, Klevering BJ. Retinitis pigmentosa caused by mutations in the ciliary MAK gene is relatively mild and is not associated with apparent extra-ocular features. *Acta Ophthalmol.* 2015 Feb;93(1):83-94.

van Huet RA, Oomen CJ, Plomp AS, van Genderen MM, Klevering BJ, Schlingemann RO, Klaver CC, van den Born LI, Cremers FP; RD5000 Study Group. The RD5000 database: facilitating clinical, genetic, and therapeutic studies on inherited retinal diseases. *Invest Ophthalmol Vis Sci.* 2014 Nov 17;55(11):7355-60.

van Huet RA, Bax NM, Westeneng-Van Haaften SC, Muhamad M, Zonneveld-Vrieling MN, Hoefsloot LH, Cremers FP, Boon CJ, Klevering BJ, Hoyng CB. Foveal sparing in Stargardt disease. *Invest Ophthalmol Vis Sci.* 2014 Oct 16;55(11):7467-78.

Nishiguchi KM, Avila-Fernandez A, **van Huet RA**, Corton M, Pérez-Carro R, Martín-Garrido E, López-Molina MI, Blanco-Kelly F, Hoefsloot LH, van Zelst-Stams WA, García-Ruiz PJ, Del Val J, Di Gioia SA, Klevering BJ, van de Warrenburg BP, Vazquez C, Cremers FP, García-Sandoval B, Hoyng CB, Collin RW, Rivolta C, Ayuso C. Exome sequencing extends the phenotypic spectrum for ABHD12 mutations: from syndromic to nonsyndromic retinal degeneration. *Ophthalmology.* 2014 Aug;121(8):1620-7.

van Huet RA, Collin RW, Siemiatkowska AM, Klaver CC, Hoyng CB, Simonelli F, Khan MI, Qamar R, Banin E, Cremers FP, Theelen T, den Hollander AI, van den Born LI, Klevering BJ. IMPG2-associated retinitis pigmentosa displays relatively early macular involvement. *Invest Ophthalmol Vis Sci.* 2014 May 29;55(6):3939-53.

van Huet RA, Estrada-Cuzcano A, Banin E, Rotenstreich Y, Hipp S, Kohl S, Hoyng CB, den Hollander AI, Collin RW, Klevering BJ. Clinical characteristics of rod and cone photoreceptor dystrophies in patients with mutations in the C8orf37 gene. *Invest Ophthalmol Vis Sci.* 2013 Jul 12;54(7):4683-90.

Other publications

Teussink MM, Lee MD, Smith RT, **van Huet RA**, Klaver CC, Klevering BJ, Theelen T, Hoyng CB. The Effect of Light Deprivation in Patients with Stargardt Disease. *Am J Ophthalmol.* 2015 May;159(5):964-72

Smailhodzic D, van Asten F, Blom AM, Mohlin FC, den Hollander AI, van de Ven JP, **van Huet RA**, Groenewoud JM, Tian Y, Berendschot TT, Lechanteur YT, Fauser S, de Bruijn C, Daha MR, van der Wilt GJ, Hoyng CB, Klevering BJ. Zinc supplementation inhibits complement activation in age-related macular degeneration. *PLoS One.* 2014 Nov 13;9(11):e112682.

Siemiatkowska AM, van den Born LI, van Genderen MM, Bertelsen M, Zobor D, Rohrschneider K, **van Huet RA**, Nurohmah S, Klevering BJ, Kohl S, Faradz SM, Rosenberg T, den Hollander AI, Collin RW, Cremers FP. Novel compound heterozygous NMNAT1 variants associated with Leber congenital amaurosis. *Mol Vis.* 2014 Jun 2;20:753-9.

Neveling K, Collin RW, Gilissen C, **van Huet RA**, Visser L, Kwint MP, Gijsen SJ, Zonneveld MN, Wieskamp N, de Ligt J, Siemiatkowska AM, Hoefsloot LH, Buckley MF, Kellner U, Branham KE, den Hollander AI, Hoischen A, Hoyng C, Klevering BJ, van den Born LI, Veltman JA, Cremers FP, Scheffer H. Next-generation genetic testing for retinitis pigmentosa. *Hum Mutat.* 2012 Jun;33(6):963-72.

Estrada-Cuzcano A, Neveling K, Kohl S, Banin E, Rotenstreich Y, Sharon D, Falik-Zaccai TC, Hipp S, Roepman R, Wissinger B, Letteboer SJ, Mans DA, Blokland EA, Kwint MP, Gijsen SJ, **van Huet RA**, Collin RW, Scheffer H, Veltman JA, Zrenner E; European Retinal Disease Consortium, den Hollander AI, Klevering BJ, Cremers FP. Mutations in C8orf37, encoding a ciliary protein, are associated with autosomal-recessive retinal dystrophies with early macular involvement. Am J *Hum Genet.* 2012 Jan 13;90(1):102-9.

Smailhodzic D, Fleckenstein M, Theelen T, Boon CJ, **van Huet RA**, van de Ven JP, Den Hollander AI, Schmitz-Valckenberg S, Hoyng CB, Weber BH, Holz FG, Klevering BJ. Central areolar choroidal dystrophy (CACD) and age-related macular degeneration (AMD): differentiating characteristics in multimodal imaging. *Invest Ophthalmol Vis Sci.* 2011 Nov 21;52(12):8908-18.

Een woord van waardering…

Op de voorkant van dit proefschrift wat voor u ligt prijkt enkel de naam van ondergetekende, maar het had er nooit gelegen zonder de hulp, begeleiding, en het vertrouwen van anderen. In tegenstelling tot wat veel mensen denken, doe je onderzoek niet alleen. Natuurlijk zit je als promovendus regelmatig dagen achter de computer data het analyseren, theorieën op te stellen, verklaring te zoeken en dit in een artikel op te schrijven, maar promoveren is zo veel meer. Het is een reis waarbij je groeit – zowel als persoon als onderzoeker – maar ook leert waar je grenzen liggen. Je leert omgaan met teleurstellingen, tegenslagen te verwerken en deze in een kracht om te zetten. (*"You live, you love, you cry, you lose, you bleed, you scream, you learn"* Alanis Morissette – You learn) Gelukkig heeft deze ontdekkingstocht wegbewijzering, staat de autoradio aan en sta je niet alleen in de file: de dagen worden gekleurd door talloze overleggen en vergaderingen, congressen en cursussen, maar vooral ook de gezellige lunches en het directe contact met collega promovendi en arts-assistenten. Kortom: promoveren doe je niet alleen en daarom is een woord van waardering en dank op zijn plaats.

Geachte prof. dr. Hoyng, beste Carel, dank voor het vertrouwen, de vrijheid en dat ik heb mogen leren van jouw jarenlange ervaring met retinadystrofieën. Jij bent de man van het overzicht en de neuzen de juiste richting op. Jij weet altijd te bewaken wat de rode lijn moest zijn, waarbij het klinische belang nooit uit het oog verloren raakt: 'wat wil ik nou weten als de patiënt tegenover me zit in de spreekkamer?' Je schroomt niet om groot te denken en gedurfde keuzes te maken. (*"That what he goes there for, is to unlock the door"* Seal – Crazy)

Geachte dr. Klevering, beste Jeroen, dank voor de leerzame discussies, jouw brede en toch gedetailleerde kennis en jouw sturing. Jij was mijn directe begeleider de afgelopen jaren, en menigmaal als ik het spoor bijster was, had jij mij binnen een paar minuten weer op het juiste spoor. Als geen ander weet jij de vinger op het probleem te leggen, waarvoor je dan meestal een eenvoudige doch effectieve oplossing hebt, die niet bij uitzondering zo logisch en vanzelfsprekend blijkt dat je je afvraagt waarom je er zelf niet op gekomen bent. (*"Nobody said it was easy."* Coldplay – The Scientist)

Geachte dr. Collin, beste Rob, voor menig clinicus lijkt de moleculaire genetica ingewikkeld, onoverzichtelijk en een ver-van-mijn-bed verhaal, om nog maar te zwijgen hoe die genetica dan in expressie komt tot een fenotype. Jij wist mij daarentegen bij te sturen als ik mij op het gladde ijs van de genetica begaf en de bocht te kort dreigde te nemen. Dank hiervoor.

Geachte prof. dr. Cremers, beste Frans, vanaf het begin van mijn promotie viel mij de laagdrempeligheid op waarmee je te benaderen bent. Overleg met jouw is altijd hardop denken en hiermee samen het juiste pad bepalen. Jij was de grote drijfveer achter het

RD5000 project, wat een grote stempel op mijn promotieonderzoek heeft gedrukt. Een van de resultaten hiervan staat in hoofdstuk 11 beschreven.

Geachte dr. Van den Born, beste Ingeborgh, menigmaal hadden wij overleg om een samenwerking te creëren (hoe meer patiënten, hoe beter!) of om resultaten en interpretaties hiervan te bespreken. Dank je voor het delen van je grote klinische kennis van retinale dystrofieën.

Geachte prof. dr. Den Hollander, beste Anneke, slechts enkele keren werkten we samen aan een project, waarbij dan voorafgaand eerst goed werd bepaald hoe het doel efficiënt behaald kon worden. Dankzij je onberispelijke Engels waren jouw correcties meteen een 'semi-native' speaker edit, iets wat zeer waardevol voor een artikel is. Dank je wel.

Geachte dr. Theelen, beste Thomas, voor hulp betreffende beeldvorming kon ik altijd bij u terecht. Je snelle en gedetailleerde beschrijvingen van de verschillende technieken brachten meer dan eens nieuwe inzichten aan het licht.

Geachte dr. Boon, beste Camiel, het was altijd fijn om met jou van gedachten te wisselen. Bij het geven van commentaren op een artikel weet jij feilloos de (soms bijna onzichtbare) zwakke punten eruit te pikken en hier eenvoudige doch stevige oplossingen voor te bieden. Dank voor je enthousiasme en kunde.

Geachte dr. Oomen, beste Clasien, wij hebben intensief samengewerkt aan verschillende onderdelen van het RD5000 project. Samen begaven wij ons in de wereld van data management, logistiek, regelgeving en gebruiksvriendelijkheid van de RD5000 database. Het volgende moment hadden we het over de website: waar moet welke tekst? Dank voor het overzicht en de prettige samenwerking binnen het RD5000 project.

Geachte prof. dr. Keunen, beste Jan, een deel van mijn promotietraject viel samen met mijn opleiding tot oogarts. U waarschuwde mij bij voorbaat voor de drukte die deze combinatie met zich mee zou gaan brengen. It was tough, but I made it! Dank voor de betrokkenheid en zorgzaamheid.

Geachte drs. Groenewoud, beste Hans, jij bent mijn statistische held. Speerpunt was altijd het vinden van de meest eerlijk en subtiele manier om deze specifieke statische vraag te beantwoorden. Ook als er overlegd moest worden over een output van een database stonden jij en je collegae klaar om hierover gedachten te wisselen, ondanks jouw drukke agenda gevuld met colleges en cursussen. Dank voor je motivatie en zorgvuldigheid.

Uiteraard ook veel dank aan mijn (oud) mede-promovendi van de afdeling oogheelkunde: Dženita, John, Mahesh, Yara, Shazia, Nicole, Freekje, Constantin, Myrte, Michel, Nathalie, Laura, Maartje, Roos en Stanley. Samen maakten we het doen van onderzoek leuk! Dank

voor het aanhoren van frustraties, alle zin en onzin die over en weer door de kamer ging, en de leuke uitjes. Een aantal van jullie is inmiddels ook in opleiding tot oogarts en ik hoop nog een aantal van jullie twee verdiepingen lager te mogen verwelkomen.

En dan kom je 'beneden', wederom een transitie van 'oudste' naar 'jongste' (will it ever stop?!?!). Pit, Jeroen, Milan, Irene, Samuel, Linda, Carla, Paulien, Ann-Laure, John, Dženita, Anita, Stefan, Jelina, Ellen, Frank, Yara, Nicole, Artin, Myrte en Anna; dank voor jullie warme onthaal en de fijne samenwerking. We zijn een leuke groep samen!

I would also like to thank my (ex-)colleagues at the department of Genetics: Susanne, Alejo, Imran, Anna, Alex, Galuh, Ellen, Marijke, Frederieke, Bjorn and Saskia. Thank you for your time and patience while answering my questions, explaining tests (results) or running certain tests.

Graag wil ik mijn collega bij de keel-, neus- en oorheelkunde, Anne Oonk, bedanken voor de fijne samenwerking. Het was verfrissend om eens verder dan het oog te kijken!

Ik ben ook zeker veel dank verschuldigd aan de dames en heren van de administratie, de verpleegpost, het trialcentrum en de optometrie. Dankzij jullie was het mogelijk om onderzoekspatiënten op de polikliniek te kunnen zien tussen het reguliere patiëntenverkeer door. Liesbeth, bedankt voor de bereidwilligheid om menig lunch op te geven om weer eens een ERG of een kleurenonderzoek voor mij te verrichten. Uiteindelijk heb je het mij zelfs geleerd om de bijzondere onderzoeken zelf uit te voeren.

Mijn vrienden Joep, Lianne, Lyvonne, Maaike, Monique, Nicky, Nienke, Wienke, Yara, Nicole, en Marleen wil ik bedanken voor het bieden van de broodnodige afleiding tussen alle avonden en weekenden werken: voor de leuke uitjes, de weekendjes weg, de hilarische impulsieve acties tussendoor, nutteloze discussies (gewoon omdat het kan), de avonden samen Wie is de Mol? kijken en de talloze spellendag (Ligretto stop!).

Mijn paranimfen wil ik graag nog apart bedanken voor de hulp bij de laatste loodjes. Maaike, bedankt voor de gezelligheid, de mooie concerten, de avonden film kijken, de nutteloze discussies gewoon omdat het kan (zijn wij toch wel experts in te noemen) en het luisterend oor als dat nodig was. Nicole, wij zaten op dezelfde golflengte vanaf seconde 1 dat ik je heb leren kennen. Jouw hilariteit, energie, en humor zijn goud waard, dank voor het delen ervan. *kinstagmus*

De personen die het belangrijkst voor je zijn worden vaak aan het eind bedankt en zo ook hier. Lieve Silf en Ivonka, lieve pap en mam, bedankt dat jullie er altijd voor me zijn geweest; altijd m'n 'back gecoverd' hebben. Ik kan niet anders dan apetrots op jullie zijn!
("*So sing your own song and never forget. N'oubliez jamais.*" – Joe Cocker N'oubliez jamais)

Lieve Frank, Ania en Adam, vanaf een afstandje – Warschau is nèt niet naast de deur – hebben jullie altijd interesse in mijn promotie getoond. Dank voor de technische hulp als de computer of telefoon B deed, terwijl ik A wilde. Dit jaar is Adam in de familie erbij gekomen, waarvoor ik – wederom vanaf afstand – voor suikeroom mag gaan spelen.☺

Lieve Nina, jij bent altijd vrolijk en staat vooraan om een knuffel te geven. Wij hebben thuis dankzij jou veel geleerd, en niemand kan mij zo goed 'aan elkaar slaan' op de Wii als jij! Dank je wel en dikke knuffel terug!
("*Met een mooie glimlach of een lief gebaar, worden al jouw dromen waar.*" – K3 – Toveren)

Lieve Niels, dank je dat je er altijd voor me bent. Ook als ik weer eens chagrijnig was omdat ik mezelf geen moment rust gunde en alleen maar tegen je kon klagen, wist jij zonder moeite de bui over te laten trekken. Dank je voor het begrip als ik weer eens ging zitten werken in plaats van samen op de bank een film kijken. Jij bent mijn thuis.
("*You are, home. Home, where I wanted to go.*" Coldplay – Clocks)